THE CUTTING PERFORMANCE OF SIALON CERAMIC TOOLS

By

ADEL FAKHRI LAFTA

BSc, MSc (M.T.T. England)

A Thesis submitted for the degree of

DOCTOR OF PHILOSOPHY

of the

University of Aston in Birmingham

Department of Production Technology
and Production Management

September 1983

Supervisor: T J Vickerstaff

THE CUTTING PERFORMANCE OF SIALON CERAMIC TOOLS

ADEL FAKHRI LAFTA

A thesis submitted to
The University of Aston in Birmingham
for the degree of Doctor of Philosophy 1983

Summary

The thesis deals with a research programme in which the cutting performance of a new generation of ceramic cutting tool material is evaluated using the turning process.

In part one, the performance of commercial Kyon 2000 sialon ceramic inserts is studied when machining a hardened alloy steel under a wide range of cutting conditions. The aim is to formulate a pattern of machining behaviour in which tool wear is related to a theoretical interpretation of the temperatures and stresses generated by the chip-tool interaction. The work involves a correlation of wear measurement and metallographic examination of the wear area with the measurable cutting data. Four main tool failure modes are recognised:

(a) flank and crater wear
(b) grooving wear
(c) deformation wear and
(d) brittle failure

Results indicate catastrophic edge breakdown under certain conditions. Accordingly in part two, the edge geometry is modified to give a double rake tool; a negative/positive combination. The results are reported for a range of workpiece materials under orthogonal cutting conditions. Significant improvements in the cutting performance are achieved. The improvements are explained by a study of process parameters; cutting forces, chip thickness ratio, chip contact length, temperature distribution, stress distribution and chip formation.

In part three, improvements in tool performance are shown to arise when the edge chamfer on a single rake tool is modified. Under optimum edge chamfer conditions a substantial increase in tool life is obtained compared with the commercial cutting geometry.

Keywords

Sialon; Metal cutting; Failure modes; edge geometry

ACKNOWLEDGEMENTS

I am extremely grateful to my supervisor, Dr.T.J.Vickerstaff, Senior Tutor, for his advice, patient and personal guidance, inspiration and many productive discussions which covered all aspects of the work.

I would like to thank Professor T.Thornley, Head of Production Technology and Production Management Department, for the provision of equipment, technical staff and other extensive departmental facilities.

Thanks are also due to the technicians in the Department of Production Technology and Production Management, especially Mr.G.Yardly for his help whilst performing the experimental part of this work.

I am also grateful to Dr.G.Barrow for the valuable discussion on the split tool dynamometer design.

I would like to thank Mrs.A.Howell for typing the manuscript.

Finally, I would like to thank my wife Alaa for her help, patience and encouragement during the preparation of this work.

To my children

NEHAL and NAWAR

No part of the work described in this thesis has been submitted in support of an application for another degree or award of this or any other University or Institute

A. F. Lafta

23.9.1983

A.F.LAFTA

LIST OF CONTENTS

LIST OF TABLES

LIST OF FIGURES

CHAPTER FIVE

CHAPTER SIX

NOTATIONS

ϕ	shear angle, degree
ψ	mean friction angle, degree
α	rake angle, degree
L_s	sticking length (mm)
x	distance along the rake face (mm)
L_c	contact length (mm)
F_s	shear force on shear plane (N)
F_{ns}	normal force on shear plane (N)
t_1	undeformed chip thickness (mm)
t_2	deformed chip thickness (mm)
R	Resultant cutting force (N)
Fr	Frictional force on the rake
Fn	normal force on tool face
T_1	Tool life (min)
V	cutting speed (m/min)
n,c'	Taylor constant
f	feed rate (mm/rev)
d	depth of cut (mm)
V_B	flank wear (mm)
V_{Bmax}	Maximum flank wear (mm)
V_n	primary groove (mm) (leading edge)
V_c	secondary groove (Trailing edge)
K_T	crater depth (mm)
r_ε	nose radius (mm)
β	symbol represent type of sialon structure

$F_x=F_t$	feed force (N)
F_y	Radial force (N)
F_z	tangential force or main cutting force (N)
γ	The partial F-value for the entry of variables to the regression equation and removing variables from the regression equation
F-value	variance ratio
T	Temperature ^oC
σ_f	normal stress on the flank
α_1	primary rake angle (degree)
α_2	secondary rake angle (degree)
L	Land width (mm)
L_1	projected land width (mm)
G	split tool "air-gap" width (mm)
τ_n	shear stress along the rake face (N/mm^2)
σ_n	normal stress on the rake face (N/mm^2)
τ	chamfer angle in the statistical model
B	feed rate in the statistical model
q	chamfer width in the statistical model
i=a	level of chamfer angle
j=b	level of feed rate
K=	level of chamfer width
e_{ijk}	error in the statistical model
Y_{ijk}	dependent variable in the statistical model

CHAPTER ONE

INTRODUCTION

CHAPTER 1

During the past decade mounting economic and social pressures have forced the major industrial nations to contain price increases to some extent, whilst the costs of production have increased rapidly. These conditions have meant, in terms of the factory environment, that the choice of the correct method of production and the use of improved materials has been even more important than before.

The history of the metal cutting industry is a good example of the benefits that can be derived by the use of improved materials. Increased output and reduction of costs have been realized through the years with the progressive use of new cutting tool materials starting with carbon steels then on to high speed steels, the cast cobalt-base alloys, cemented carbides, ceramics, and more recently, cubic boron nitrides and polycrystalline diamonds. However, the choice of a cutting tool material for a particular application is usually a compromise between conflicting technological requirements, both production and metallurgical, and economic criteria.

The performance of any cutting tool largely depends upon tool material properties and cutting geometries. Having selected the optimum material and geometry, the correct cutting conditions can then be established. The tool material and edge geometry can be considered to be

dependent variables since the correct geometry allows the use of harder, more brittle, tool materials while the choice of tool material places limits on the geometry which can be employed.

More recently, in the course of developing a new ceramic cutting tool material, Lucas Industries have found sialon compositions with outstanding mechanical and thermal properties which have been patented and trademarked Syalon. It is claimed that this material offers an attractive combination of properties which are not available in other materials, and can be modified to suit the particular needs of the user. Such compositional flexibility is not available in other high performance ceramics and this enables considerable performance advantages to be gained with significant cost savings.

The characteristics of Syalon ceramics have been listed in [1]* and can be summarised as follows;

- High mechanical strength at room and elevated temperatures.
- High specific strength resulting in weight savings over metallic systems thus leading to cost comparability.

* Figures in parenthesis [1] refer to references in the Bibliography.

- High hardness, high toughness and low coefficient of friction. These combinations result in
  - Good wear resistance.
  - Good abrasion resistance.
  - Good erosion resistance.
- Low thermal coefficient of expansion leading to good thermal shock resistance.
- Chemical inertness resulting in resistance to attack by molten metal environments.
- Creep and oxidation resistance.

Field trials with Syalon ceramic tools on a range of industrially used materials, have shown that this new material is capable of machining under cutting conditions which previously were not achievable. The results encouraged two of the world's major tungsten carbide suppliers (Sandvik and Kennametal) to take up licences to manufacture and market the material. Although the commercial Kennametal product named Kyon 2000 appeared on the market, the data available on its cutting performance is minimal and therefore, it is important that its characteristics as a cutting tool are evaluated so that appropriate areas of application can be defined.

The objective of the work reported in this thesis

was to evaluate the cutting performance of this new generation of tool material, under a wide range of cutting conditions. The cutting edge geometry currently specified for Kyon 2000 is similar to that conventionally used for carbide and coated carbides; and therefore, an additional objective was to decide if this is the most satisfactory, and if not, to recommend alternatives.

In Chapter 2, a survey of the literature relevant to chip formation process is given with an indication of the basic mechanics of the metal cutting process in relation to the current problem. Chapter 3, is devoted to the provision of a fundamental understanding of the variables affecting the cutting process. A discussion of the types of cutting tool wear, the criteria of tool failure and the methods of measuring tool wear are included.

Chapter 4 demonstrates the electrical, thermal and mechanical properties of sialon ceramic and a review of previous work on sialon material as a cutting tool is also given. Following a description of test equipment and experimental procedures in Chapter 5, Chapter 6, presents experimental results obtained using standard Kyon 2000 ceramic inserts. The object of the work in this chapter was to formulate a pattern of machining behaviour in which tool wear could be related to a theoretical interpretation and a direct measurement of cutting data.

A number of authors have suggested the use of double rake tooling as a means of overcoming some of the problems identified in Chapter 6. Accordingly, following a review of the double rake literature, the cutting performance of sialon ceramics with double rake geometry was studied in Chapter 7. Orthogonal cutting was used for the purpose of this investigation and the results are discussed in the light of temperature and stress measurements made in the cutting area.

In Chapter 8, the results of tests with a more standard edge geometry are reported. The edge chamfer on a single rake tool was modified and the cutting tool was evaluated under oblique cutting experiments. It is clear from this work that significant improvements in the tool life of sialon ceramic inserts can be obtained from the correct selection of cutting edge geometry.

Chapter 9 presents conclusions and suggestions for future work.

CHAPTER TWO

THE METAL CUTTING PROCESS

2.1 INTRODUCTION

Research into the metal cutting process can be traced as far back as the 17th century, though most of the work has been done during the past four to five decades. It is impossible to review the entire historical development of this field of research, but is is intended here to give some of the more important steps that have been made.

In 1956 Finnie[2], reported a historical review of work in metal cutting for the period of one hundred years previous to the date of his publication. Early research in this field started with Cocquilhat[3] in 1851, who dealt with the drilling operation. Research into chip formation was carried out by Timme[4], who stated that the chip is formed by fracture along shear planes which are inclined in the direction of cutting. Tresca[5] developed some of the basic concepts of plasticity and described the mechanism of the chip formation as a compression of the work material in front of the tool with subsequent shearing in a plane parallel to the cutting direction. In 1881 after examining polished and etched chips, Mallock[6] described chip formation as a shearing of the work material, like a "sliding deck of cards". He emphasized the effect of friction occurring on the tool face as the chip was removed.

In 1907, the famous article "On the art of metal cutting" by Taylor[7] was published, which reported the results of extensive work. Taylor was interested in the application of piece-work systems in machine shops, where a time allowance was set for a particular job and a bonus was given to the workman performing his task in the allotted time. To assist in the application of such a system Taylor investigated the effect of tool material and cutting conditions on tool life during roughing operations. The principal object was to determine the empirical laws that allow cutting conditions to be established. It is important to note that some of Taylor's findings are still used today. Following the publication of Taylor's work, research into metal cutting started to increase gradually, but most of the work in this field has been carried out after Merchant's[8] publication in 1941, which proposed the mechanism of the simple thin shear plane process.

2.2 THE METAL CUTTING PROCESS

The cutting of metals is one of the most common and the most economical methods of producing components in engineering. The process itself basically involves the removal of a thin layer of work material, known as the swarf or the chip, by the action of a wedge-shaped tool driven asymmetrically into the workpiece material. The metal removed impinges upon the rake-face of the tool and moves over it in a direction away from that in which the body of the metal is moving and so is parted from it. An understanding of the mechanics of the metal cutting process is very important, although it is somewhat complex, and its full appreciation requires consideration of some aspects of solid state physics, physical metallurgy, engineering mechanics, thermodynamics, theories of wear and lubrication and their inter-relation in metal cutting. Thus, understanding the process refers to conditions involving intense deformation of metal, combined with high local pressure and steep temperature gradients at the chip-tool interface.

2.3 THEORIES OF METAL CUTTING

The mechanics of chip formation have been studied by many authors and it is now widely accepted that chip formation is a plastic shearing process and that the deformation is extremely localised.

Basically, the chip formation process can be best explained by considering the two-dimensional simple case - "orthogonal cutting" in which a single cutting edge is perpendicular to the relative motion between the tool and workpiece. In practice, actual cutting operations often involve a cutting edge which is inclined at some angle other than 90^{o} to give "oblique cutting". However, the nature of the chip formation process is similar in both cases.

The first complete analysis providing a so-called "shear angle solution" was presented by Ernst and Merchant[8]. In their analysis the chip was assumed to act as a rigid body which is held in equilibrium by the action of the forces transmitted across the chip-tool interface and across the shear plane. Figure (2.1) shows the system of forces in orthogonal cutting with a continuous chip.

Merchant derived the following well-known relationship by assuming that the deformation process adjusts itself to give minimum energy consumption.

$$\Phi = \frac{\pi}{4} - \frac{1}{2} (\psi - \alpha) \quad \ldots\ldots\ldots 1$$

It is assumed that ψ, α are independent of Φ. Equation 1 does not fit in well with experimental data and Merchant[9] modified it by assuming that the shear stress on the shear plane is linearly proportional to the normal stress to give

$$\Phi = C - \frac{1}{2} (\psi - \alpha) \quad \ldots\ldots\ldots 2$$

where C is a material constant.

Lee and Shaffer[10] arrived at a different equation by applying the theory of an ideal rigid plastic body.

$$\Phi = \frac{\pi}{4} - (\psi - \alpha) \quad \ldots\ldots\ldots 3$$

Neither theory gives a totally satisfactory explanation of actual cutting data. Other workers, such as Shaw et al[11], Oxley[12,13] and Colding[14], suggest various shear angle relationships, but none of them has been found to be completely satisfactory either. In general, the shear angle relationship can be expressed as

$$\Phi = C_1 - C_2 (\psi - \alpha) \quad \ldots\ldots\ldots 4$$

where C_1, C_2 are constants depending on the tool-work pair[15]. However, there are conflicting ideas about the actual shape of the plastic-flow region. Piispanen[16] Ernst[8] and Merchant[9] support the thin shear zone model. Palmer and Oxley[17], Okushima and Hitomi[18] propose thick deformation zone models, as shown in

figure (2.2). Bitans and Brown[19] suggest that under different machining conditions the deformation approximates to one or other of these shear models. After examining motion picture film and photo-micrographic evidence, they conclude that, especially when the metal is in an annealed state, the "thick zone" model is more appropriate at low cutting speeds. At the high cutting speed region the situation approaches the "thin zone" model.

2.4 TOOL STRESSES IN THE CUTTING PROCESS

One of the most important aspects of the chip formation process is the nature of the mean compressive and shear stress acting on the tool and the way that it is distributed along the rake face. In fact cutting tools are rarely, if ever, designed on the basis of stress calculations; trial and error methods and accumulated experience form the basis for tool design. However, in trying to understand the properties required of tool materials, it is useful to have some knowledge of the general character of these stresses. Zorev[20] suggested that the normal and shear stresses on the rake face are distributed as shown in figure (2.3). The normal stress is assumed to decrease exponentially from a maximum value at the tool edge to zero at the point of chip separation. In the region $L_s < x < L_c$ the normal stress is relatively low, so that the proportion of the real area to the apparent area of contact is small enough to allow the chip to slide along the tool face. This zone is known as the sliding (friction) region. In the zone $x < L_s$ the normal stress is so high that seizure occurs between the chip and tool materials, as a consequence of which the shear stress becomes equal to the shear yield stress of the chip material. The zone is known as the sticking (friction) region. However, this picture may be oversimplified, since it has been deduced from limited data obtained from photoelastic studies.[21,22] Kudo[23] evaluated rake face stress near the cutting

edge by applying the theory of plasticity for rigid plastic non-hardening materials. His results indicate that the normal and shear stresses would, to a large extent, be uniform over the sticking length, while the normal stress decreases and the shear stress increases as the tool tip is approached.

Recently, Kato et al[24] and Barrow[25] have determined the stress distribution at the chip-tool interface by means of a split-tool dynamometer. This technique has made possible the presentation of a reasonably accurate picture of the stress distribution and is discussed in more detail in Section 5.11.

2.5 STRAIN AND STRAIN RATE IN METAL CUTTING

In metal cutting the plastic deformation takes place over two main regions. The region (figure 2.4) around the so-called shear plane, known as the 'primary zone', and the region adjacent to the rake face of the tool, known as the 'secondary zone'. The deformation process presents unique conditions for the study of plastic flow characteristics. The flow stress of a metal under conditions occurring in the primary and secondary zone is influenced by the temperature of deformation, the degree of deformation or strain and the rate of deformation or strain rate. The degree of dependency of the flow stress upon these variables varies considerably for different materials. Moreover, in the contact area, variations in strain and strain rate can alter both the chip heating and the chip flow. The very large strains, which are estimated by Zorev[26] to be as high as forty at a distance of 0.025 mm from the rake face for the cutting of medium carbon steel at 18 m/min, have fallen to six at a distance of 1 mm from the rake face. These very large strains tend to break up the structure of two phased materials[27], e.g. steels. This is an additional complication in the interpretation of the flow stress behaviour of the chip material next to the rake face.

The behaviour of metals under the extreme conditions

operating at the chip/tool interface, the relationships between strain, strain rate and temperature variation, and chip flow are by no means fully understood.

2.6 HEAT IN METAL CUTTING

During machining operations, high temperatures are generated in the cutting zone as a result of the chip formation process where the power consumed in deforming the work materials is largely converted into heat. Increasing the metal removal rate above a certain limit produces a very high temperature, which has a controlling influence on the rate of wear of the cutting tool, as well as on the friction between the chip and the tool. The combined effect of the high temperature and the stress imposed on the cutting tool tends to cause the cutting edge to collapse.

Heat is generated in three major zones[28,29,30]

1. The primary shear zone.
2. The secondary shear zone.
3. On the flank face of the tool.

Figure (2.4) shows the heat generation during orthogonal cutting in the turning operation. The temperature distribution in the primary and secondary shear zones depends on a great many factors. The nature of the work-piece is of particular importance, since its thermal properties play an important role in the heat generated. The tool chip contact area also affects the secondary shear zone temperature.

It has proved difficult to measure the temperature in metal cutting and to obtain the temperature gradients. Several methods of measuring cutting temperature (both average values and distribution) have been used. These can be categorised as follows[31]:

a) Thermo - e.m.f (thermocouples).

b) Radiation (pyrometry, infra-red photography, etc.)

c) Thermo-chemical reactions (thermo-colours)

d) Constant Melting point powders.

2.6.1 Heat in the Primary Shear Zone

As reported earlier[7], the energy involved in plastic deformation goes largely into thermal energy. The extent to which this energy transformation occurs depends upon the strain energy involved in the process.

Under most machining conditions, the largest amount of the work is carried out in forming the chip. The temperature of the chip can affect the cutting performance of the tool only as long as the chip remains in contact with the tool. As contact ends, heat leaves the system with the chip. However, some of the heat from the deformed layer of work material is conducted back into the workpiece and raises the temperature of the machined part.

Summarising, most of the heat resulting from the

work done on the shear plane to form the chip remains in the chip and is removed from the cutting zone in the chip. Trent[30] estimated that 99% of the heat generated in cutting was present in the chip.

2.6.2 Heat in the Secondary Shear Zone

The heat generated at the tool/work interface is of major importance in relation to tool performance. Furthermore, it is particularly significant in limiting the rates of metal removed in cutting steels and other alloys of high melting point. The amounts of strain in the flow zone near the tool surface are very large and are caused by what is known as SEIZURE. The ability of metals to withstand such enormous shear strains in the flow zone without fracture, must be attributed to the very high compressive stresses in this region. Compressive stress at the rake face decreases, as the chip moves away from the cutting edge. The material from which the flow zone is composed changes continuously as new material is fed in near the cutting edge. It is continuously sheared as is flows over the rake face until it leaves the tool as a thin layer under the surface of the chip. Thus, unlike the material in the body of the chip, it is continuously being sheared and progressively heated by the work done and therefore, the temperature can be expected to increase as it flows away from the cutting edge. The tool thus acts as a sink

into which heat flows from the flow zone, while a stable temperature gradient is built up within the tool. The heat flowing into the tool from the flow zone raises its temperature, which is the most important factor that limits the rate of metal removal when cutting the higher melting point metals.

2.6.3 Heat on the Flank Face of the Tool

As shown in figure (2.4), a third heat source would be present owing to friction between the tool and the workpiece surface. In this case the clearance angle of the tool has an influence on the heat generated because if it is large enough, it can ensure that separation of freshly cut workpiece surface is performed without rubbing against the tool face. However, a very large value of clearance angle is not recommended since it weakens the tool and therefore,a compromise value should be adopted. Furthermore, it has been mentioned[32] that the temperature on the flank will be also influenced by the rake-face temperature.

However, if the tool is severely worn, the generation of high temperatures in this region is usually followed immediately by collapse of the tool.

2.7 FORMATION OF CHIPS

The type of chip produced during metal cutting depends on the material being machined and the cutting conditions used. However, the types of chip produced can be conveniently classified into four groups, as described by Boothroyd[32] and Reeht[33]:

1) The continous chip
2) The continuous chip with built-up edge
3) The discontinuous chip and
4) The saw tooth chip.

2.7.1 Continuous Chip

As a result of machining ductile materials such as wrought iron, mild steel, copper and aluminium, a continuous chip is produced. Basically this operation is one of shearing the work material to form the chip and of sliding the chip along the face of the cutting tool. To deform the material in this manner the forces that must be transmitted to the chip across the interface between the chip and the tool, are sufficient to deform the lower layers of the chip, as it slides along the tool face.

2.7.2 Continuous Chip with Built-up Edge

It has been observed that under certain cutting

conditions and with certain work materials a chip or part of it is welded to the cutting edge. The presence of this welded material increases the friction between the chip and the tool and in turn this friction leads to the building up of layer upon layer of chip material. The resulting pile of material is known as a built-up edge. Often the built-up edge continues to grow, until it reaches an unstable point and then breaks down, the broken pieces being carried away by the underside of the chip and the new workpiece surface. Built-up edge formation in metal cutting is undesirable, as it is one of the principal factors affecting surface finish and can have a considerable influence on cutting tool life.

2.7.3 Discontinuous Chip

The discontinuous chip is produced whenever the material being machined is brittle and the chip undergoes severe strain.

This kind of chip is always formed during the process of machining brittle materials, such as cast iron or cast brass, or when machining ductile materials at very low cutting speeds and high feeds. Figure (2.5) shows the various forms of chips (after Boothroyd[32]).

2.7.4 The Saw-Tooth Chip

This type of chip has been described by Reeht[33]. It is called by the above name, because the top of the chip shows a saw-tooth waveform. It has been postulated that this form of chip is the result of catastrophic shear, which occurs when local temperature gradients offset the effects of strain hardening. In this case, the burden of plastic strain is supported by a small proportion of the metal and this can explain the saw-tooth waveform, which in section shows planes of distinct shear separated by regions which are only lightly strained.

2.8 CHAPTER CLOSURE

The metal cutting process is extremely complex with many factors influencing the performance of the cutting tool and the quality of the workpiece produced. The survey indicates that an understanding of the process mechanics involves a knowledge of solid state physics, physical metallurgy, engineering mechanics and thermodynamics as well as some basis of the theories of wear and lubrication. In any study of cutting tool performance many of these factors will have to be considered.

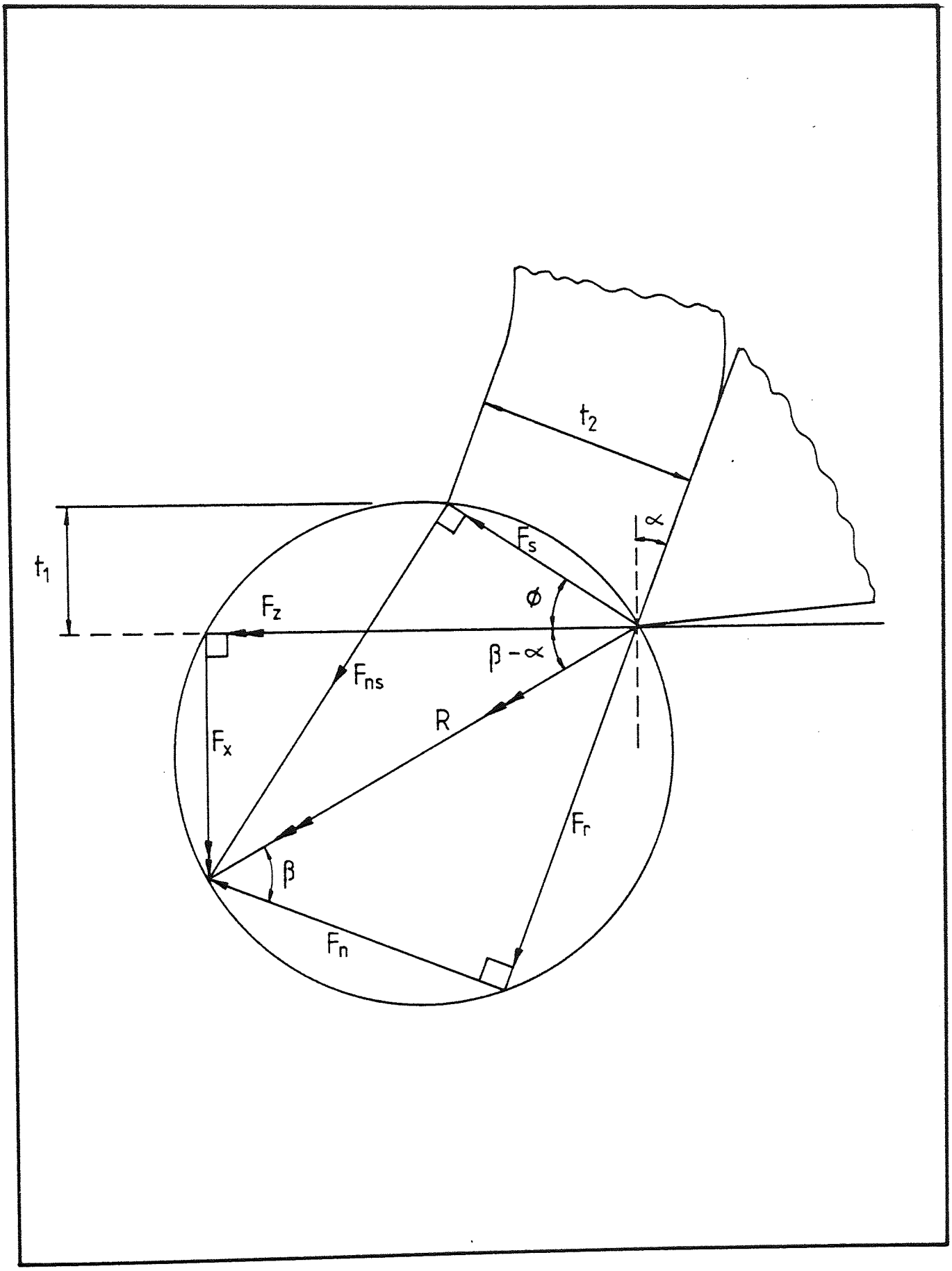

Figure 2.1 System of Forces on Orthogonal Cutting

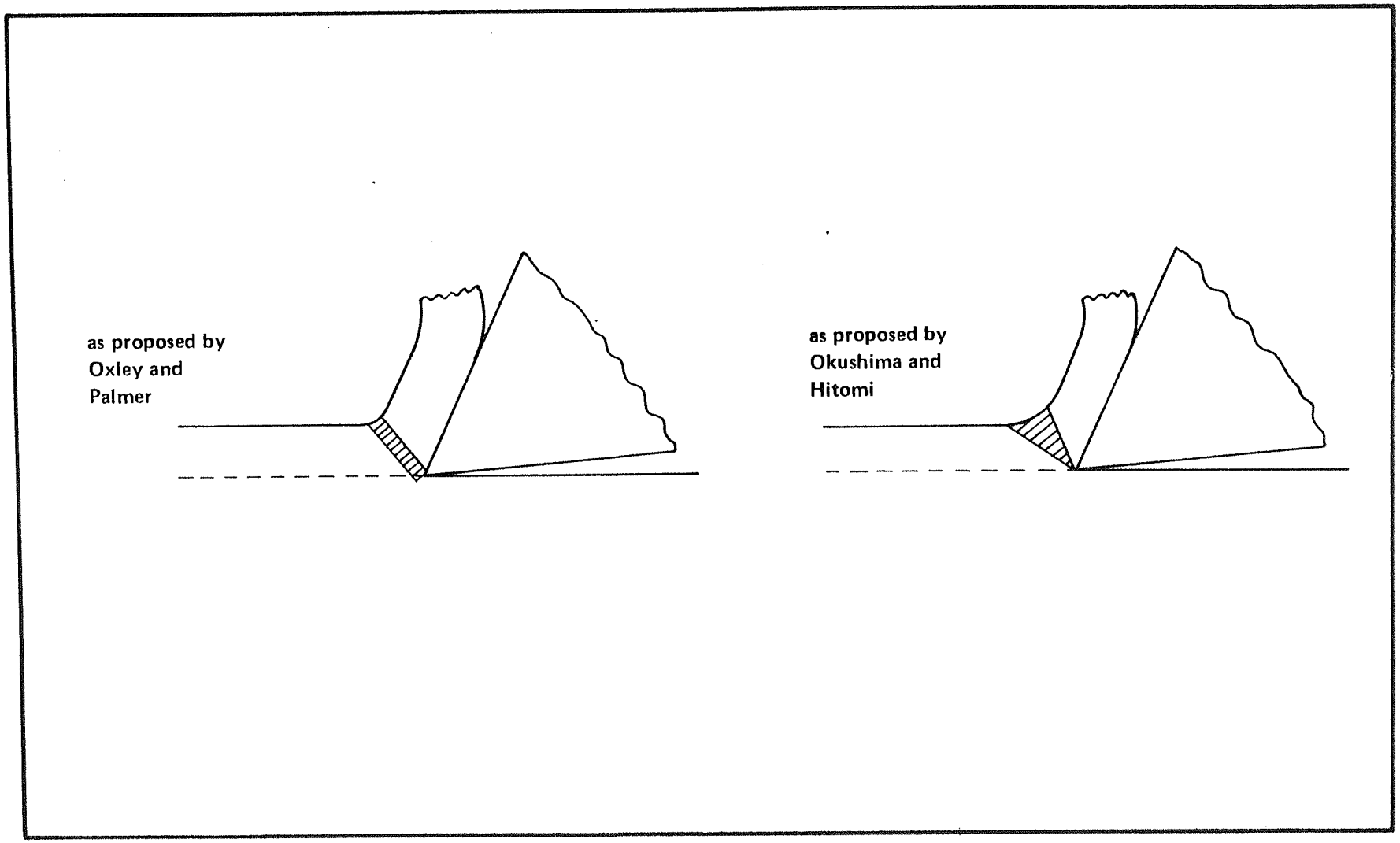

Figure 2.2 Thick Shear Zone Models

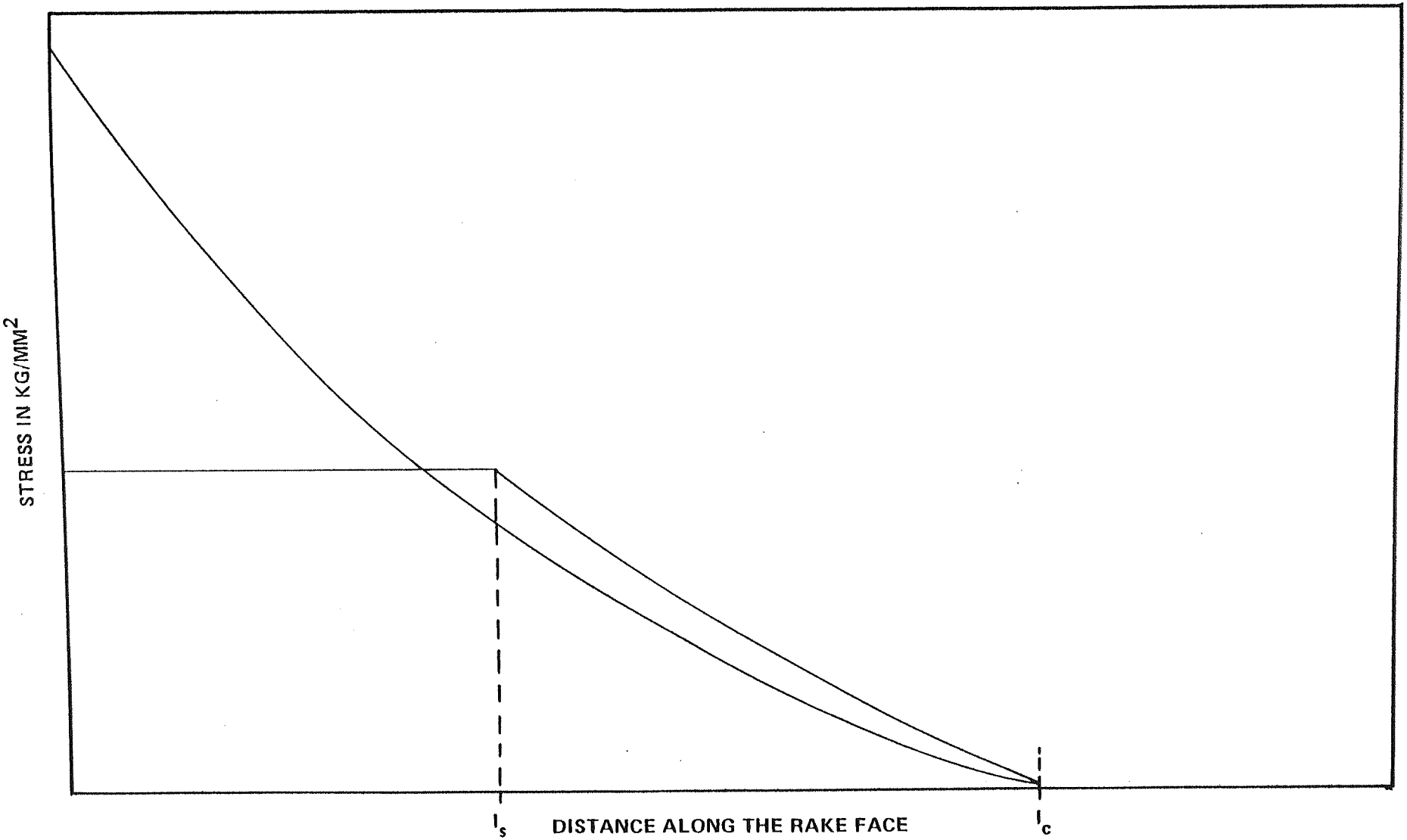

Figure 2.3 The Stress Distribution Proposed by Zorev

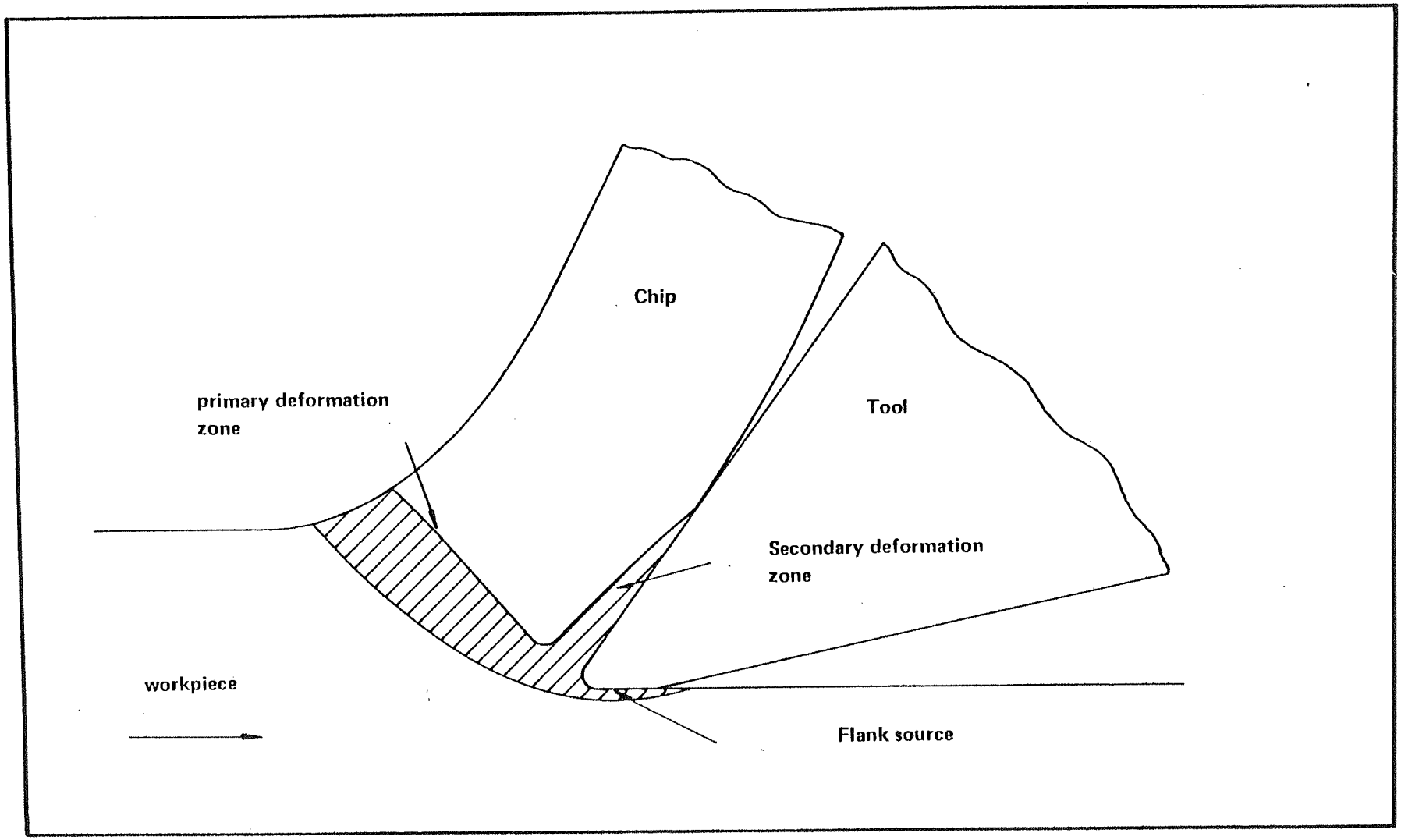

Figure 2.4 Generation of Heat in Orthogonal Cutting

Figure 2.5 Types of Chip Produce during Metal Cutting (After Boothroyd (32))

CHAPTER THREE

FACTORS AFFECTING THE CUTTING PROCESS

3.1 INTRODUCTION

As mentioned in the previous chapter, the cutting process is a complex phenomenon and involves different processes which take place at the same time during machining.

The machining process is subject to variables such as the nature of the cutting tool, the conditions of cutting, the nature of the workpiece material and many other factors. It is the purpose of this Chapter to provide a fundamental understanding of these variables and how they affect the cutting process. Furthermore, a discussion of the types of cutting tool wear, the criteria of tool failure and the methods of measuring tool wear are included.

3.2 MACHINE VARIABLES

Three important factors have been identified

- Cutting speeds
- Feed rates and depth of cut
- Rigidity of the machine tool set-up.

3.2.1 Cutting Speed

The influence of cutting speed on the chip formation process has been reported by many researchers and an early paper relating tool life to cutting speed was published by Taylor in 1907[7]. As mentioned in Chapter 2, Taylor carried out experiments in order to determine optimum tool life in terms of cutting speed. From these investigations, the well-known Taylor tool life / cutting speed equation was developed:

$$V T_1^n = C'$$

Furthermore, the effects of speed on the cutting of a variety of different materials have been reported[34,35], showing the dependence of the tool forces, shear angle, and coefficient of friction on speed. In all cases the cutting forces decrease with increase in speed - especially when cutting at negative rake angles, and the shear angle increases with speed. These observations are attributed to the effect of speed on the friction at the chip-tool

interface, which is related to the temperature distribution and thermal properties of the material.

Generally in metal cutting, increase of speed results in an increase in the temperatures on the tool face.

3.2.2 Feed Rate and Depth of Cut

In combination with tool geometry these variables determine the cross sectional area of the chip and therefore determine the amount of cutting pressure acting on the tool.

The depth of cut is of less significance than feed rate. The cutting pressure creates a torque or force against the workpiece which often limits the amount of chip area. Moreover, some other factors can limit the feed or depth of cut, such as

1. Tool clamping force - the higher the chip area, the more clamping force is needed.

2. Distortion of the workpiece; thin fragile workpieces may be distorted by the use of too heavy a feed or depth of cut.

Therefore, the rigidity of the workpiece may be a limiting factor.

3.2.3 Rigidity of Machine Set-up

It has been pointed out previously[36,37] that for a successful cutting tool application, the machine tool set-up must be sufficiently rigid. This means that spindle bearings should be adequate and well-fitted. All sliding parts need to be adjusted, so that they are free from play. These conditions are absolutely vital, since there is nothing which causes more deterioration to cutting edges than vibration of machine or workpiece.

However, another important prerequisite for successful use of cutting tools is the rigidity of the tool shank and the tool holding device. Even if the machine and the work are rigid, a non-rigid tool shank or a poor tool holder can lead to early tool failure. With a cutting tool lacking toughness and where brittleness characteristics play an important role on its life, the problem of rigidity needs to be carefully considered.

3.3 TOOL VARIABLES

3.3.1 Tool Geometry

The shape and the position of the tool relative to the workpiece have a very important effect on the tool performance, when other conditions remain the same. For this reason, accurate engineering practice in the machine shop requires that tools be carefully designed or selected for the particular job for which they are to be utilized. Only then can the best performance be expected from the tool.

In practice of course there may be economic limits on the available tool geometry. For example, in the manufacture of carbide and ceramic inserts only a limited range of geometries can be made available. It is therefore very important to know what are the critical aspects of the tool geometry so that a satisfactory selection can be made.

Later sections of this work are concerned with Kyon 2000 sialon ceramic cutting tools and because these are produced in the USA the following discussion of cutting tool geometry uses the American standard nomenclature, (see figure 3.1).

3.3.1.1 The Side Rake Angle

The side rake angle is the angle between the ground top face of the tool and the top or bottom plane of the tool. This angle needs to be made as large as possible, since it facilitates the chip flow. It depends largely on the following factors:

- The strength of the cutting tool material being used. The stronger the tool material, the greater the side rake can be.

- The strength and hardness of the material being machined. A small side rake angle is required for hard or high tensile strength materials.

- Heat generation during cutting. Materials that generate high heat require a small side cutting angle.

- The amount of feed per revolution. Smaller side rake angles are used with heavy feeds rather than with light ones.

In order to attain a greater strength at the cutting edge and a better heat dissipation, negative rake angles can be used. These angles place the edge in compression, a condition important for difficult to machine materials. However, the use of high negative rake angles creates vibration problems due to the increase in radial force.

Although positive rake angles require less power and generate less heat during the cutting process, they are not recommended for material which is difficult to machine.

3.3.1.2 The Back Rake Angle

The back rake angle, formerly called the back slope angle, is the angle between the ground top face of the tool and the top plane of the tool. It may be positive, neutral or negative. As is the case with the side rake angle, the back rake angle is important for the cutting process, since it acts in a way similar to the side rake angle. It controls the direction of the chip flow, prevents distortion on long slender workpieces, and protects the finishing point of a tool. Negative back rake angles, like the side rake angles, strengthen the cutting edge and provide a wider area for heat dissipation. The tool material and the workpiece material represent important factors in specifying this angle.

3.3.1.3 The Side Relief Angle

One of the most important requirements for the cutting edge is that it can be moved or fed into the workpiece and cut freely without interference. Therefore, the cutting edge needs to be provided with a certain relief. Specification of the side relief angle depends

on the strength of both the tool material and workpiece being machined. In addition, the hardness of the workpiece plays an important role. A small relief angle may result in contact between the side cutting edge and the workpiece, leading to an increase in the cutting forces and heat generated due to the rubbing action. Moreover, the surface finish of the work may deteriorate.

However, in the case of a large side relief, the side cutting edge may chip as a result of insufficient cutting edge support. To avoid either of these unfavourable developments a compromise value is necessary.

3.3.1.4 The End Relief Angle

The end relief angle is closely associated with the side relief in that both act to preserve the cutting edge and therefore to allow as much work as possible. The end relief angle needs to be as large as possible without causing the end cutting edge to chip or crumble even minutely. Briefly, the amount of the end relief should vary according to the following two factors:

1. The shear and impact strength of the cutting tool material. The greater the shear and impact strength is, the greater the end relief needs to be.
2. The type of material being machined. A small end relief angle is required to machine hard,

strong, or tough materials, while larger angles are better for machining the weaker and softer materials.

3.3.1.5 The Side Cutting Edge Angle

The side cutting edge angle is one of the most important angles on a cutting tool. Increasing this angle yields several significant advantages. Firstly, the conditions at the start of the cut can be improved, because the initial impact force is incident farther back from the cutting edge. This often reduces the chatter and vibration in the machine tool. Secondly, the longer length of contact between the tool and the workpiece and the consequent reductions in both load per unit area and chip thickness, lower the pressure and temperature on the cutting edge. Thirdly, the side cutting edge angle increases the included angle at the finishing point of the tool and thereby strengthens this area. Finally, it positively affects the direction of chip flow.

These advantages are expected to reduce the tool wear rate and, consequently increase the cutting edge tool life. However, the size of this angle does have an influence on chatter. Too great an angle will cause severe chatter and lead to tool breakdown and / or an unacceptable workpiece surface.

3.3.1.6 Nose Radius

It is a well-known fact that the provision of a nose radius on the cutting edge is preferable to a sharp point because of the increased resistance at the point where the side cutting edge and end cutting edge join. Increasing the nose radius produces an increase in the length of the cutting edge in contact, a lower unit chip load and temperature and, hence, an improvement in the tool life and surface finish. However, when turning slender workpieces of insufficient stiffness with any type of tooling having a very large nose radius, chatter may occur resulting in chipping of the cutting edges. Thus, vibration or chatter and the resulting rapid failure of the cutting edge may limit the nose radius value.

3.3.2 Tool Material

The production and economic advantages of utilizing the proper tool material in any machining operation are considerable. A great many companies have not changed their machining conditions over the years, even though cutting tools have greatly improved. Employing conservative cutting speeds and feeds in an industry where billions of pounds are spent annually in cutting chips is a costly matter. Undoubtedly there are also appreciable losses in productivity and higher production costs as a result of the fact that a large portion of the industry does not use the new tool materials made available

in recent years.

Cutting tools are getting better. New and improved materials have replaced or supplemented traditional cemented tungsten carbide and high-speed steel cutting tools over a wide spectrum of metal cutting applications.

Industry is increasingly recognising the importance of maximum metal removal rate, which can form the starting point to understand the relationship between the low cost of the tool versus the large cost of direct labour. However, a wide range of cutting tool materials are available in industry today such as:

1 - High speed steel tools.

2 - Carbon steel tools.

3 - Carbide tools.

4 - Micrograin carbide tools.

5 - Ucon tools.

6 - Ceramic tools.

7 - Cubic boron nitride tools.

8 - Diamond tools.

3.3.3 Requirements of Tool Material

In general, the machining process can be sub-divided into rough, semi-finish and finish. It may be classified as intermittent, continuous, and so on. Such classification produces different modes of chip formation

depending on the workpiece machined and the tool used.

If a specific workpiece needs to be machined, the choice of a suitable cutting tool depends on a great many factors, such as the nature of the cutting operation, the rigidity of the machine tool, the composition and slenderness of the workpiece, the type of coolant used and the cutting conditions (feed, speed, depth of cut). In "Requirements of Tool Material" Loladze[38] reports that the tool must possess two basic qualities, sufficient strength to avoid tool failure, and high wear resistivity for increased accuracy and efficiency of machining. Trent[39] also catalogues the parameters that are needed in the tool material.

An ideal situation can exist when the tool possesses the following properties:-

1 - High hot hardness in order to enable the tool to work at high cutting temperature.
2 - Wear resistivity to all types of wear.
3 - High thermal conductivity and low specific heat.
4 - Low apparent coefficient of friction.
5 - Chemical inertness with the workpiece.
6 - Sufficient toughness to resist impact loading.
7 - Resistance to attack by cutting oils and lubricants.
8 - Resistance to fatigue loading.
9 - Resistance to oxidation.
10 - Economic in costing.

3.4 WORKPIECE VARIABLES

The properties of the work material are important in chip formation and have a large influence on both the nature and the rate of cutting tool wear. Small variations in the microstructure of the work material cause considerable alterations in the cutting characteristics and in the performance of the tool. Concerning the work material variables, three factors are taken into account:

- The chemical composition.
- The mechanical properties.
- The thermal properties.

3.4.1 Chemical Composition

To control the properties of the work material in order to improve the machining operations, the metallurgist can alter the microstructure and the matrix properties of the alloy either by adding free machining additives or by mechanical treatments, such as cold working and heat treatment. Empirical attempts to relate chemical composition to machinability have been made by a number of research workers[40,41,42]. Boulger[40] evaluates the effects of carbon, silicon, phosphorous and sulphur on machinability. He reports a deteriorating effect on machinability as the silicon content of the steel increases. Paliwoda[41] and Schrader[42] give

statistical analyses of the observed machinability for a number of free cutting low carbon steels, which have minor differences in their chemical composition. They relate the percentage of the chemical constituents of the steels to the cutting speed to give a tool life of 60 minutes. Although the analyses show a linear trend, the results are scattered and cannot be explained in terms of chemical composition of the steels alone.

3.4.2 Mechanical Properties

The properties of the work material are important in chip formation. If the material exhibits a high hardness and strength, resistance to plastic flow during machining is high. The combination of high hardness and resistance to plastic flow increases the specific power requirements during machining and the metal removal rates are then limited and relatively low. Tool wear increases due to the repeated contact of the cutting edge with a hard work material, as well as thermal softening and thermally activated wear accompanying high tool chip interface temperatures. Several investigators[43,44] report a correlation between hardness and tool life.

Work material ductility is a further important factor in the machining process. Materials with high ductility permit extensive plastic deformation of the chip during cutting, which increases work, heat generation,

and temperature. Furthermore, high ductility results in longer, "continuous" chips that remain in contact with the tool face, for longer periods, thus causing more frictional heat. Moreover, the work hardening of the material is more important than the initial hardness in determining the power required and heat generated in the cutting zone.

3.4.3 Thermal Properties

It is widely accepted that the thermal properties of the workpiece material have an influence on the chip formation process. The coefficient of thermal expansion, thermal conductivity and specific heat properties play an important role in the local temperature produced in the cutting zone. High thermal conductivity of the workpiece material causes the chip to weld or adhere to the cutting edge of the tool, thus forming the built-up edge which affects the dimensional accuracy of the pieces produced. Low thermal conductivity and specific heat, on the other hand, cause the heat generated to be carried away from the cutting zone through the chip produced, and hence positively affect the tool life. However, the coefficient of thermal expansion can have an unfavourable effect on the dimensional accuracy.

3.5 THE EFFECT OF CUTTING FLUID

Cutting fluids are employed for two main reasons, namely, to cool and to lubricate the cutting zone. This zone comprises the region of the tool cutting edges and the tool-workpiece interface. During a machining operation the cutting tool induces a continuous wave of dislocations, which travel ahead of the cutting edge, deforming and shearing the workpiece metal into continuous or discontinuous chips. The energy required for this deformation is primarily converted into heat. Simultaneously, frictional heat is generated at the point where the tool rubs against the new surface and the chip rubs against the cutting face of the tool. These combined effects raise the tool temperature to a level that might affect its life, since the wear mechanism of the cutting tool is temperature dependent. Consequently, using a cutting fluid for cooling purposes is often effective for improving tool life and the surface finish of the machined parts.

The aim of the lubricating action is to reduce friction between tool and workpiece, i.e. to prevent adhesion by deliberately producing a mild form of corrosion. However, the effects of lubricants in machining are not fully understood yet, as their effects are different from those observed in conventional sliding experiments. This is because the lubricating action may accelerate the total rate of tool wear, if the increase in corrosive wear offsets the decrease in adhesive wear[45].

3.6 TOOL WEAR

3.6.1 Introduction

It is generally accepted that tool wear is of crucial importance in metal machining. It represents a major index of the performance criteria of a cutting tool, since useful tool life is limited by wear. Acceptable surface quality and integrity, dimensional accuracy and, consequently, the overall economics of machining are directly influenced by tool wear. Furthermore, the continued development of new and sophisticated alloys, new cutting tool materials, and N.C machine tools present increasing problems that relate to the performance of tools and in particular to tool wear.

The manner in which a tool wears, the part of the tool that wears most and the practical consequences of tool wear vary both with cutting conditions and with the quality specifications of the part being machined. As a result, the concept of "tool life" can be interpreted differently in different contexts. Similarly, "wear rate" will have different meanings for different people.

3.6.2 Wear Mechanism

Failure in cutting tools is usually brought about by one or a combination of the following wear mechanism:

- Gradual wear
- Brittle fracture
- Plastic deformation.

However, under properly controlled cutting conditions and with a proper selection of tool material, tool geometry etc., a cutting tool usually fails as a result of gradual wear, that is, through progressive loss of tool material caused by mutual interactions between the tool and the workpiece, as well as between the tool and the chips.

3.6.3 Gradual Wear

Current knowledge of the tool wear process indicates several basic types causing the tool to gradually wear away.

These may be listed as follows:

- Abrasive wear.
- Attrition wear.
- Diffusion wear.
- Oxidation wear.

3.6.3.1 Abrasive Wear

Abrasive wear is caused by the hard constituents of workpiece material, such as carbides, oxides and

nitrides. These include fragments of built-up edge which plough into the tool surfaces as they sweep over the tool. The relative hardness of the two bodies in contact, the stresses acting on the sliding surfaces and the cutting media greatly influence the rate of abrasive wear.

Although abrasion may be caused by hard inclusions Trent[46] reports the presence of ridges on worn tool surfaces emanating from wear resistant inclusions. These are in the surface of the tool and force work material to flow around them cutting channels at either side of the ridge and giving rise to a scratched appearance which may be wrongly attributed to abrasion. Trent concedes that abrasion may possibly occur in the machining of a rough casting with trapped sand pockets or alloys which contain aluminium oxide.

Abrasive wear is unlikely to make a significant contribution, under the vast majority of cutting conditions to the wear of carbide based tools as these tools are characterised by their relative hardness. In general, the abrasive action is relatively more severe on the flank because of the nature of the contact.

3.6.3.2 Attrition Wear

Attrition wear is the most dominant type of wear

during machining if nascent surfaces exist and there is a relatively small area of actual tool / work contact. It is particularly evident when cutting at relatively low speeds, where temperature is not sufficiently high for wear based on diffusion to be significant.

During cutting the built-up edge changes continually, with work material being built on the cutting edge and with fragments being sheared away due to cyclic stress fluctuations[47]. If only the outer layers are sheared away, while at the same time the part of the built-up edge adjacent to the tool remains adherent and unchanged, the tool continues to cut for long periods of time without wear. However, the shearing of interfacial weld areas leads to the plucking out of material from the tool. Subsequently, this is carried away by the newly created workpiece surface or the chip. Trent[48] mentioned that fragments are broken away because of localised tensile stresses imposed by the unevenly flowing metal. Moreover, these tensile stresses may act where the strength of the tool constituents are low in relation to the bulk properties of the tool, which then results in an acceleration of wear.

Since the metal flow around the tool edge tends to become more laminar as the cutting speed increases, the rate of wear by attrition may increase as the cutting speed falls. Therefore, to improve tool life where attrition wear is significant, a rigid machine free from

vibration and with adequate clearance angles on the tools should be used.

3.6.3.3 Diffusion Wear

If in metal cutting processes the machining is performed at a high speed and a high feed rate, the cutting temperature increases and a crater is formed on the rake face of the tool. It has been demonstrated[49,50] that at high temperatures, diffusion mass transfer may take place at the interfaces, where the chips slide over the contact surface. This means that in favourable conditions temperature and time, atoms of different elements in the tool material are simultaneously introduced into the work material. However, Opitz and Konig[51] report that the effect of the diffusion is not based on transfer of atoms, but on the formation of new complex carbides, which results in the weakening of the microstructure. They propose a model for diffusion processes, as shown in figure (3.2). In the case of high cutting speeds, an austenitic structure might be found on the underside of the chips, when machining steel. The complete solubility of the components, austenite on the one side and cobalt or nickel on the other, makes it possible to form iron-cobalt or iron-nickel solid solution crystals. Iron diffuses into the cobalt-phase and brings about two reactions which increase the rate of dissolution. In the first place, it may enter into complex carbides. Secondly, it increases the solubility of carbon in cobalt.

This in itself is a required condition for initiating the dissolution process of tungsten monocarbide. Carbon set free in the dissolution process of tungsten carbide diffuses into the steel, as may be seen in figure (3.2). Various investigators would appear to be agreed on important points, as stated in [51].

1. Diffusion of iron into the cobalt phase of the tool.
2. Diffusion of cobalt into forming a continuous solid solution.
3. Dissolution of tungsten carbide and the formation of double carbides.
4. Diffusion of free carbon in the tool in the direction of the workpiece.

Cook[52] on the other hand reports that, as a consequence of diffusion bringing about structural degradation of the tool surface, mechanical removal of the carbide particles subsequently takes place. Trent[53] however, has not found any evidence for the Cook phenomenon.

Summarising, it has been established that, at high temperatures, the wear rate of the cutting tool used at high speed is greatly influenced by the chemical stability of the tool constituents and by the relative affinity of both tool and workpiece material.

3.6.3.4 Oxidation Wear

Generally, a relatively high cutting temperature is generated when cutting is performed at high cutting speeds. Consequently, this may sometimes cause tool oxidation. In addition, if the tool is in contact with the workpiece at high cutting speeds, oxidation of the tool takes place at the periphery of the cutting zone. This happens because the atmospheric oxygen is excluded from the media. It has been reported that a high wear rate, partly caused by oxidation, is often found on the trailing and leading edges of the tool [54].

Moreover, as the oxide film is only loosely adhered to the tool surface it is easily detached and carried away by the chip and workpiece, thus causing abrasion[55].

3.6.4 Fracture

Brittle fracture of the cutting tool has been regarded as one of the most serious problems in practical production. Brittle tool failure involves the development and propagation of micro-cracks in the tool material. Micro-cracks develop at so called dangerous points when the stress state is such that it causes local rupturing of the inter-atomic bonds.

Generally, brittle fracture of the cutting tools is categorized into two types of fracture, namely the

mechanical fracture and the thermal fatigue type of fracture.

Thermal fatigue cracks rarely occur when turning, but are quite common when milling. These cracks are due to the fact that the cutting tool is subjected to the alternation of heating and cooling. As in the case of intermittent cutting action, temperature gradients are introduced into the surface layers[56], producing high tensile stresses which result in parallel cracks appearing in the tool, approximately perpendicular to the cutting edge, but possibly inclined to the direction of the chip flow.

Tools may fail mechanically as a result of chipping (gradual damage of the cutting edge) or of breakage (fracture of a large portion of the tool wedge). The mechanical failure could be explained as follows. The relatively brittle, carbide tools may deform plastically when the conditions of stress and temperature exceed the hot yield strength of the material. Any protrusions or other adverse cutting geometry modification arising from deformation are easily chipped off the tool, which may initiate a process of rapid edge breakdown[57]. Mechanical fracture may be initiated by stress fluctuations which are due to machine tool chatter and workpiece discontinuities or inhomogeneity. Chipping and fracture can also result from poor handling and lack of care in the setting up. Poorly designed tool holders can have

the same effect, if they fail to provide sufficient backing up support for the tool, thus allowing it to move or to be subjected to bending moments.

3.6.5 Plastic Deformation

This form of wear or damage was first reported in 1907 in a comprehensive paper on metal cutting by Taylor[7]. He states that "according to the part which heat has played in producing wear, worn out tools may be properly divided into 3 classes: wear of 1st class - Tools in which heat..... has been so slight as to have no softening effect upon the surface of the tool"..... "wear of 3rd class - Tools in which the heat has been so great as to soften the tip surface of the tool beneath the chips almost at once, after starting the cut, and in which.....heat has played the principal part in the wear of the tool."

Since Taylor's work, other studies[58,59] have focussed on the deformation of the cutting tool, as it takes place under high stresses and temperatures when cutting is performed at high speeds and feeds. The result of these investigations can be summarized as follows:

1. Failure due to deformation is more probable at a high feed rate.
2. The plastic deformation mode of failure is more significant when cutting materials are of high hardness.

3. Carbide grades with low cobalt contents can be used at high speed and feed rates because of their increased resistance to deformation.
4. Maximum deformation occurs predominantly at the nose of the cutting edge.
5. Deformation on the tool can be observed as a bulge on the flank and rake faces.
6. Fine grain alloys are considered to have greater resistance to plastic deformation.

3.6.6 Tool Wear Patterns

The patterns of cutting tool wear vary, depending on a great number of factors involved in the machining processes. These include tool material, work material, tool geometry etc. According to Venkatesh and Colding[60] the general forms of tool wear for different tool materials (such as carbide tool, high speed steel tool and ceramic tool) which may be produced gradually during metal cutting processes are shown in figure (3.3).

Six basic forms of wear can be established:

1. Flank wear (wear land)
2. Crater wear
3. Primary groove (outer diameter groove or wear notch)
4. Secondary groove (oxidation wear)
5. Outer chip notch
6. Inner chip notch.

Most of the research in this field has taken the flank wear and the crater wear as a criteria for tools failure, although the other forms of wear are known to have an influence on the tool failure as well.

3.6.7 Tool Life Criteria

Tool failure is said to occur if the tool no longer performs the desired function. In practice, there exists a wide range of cutting conditions; and therefore, this makes it essential for tool life tests to specify the end point of the tool. To avoid catastrophic tool failure and according to ISO recommendations, the cutting tool failure criteria may be specified according to the tool material, see figure (3.4).

For flank wear; sintered carbide and ceramic tools are either

1) $V_B = 0.3$ mm

or

2) $V_{Bmax} = 0.8$ mm, namely if the flank is irregularly worn, scratched, chipped badly grooved in zone B)

For high speed steel tools the following applies;

1) $V_{Bmax} = 0.8$ mm

As far as crater wear is concerned it appears that the

following equation is acceptable:

$$KT = 0.06 + 0.3f$$

3.6.8 Methods of Measuring Tool Wear

It is generally recognized that tool wear represents one of the most vital problems in metal cutting. This has led many investigators to try to find a way to evaluate tool life.

Micheletti et al[61] 1976 provide a comprehensive survey which presents different methods of assessing the cutting tool. Only an outline is offered here, as it is not intended to give full details of each method. Tool wear sensing set-up can be based on two general types of approach:

1) Direct measurement;

With this type of measurement the device evaluates the volumetric loss from the tool due to the tool wear. Different ways can be used with direct measurement, such as:

a. Optical (light reflection, fibre optics, T.V. camera) sensors.
b. Electrical resistance sensors.
c. Radioactive sensors.
d. Pneumatic sensors.

2) Indirect measurement;

In the second case, equations are established to describe the correlations between tool wear and other parameters which are easier to measure. The measuring parameter can be:

a. The cutting force and / or torque.

b. The vibrations and sonic analysis (noise)

c. The roughness of machined surfaces.

d. The workpiece dimension change.

e. The distance between tool post and the workpiece.

f. Temperature and thermoelectric effects.

g. The energy input to the system.

The general requirements for a tool wear sensing set-up can be summarized as follows:

1. The produced signal which describes the trend of a parameter, needs to correlate linearly with tool wear.
2. The signal needs to have a short time delay of sensing.
3. The measuring set-up must be capable of providing a reliable tool wear trend.
4. The measuring set-up must be easy to operate, require little adjustment and be adaptable to the production floor.
5. The cost of equipment must be reliable.

3.7 CHAPTER CLOSURE

In this chapter the factors affecting the chip formation process were analysed. Tool wear processes and the criteria of tool failure were discussed and methods of determining such criteria were reviewed.

1 Side rake angle
2 Back rake angle
3 Side relief angle
4 End relief angle
5 Side cutting angle
6 Nose radius
7 End cutting angle

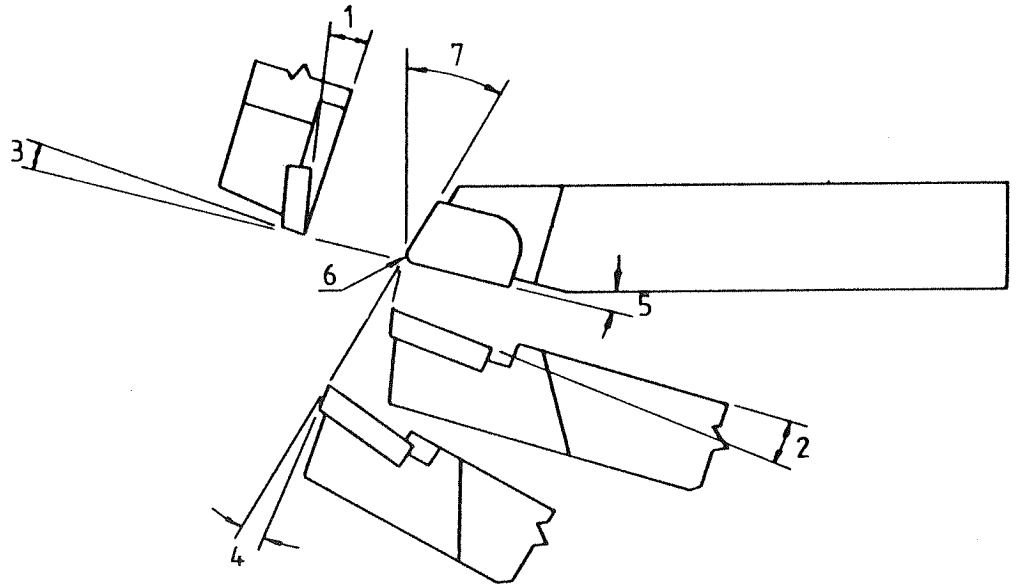

Figure 3.1 A.S.M.E Tool Nomenclature

Figure 3.2 Simplified Model of the Diffusion Processes

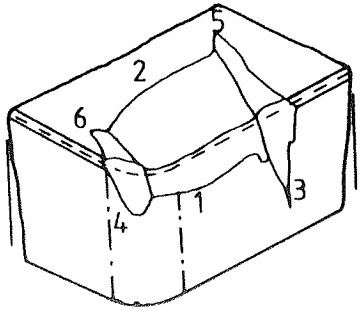

(b) Wear forms on H S S tool

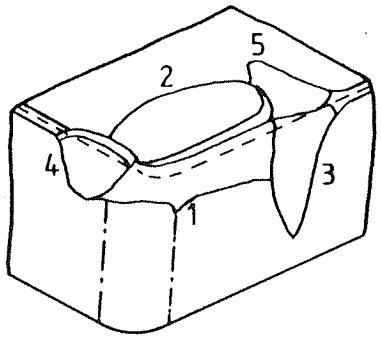

(a) Type of wear forms on carbide tool

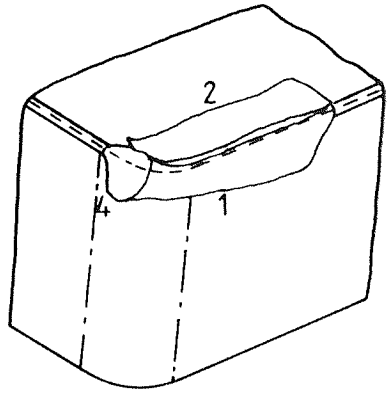

(c) Oxide ceramic tool wear forms

1 Flank wear (wear land)
2 Crater wear
3 Primary groove (outer diamter groove or wear notch)
4 Secondary groove (oxidation wear)
5 Outer chip notch
6 Inner chip notch

Figure 3.3 Wear Forms on Cutting Tools

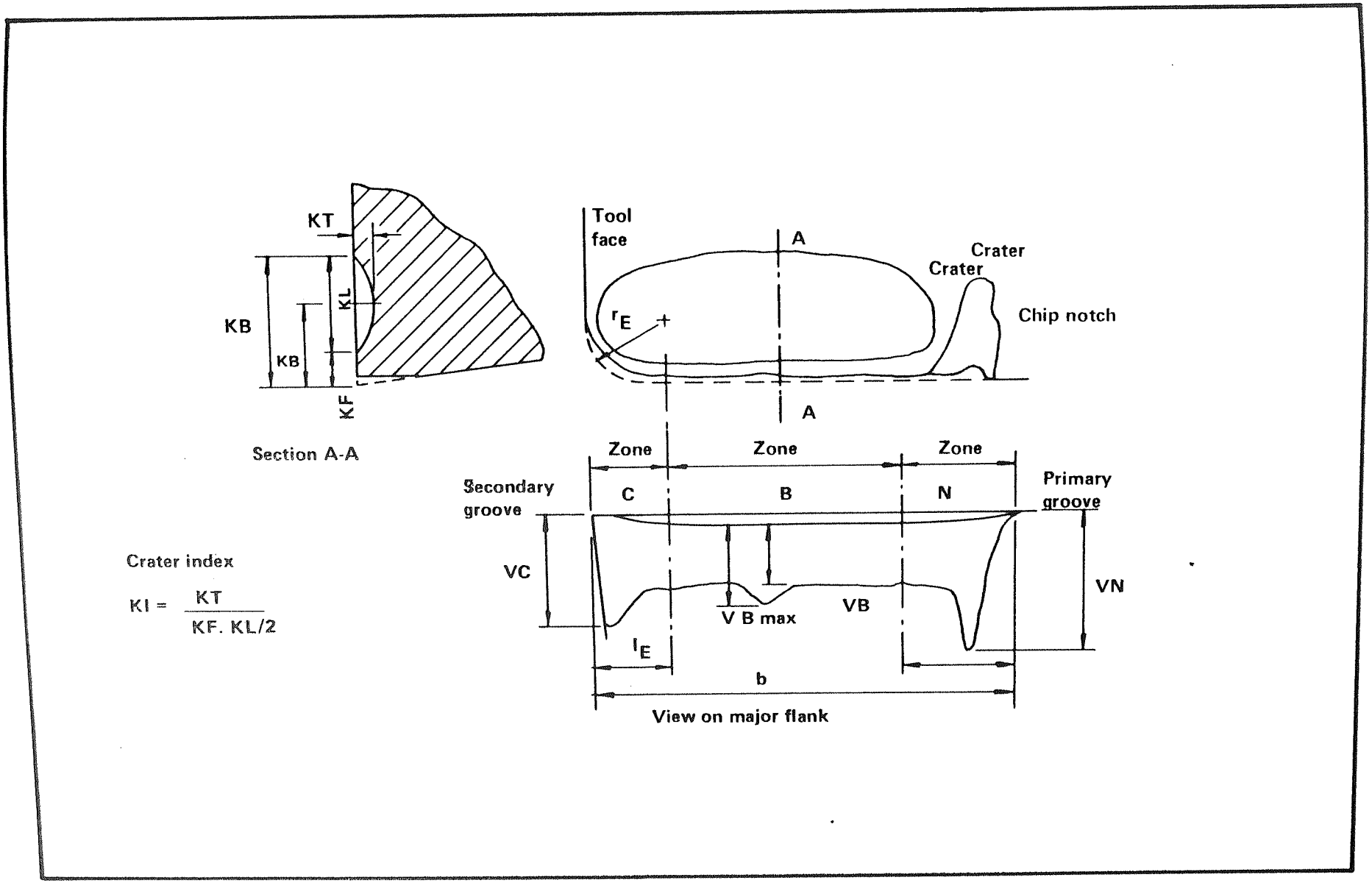

Figure 3.4 Criteria based on features of tool wear

CHAPTER FOUR

PROPERTIES OF SIALON CERAMIC MATERIALS

4.1 INTRODUCTION

With the development of more efficient and more rigid machine tools, the demand for a tool material which can cut at high speeds and feed rates have been increased. No single tool material provides the complete answer to all machining operations but there is no doubt that for certain cases high hot hardness, chemical inertness and reasonable impact strength will be of considerable advantage.

Ceramic tool materials would seem to be the best choice for high speed machining because of their ability to retain their physical and chemical properties at elevated temperatures. However, these tools have not been entirely successful in industry partly due to their brittleness and partly because of a lack of sufficiently rigid machine tools.

In searching for an improved solution to high speed machining, silicon-nitride has been forwarded as the engineering material of the future. The material has a very good combination of high strength, wear resistance and thermal shock. However, the production route makes it relatively expensive and the end product is limited to fairly simple shapes. As a consequence of development of silicon nitride Lucas Industries have produced a material called Syalon and it is claimed to be very efficient in the metal cutting field[62].

The object of this chapter is to discuss the properties and previous work carried out on this material since it is used as the cutting tool material for this research project.

4.2 MATERIAL SYNTHESIS

Sialons are synthesized[62] by reacting together silicon nitride, aluminium nitride, alumina and yttria oxide. The powder charges for sintering are prepared by milling weighed quantities of the basic constituents mentioned above. Depending upon the relative proportions of these constituents the final product can range from one having a glassy intergranular phase to one having such a phase that is crystalline, with resultant variations in the final mechanical and thermal properties. These properties can, therefore, be varied to suit the particular product concerned by adequate consultation at the design stage. Using isopropyl alcohol as the matrix, the particle size during the milling stage needs to be less than 5 μm in order to ensure homogeneity of the composition. The resultant powders are dried and sieved before compacting. The material is preformed by cold-isostatic pressing in rubber envelopes at a pressure of 140 MN/m^2 or by slip casting.

The preforms are enclosed in a bed of boron nitride within a graphite container fitted into the susceptor of an induction furnace. The sintering cycle consists of a one-hour period at up to a maximum of 1800°C, at which isothermal sintering can occur for one hour before the furnace is switched off and allowed to cool. The resulting product of the above process is a single phase material having a silicon-nitride crystal structure with a slightly

enlarged unit-cell. It has the same crystal structure and physical properties as those of β silicon-nitride, but because of its composition the chemical properties are more like those of alumina.

Most of the development work has been carried out on the so-called 'glassy' sialon materials, where the glassy-grain-boundary phase is evident. However, research has resulted in crystalline-grain-boundary phase as well. With these materials the crystalline-grain-boundary phase is the controlling factor so far as high-temperature properties are concerned. Despite a fairly large change in dimensions with both of these material types during their formation by sintering, allowance can be made to enable the production of accurate final products.

4.3 MATERIAL PROPERTIES

4.3.1 Modulus of Rupture

Measurement of modulus of rupture of sialon ceramic has been carried out as reported by Katz[63] and Lumby et al[64]. Test pieces were prepared from sintered samples by lapping all the faces and the edges with diamond paste on a cast iron lap. At room temperature testing has been performed in three point bending with a span of 1.9 cm and a cross head speed of 0.05 cm/minute. For the high temperature measurements similar test bars, geometry and cross head speed were used. The values quoted for room temperature are the average of sixteen breaks whilst at the high temperatures values are an average of two breaks.

The results of these tests were compared with other high-temperature ceramics such as hot pressed silicon nitride, hot pressed silicon carbide and Refel silicon carbide. The sintered sialon 1 material as is seen in figure (4.1) shows a much higher level of strength retention between 1000 and 1400^{o}C without the substantial decrease experienced by Refel silicon carbide at 1400^{o}C. Since then, a glassy-grain-boundary form of sintered sialon ceramic has been developed, termed Sialon 3 in figure (4.1), giving a room-temperature modulus of rupture of 828 MN/m^{2}.

4.3.2 Creep Resistance

Measurements have been performed to assess the ability of sialon ceramic to resist creep[64]. Figure (4.2) shows the strain / time relationship for five different materials produced at just over 1200°C and 77 MN/m^2. A comparison of performance of sintered sialon with that of hot pressed silicon nitride, hot pressed silicon carbide, reaction bonded silicon nitride and Refel silicon carbide reveals that the creep resistance of sintered sialon is bettered only by hot pressed silicon carbide.

4.3.3 Thermal Diffusivity

Figure (4.3) shows the thermal diffusivity-temperature relationship of sintered sialon compared with that of other high temperature ceramic materials[64,65].

The graph plots thermal diffusivity against temperature for a number of different sialon ceramics. These different materials have varying composition and porosity and it is clear that thermal diffusivity is a function of both composition and porosity. Reducing the porosity is expected to yield higher levels of thermal diffusivity especially at lower levels of aluminium and oxygen content.

4.3.4 Oxidation Resistance

Tests on hot pressed silicon nitride show that this material is not immune from oxidation[64]. A weight gain of 300 to 800 mg/m^2 on heating at 1400°C for 70 hours has been found. When sintered sialon was tested for oxidation resistance at 1000°C for 100 hours, results show virtually no weight gain, a mere 0.1 to 0.2 mg/m^2 at 1227°C but a somewhat higher figure of 2 to 5 mg/m^2 at 1380°C. Research to further increase the already high resistance to oxidation is still continuing.

4.3.5 Thermal Shock Resistance

Thermal shock resistance of sintered sialon ceramic material has been assessed on the basis of measuring the modulus of rupture at a given thermal shock. Thermal shocks of increasing severity are applied until at a particular temperature a significant reduction in the room temperature modulus has been obtained[62].

4.3.6 Fracture Toughness

Fracture toughness of sintered sialon has been measured[62]. The results show a mean critical stress-intensity factor of 6.0 $MN/m^{3/2}$ and comparing this result with the values for hot pressed silicon nitride and hot pressed sialon shows a large similarity. A rapid increase in critical stress-intensity factors has

resulted with hot pressed sialon ceramic when temperature is increased to 1100°C, see figure (4.4). However, recent tests on sintered sialon indicates that there is no increase in the above factor up to a temperature of 1300°C.

The rapid increase in critical stress-intensity factors reveals that a viscous deformation of the grain boundary layer has taken place. The higher temperature at which this occurs with the sintered material is a reflection of its higher creep resistance at elevated temperatures.

4.3.7 Thermal Conductivity

Results of measurements of thermal conductivity of sialon ceramic have been reported by Rama et al[66]. Figure (4.5) shows a thermal conductivity / temperature relationship for four sialon ceramics differing only in their number of substituted atoms of aluminium and oxygen. Results show that thermal conductivity decreases with increasing concentration of aluminium-oxide, with a larger effect at lower temperatures. At 1000°C the values for all four samples are very similar.

4.3.8 Electrical Properties

The a c electrical conductivity of sialon ceramic material is shown in figure (4.6) as a function of temperature at different frequencies[66]. The lack of

thermal hysteresis indicates that no compositional changes occurred during the measurements. At high temperatures, the conductivities are almost entirely independent of frequency, whereas below approximately 700^{o}C there is a relatively large dispersion of the conductivity with frequency, with a concomitant lessening of the temperature dependence.

4.4 PREVIOUS ASSESSMENT OF SIALON AS A CUTTING TOOL INSERT

Sialon ceramics offer an attractive combination of properties which are not available in other materials and can be modified to suit the particular needs of the user. Such flexibility in composition is not available in other high performance ceramics and enables considerable performance advantage to be gained with significant cost savings.

A number of authors have reported results in which they compare silicon ceramics with other cutting tool materials and a range of workpiece materials have been used.

4.4.1 Machining Cast Iron

Results reported from the USA indicated that sialon has superior performance to standard ceramics at speeds up to 600 m/min[67]. Similar data was given by Lumby et al[64] and by Cother and Hodgson[68]. Bhattacharya[69] obtained 10 to 15 times longer tool life with sialon when compared to coated carbide or Al_2O_3 based ceramics for machining an automotive cast iron. Machining trials on grade 14 heavy duty cast iron gave a 14X increase in tool life compared with coated carbide. Bhattacharya[69] also claimed that sialon could be used for the intermittent cutting of cast iron.

The commercial sialon ceramic, Kyon 2000 has been used by Kennametal to machine cast iron. Results are shown in figure (4.7) which includes comparisons with aluminium oxide coated carbides and hot pressed composite ceramics. As shown in figure (4.7) the inability of hot pressed composites to withstand high feed rates limits their effectiveness. On the other hand it is the cutting speed which limits the effectiveness of coated carbides. Kennametal claim that Kyon 2000 has a mixture of the best points of each of their competitors and so represents a good choice.

4.4.2 Machining Steels

Lumby[64] claimed that sialon could be used successfully to machine mild, medium carbon and high carbon steel. In particular it was reported that EN31 in the hardened condition (60 Rc) could be machined in conditions where carbide and coated carbide failed at the moment of contact between the tool and the workpiece.

Bhattacharya[69] machined a medium carbon steel, EN9 and compared results with coated carbide. Under similar conditions the coated carbide tool life of 8-15 minutes was increased to 25 minutes for sialon.

4.4.3 Nickel Based Alloys

The aerospace and related industries are making increasing use of nickel based alloys and they are notoriously difficult to machine. It is not surprising therefore that tests have been carried out in this area.

Figure (4.8) presents data published by Kennametal on the use of Kyon 2000 for machining nickel alloys. Kennametal argue that the hardness, abrasiveness and toughness of these alloys makes them very difficult to cut and with conventional tests the tool life is always unpredictable and frequently short. Comparative tool life curves for machining Inconel 718 show substantial advantages for Kyon 2000 compared with a hot pressed composite ceramic. To avoid work hardening of the work material Kennametal recommend a minimum feed rate of 0.2 mm/rev.

Bhattacharya[69] has also done test work in this area but in his case Inconel 901 was used and comparisons were made with coated carbides and Al_2O_3 ceramics. Once again sialon proved superior giving both longer and more reliable tool lives.

4.5 CHAPTER CLOSURE

For certain workpiece material groups i.e. cast irons, steels and nickel based alloys, there is good evidence to suggest that sialon ceramic inserts have significant advantages. Kennametal, the commercial company who market the sialon ceramic, Kyon 2000, claim the same advantages for their product.

However, apart from a generally held belief that sialon has hybrid properties, combining the best features of coated carbides and hot pressed composite ceramics, there is little data available on the performance of such tools. The principal objective of this report is to study the performance of sialon ceramics to determine their wear characteristics and optimum geometry for certain applications. Kyon 2000 inserts are used because of their availability and because they are the only commercial product being used.

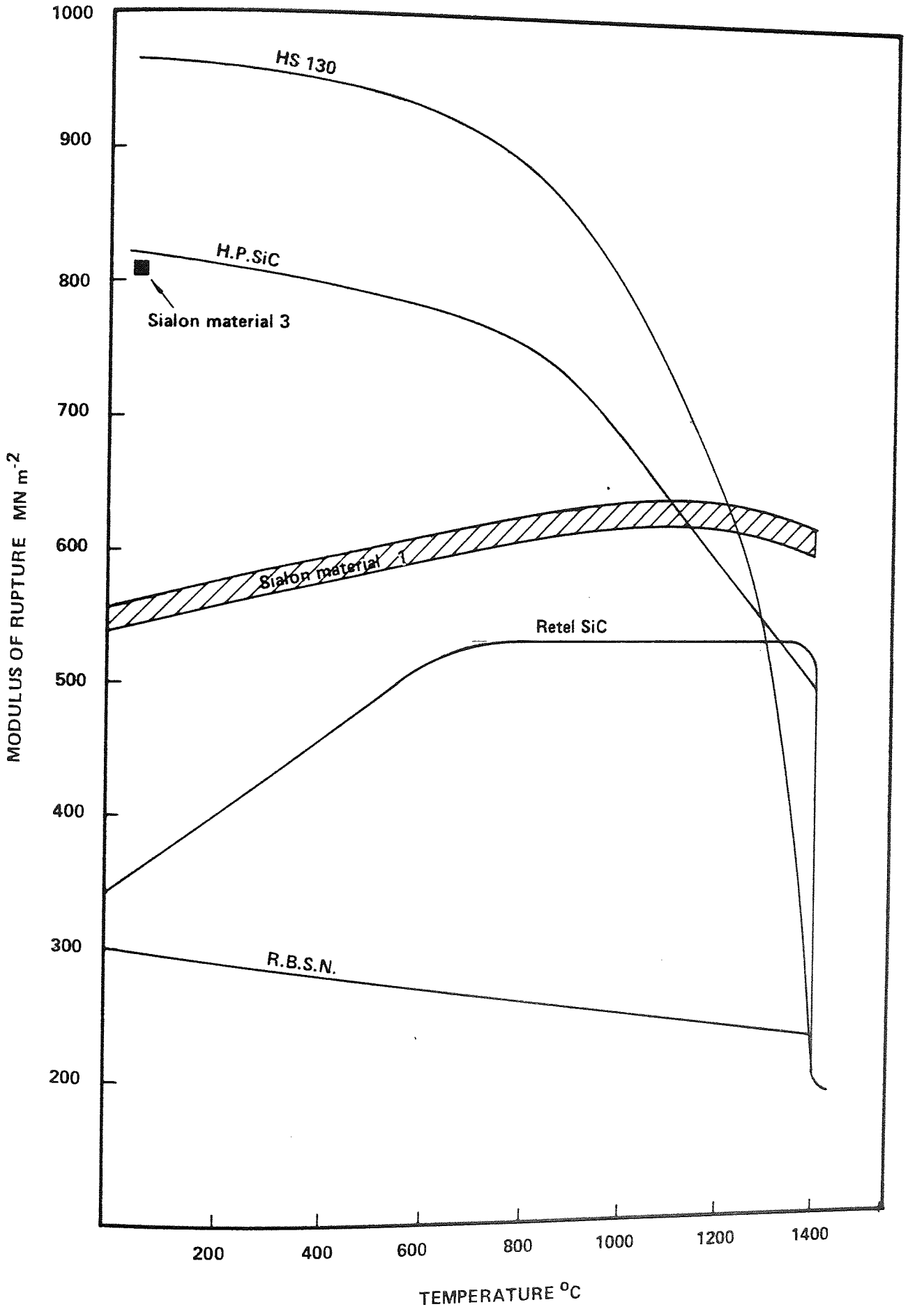

Figure 4.1 Variation of Modules of Rupture with Temperature

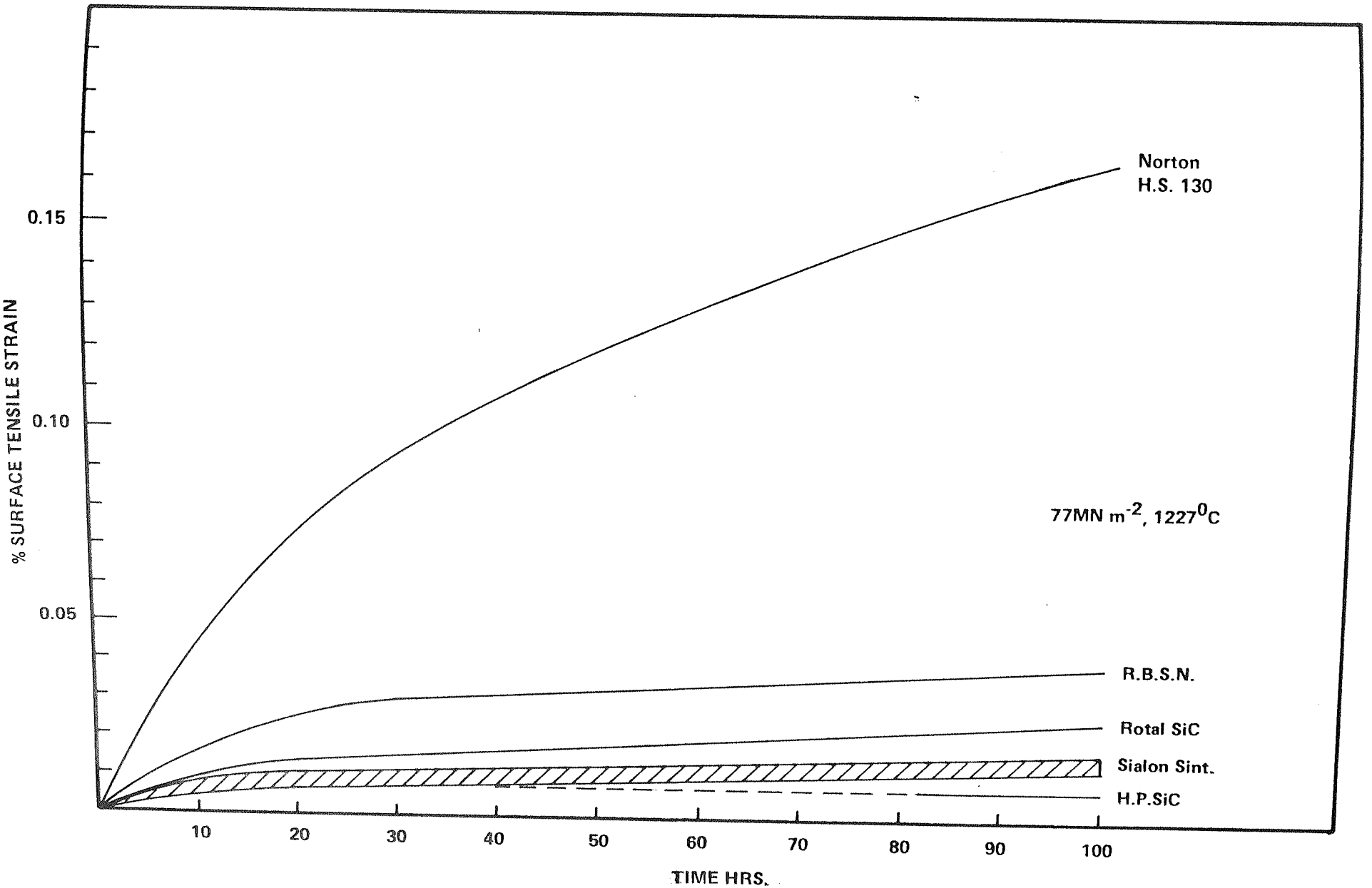

Figure 4.2 Creep at 1227^{o}C – 77 MNm^{-2}

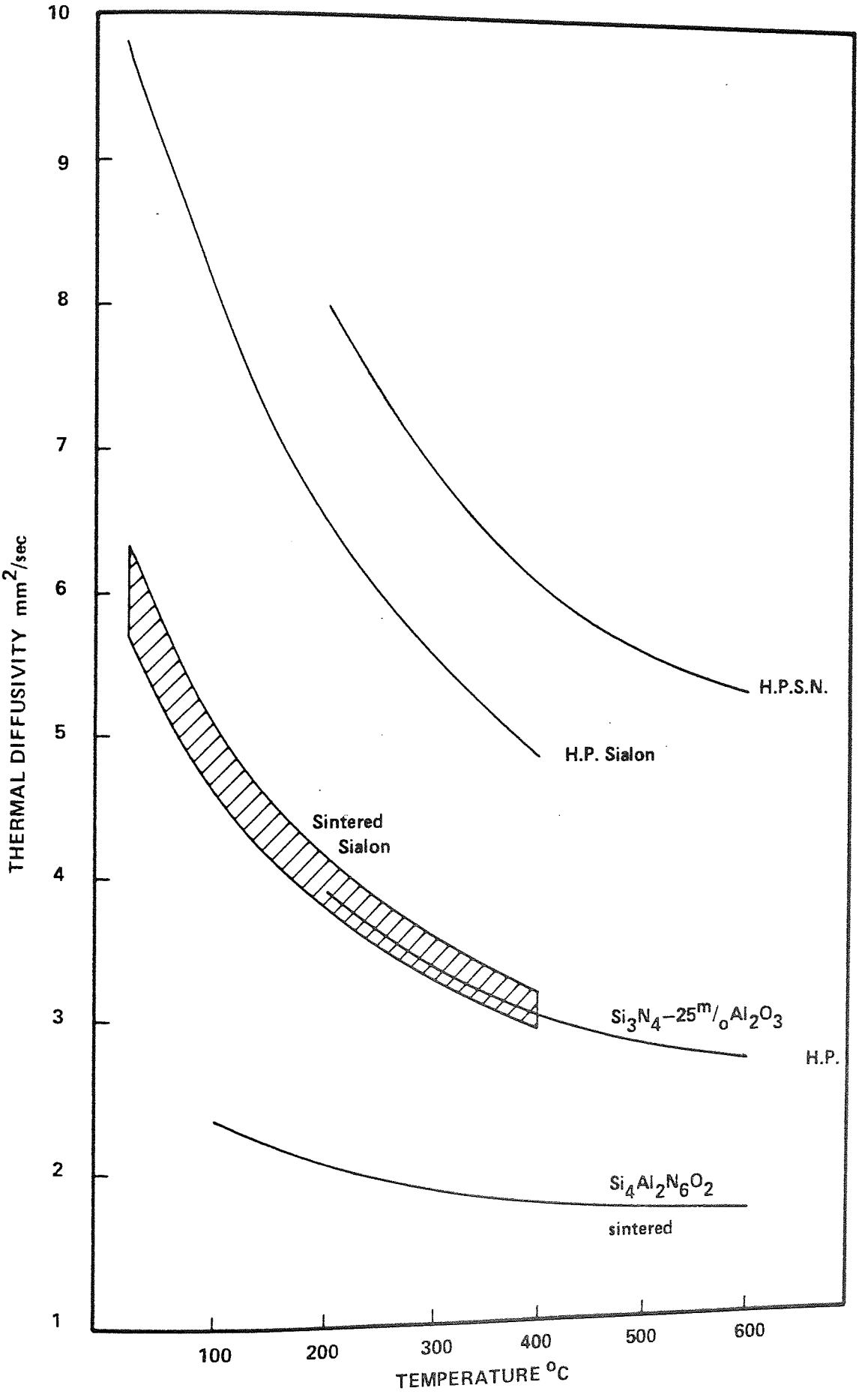

Figure 4.3 Variation of Thermal Diffusivity with Temperature

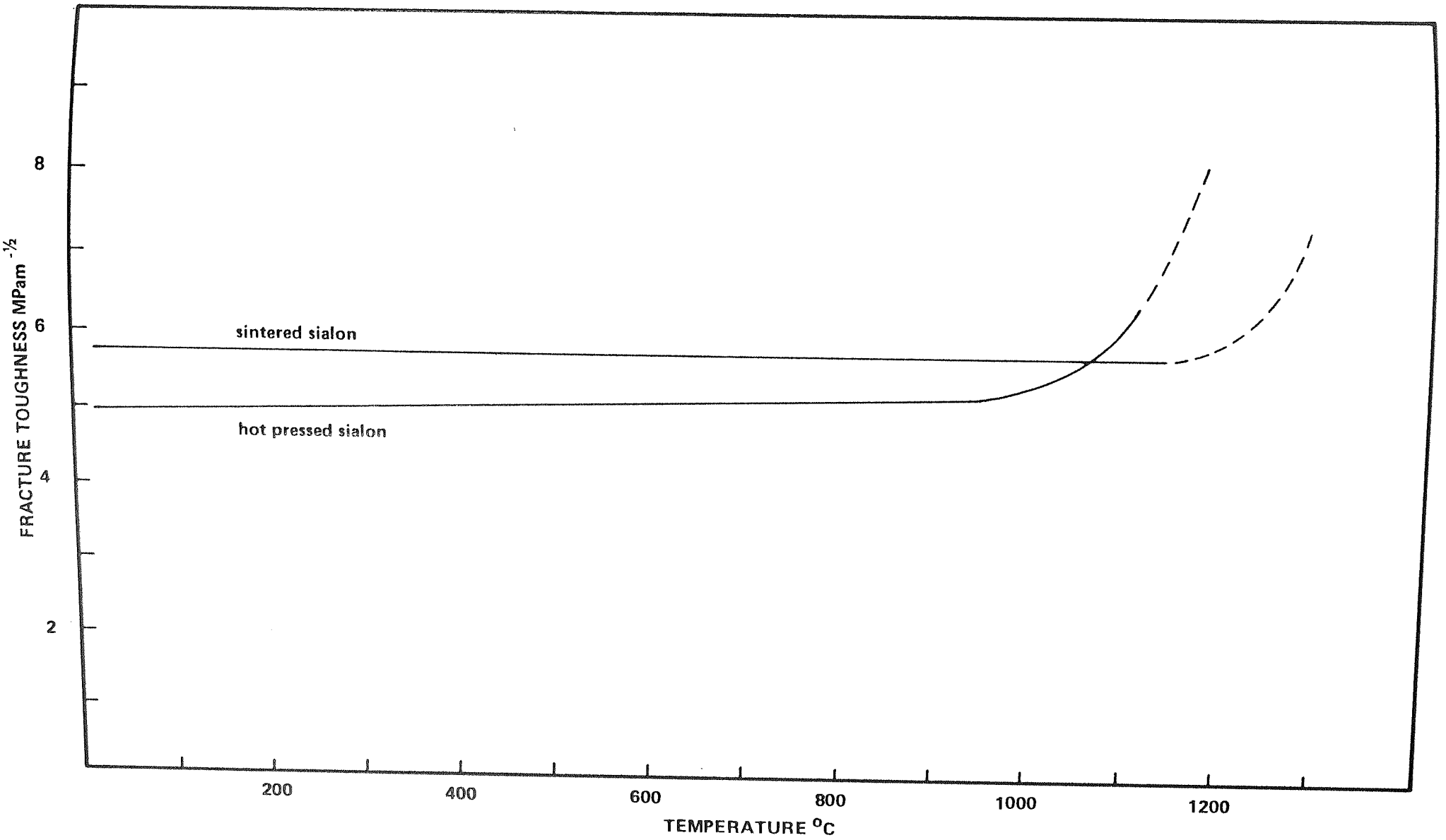

Figure 4.4 Variation of Fracture Toughness with Temperature

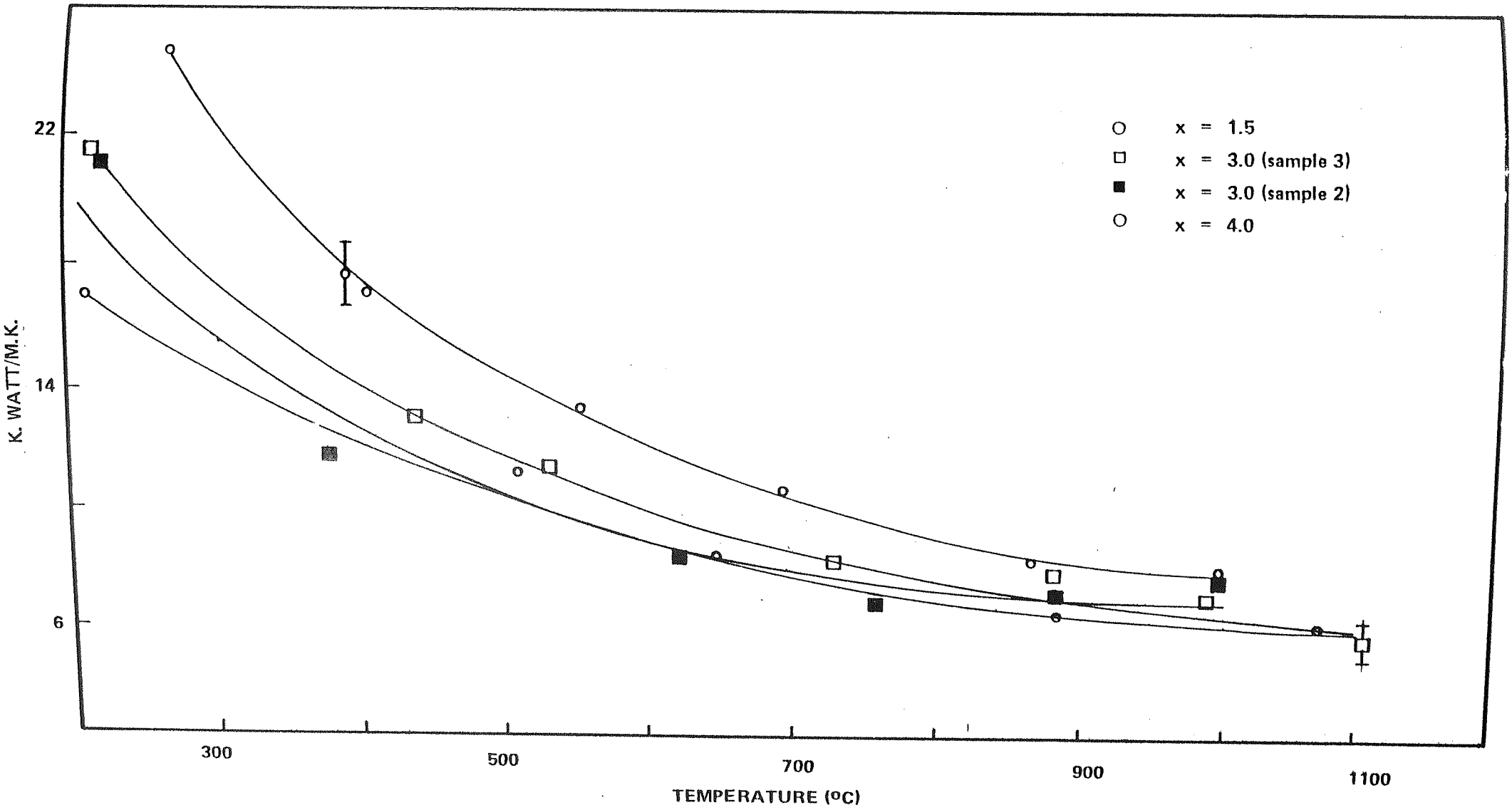

Figure 4.5 Thermal Conductivity of Sialon Ceramics

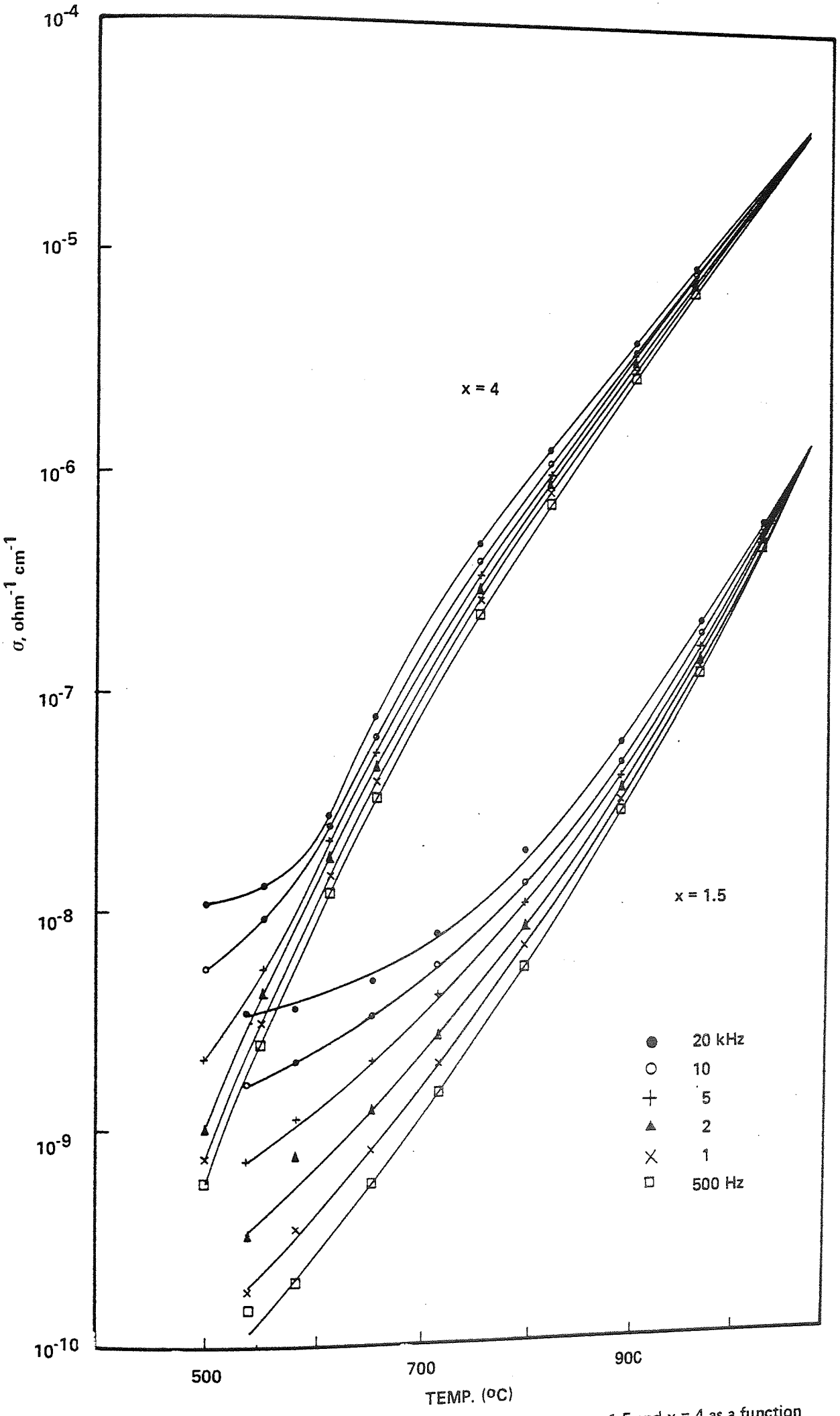

Figure 4.6 AC Electrical Conductivity of Compositions with x = 1.5 and x = 4 as a function of temperature and frequency

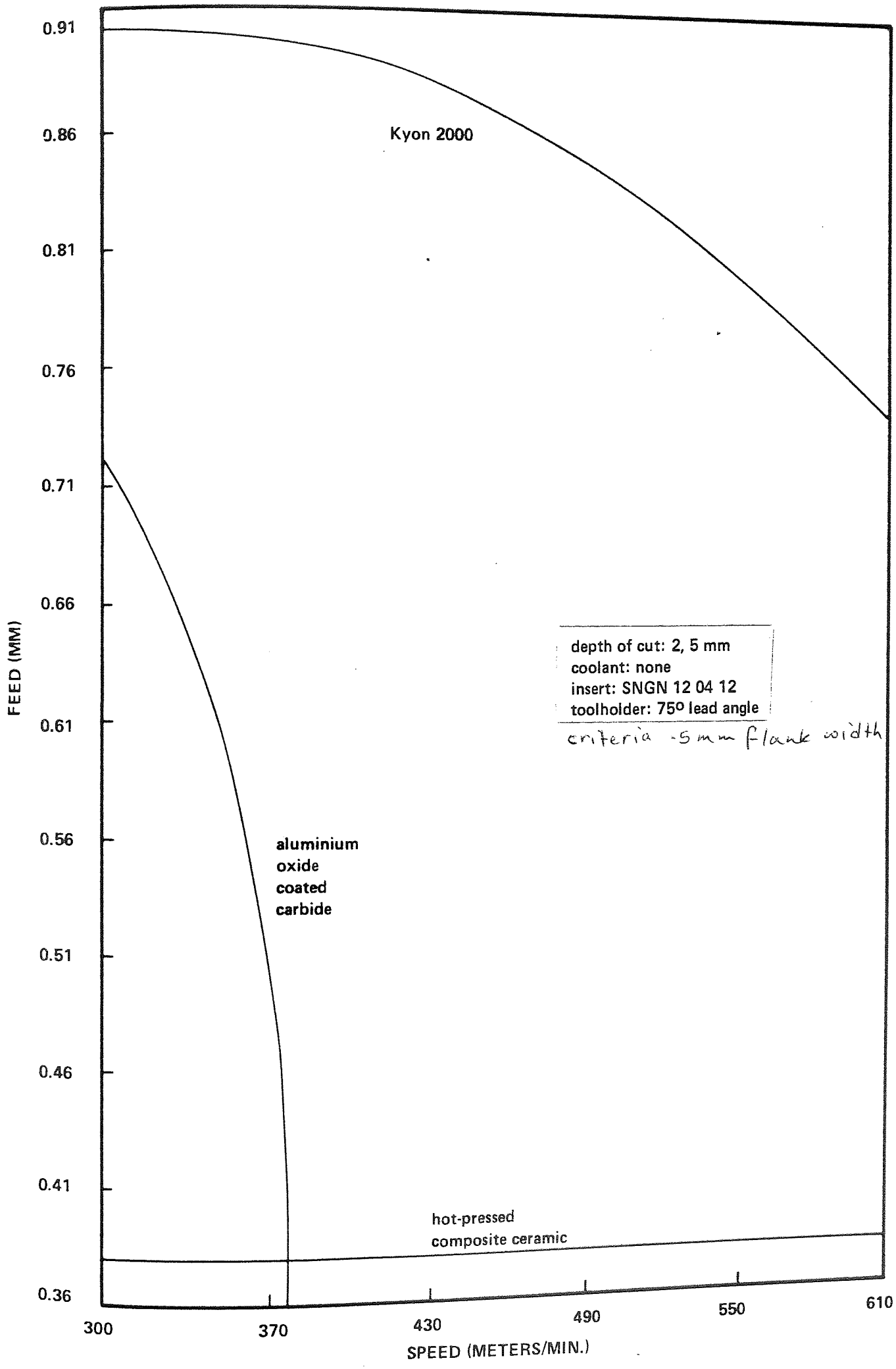

Figure 4.7 Comparative Tool Life Curves (Cast Iron)

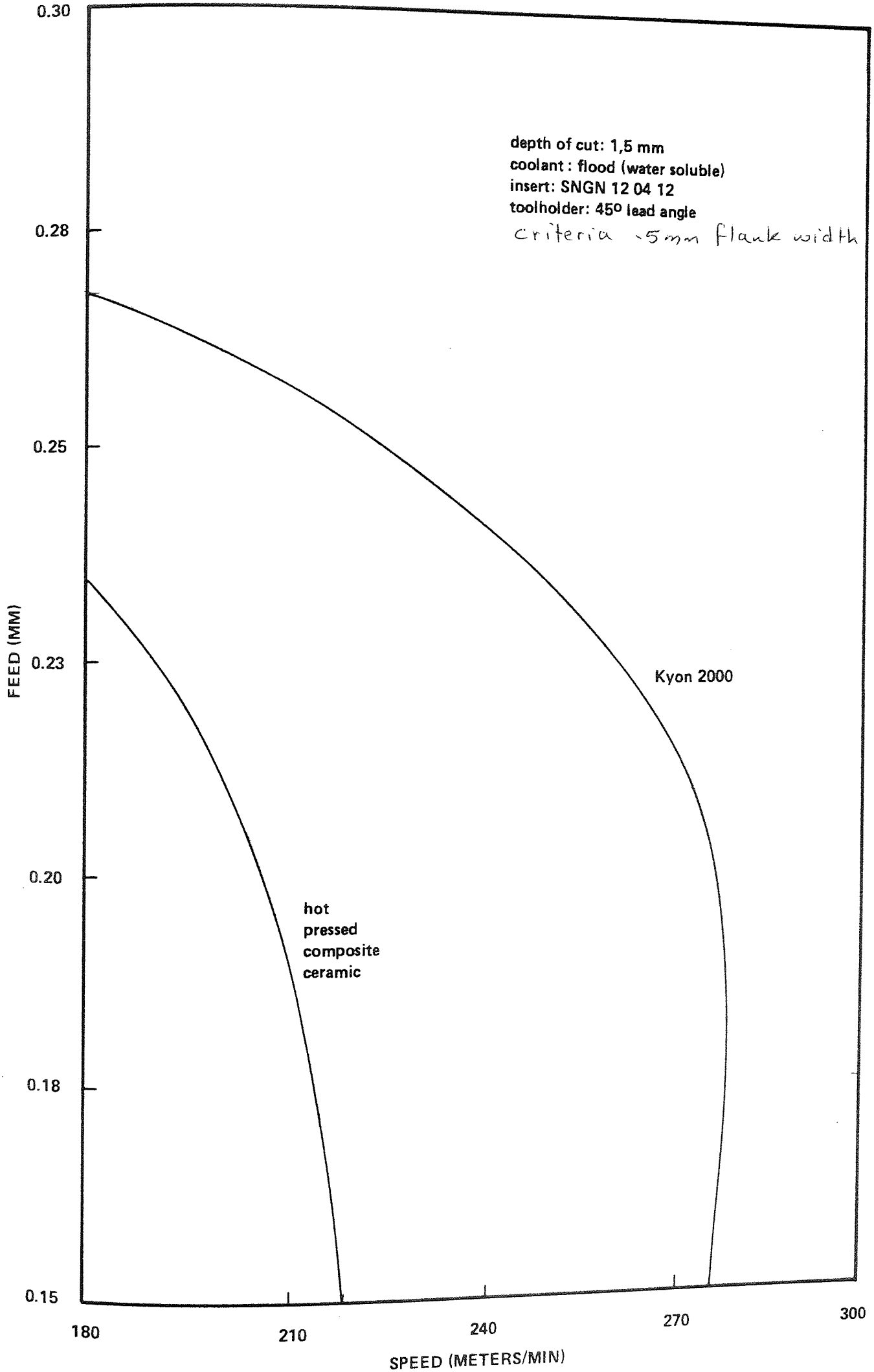

Figure 4.8 Comparative Tool Life Curves (Inconel 718)

CHAPTER FIVE

EXPERIMENTAL EQUIPMENT AND PROCEDURES

5.1 INTRODUCTION

It is seen from Chapter 4 that Kyon 2000 ceramic cutting tools appear to be capable of achieving a significant improvement in cutting performance when compared with other tool materials. An experimental programme was developed to conduct cutting tests in order to study the performance of this new generation of ceramic cutting tools.

The aim of this chapter is to present a description of the test equipment and experimental procedure used.

5.2 TEST MACHINE (THE LATHE)

The machine used for all the experimental work was a SWIFT 12/18 inches swing lathe. The lathe was fitted with a 10/30 horse-power motor having infinitely variable spindle speeds from 8 rpm to 2100 rpm.

A tachometer was used for the checking of spindle speeds. Nine feed rates in the range of 0.05 to 2.0 mm/rev. were available.

A four jaw independent chuck was used for holding the workpiece instead of the standard three jaw chuck. The superior gripping power and flexibility in setting provided by a four jaw chuck gave added safety and less possibility of the workpiece moving during an operation.

The set-up for the turning operation is shown in figure (5.1).

5.3 WORKPIECE MATERIAL

Four types of workpiece materials were used as follows:

a) EN 26 53 Rc

b) EN 26 46 Rc

c) EN 9 and

d) Cast Iron grade G 17

A chemical analysis of each material is given in appendix II.

The workpiece material used in both Chapters 6 and 8 were high strength alloy steel EN 26. Bars 125 mm diameter and 610 mm long were heat treated to give two levels of hardness 53 Rc and 46 Rc. Machining was terminated when the length to diameter ratio of the turned length reached 10.

In Chapter 7, tubular workpieces of outside diameter 75 mm and 230 mm in length were prepared from bar stock. Prior to each cutting test, the wall thickness was reduced to 3.5 ± 0.025 mm by boring and turning the workpiece.

5.4 THE CUTTING TOOLS

In the initial tests on commercially available tools (Chapter 6), solid Kyon 2000 inserts 12.7 mm square and 4.76 mm thick with a 1.2 mm nose radius were used. The tool holders were selected to give tool geometry -5^{o}, -5^{o}, 5^{o}, 5^{o}, 1.2 mm and with plan approach angles of 15^{o} and 45^{o}. The edge chamfer was 0.2 mm land width at 20^{o}, giving a chamfer angle of presentation to the workpiece of 25^{o}. However, the edge geometries were later modified to give either a double rake negative / positive combination or a different edge chamfer.

5.5 TOOL WEAR CRITERIA

In early tests flank wear was observed to be more significant than crater wear and so flank wear was selected as the criterion of tool failure. It is essential that the end of the life of a cutting tool is specified in a reliable and repeatable way and so when comparing the performance of tools by flank wear rates and maximum flank wear values, see figure (3.4), the wear measurements used should be related to the region of the cutting edge where each tool would be expected to eventually collapse.

Authorities differ on what represents an acceptable wear land before the tool is changed and because sialon ceramic is relatively new there are no recommendations available. However, a figure of 0.75 mm is often quoted for carbide tools and so it was used in these tests. The procedure of measurement was to allow the tool to cut for a certain length of time. It was then retracted from the workpiece and the insert taken out from the holder for examination. After the flank wear was measured, the insert was carefully replaced, and the cutting operation resumed. This procedure was repeated at specified time intervals until the tool showed a flank wear of 0.75 mm. All the cutting tools were tested in similar fashion.

5.6 EXAMINATION OF WEAR AREAS

A universal measuring microscope type MU.214B, (figure (5.2))was used for measuring the extent of tool wear on the flank.

Stylus probe examination using Rank Taylor Hobson Talylin equipment, was employed to give an indication of crater topography. The crater measurement was recorded at a fixed distance from the leading edge. The cutting insert was mounted in a special fixture manufactured for this purpose (figure (5.3)).

In order to obtain a permanent visual record of the wear mechanism, inprocess photography was used showing both flank and crater profiles. An Olympus zoom stereo microscope model SZ-Tr fitted with Olympus camera system was used for this purpose (see figure (5.4)).

A scanning electron microscope fitted with simultaneous energy dispersive X-ray fluorescence analyser was used in order to provide additional scope for tool wear identification. The SEM has a much greater depth of focus and can be used at much higher magnifications than can be attained in optical metallography.

5.7 MEASUREMENT OF CUTTING FORCES

Cutting forces were measured using a Kistler three-component piezo electric force dynamometer type 9263, see figure (5.1). The signal produced was fed into an a appropriate charge amplifier and then to a galvanometer amplifier. The output was recorded on a UV recorder. Cutting force measurements were carried out during oblique and orthogonal cutting tests using both commercially available and modified cutting tool geometries. Those forces were determined simultaneously and recorded throughout the machining process.

5.8 SURFACE FINISH MEASUREMENT

Surface finish measurements were carried out for the oblique machining process. The results for both effects of changing feed rates and cutting speeds during dry cutting when using both commercially available and modified cutting tool geometries were determined after each pass using a portable Talysurf model 100. Measurements were made in centre line average values. The equipment did not have a permanent trace recording facility, but could conveniently be used in situ on the test machine.

5.9 MEASUREMENT OF CHIP THICKNESS AND CONTACT LENGTHS

During the tests of orthogonal cutting, the chips were collected after each test and the thickness measured using a 0.0002 mm clock gauge equipped with a special pointed anvil designed for this purpose. The value used for calculation of the shear angle was the average of five readings.

The contact length between the chip and the cutting edge on both the primary and secondary cutting edges was measured using the Universal measuring microscope MV.214B, see figure (5.2).

5.10 MEASUREMENT OF TEMPERATURE

The main methods used to measure the cutting temperature as mentioned in Chapter 2 are embedded thermocouples, tool-chip thermocouples, radiation pyrometer, thermocolours techniques, and so on. The usual method of measuring the temperature distribution within the tool is the embedded thermocouple technique. However, this latter technique is not so useful to measure temperature distribution in cutting with very hard tools such as sialon ceramics (Kyon 2000). The tool-chip thermocouple technique is convenient but employed only to measure the mean temperature along the tool-chip interface, and its use is restricted to the couples between electric conductors. Radiation pyrometer and thermocouple techniques are sometimes very useful to measure distribution of surface temperature and tool-chip interface temperature.

Therefore, in order to overcome the above mentioned problems, temperature distribution was determined by using the constant melting point powders technique[70]. The tool was divided into two parts along a plane normal to the cutting edge and parallel to the direction of chip flow (see figure (5.5.)). The split surfaces were coated with a powder of known melting point, bonded to the surface with an aqueous solution of sodium silicate. The two parts of the tool were then assembled in a special tool holder designed for this purpose, and used

in the normal way. After completing the test the tool was split apart to reveal the coated area and the boundary between melted and unmelted powder was the isothermal appropriate to the melting point of that particular powder. By using a range of different powders an isotherm map was built up.

On this technique it must be emphasized that the calibration is not needed because the melting point is peculiar to the material. However, care needs to be taken in setting the two divided tools in order to avoid the chip getting between the two surfaces during machining.

5.11 MEASUREMENT OF STRESS DISTRIBUTION

For measurement of stress distribution along the rake face a split tool dynamometer was used[71]. Once again the tool was separated into two parts, but in this case the parting line was parallel to the cutting edge. The two parts were mounted in the dynamometer in such a way that the force on only one part was measured. By using several tools with split lines made at different distances from the cutting edge a pattern of forces and hence stresses along the rake face was determined. The split tool dynamometer was built around the Kistler 3 component turning dynamometer type 9263 (see figure (5.6)), it consists of two parts as shown in figures (5.7) and (5.8).

a) Back Tool-holder

It was basically a 25x25x153 mm EN26 steel bar machined as shown in figure (5.8). The back insert can be edged forward by screwing in the taper-ended screw. The slider acts as the intermediate piece in the arrangement. A special clamp was used to fasten the tool and the slider in the tool holder.

b) Front Tool-holder

This part is shown in figure (5.9). It was machined from mild steel. The front insert was carried

in a slider, and a special clamp was used for fixing the tip in the right position after the height setting. A high power microscope was used for setting the two tips.

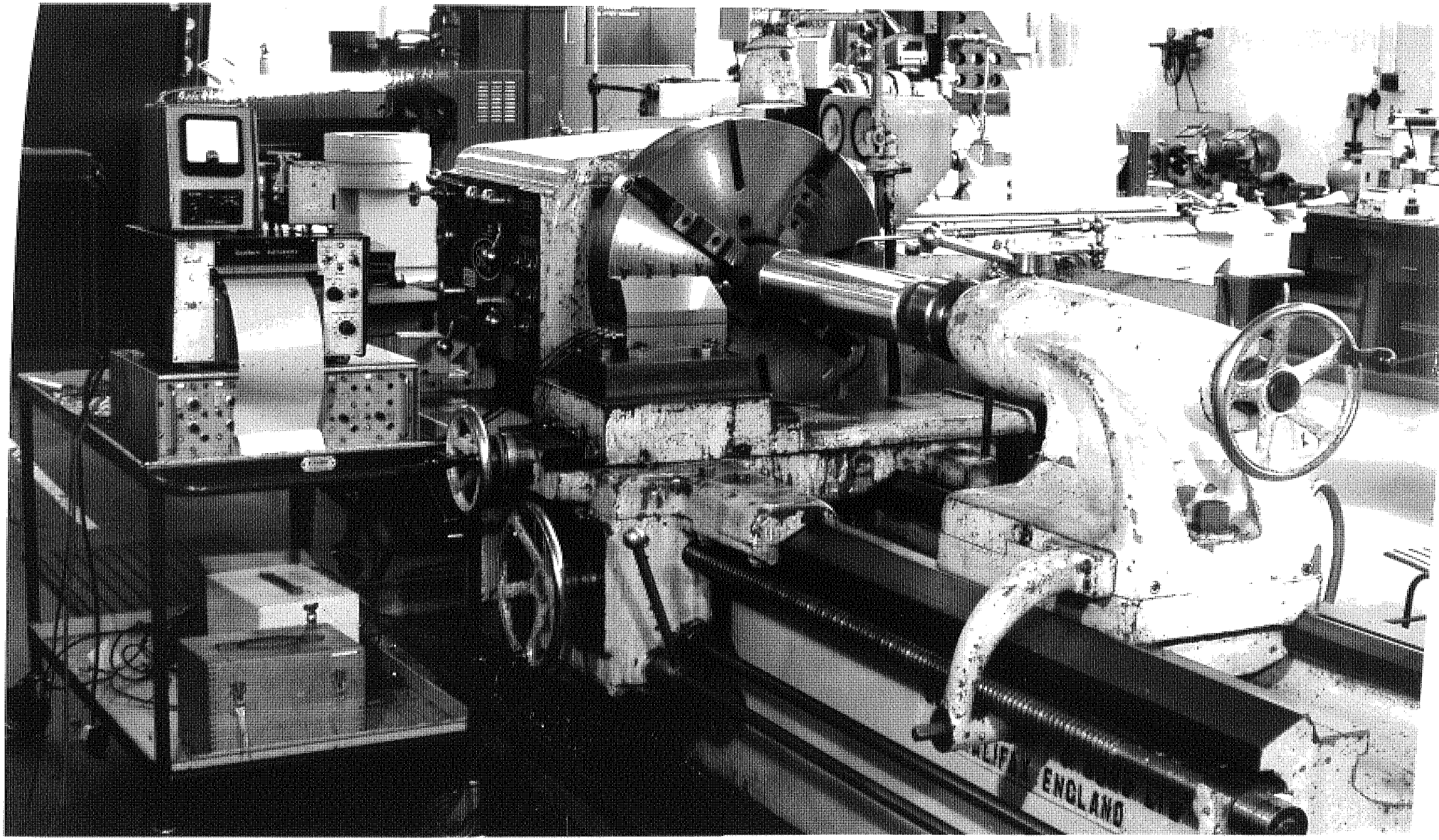

Figure 5.1 Turning operation set-up

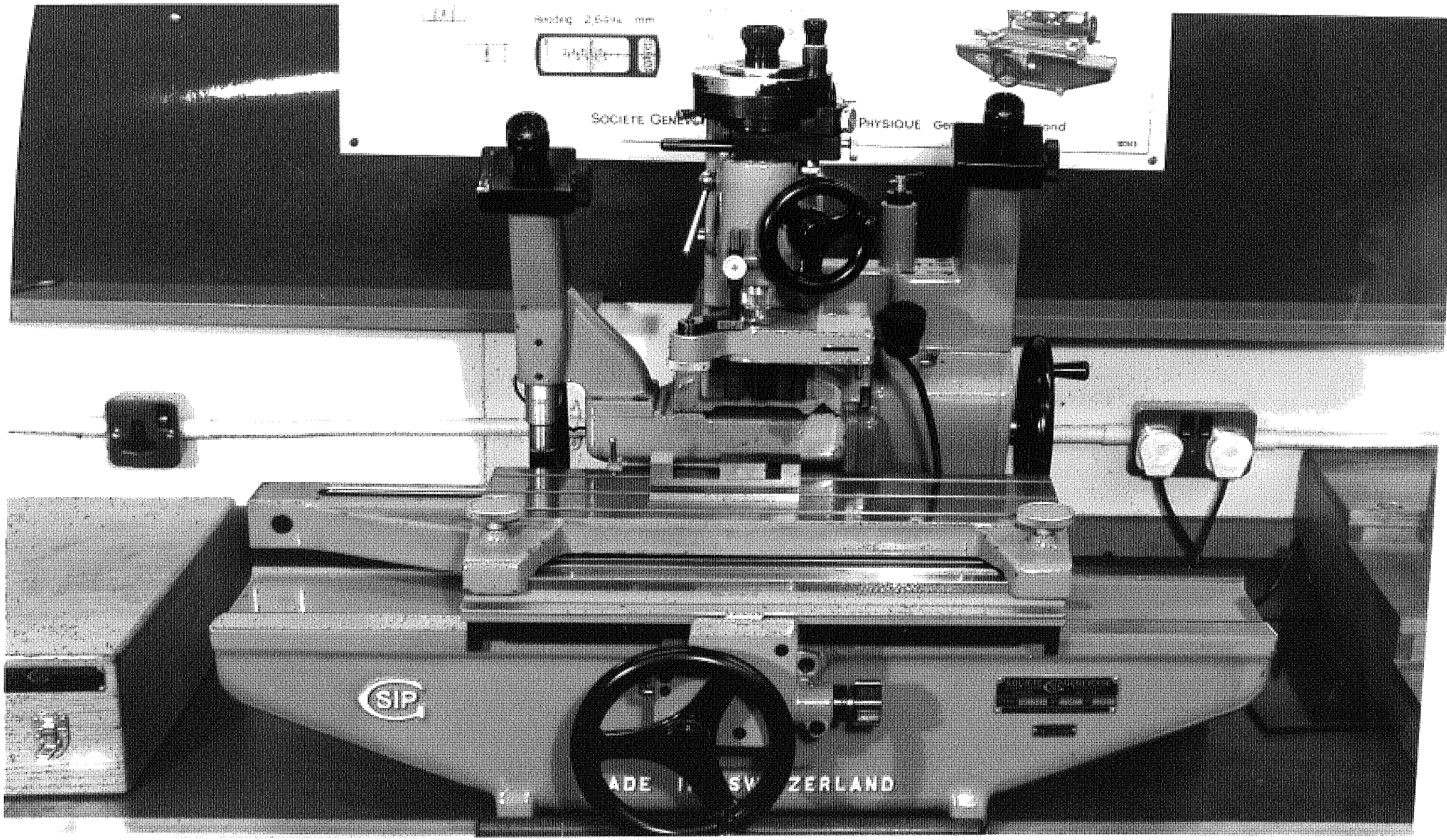

Figure 5.2 Universal measuring microscope

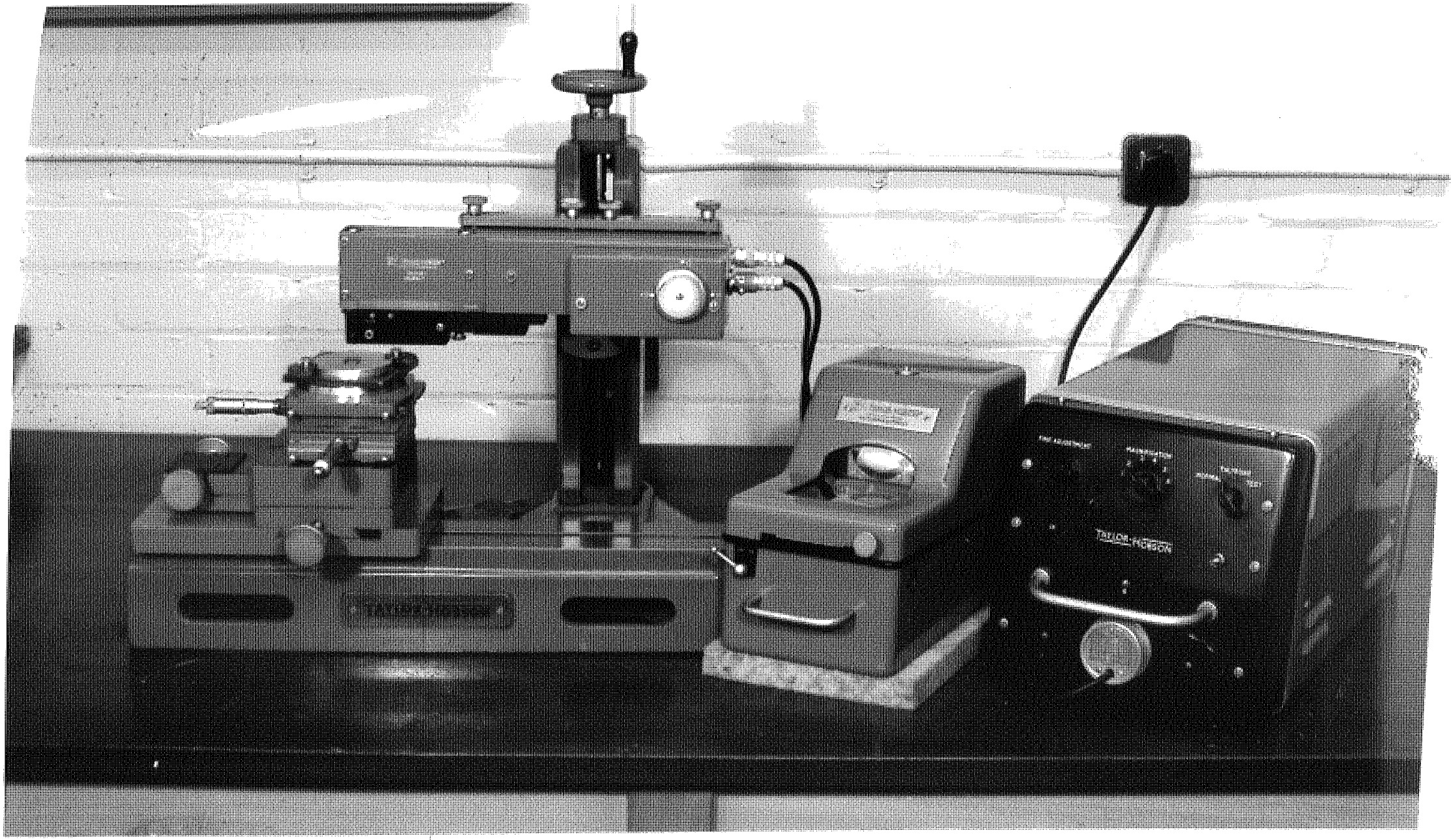

Figure 5.3 Rank Taylor Hobson Talylin

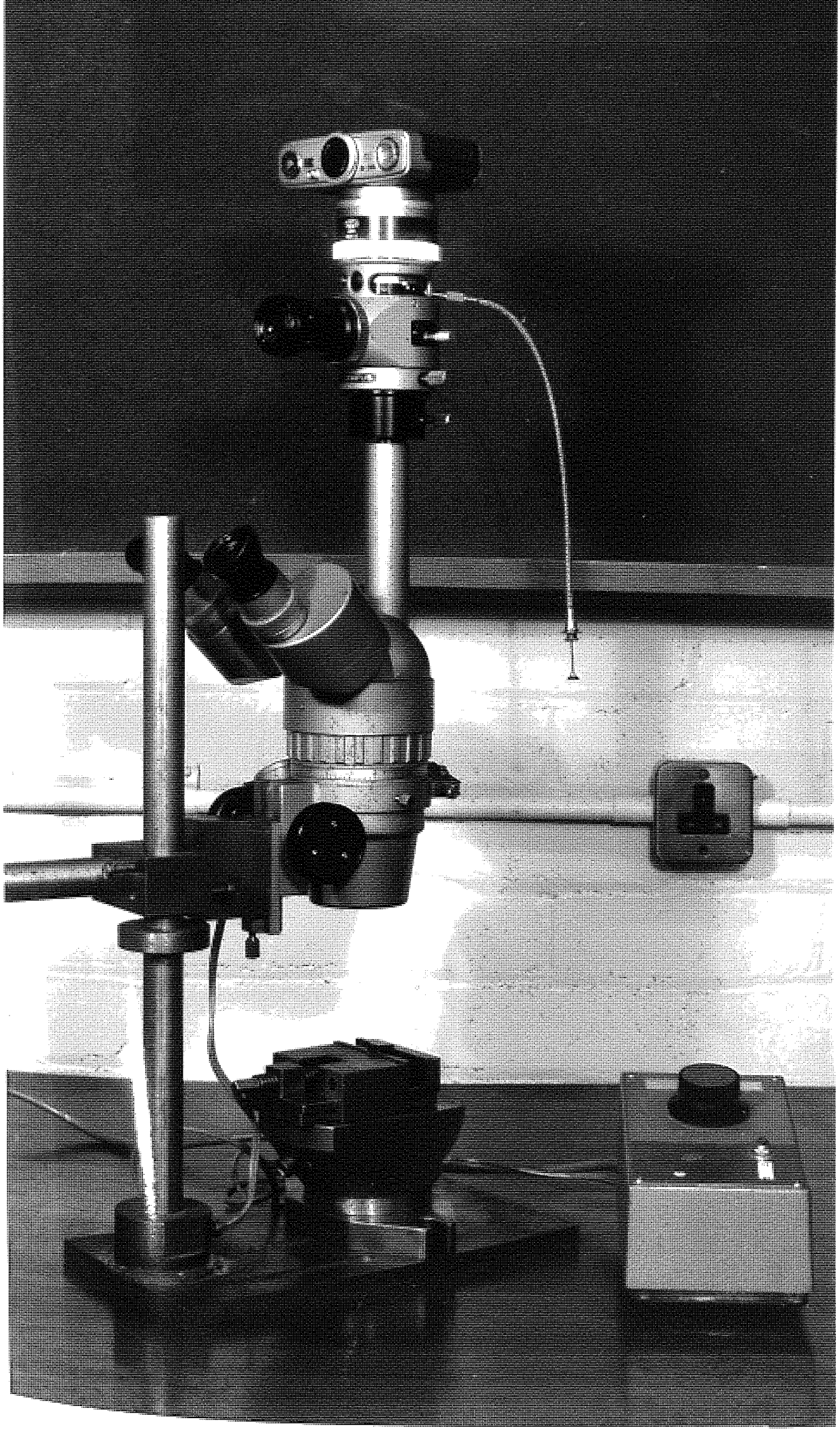

Figure 5.4 Olympus zoom stero microscope

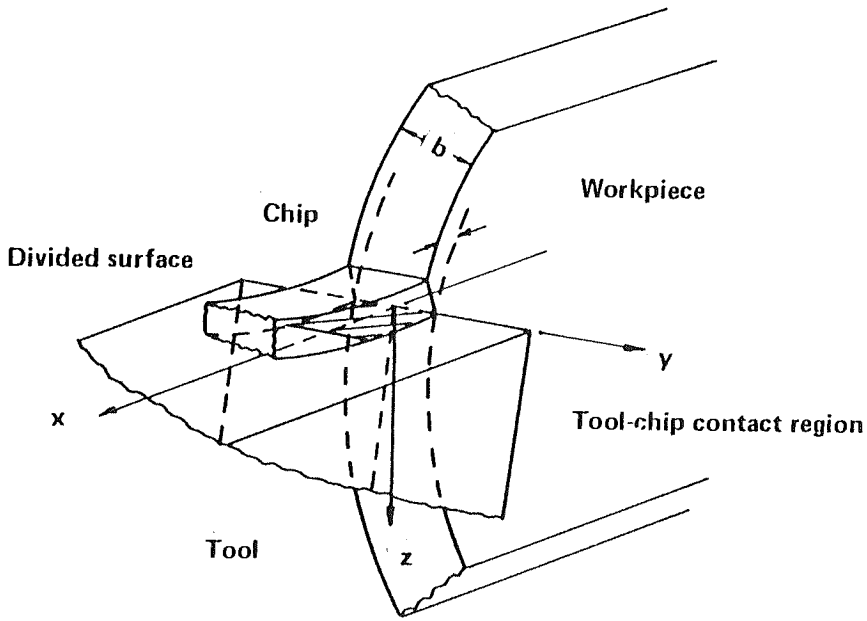

Figure 5.5 Appearance of Cutting

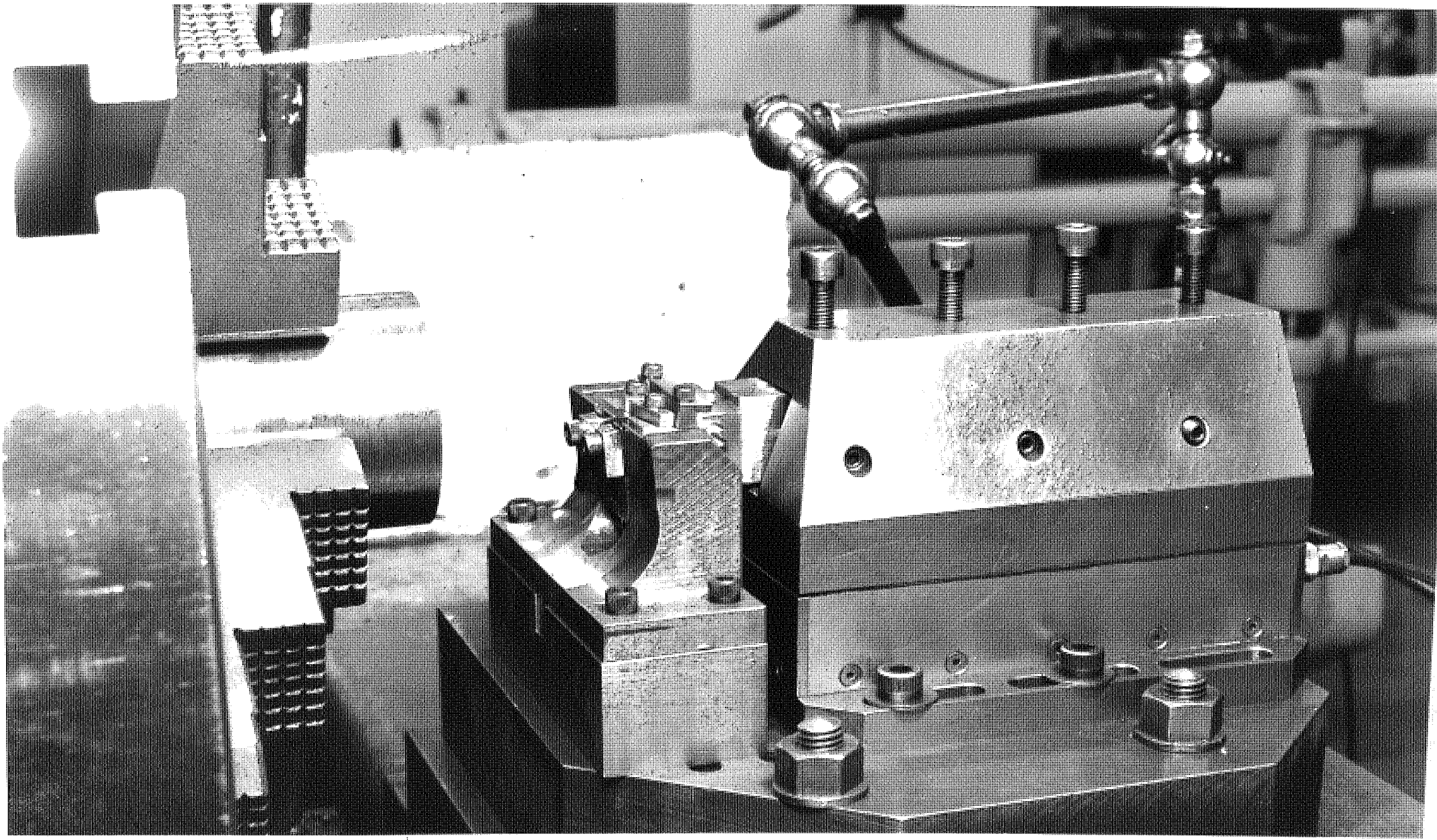

Figure 5.6 Split-tool dynamometer set-up

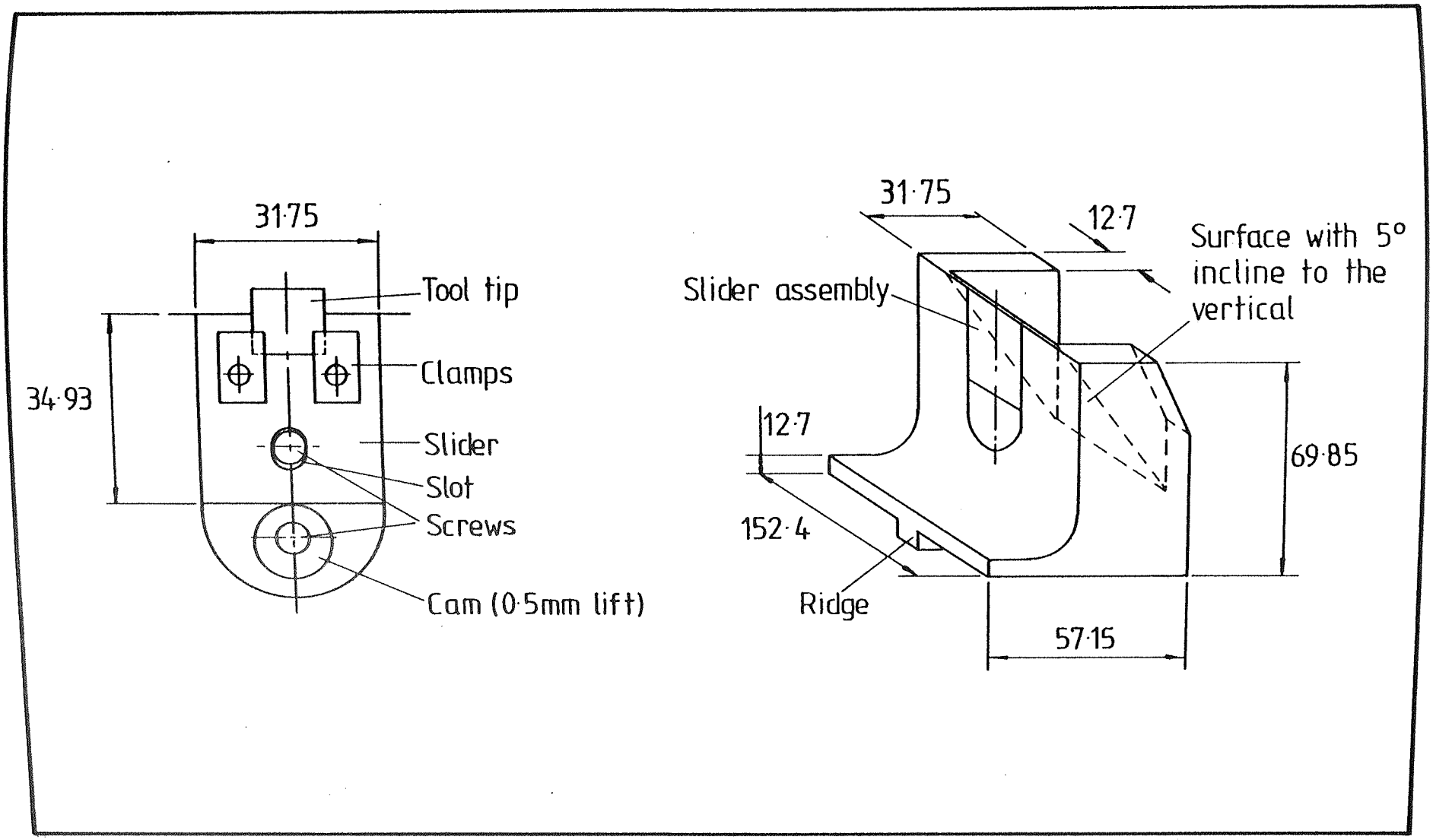

Figure 5.7 Front tool holder (split-tool)

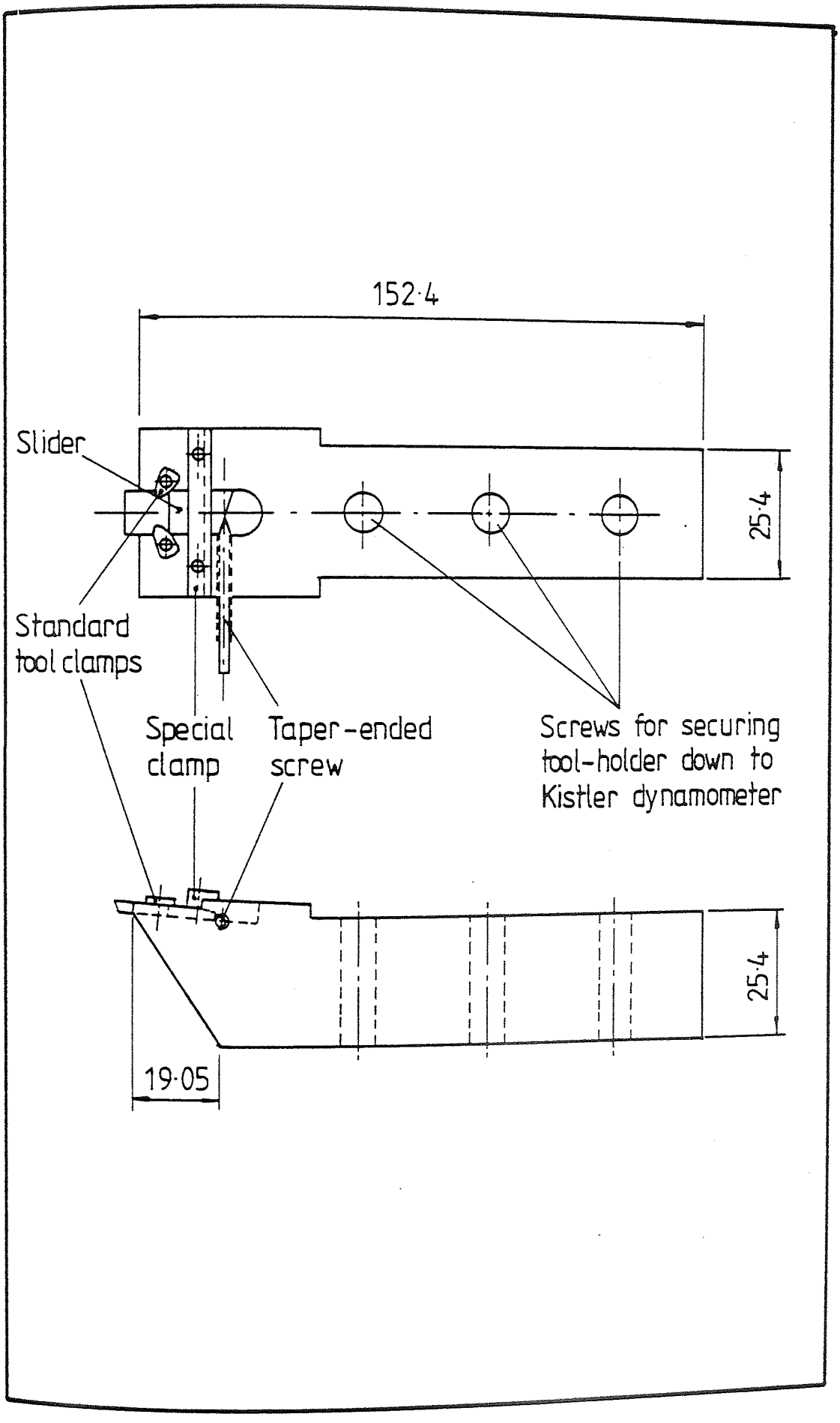

Figure 5.8 Back tool holder (split-tool)

CHAPTER SIX

AN ASSESSMENT OF KYON 2000 FOR CUTTING A HARDENED ALLOY STEEL

6.1 INTRODUCTION

It has already been mentioned in Chapter 4 that Kyon 2000 sialon ceramic inserts have recently appeared on the market. Because the literature available on the performance of this material as a cutting tool was so little, it was decided at the early stage of the research to carry out a series of cutting tests (see Table 6.1). They were performed by using standard negative rake sialon ceramic inserts produced by Kennametal, to machine hardened EN26 (53Rc) varying the cutting speed and feed rates. The main objectives of these tests were

1) To confirm that the flank wear on the cutting tool followed the classical wear pattern as shown in figure (6.1).

2) To establish the procedure for measuring the wear on the cutting edge.

3) To select suitable cutting conditions for the main programme of the work.

		CUTTING SPEED IN M/MIN			
f \ V		90	150	200	400
FEED RATE IN MM/REV	.056	a	a	a	b
	.17	a	a	a	b
	.33	a	a	a	b
	.5	a	a	a	c
	1	c	c	c	c

Table (6.1) Block diagram of initial tests on Kenametal sialon

The results obtained were as follows:

Group (a) (refer to Table 6.1), wear on the flank and on the crater was measurable; no fracture of the cutting edge was observed

Group (b) cutting edges were broken in less than 30 seconds cutting time.

Group (c) Cutting edges were broken at the instant of contact between the tool and the workpiece.

The conclusions that may be drawn from the results of the above series of test can be summarised below:

1. Flank wear has a considerable effect upon cutting conditions and followed a classical wear pattern.
2. Crater wear, on the other hand, has little effect upon the basic machining conditions.
3. Another type of wear which appeared to be important was the grooving wear.
4. There was a range of limits for the cutting conditions to be used; the cutting performance of the cutting inserts above and below these limits are expected to be poor.

6.2 DESIGN OF MAIN PROGRAMME

On the basis of the preliminary work reported in Section 6.1 a test programme was set out to investigate the types of wear associated with Kyon 2000 inserts when machining a difficult material. A large number of cutting tests were performed using the standard conventional available cutting inserts, Kyon 2000.

The above work was aimed at answering the following questions:

1. What cutting conditions give the best performance?
2. How does the workpiece affect the cutting process?
3. Is it possible to predict the best cutting conditions from measuring the cutting forces?
4. What are the types of wear associated with Kyon 2000?

The cutting variables investigated for the above purposes were: cutting speed, feed rate, approach angle, hardness of the workpiece, and type of cutting. Four levels of both speed and feed rate were used; two levels of hardness of the workpiece and approach angle were used. Most of the cutting tests were conducted without coolant. However, in some tests a cutting coolant was employed. The complete tests plan is shown in Table 6.2. It is evident from the table that the

HARDNESS		FEED RATE IN mm/rev (f)		CUTTING SPEED IN M/MIN (V) 90	150	175	200
	53 Rc		.17	a,d	a,c,d	a,d	a,d
			.25	a,d	a,c,d	a,d	a,d
			.33	a,d	a,c,d	a,d	a,d
			.5	a,d	a,c,d	a,d	a,d
	45 Rc		.17	b	b,c,d	b	b,d
			.25	b	b,c,d	b	b
			.33	b	b,c,d	b	b
			.5	b	b,c,d	b	b

Depth of cut 2 mm

a - Material hardness 53 HRc,

b - Material hardness 45 HRc,

a,b - Dry cutting tests

c - Approach angle tests

d - Coolant cutting tests

Table (6.2) Block diagram of the main tests plan

cutting variables were chosen to cover a wide range of cutting conditions. Furthermore, a complete block diagram of the variables being investigated and the cutting parameters being measured during the cutting process is presented in figure (6.2)

6.3 FLANK WEAR

The following section presents the results of machinability testing carried out by the author on high strength alloy steel EN26 at two levels of hardness 53Rc and 46Rc respectively, and serve to demonstrate some features of the wear characteristics associated with Kyon 2000 sialon ceramic inserts.

6.3.1 Material EN26 53Rc

In these series of tests a standard Kyon 2000 insert, 12.7 mm square and 4.76 mm thick with a 1.2 mm nose radius was used. The tool holder was selected to give tool geometry of -5^{o}, -5^{o}, 5^{o}, 5^{o}, 1.2 mm and with a plan approach angle of 45^{o}.

The flank wear curves can be seen in figures (6.3-6.8). The graphs are drawn for a variety of feeds and speeds ranging from .17 - .5 mm/rev and 90 - 200 m/min respectively. From figures (6.3-6.4) it is clear that for the conditions being used in these tests(cutting speed 90 and 150 m/min) the selected feed rate is very important. At 0.17 and 0.25 mm/rev the flank wear is similar, but an increase to feed rate of 0.33 mm/rev gives a substantial reduction in flank wear rate and a consequent increase in tool life. Further extensions of feed rate above and below these values gave unsatisfactory conditions. At 0.5 mm/rev the tool broke under the

high cutting forces after less than one minute cutting time, while at 0.05 mm/rev failure occurred after a similar time due to severe vibration caused by the tool rubbing instead of cutting and the formation of many grooves on the cutting edge. When the cutting speed was increased to 175 and 200 m/min, the tool survived only for a feed rate of .17 mm/rev and the flank wear rate was higher as shown in figure (6.5). The above finding will be discussed in more detail later in Section 6.14.

The data on cutting speed variation is shown in figures (6.6-6.8). The flank wear graphs are drawn in these figures for a variety of feed rates. The results reveal that the rate of flank wear increases as the cutting speed increases. However, higher cutting speed up to 200 m/min does not give much further increase in flank wear for the case when small feed was used. The effect of increased cutting speed upon the tool performance can be explained as follows. For most tool workpiece combinations, increasing cutting speed will result in a reduction in average shear strength due to an increase in temperature. Although it was not possible to measure temperatures whilst this work was carried out, it is expected that increasing cutting speed would increase the temperature generated and, consequently cause considerable softening of the cutting edge, followed by deformation of the cutting edge to cause a bulge on the rake face. This in turn would lead to increased cutting forces which were in fact evident from

the measurement of the cutting forces during the tests carried out, and finally to failure of the whole cutting edge. The flank wear might only be very small and as shown in figures (6.5 and 6.6) this is true for feed rates above 0.17 mm/rev. However, the implication of the results obtained at the lower feed rate of .17 mm/rev, as shown in figure (6.6), is that Kyon 2000 is insensitive to speed variation (after V=150 m/min) and optimum cutting conditions might therefore be sought at the higher speeds for a low feed.

6.3.2 Material EN26 46Rc

The results of flank wear-cutting time tests are presented in figures (6.9-6.12) for feed rate variation and in figures (6.13-6.16) for speed variation using similar geometry to that used in the previous section.

As shown in figures (6.9-6.12) the tool gives similar results for those obtained with material hardness of 53Rc as regards the improvement in the tool performance when feed rate is increased up to .33 mm/rev. As expected from the lower hardness the wear rate in this series of tests is much lower than the case when machining material hardness of 53Rc. In addition the results also indicate that the cutting edge of the tool survived at a feed rate higher than .33 mm/rev whereas with the higher hardness materials .33 mm/rev could not be exceeded because the edge failed almost immediately. In most cases the flank wear increased gradually with time up to about the

criterian of tool failure specified.

Figures (6.13-6.16) present the effect of speed variation on tool flank wear. It is clear from these figures that for all the feed rates tested the flank wear rate increases as the cutting speed increases. However once again similar to the case of the harder material, the flank wear rate did not increase much at the speed range above 150 m/min for all the feed rates tested.

6.4 CRATER WEAR

6.4.1 Material EN26 53Rc

The developments of crater wear during machining were measured using a stylus type surface measuring instrument which was described in Chapter 5. The maximum crater depths at the mid-point of the crater length were recorded.

The results are shown in figures (6.17) and (6.18) for changes in both cutting speed and feed rate. The prime feature exhibited by both sets of graphs is the steady state condition of crater progression during the tests. Figure (6.17) shows that at a fixed feed rate of .17 mm/rev, the crater wear rate increases as cutting speed increases which is expected since the cutting temperature will increase and consequently affect the shear strength in secondary zone which will directly influence the rate of crater wear[72]. On the other hand results in figure (6.18) where feed rate has been varied at a fixed speed of 90 m/min show that the crater wear rate also has a feed dependency, i.e. the higher the feed rate the higher the crater rate. Although the cutting temperature is expected to be approximately the same because of the fixed speed, a higher normal stress is expected to occur at the higher feed rate range, and therefore an increased crater wear rate. Similar results have been reported by Kurimoto and Barrow[73] for high

speed steel tools.

The nature and location of the crater was examined by using both the stylus instrument and, as will be shown later, by the use of a scanning electron microscope. Stylus traces were taken along the rake face of the tool parallel to the chip flow direction for all the tests and an example of the results is shown in figure (6.19). As far as the location of the crater is concerned, it is evident from the figure that as feed increases from 0.17 to 0.5 mm/rev the crater moves farther back, away from the cutting edge. Furthermore, figure (6.20) shows the development and progression of the crater at cutting conditions of 0.33 mm/rev and 90 m/min, and it is clear that the depth of the crater increases as cutting time increases. It is also evident that the shape of the crater changed as cutting proceeded and this will be discussed later in Section 6.14. It is worthwhile to mention in this context that crater depth measurements were conducted for all the experiments and results show a dependency on feed and speed. Further discussion on the nature of the crater is included in Section 6.12.

6.4.2 Material EN26 46Rc

As with the previous section, crater depths were measured. Typical results of crater depth-time relationships are shown in figures (6.21-6.22) for a variety of cutting speeds and feed rates. Figure (6.21) shows once

again that the crater depth for a fixed feed rate of .17 mm/rev is speed dependent and this also applies to the high feed rates. However, higher values of crater depth are obtained at the higher feeds.

Figure(6.22) reveals similar results to those obtained in the previous section for feed variation. It is also evident from the figure that using a higher feed rate of .5 mm/rev results in a substantial increase in crater depth. Furthermore, as with the previous section, figure (6.23) shows the progression of the crater with cutting time.

The reasons for the above trends in this set of graphs are the same as those previously outlined in Section 6.4.1.

6.5 GROOVING WEAR

Grooving wear has a particular influence on surface finish and dimensional accuracy and is evident from the appearance of a groove on the trailing edge. The grooving effect and its relationship to flank and crater wear is shown in figure (6.24).

A similar groove may appear on the leading edge of the cutting tool, as also shown in figure (6.24), and the presence of this type of groove can again influence the dimensional accuracy. When the leading edge groove becomes large enough the cutting edge will fail totally due to edge break away.

The phenomenon of groove wear has been noted by a number of authors, and a number of reasons for groove formation have been put forward[74-77]. Mechanisms of groove formation that have been proposed include:

1. Work hardening of the surface layer of the work material from a previous cut will cause grooving. Reported test cuts on annealed and non-annealed work material have shown less grooving wear with the former.

2. Flow of built-up edge material outwards along the cutting edge of the tool will be dragged down the flank of the tool at the outside edge of the cut causing concentrated wear at this point.

3. Stress concentration and temperature concentration at the free surface.

4. A higher velocity at the outside diameter.

5. It occurs as a result of the abrasive action of the particles of the build-up-edge already deposited on the workpiece.

6. Presence of an abrasive oxide layer on the previously cut surface.

7. Chemical effects at the tool / work / atmosphere interface i.e. fretting corrosion.

8. Fatigue of the tool material due to the fluctuation of force at the free surface which accompanies the small lateral motions of the edge of the chip.

9. Vibration which is brought about by machining system instability.

It may appear, therefore, that groove wear is a complex phenomenon, and the real cause appears to be the result of a combination of several factors, the relative importance of each depending on the particular tool and workpiece combination, the machining system and the cutting conditions.

From observations carried out in this work, it is clear that Kyon 2000 cutting tools are prone to severe

formation of grooves. These grooves were observed to develop on both the trailing edge and leading edge. On the trailing edge a groove first appeared at a distance from the leading edge, as it progressed further a second and then a third groove developed. The distance between each groove shows a dependency on feed rate, and this was reported in [73] when machining a similar workpiece material.

Figures (6.25) and (6.26) show scanning electron microscope pictures of a typical formation of groove wear on the trailing edge and leading edge of the tool. It is clear from the above, that a series of grooves were formed and this had an effect on the surface roughness during the test as shown in Section 6.11. Moreover, results obtained also showed that both the groove depth and length were dependent on the cutting time, i.e. the cutting length.

It is interesting to mention in this context that feed rate has an influence on the formation of the grooves. Figures (6.27-6.28) show results obtained when the feed rate is increased from 0.056 mm/rev to 0.33 mm/rev. It is clear that the grooves were reduced in number and depth when the feed increased and this change can be attributed to stability of the system since as was mentioned in Section 6.3 the tool with the lower feed rate rubs and does not cut efficiently.

6.6 THE EFFECT OF CUTTING SPEED ON CUTTING FORCES

The influence of cutting speed on the main cutting force (F_z), radial force (F_y) and feed force (F_x) are shown in figures (6.29-6.36), where the cutting forces are plotted as a function of cutting speed, at speeds rates of .17, .25, .33 and .5 mm/rev. The depth of cut was maintained at 2 mm throughout all the tests.

Figures (6.29-6.32) show the speed / force relationships for machining material EN26 of hardness 53Rc, while figures (6.33-6.36) show similar relationships of the same material but at a hardness of 46Rc. However, before discussing the results of these tests, it is worth pointing out that cutting theory has generally related the cutting forces to chip-tool interaction and material strength. The cutting forces are therefore highly affected by the nature of the chip formation process, which in turn determines the chip-tool interaction.

As would be expected when machining a material with hardness of at least 46Rc the cutting forces recorded in figures (6.29-6.36) are relatively high. It is clear from the figures that similar trends are obtained for both main cutting force and feed force. In both cases, machining either 53Rc or 46Rc materials, both forces tend to fall as cutting speed increases. The reduction in the main cutting force and feed force can

be attributed to the reduction in shear strength in the secondary zone brought about by increasing the cutting temperature produced during cutting.

However, the results obtained for radial force reveals different trends from those obtained for both main cutting force and feed force. It is seen from the graphs that in most cases the radial force has the tendency to increase after a speed of 150 m/min is reached and this may be attributed to the deformation which takes place on the cutting edge in the form of a bulge on the rake face. Further discussion of this point is included in Section 6.14. Furthermore, it is noticed that at a feed rate of .5 mm/rev and when machining material with hardness 53Rc, the main cutting force exhibits a continuous increase as the cutting speed increases. This was due to the higher feed used, which led ultimately to tool failure.

6.7 CORRELATION BETWEEN FLANK WEAR, CRATER WEAR AND CUTTING FORCES.

It is well known that the cutting forces are dependent on the chip formation process and therefore, it is to be expected that cutting tool wear will have a significant influence on the cutting forces. Therefore, during this work monitoring of cutting forces during machining was done in order to reach more detailed knowledge of the influence of the development of both flank and crater wear on the cutting forces.

The results reported here are for a variety of feed rates ranging from .17 - .5 mm/rev and a constant cutting speed and depth of cut of 90 m/min and 2 mm respectively and are shown in figures (6.37 - 6.38). Figure (6.37) shows the results obtained when material EN26 at 53Rc is used. It is clear from the sets of graphs that the initial rapid rate of tool wear on both the flank and the crater is accompanied by a similar increase in all of the cutting forces. The increase was observed when the cutting time was increased from 0 - 1 minute. As the cutting process was continued beyond this initial period a steady wear rate was brought about for a limited period of cutting time and then for some cases when the wear on the cutting tool accelerated, the cutting forces also increased. The implication of the above results is that as the tool wears cutting becomes less efficient and the forces necessary to produce the chip will increase.

Furthermore, it can also be seen from the graphs that increasing the feed rate results in an increase in the cutting forces. However, with the feed rate of .5 mm/rev it was not possible for the cutting edge of the tool to withstand the very high, suddenly developed cutting forces, and therefore, the tool broke and no measurable value of either flank or crater was obtained.

Examining the results presented in figure(6.38) where a material EN26 of a hardness 46Rc were used shows similar results to those obtained in figure (6.37), although the rate of wear is slower in this case. It is also clear that a significant increase in the radial force value was observed at feed rate of .5 mm/rev probably due to rake face bulging. Tests carried out at speeds greater than 90 m/min produced increased flank and crater wear as discussed in Section 6.3 and 6.4. However the relationship between wear and forces reported here for a speed of 90 m/min were similar at the higher speeds.

6.8 THE EFFECT OF HARDNESS OF THE WORKPIECE

Two different levels of hardness 53Rc and 46Rc were used for the EN26 alloy steel used in this work.

Tests to examine the microstructure of the two types of heat treated high strength alloy steel were conducted. Small samples of each specimen were taken after the heat treatment and mounted in bakelite for optical examination. They were mechanically polished on silicon carbide papers down to 1200 grade and then diamond polished using grit sizes of 6μ and 1μ. Final polishing was done on a soft cloth impregnated with 0.3 gamma alumina powder and 0.05 powder in succession before etching to reveal the microstructure. The samples were etched using 2% Nital Solution. Examination of the microstructure of the heat treated steels under SEM shows that a martensitic structure was obtained when the steel was heat treated to obtain a hardness value of 53Rc. However, the microstructure of the second case reveals different results. A bainite structure was distinguished clearly, and this of course is the reason for the lower hardness value.

It is noticeable from the series of tool wear tests carried out on machining both types of steel, that the wear rate in general was less and developed more slowly with the lower hardness material, as can be seen from the results obtained in Sections 6.3 and 6.4. Moreover,

under certain conditions the tool failed when the higher hardness material level was machined. It is therefore evident that as the hardness and strength of the workpiece increases secondary shear strength of the chip and intensity of energy expenditure in secondary shear zone will increase, thus, generating higher temperatures and stresses. As tool wear is temperature dependent, higher rates of wear are expected to result[78] and this was quite evident from the tests carried out using Kyon 2000 sialon ceramic inserts.

6.9 THE INFLUENCE OF PLAN APPROACH ANGLE

Tests were carried out with two plan approach angles 15^{o} and 45^{o}. At the higher angle two important advantages can be expected. Firstly, the conditions at the start of the cut are improved because the initial impact force is incident farther from the cutting edge. Secondly, the longer length of contact between the tool and the workpiece and the consequent reductions in both load per unit area and chip thickness lower the pressure and temperature on the edge.

These advantages should lead to a reduction in tool wear rate and this is shown in figure (6.39) where cutting conditions of 150 m/min cutting speed, 2 mm depth of cut and a range of feed rates between .17 mm/rev and .5 mm were used. The material being used for these series of tests was EN26 at hardness level of 53Rc.

Results show that at a feed rate of 0.17 mm/rev, the flank wear rate is lower at approach angle 45^{o} than at 15^{o}. It is also evident from the tests and equally important, is that at 45^{o} plan approach angle, feed rate could be increased to 0.33 mm/rev,whereas, at 15^{o} all tools broke at feed rates greater than 0.17 mm/rev. The contact distance from the cutting edge at 15^{o} plan approach angle was clearly too short to absorb the higher forces.

6.10 THE INFLUENCE OF CUTTING FLUID

Tests involving cutting fluid were carried out using Cincinnati Cimperial 20 water soluble at a ratio of 1 to 9 and at a flood rate of 4.5 litres/min. Cutting speed of 150 m/min, depth of cut of 2 mm and feed rates between .17 mm/rev and .5 mm/rev were employed.

Results showed that the rate of development of flank wear is not significantly influenced by using a cutting fluid. However, as shown in figure (6.40) where a work-piece material of 53Rc is used, there is a much greater tendency for the tool edge to fail due to breakage when a cutting fluid is used in the manner adopted for these tests. The forces developed during cutting, which are shown in figure (6.41) provide an explanation for this tendency. In dry cutting the tool / chip interface temperature will be high and although this may be a problem with certain tool materials, Kyon 2000 sialon ceramic insert has the necessary hot hardness to continue to operate satisfactorily. Moreover, the cutting edge only broke during dry cutting when the feed rate was raised to 0.5 mm/rev. However, when a cutting fluid is used the chip temperature is reduced and the strength of the workpiece remains high, leading to high radial feed forces. As indicated in figure (6.41) the forces eventually become high enough (especially at a higher feed rate level i.e. .25 mm/rev and over) to cause breakage of the tool. When the cutting tests were performed

using a material of hardness 46Rc, similar results were obtained as shown in figure (6.42). Once again there is not much improvement gained in tool life by using the cutting fluid. Similar results have been reported by Phillips[79] for machining high strength, low alloy steels.

6.11 SURFACE FINISH

As far as the surface finish of the machined surface is concerned, it is well known generally that the surface finish is dependent on the nature of the tool edge in contact with the workpiece. During the cutting tool wear tests performed using Kyon 2000 ceramic inserts, surface finish values were measured relative to cutting time. The results are plotted in figures (6.43) and (6.44) for both effects of cutting speed and feed rates during dry cutting when a material EN26 of 53Rc hardness is machined.

It is clear from the graphs in figure(6.43) that increasing the cutting speed has improved the surface finish of the machined surface, although as cutting time increases the value of the surface roughness increases as well due to wear developed on the cutting edge. Surface finish is also dependent on feed rate as can be seen from figure (6.44), an increase in feed giving an increase in surface roughness. It is evident from figure (6.44) that the feed rate has a much greater influence on surface finish than does cutting speed.

The surface finish obtained when machining the lower hardness material exhibited similar results to those presented in figures (6.43 - 6.44).

6.12 X-RAY MICRO ANALYSIS OF THE RAKE FACE

To display more analytical information on tool wear, x-ray microanalysis of the ridge area at the rake face was carried out. The main objective of this exercise was to study whether there had been any transfer of the work material to the wearing area of the tool. Workpiece hardnesses of both 53Rc and 46Rc were used.

Results of examination on the harder material gave Fe, Mn, Ni, Cr as primary deposits, while machining the lower hardness produced Fe, Mn, Mo, Sn as shown in figure (6.45). The x-ray map photographs, see figure (6,46 a,b,c,d), show dot patterns which indicate the level of concentration of a particular material transferred to the rake face. It is clear that the dot intensity varies for different positions on the rake face and the variation is random. Nevertheless although the quantity of transferred work material varies there is no doubt that transfer has taken place.

6.13 EXAMINATION OF WEAR AREAS

It is important to gain an understanding of the development of tool wear as machining proceeds. For the above purpose tool wear was regularly monitored using an Olympus zoom stereo microscope fitted with a camera as described in Chapter 5.

Figures (6.47) and (6.48) show a series of photographs for both flank wear and crater wear area development during machining. These results were obtained at a cutting condition of V = 90 m/min and f = .17 mm/rev when machining EN26 at 46Rc. It is noticeable from figure (6.47) that in general uniform wear patterns occurred. However, as the cutting time increases, a series of grooves is formed, and these are shown at case C in the figure.

Furthermore, it is apparent from figure (6.48) where a series of photographs of crater wear development are presented; that as the cutting time increases the crater width is increased a little. It is also clear that a uniform crater has been formed and no notching has appeared. However, at high feed rates this was not so and a series of notches were observed.

The nature of the craters were also examined using the scanning electron microscope. Figure (6.49) shows a typical crater and the ridge formation on the crater

surface is clear. The ridges formation is typical of diffusion wear and this has also been reported by Bhattacharya et al[80]. Furthermore, an examination of the wear areas of different cutting inserts at high magnification shows no sign of a crack being found.

6.14 MODE OF TOOL FAILURE

As mentioned in the literature, the mode of failure of any type of cutting tool is largely dependent on both the localised stresses acting on the cutting edge and the heat generated in the cutting zone. Cutting tests on Kyon 2000 ceramic inserts show that the possibility of tool failure is influenced by the cutting conditions involved in the machining process.

Tests on EN26 at 53Rc at high cutting speeds (175, 200 m/min) and high feed rates (.33, .5 mm/rev) result in a fracture of the cutting edge of the insert. A picture of the cutting edge using a scanning electron microscope for a cutting condition of f = .33 mm/rev and V = 200 m/min is shown in figure (6.50). The cutting edge only survived for 50 seconds and it is clear from the figure that fracture has occurred on the rake face of the cutting edge. This can be attributed to the damage caused on the cutting edge by the very high cutting temperature generated in the cutting zone since a large energy was dissipated to form the chip. This is evident from the measurement of the cutting force produced during machining as shown in figure (6.31). It should be mentioned here that the measured cutting forces during all the tests, where high speeds and high feed rates were involved, was not stable indicating that the shape of the cutting edge had changed during the cutting operation. The use of a high cutting speed and a small

feed rate also resulted in severe tool fracture as shown in figure (6.51). (Cutting condition of f = .056 mm/rev and V = 400 m/min).

Experiments on EN26 at hardness level of 46Rc showed that the tools were plastically deformed and this was evident from the results obtained at high speed and feed rate. Figure (6.52) shows a deformation wear which occurred on the nose of the cutting edge before the cutting tool failed. It is also clear that some work material has adhered to the tool.

The developments of the deformation wear were monitored as shown in figure (6.23). However, deformation wear had also occurred when machining the higher hardness material at low speed, see figure (6.20). As mentioned in Section 6.4, it is quite clear from the above figures that the shape of the cutting edge was continuously changing during the tests.

It would appear from the results discussed so far that the type of deformation occurring with Kyon 2000 is a combination of (i) and (ii) of figure (6.53)[57] i.e. a small localised bulge and an upwards deformation of the cutting edge. The first is due to the high load or tangential force acting on the rake face and the second deformation is the result of a force acting mainly in the direction of the feed. If the cutting edge is deformed only locally, therefore, it is expected

that the small ridge will break off and may result in tool failure. In other words the downwards deformation of the rake face will increase the clearance angle (case i) and produce a more negative rake angle which causes an increase in radial force F_Y, temperature and stresses on the cutting edge. At a certain stage the upward deformation will eliminate the clearance angle, and as mentioned earlier the bulge will break off and thus lead to tool failure. Furthermore, as mentioned in [81] it would appear that with higher hardness, the above conditions will occur simultaneously and result in tool fracture.

6.15 COMPUTER ANALYSIS

6.15.1 Introduction

In designing the experimental work for the tool wear tests and as shown in Section 6.2 a large number of variables have been used. A statistical analysis of the results was carried out to isolate the effects of individual variables[82].

A statistical package of social sciences, SPSS, were used for the above purpose. In general, this package is an integrated system of computer programs designed for the analysis of experimental data. The system provides a unified and comprehensive package that enables the user to perform many different types of data analysis in a simple and convenient manner. SPSS allows a great deal of flexibility in the format of data. It provides the user with a comprehensive set of procedures for data transformation and file manipulation, and it offers the researcher a large number of statistical routines commonly used in experimental data analysis.

In addition to the usual descriptive statistics, simple frequency distributions and cross-tabulations, SPSS contains procedures for simple correlation, partial correlation, means and variances, one-way and n-way analysis of variance, multiple regression, discriminant analysis, scatter diagrams, factor analysis and Guttman

scaling. Facilities are also available which enable the user to generate new variables, to recode variables and to sample, select or weigh specified cases.

The section of the SPSS used in this analysis was the subprogram "REGRESSION", used for a multiple regression and variance analysis for the data obtained. The partial F-value for the entry of variables to the regression equation and removing variables from the regression equation was set at the $\gamma = 0.05$ level, i.e. F value = 3.8. The details of the SPSS mathematical formulation of multiple linear regression subprogram analysis can be found in [83].

6.15.2 Subprogram Regression

The SPSS multiple regression subprogram combines standard multiple regression and stepwise procedures in a manner which provides considerable control over the inclusion of independent variables in the regression equation. The variable transformation procedures of the SPSS package allow the regression subprogram to be used for a variety of multivariate analyses, such as polynomial regressions, dummy regressions and analysis of variance and covariance. In addition the subprogram allows the user to examine the residuals and predicted values for later analyses. Input to the regression subprogram may consist of either raw data cases or a correlation matrix. If the input consists of raw data

cases any of the SPSS variable-transformation features may be used and several options are available for handling missing data (83).

6,15.3 Printed Output Subprogram Regression

The output from a multiple regression computer 'run' can be varied by selecting from the options available the manner in which the data is treated and the statistics produced. All the 'runs' made for this part of the work involved the following section:

OPTIONS -1 This option causes the subprogram to include all cases in the calculation of correlation coefficients.

STATISTICS-2 This statistic causes means, standard deviations and number of valid cases to be printed in a table.

The output is divided into two parts:

(1) step-by-step results, and

(2) a summary table.

The first part provides relevant statistical information for each regression equation calculated. By choice each step involves the addition of one independent variable to the regression equation for ease of analysis and inclusion of only 'significant' variables.

The summary table of the output is printed after the final step in the anlysis and provides a brief synopsis of changes occurring at each step. Each step-by-step section is headed with the step number and a list of independent variables entered on the current step. Below it is a list of statistics relevant to the prediction equation. The statistics are:

(1) the multiple correlation coefficient (Multiple R)
(2) the value of R^2
(3) the adjusted R^2
(4) the standard error of estimate for the prediction equation.

On the right side is an (ANOVA) table which presents all of the information relevant to a test for R^2, the overall test for goodness of fit of the equation. Immediately below the foregoing information the step-by-step output is divided into subsections labelled "variables in the equation" and "variables not in the equation". Within the former, regression statistics are given for all variables entered into the equation up to and including the current step.

The unstandardized regression coefficients are listed under the column head B. The last value in this column (constant) is the Y intercept. Standardized partial-regression coefficients are listed under the

column (Beta). The column (std Error B) contains the standard errors for each of the unstandardized regression coefficients, which can be used in a t-test or in establishing confidence limits for the Beta's. The F-ratios in the column (F) are used in tests of significance for the individual Beta's.

Variables that have not been entered into the equation, but that appear in the predictor list, are treated in the "variables not in the equation" segment. The first column, headed "Beta in", is the standardized partial regression coefficient that a variable would have if it alone were entered on the very next step. Under the column head "partial" is the partial-correlation coefficient for each variable with the dependent variable, after variables already in the equation have been partialled out. The remaining two values, "Tolerance" and "F". are used by SPSS when a stepwise mode of analysis is called for. In order to be entered in a stepwise regression, the tolerance and F values must exceed those specified in the parameters section of the regression design statement. From the variables whose tolerance and F values are satisfactory, the variable with the largest partial-correlation coefficient is selected for entry on the next step.

A summary table appears near the end of the printout. It should be noted that the summary table treats variables as if they had been entered one by one, even

when variables are entered in blocks or in a single step.

The simple correlation coefficient between the dependent variable and each of the independent variables appears under the column head "Simple R".

6.15.4 Results of Regression Analysis

The SPSS package was used to investigate the effects of the cutting variables on both the tool life and the cutting forces.

The results obtained as follows:

6.15.4.1 Material EN26 53HRC

The tool life regression model obtained is

$$T = 24.354 - 36.94f - 0.115V + 0.167\,fV$$

The multiple R value is 87.129%

And the corresponding analysis of variance tables are (see Appendix I):

a) Cutting speed

A.O.V	DF	S.S	M.S	F
Regression	1	106.719	106.719	16.89
Residual	14	88.45	6.318	

b) Feed rate

A.O.V	DF	S.S	M.S	F
Regression	2	137.06852	68.53426	15.3345
Residual	13	58.10045	4.46927	

c) Interaction between feed rate and cutting speed

A.O.V	DF	S.S	M.S	F
Regression	3	148.16186	49.38729	12.6076
Residual	12	47.00712	3.92	

It is clear from the value of Multiple R that 87.129% of the variation is explained by the variables of feed rate, cutting speed and the interaction between the two.

It is also clear that the variables are highly significant at 5% level.

6.15.4.2 Material EN26 46HRC

The tool life regression model obtained are:

$$T = 29.644 - 21.92f - 0.13V + 0.1fV$$

The multiple R vale is 86.56%

And the corresponding analysis of variance tables are (see Appendix I):

a) Cutting speed A.O.V. table

A.O.V	DF	S.S	M.S.	F
Regression	1	260.66016	260.66016	34.4027
Residual	14	106.07422	7.57673	

b) Feed rate

A.O.V	DF	S.S	M.S	F
Regression	2	270.77386	135.38693	18.3411
Residual	13	95.96052	7.38158	

c) Interaction between feed rate and cutting speed A.O.V. table

A.O.V	DF	S.S	M.S	F
Regression	3	274.77525	91.59175	11.952
Residual	12	91.95913	7.66326	

As with the case of EN26 53HRC the R value explains in this case 86.559% of the variation caused by the above specified cutting variables. The variable are also highly significant at 5% level.

Cutting force

The results obtained using SPSS are presented in Tables 3-8 for both material hardness 53Rc and 46Rc.

Examining the value of multiple R, it can be noticed that a good correlation has been obtained and the cutting variables (cutting speed and feed rate) can explain the variation in the cutting forces. An example of the print-out obtained from the computer is shown in Appendix I.

Type of force N	V m/min	f mm/rev	Regression model	Multiple R
Feed Force (F_x)				
F_{x1}	a,b,c,d	1	$F_{x1} = 2294.7+0.054V^2-0.000255V^3$	99.7%
F_{x2}	a,b,c,d	2	$F_{x2} = 3418.43-9.145V+0.0187V^2$	99.34%
F_{x3}	a,b,c,d	3	$F_{x3} = 3185.9-9.25V+0.000133V^3$	99.94%
F_{x4}	a,b,c,d	4	$F_{x4} = 2668.3+0.0341V^2-0.000272$	99.88%
F_{x5}	a	1,2,3,4	$F_{x5} = 2714.535-4495.604f^2+9181.455f^3$	54.532%
F_{x6}	b	1,2,3,4	$F_{x6} = 3398.472-4646.293f+11373.16f^3$	98.743%
F_{x7}	c	1,2,3,4	$F_{x7} = 3117.463-3201.864f+6102.52f^3$	99.932%
F_{x8}	d	1,2,3,4	$F_{x8} = 2323.499+4477.68f^2-12702.91f^3$	97.955%

$V_{90} = a$ $\quad f_{.17} = 1$

$V_{150} = b$ $\quad f_{.25} = 2$

$V_{175} = c$ $\quad f_{.33} = 3$

$V_{200} = d$ $\quad f_{.5} = 4$

Material EN26 53Rc

Table (6.3) Summary of computer results of predicted models of feed force

Type of force N	V m/min	f mm/rev	Regression model	Multiple R
Radial force (F_y)				
F_{y1}	a,b,c,d	1	$F_{y1} = 2567.5-9V+0.000446V^3$	89.8%
F_{y2}	a,b,c,d	2	$F_{y2} = 3446.8-12.46V+0.00048V^3$	87.6%
F_{y3}	a,b,c,d	3	$F_{y3} = 5026.106-25.6V+0.00039V^3$	98.4%
F_{y4}	a,b,c,d	4	$F_{y4} = 2519.3+27.635V-0.000365V^3$	99.8%
F_{y5}	a	1,2,3,4	$F_{y5} = 2249.415+6138.345f^2-10350.77f^3$	82.128%
F_{y6}	b	1,2,3,4	$F_{y6} = 1526.547+5425.57f-4219.743f^2$	98.259%
F_{y7}	c	1,2,3,4	$F_{y7} = 2737.413+11993.63f-22090f^2$	98.9%
F_{y8}	d	1,2,3,4	$F_{y8} = 3898.47+4987.6f-13722.4f^2$	96.1%

Material EN26 53Rc

Table (6.4) Summary of computer results of predicted models of radial force

Type of force N	V m/min	f mm/rev	Regression model	Multiple R
Main Cutting force(F_z)				
F_{z1}	a,b,c,d	1	$F_{z1} = 2689.7+8.621V-0.000383V^3$	88.5%
F_{z2}	a,b,c,d	2	$F_{z2} = 4144.454-2.4V-0.0002V^3$	95.1%
F_{z3}	a,b,c,d	3	$F_{z3} = 6608.954-39.26V+0.00057V^3$	99.7%
F_{z4}	a,b,c,d	4	$F_{z4} = 5150.5-28.24V+0.000665V^3$	99.6%
F_{z5}	a	1,2,3,4	$F_{z5} = 2285.67+6058.674f-18685.48f^3$	84.918%
F_{z6}	b	1,2,3,4	$F_{z6} = 3233.33-1952.366f^2+2732.173f^3$	29.99%
F_{z7}	c	1,2,3,4	$F_{z7} = 749.58+5425.141f+2839.118f^3$	98.60%
F_{z8}	d	1,2,3,4	$F_{z8} = 774.318+3014.72f+9847.47f^2$	99.95%

Material EN26 53Rc

Table (6.5) Summary of computer results of predicted models of main cutting force

Type of force N	$V_{m/min}$	f mm/rev	Regression model	Multiple R
Feed Force F_x				
F_{x1}	a,b,c,d	1	$F_{x1} = 2588.123-0.0627V^2+0.0003026V^3$	99.98%
F_{x2}	a,b,c,d	2	$F_{x2} = 2473.983-7.125V+0.00019V^3$	81.08%
F_{x3}	a,b,c,d	3	$F_{x3} = 2034.4+0.000081V^3$	97.14%
F_{x4}	a,b,c,d	4	$F_{x4} = 1200.68+7.3478V-0.000064V^3$	57.4%
F_{x5}	a	1,2,3,4	$F_{x5} = 2622.83-2501.5f+1966.64f$	87.7%
F_{x6}	b	1,2,3,4	$F_{x6} = 2034.6+2924.46f^2-7109.96f^3$	51.5%
F_{x7}	c	1,2,3,4	$F_{x7} = 1593.673+5359f-7304.17f^2$	98.86%
F_{x8}	d	1,2,3,4	$F_{x8} = 2265.368+10500.4f^2-22673.8f^3$	96.547%

Material EN26 46Rc

Table (6.6) Summary of computer results of predicted models of feed force

Type of force N	V m/min	f mm/rev	Regression model	Multiple R
Radial force F				
F_{y1}	a,b,c,d	1	$F_{y1} = 6077.777-42.2V+0.000772V^2$	97.09%
F_{y2}	a,b,c,d	2	$F_{y2} = 4098.43-21.88V+0.0005V^3$	99.9%
F_{y3}	a,b,c,d	3	$F_{y3} = 4122.225-17.97V+0.000412V^3$	99.7%
F_{y4}	a,b,c,d	4	$F_{y4} = 8692.15-80.5V+0.2272V^2$	99.1%
F_{y5}	a	1,2,3,4	$F_{y5} = 3304.525-3833.772+18592.42f^3$	98.1%
F_{y6}	b	1,2,3,4	$F_{y6} = 2164.541+3195.16f^3-881.4773f^3$	90.8%
F_{y7}	c	1,2,3,4	$F_{y7} = 2864.193+2312.8f^2-2168.218f^3$	99.1%
F_{y8}	d	1,2,3,4	$F_{y8} = 3628.869+1482.2f^2-2764.16f^3$	80.9%

Material EN26 46Rc

Table 6.7 Summary of computer results of predicted models of radial force

Type of force N	V m/min	f mm/rev	Regressive model	Multiple R
Main cutting force(F_z)				
F_{z1}	a,b,c,d	1	$F_{z1} = 6587.904-41.97V+0.00659V^2+0.0004V^3$	99.8%
F_{z2}	a,b,c,d	2	$F_{z2} = 3333.88+7.2V-0.000363V^3$	99.0%
F_{z3}	a,b,c,d	3	$F_{z3} = 4534.4-12.74V+0.0000583V^3$	90.4%
F_{z4}	a,b,c,d	4	$F_{z4} = 2839.445+1.81V-0.000013V^3$	70.5%
F_{z5}	a	1,2,3,4	$F_{z5} = 2461.66+5056.1f-16071.83f^3$	84.0%
F_{z6}	b	1,2,3,4	$F_{z6} = 3217.84-4870.762f+7545.43f^2$	94.5%
F_{z7}	c	1,2,3,4	$F_{z7} = 635.7+7619.4f-4745f^2$	94.1%
F_{z8}	d	1,2,3,4	$F_{z8} = 1204.81+1798.107+3927.4f^2$	99.9%

Material EN26 $46R_C$

Table (6.8) Summary of computer results of predicted models of main cutting force

6.16 CHAPTER CLOSURE

The cutting performance of commercially available Kyon 2000 ceramic inserts was studied when machining high strength hardened alloy steel under a wide range of cutting conditions. Results were explained on a theoretical and experimental basis.

Four main tool failure modes were recognised:

a) flank and crater wear

b) grooving wear

c) deformation wear and

d) brittle failure.

Furthermore, a statistical analysis of the results obtained were carried out. A very good correlation between the process variables was achieved.

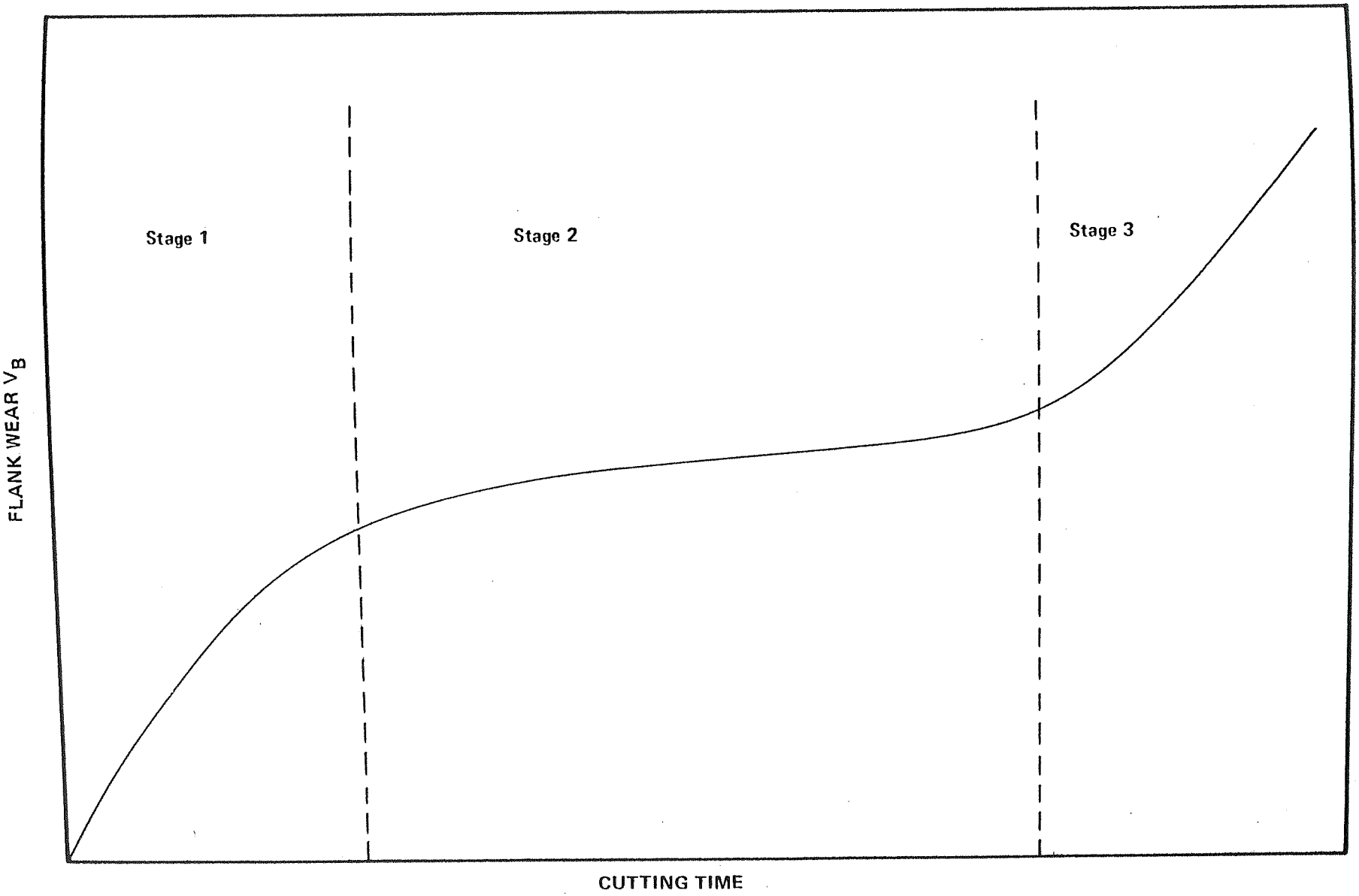

Figure 6.1 Typical Flank Wear Curve

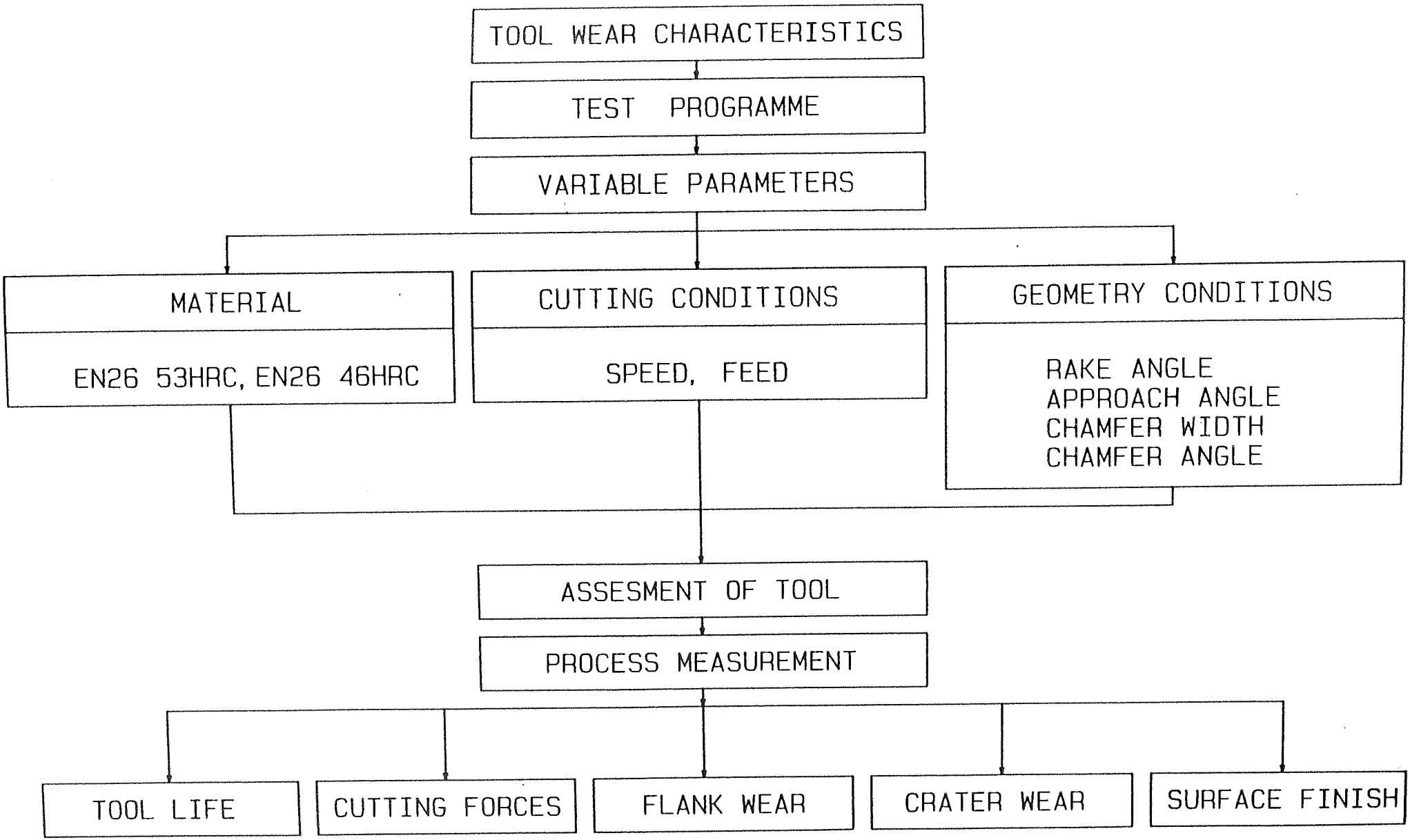

Figure 6.2 Block Diagram of Work Plan

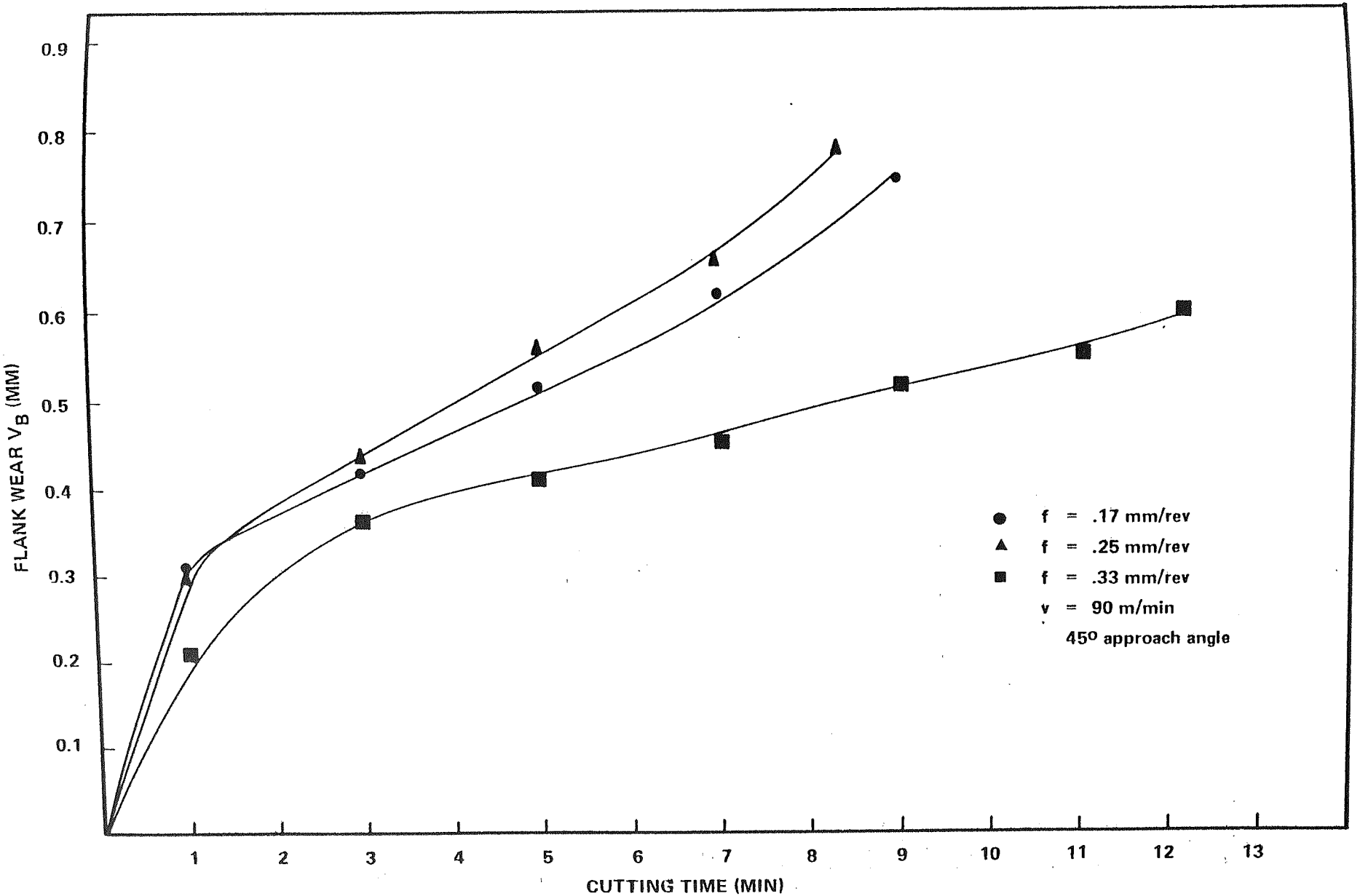

Figure 6.3 Influence of Feed Rates on Flank Wear

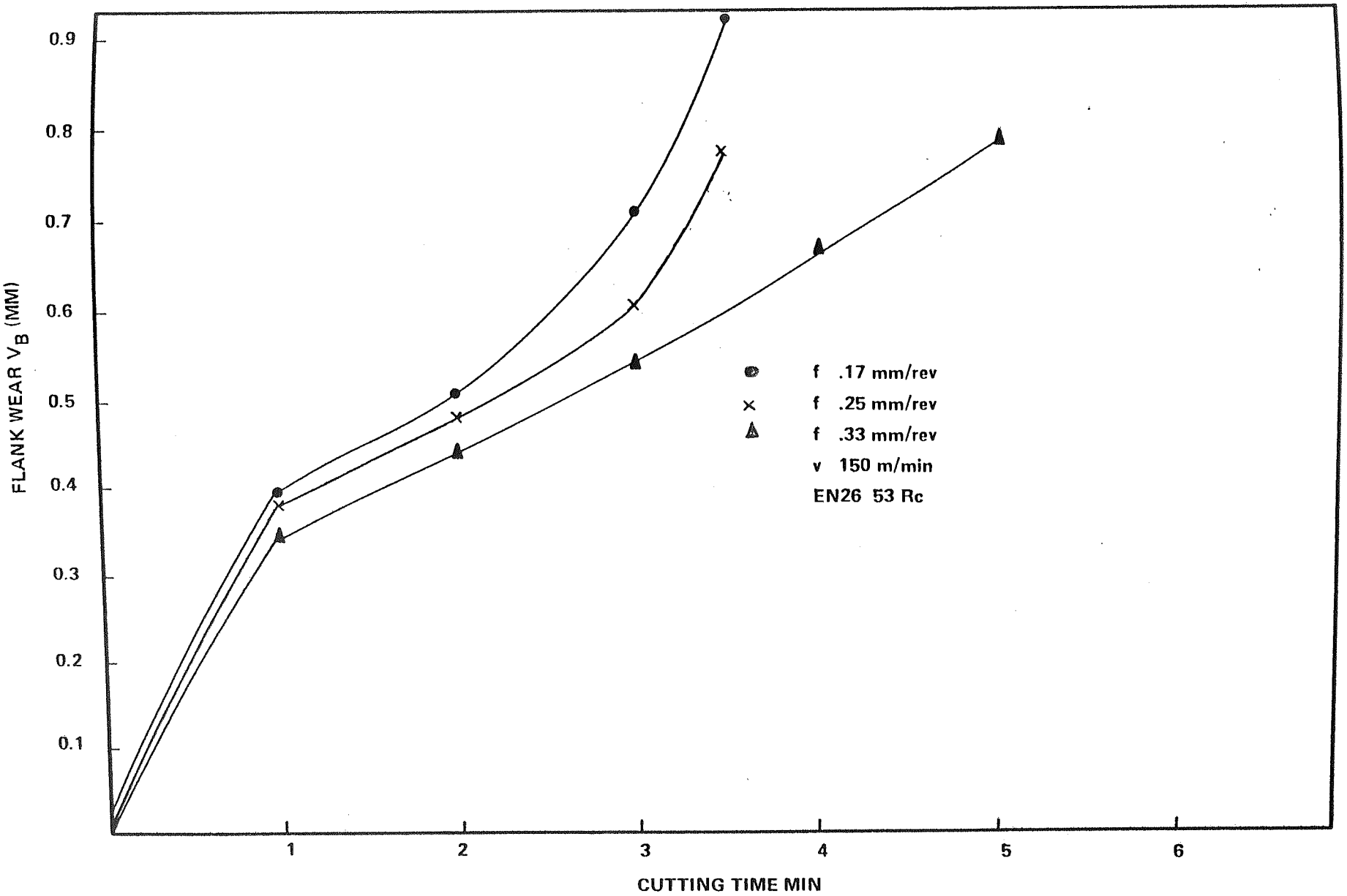

Figure 6.4 Influence of Feed Rates on Flank Wear

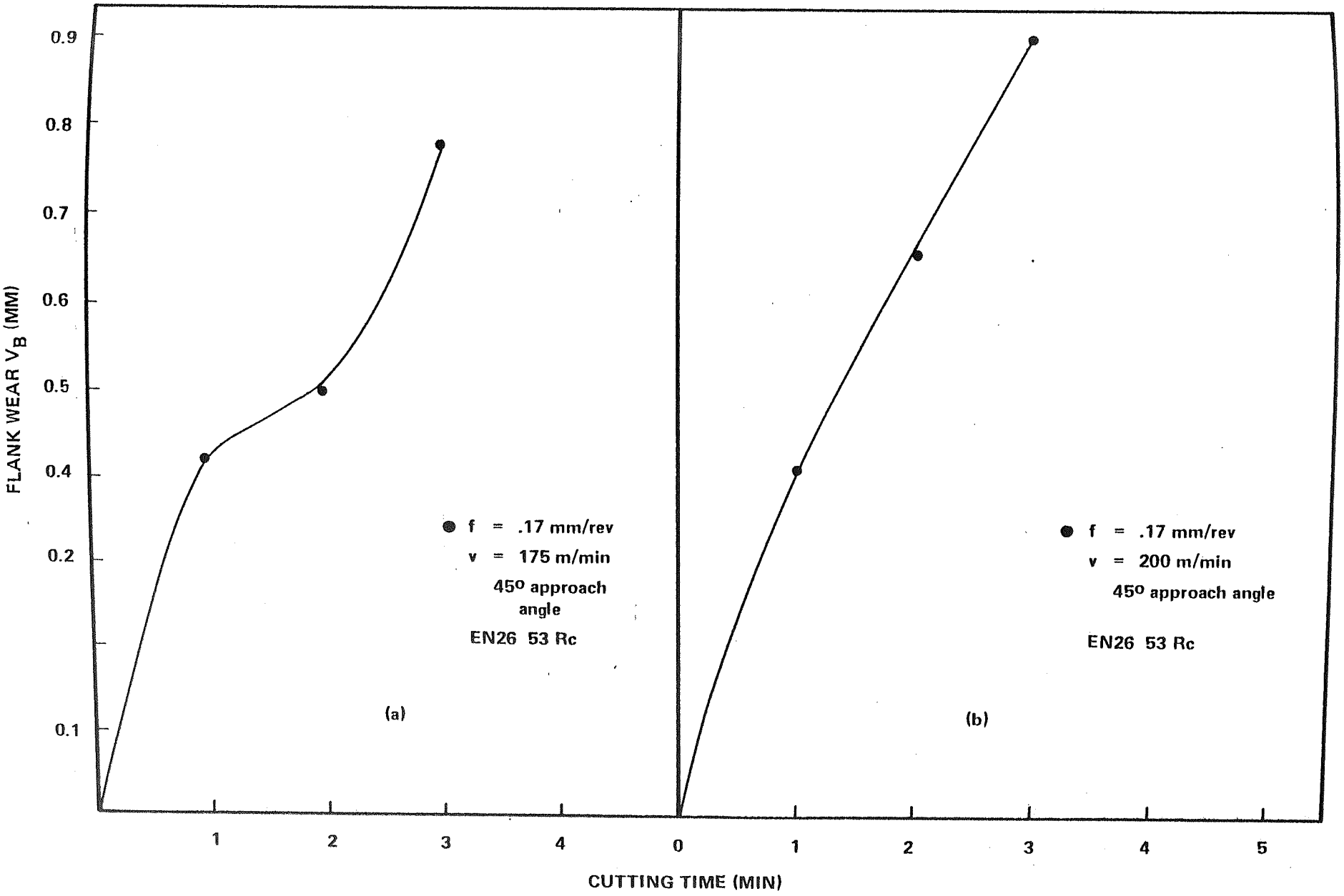

Figure 6.5 Influence of Feed Rates on Flank Wear

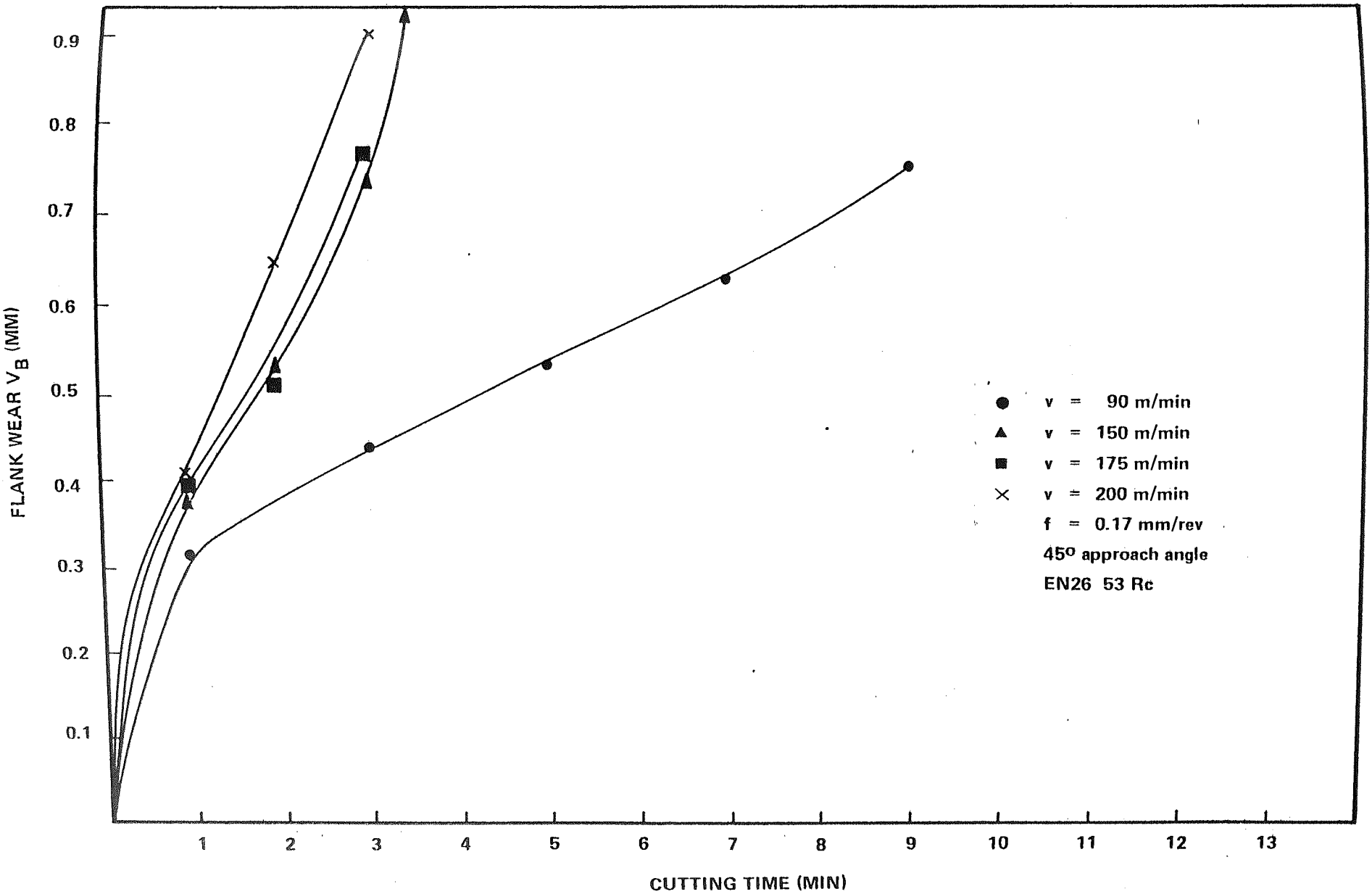

Figure 6.6 Influence of Cutting Speeds on Flank Wear

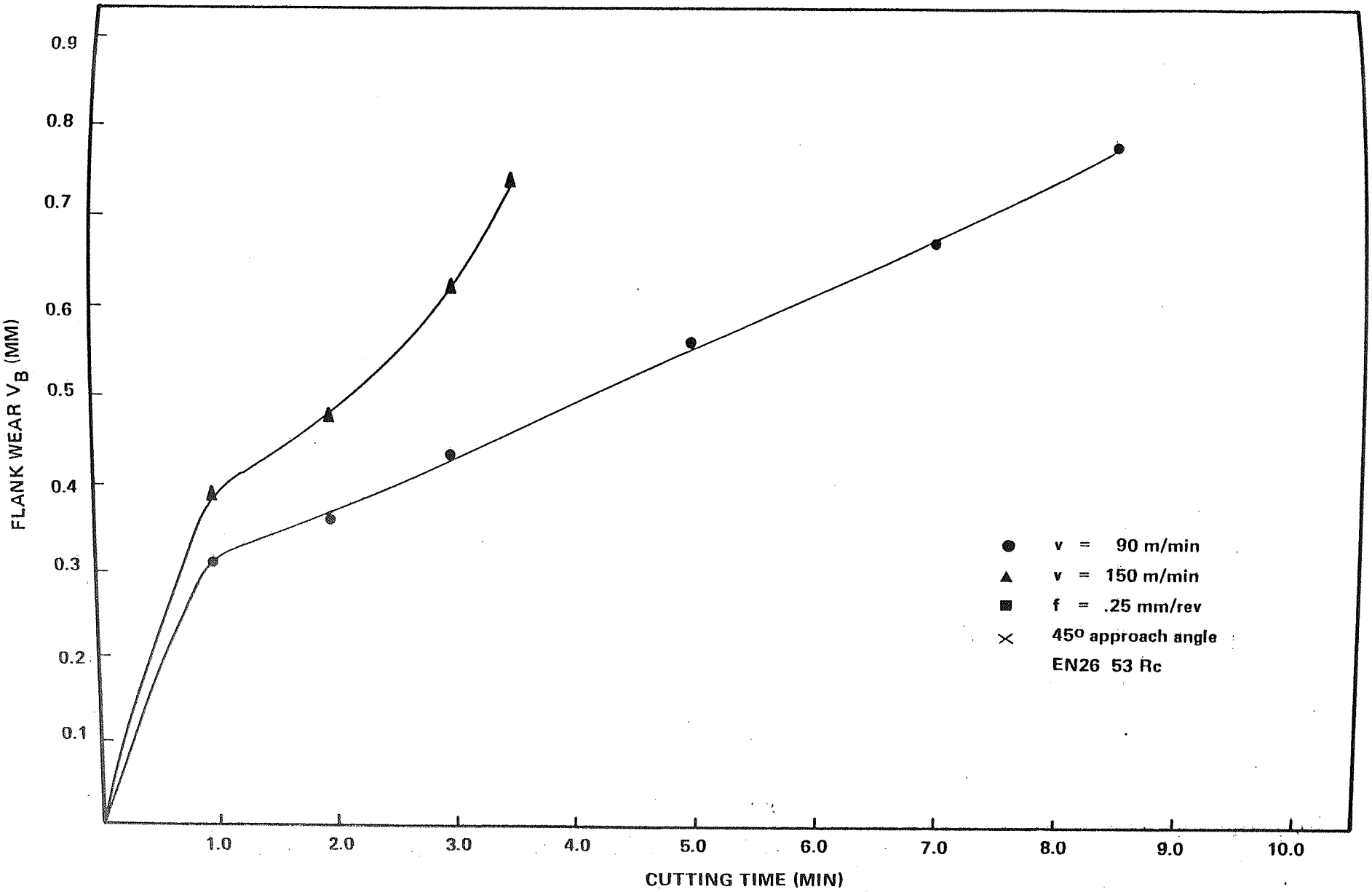

Figure 6.7 Influence of Cutting Speeds on Flank Wear

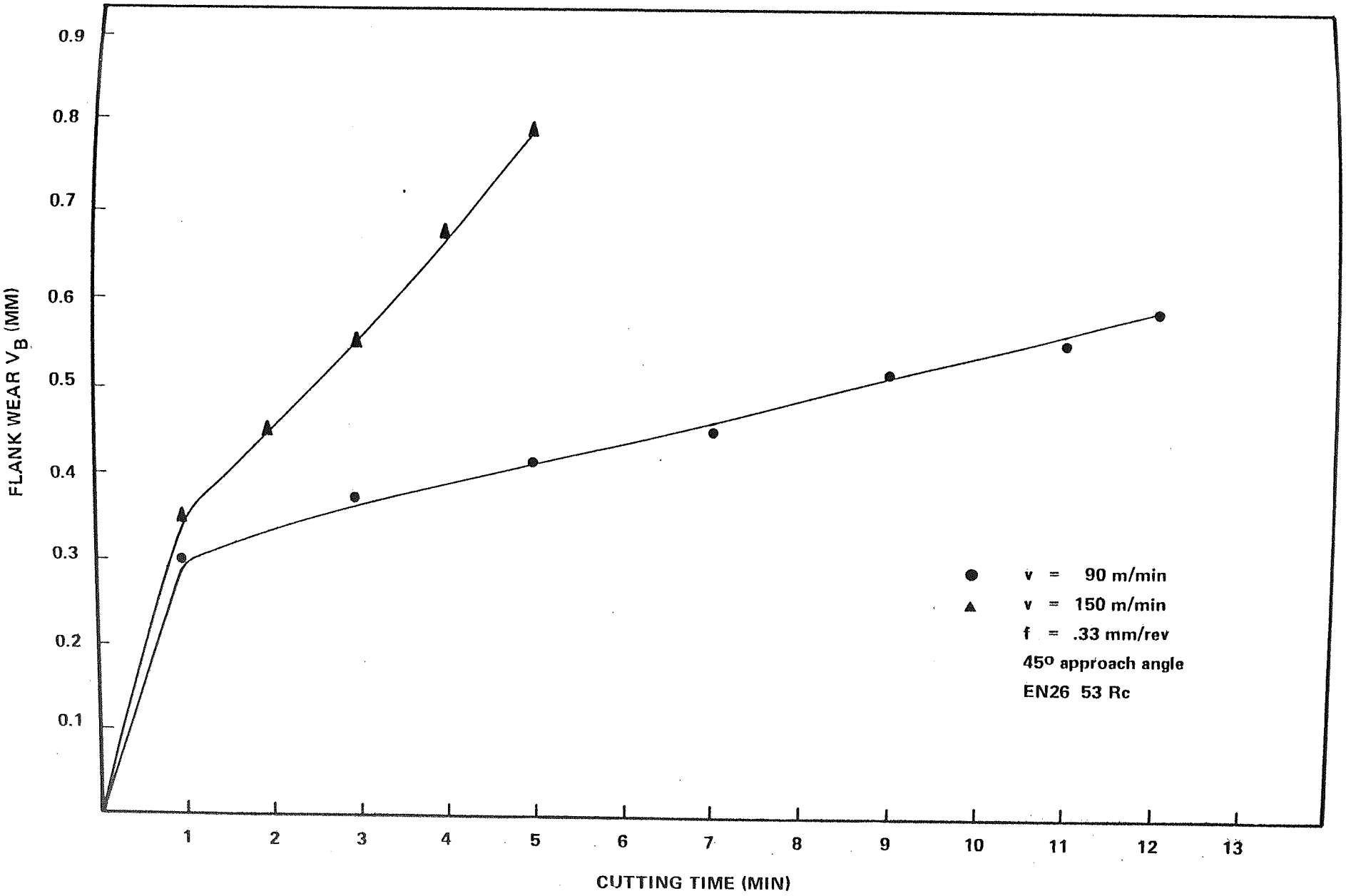

Figure 6.8 Influence of Cutting Speeds on Flank Wear

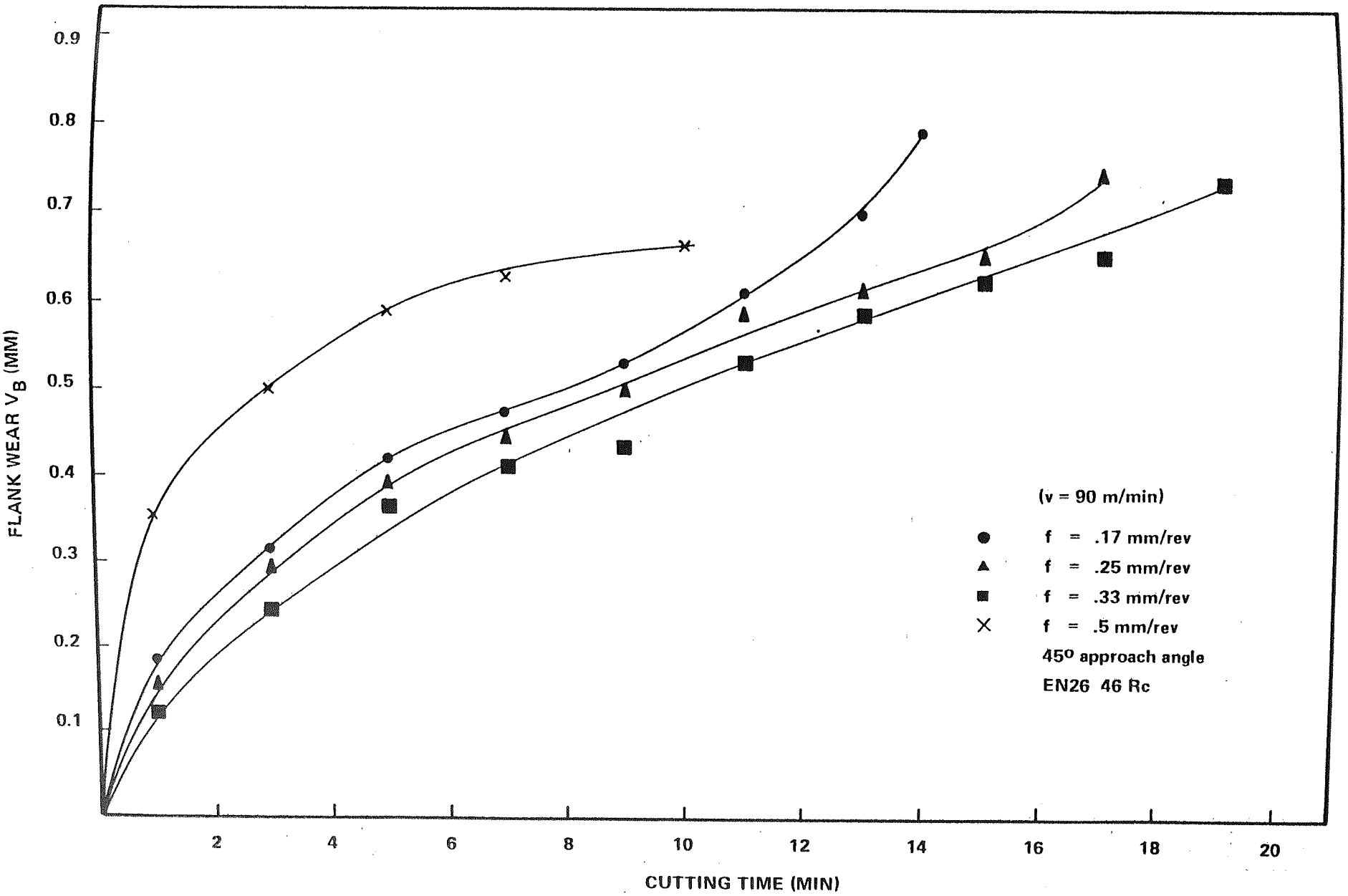

Figure 6.9 Influence of Feed Rates on Flank Wear

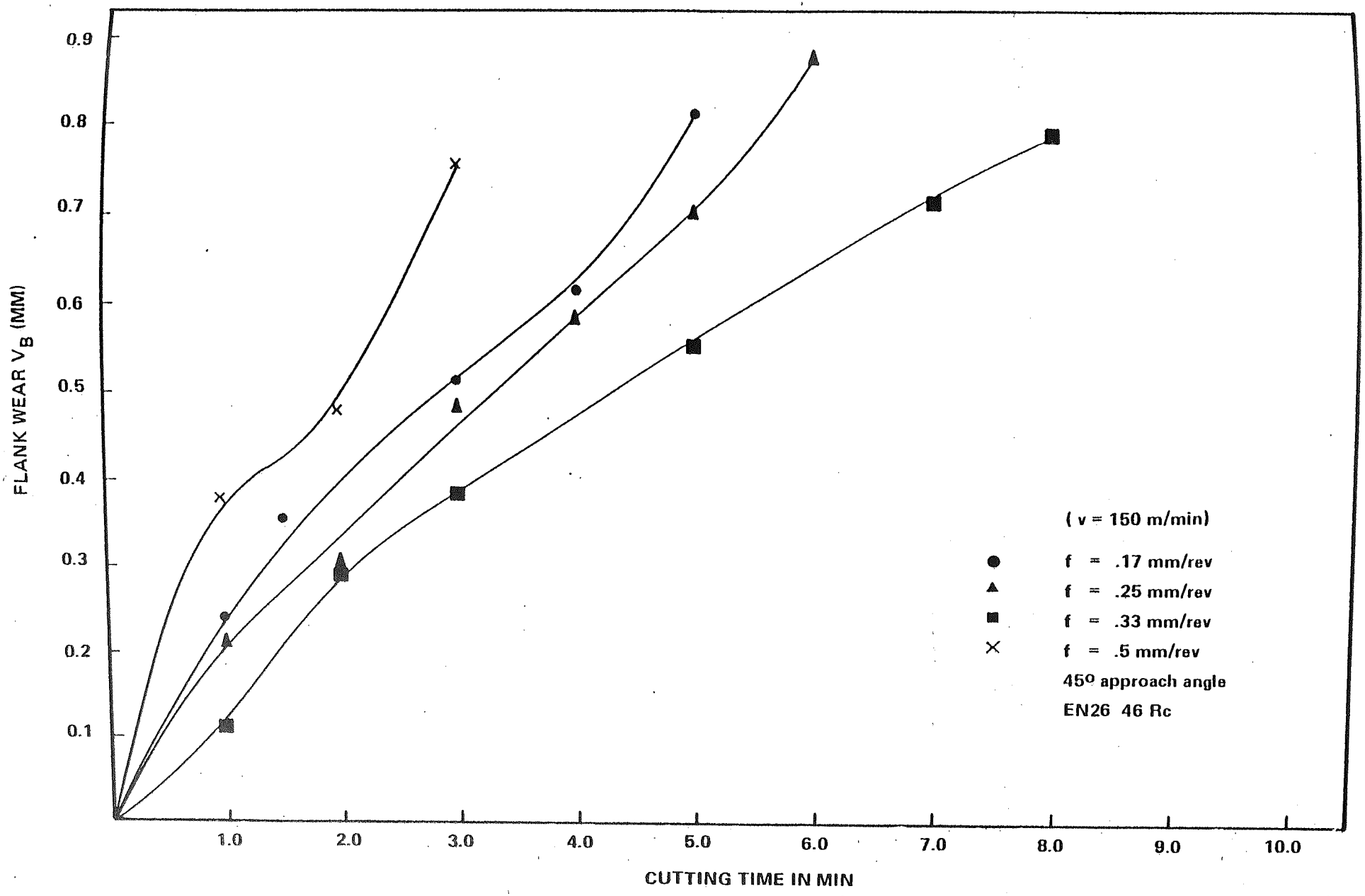

Figure 6.10 Influence of Feed Rates on Flank Wear

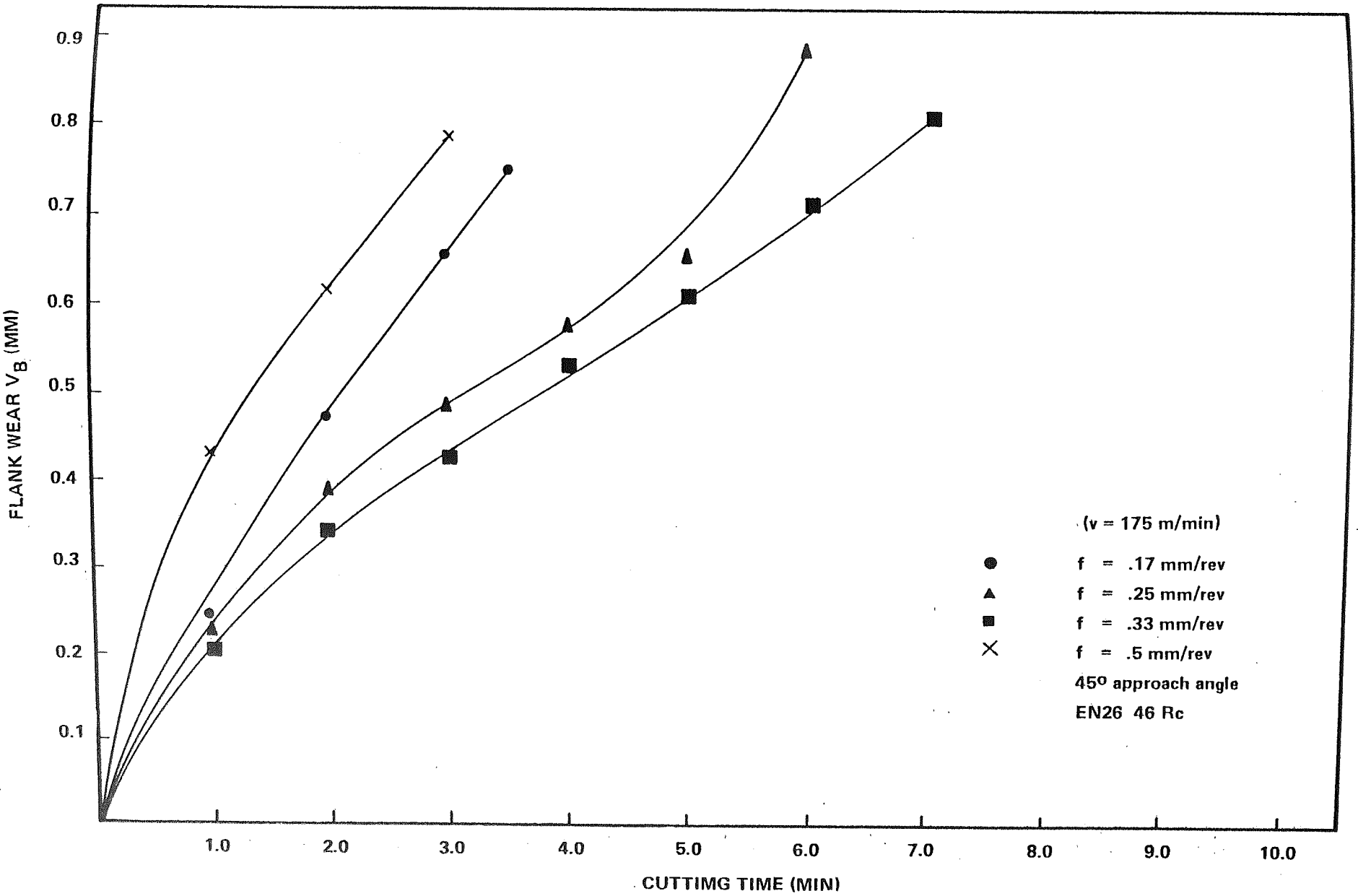

Figure 6.11 Influence of Feed Rates on Flank Wear

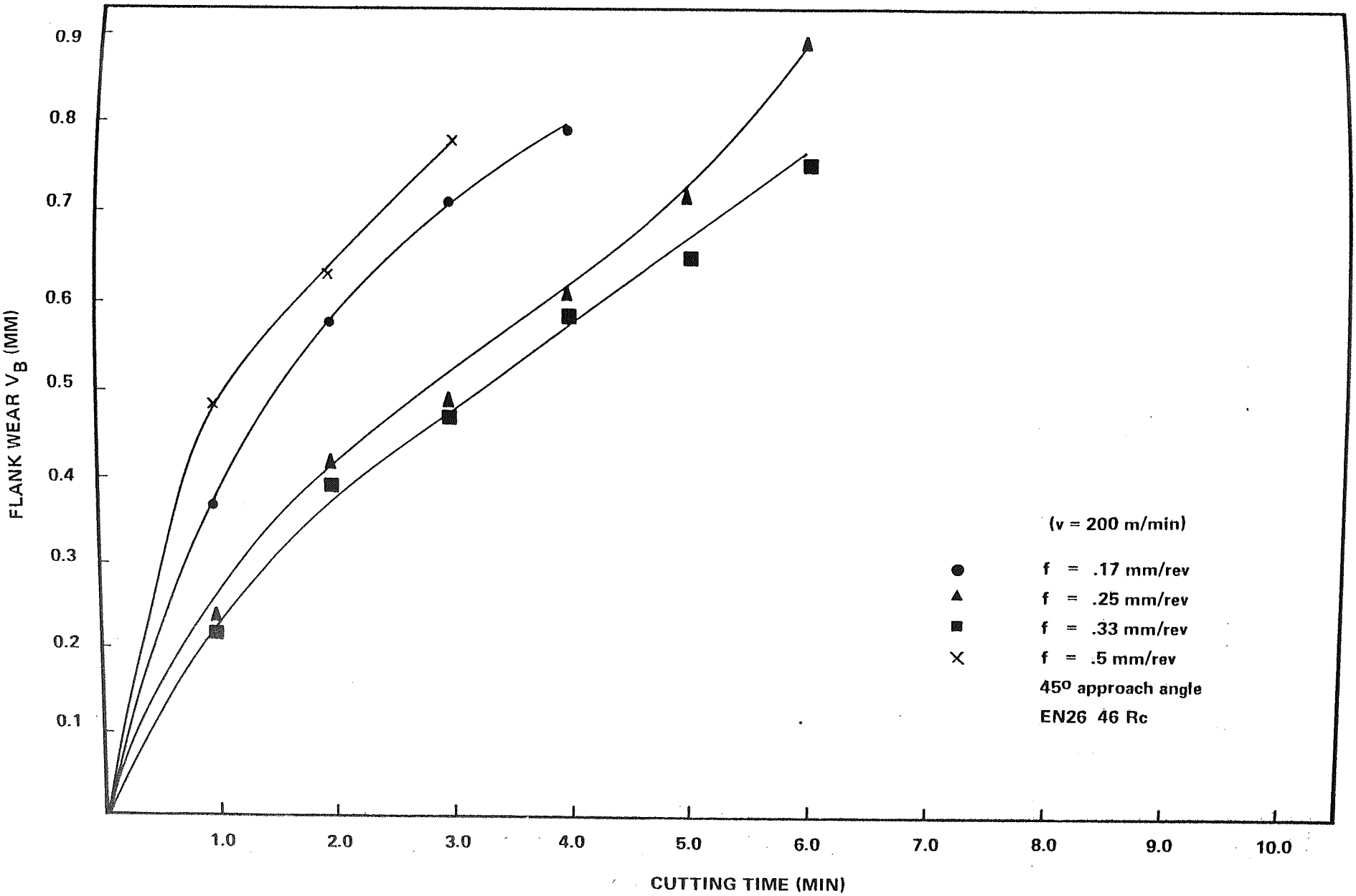

Figure 6.12 Influence of Feed Rates on Flank Wear

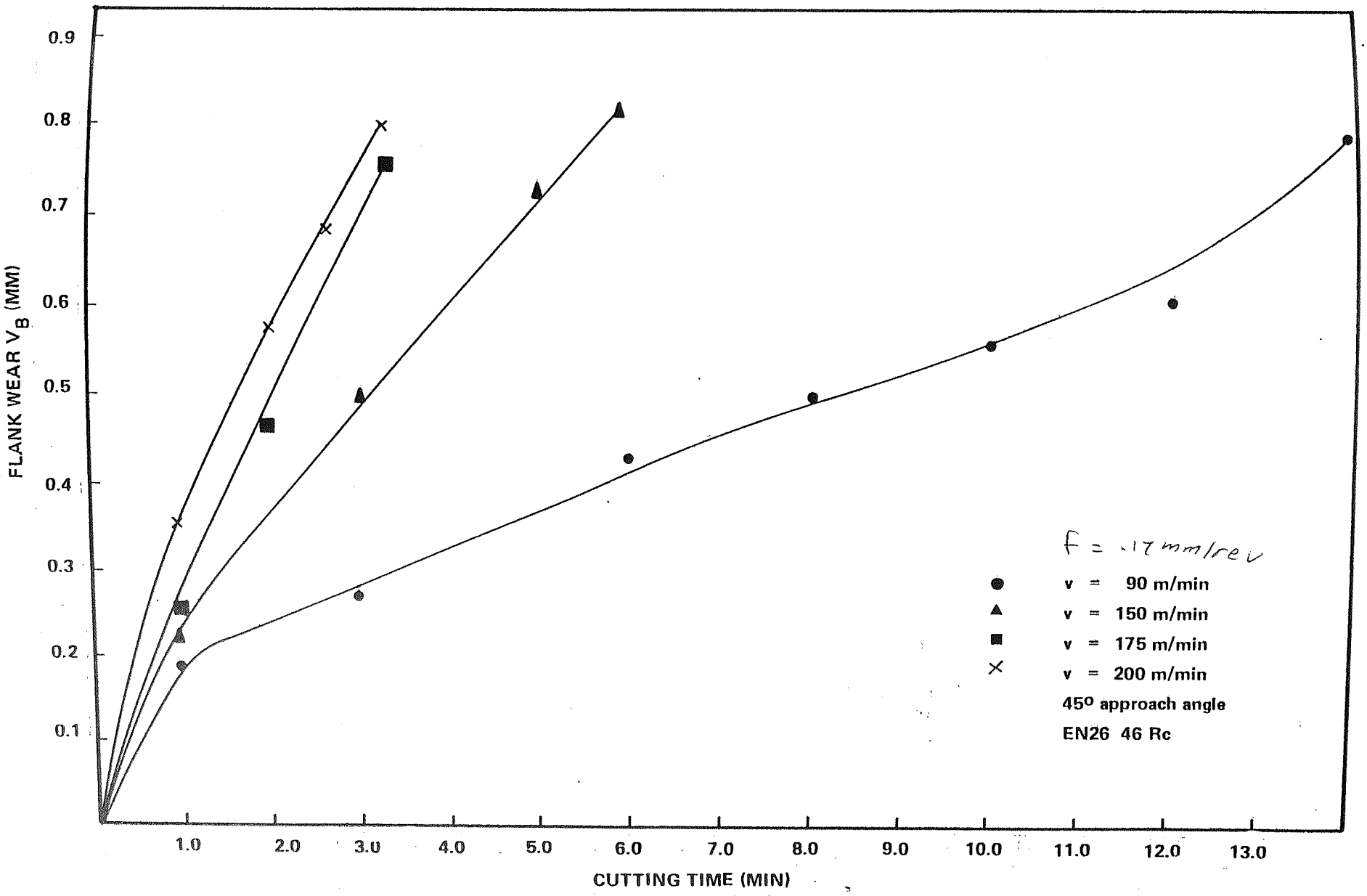

Figure 6.13 Influence of Cutting Speeds on Flank Wear EN26 46R_c

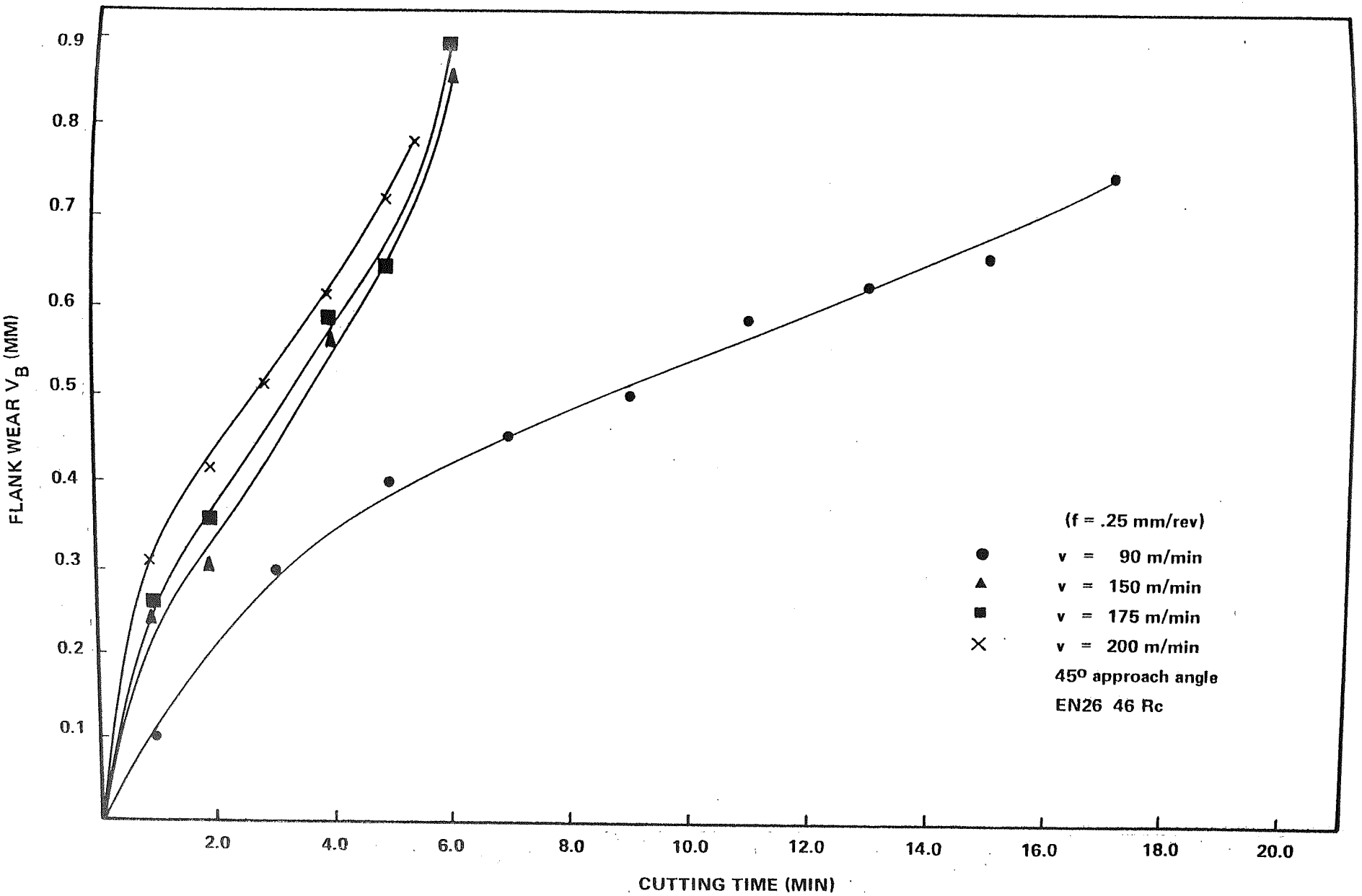

Figure 6.14 Influence of Cutting Speeds on Flank Wear

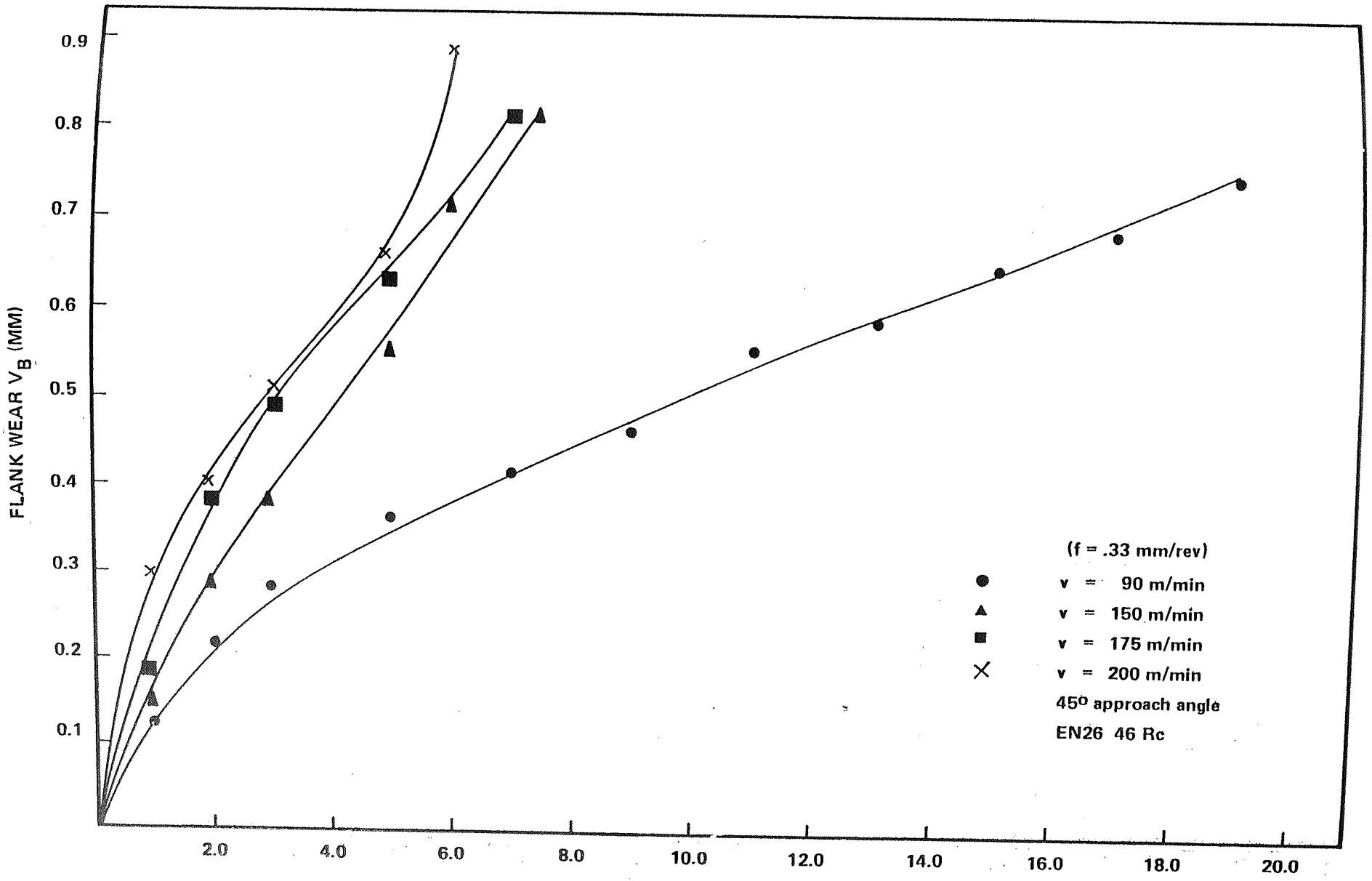

Figure 6.15 Influence of Cutting Speeds on Flank Wear

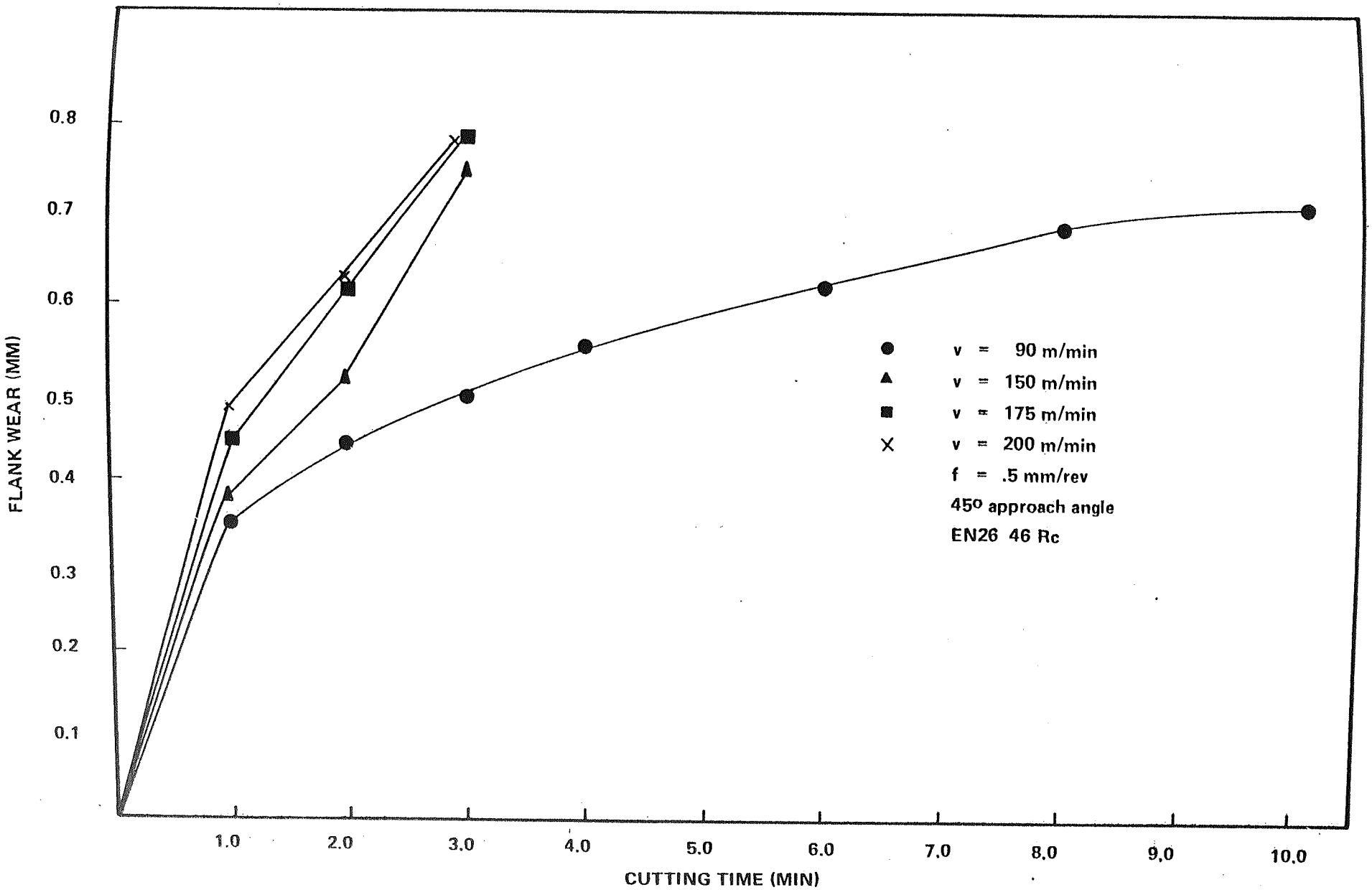

Figure 6.16 Influence of Cutting Speed on Flank Wear

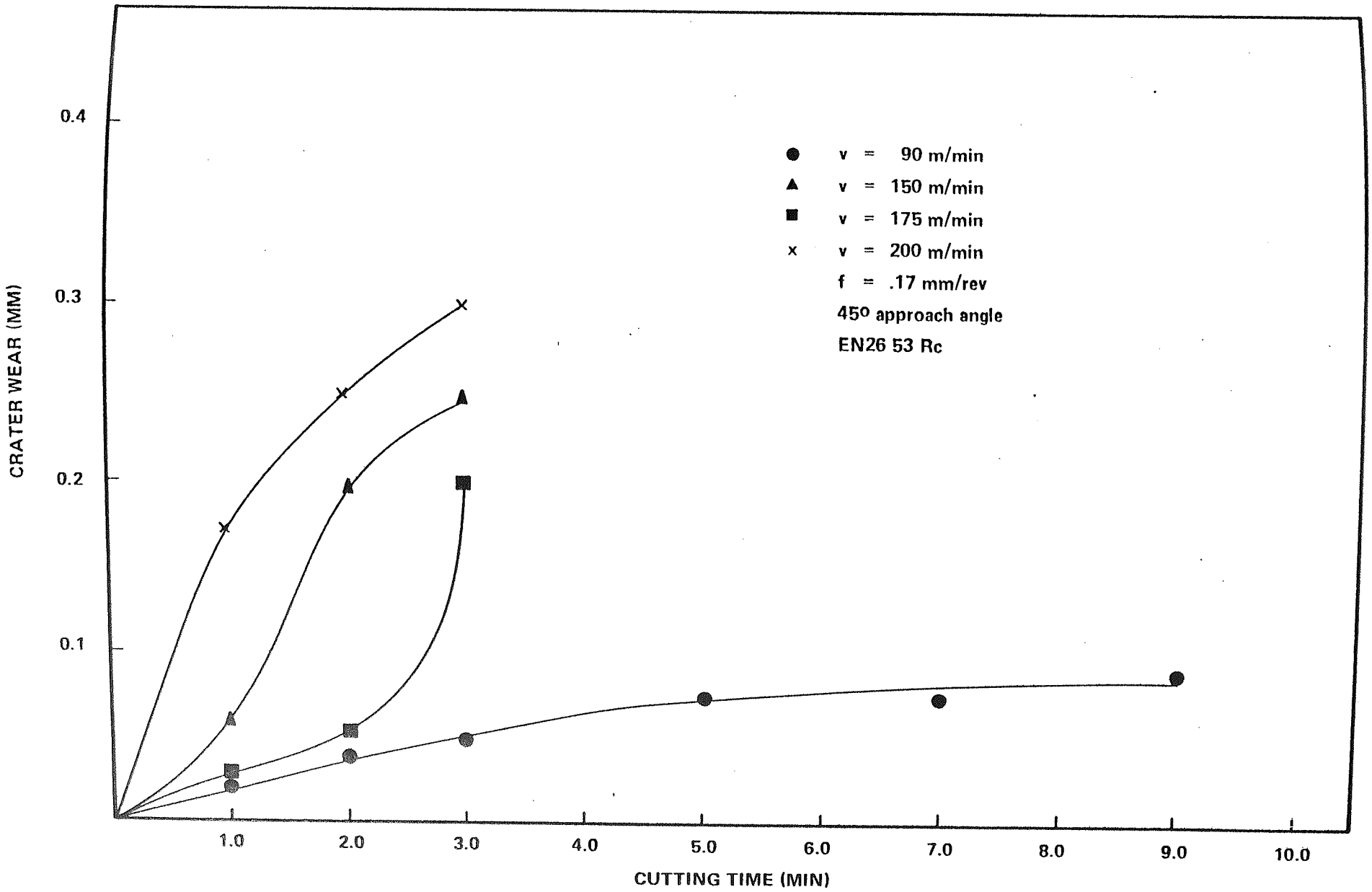

Figure 6.17 Influence of Cutting Speed on Crater Wear (EN26 53 Rc)

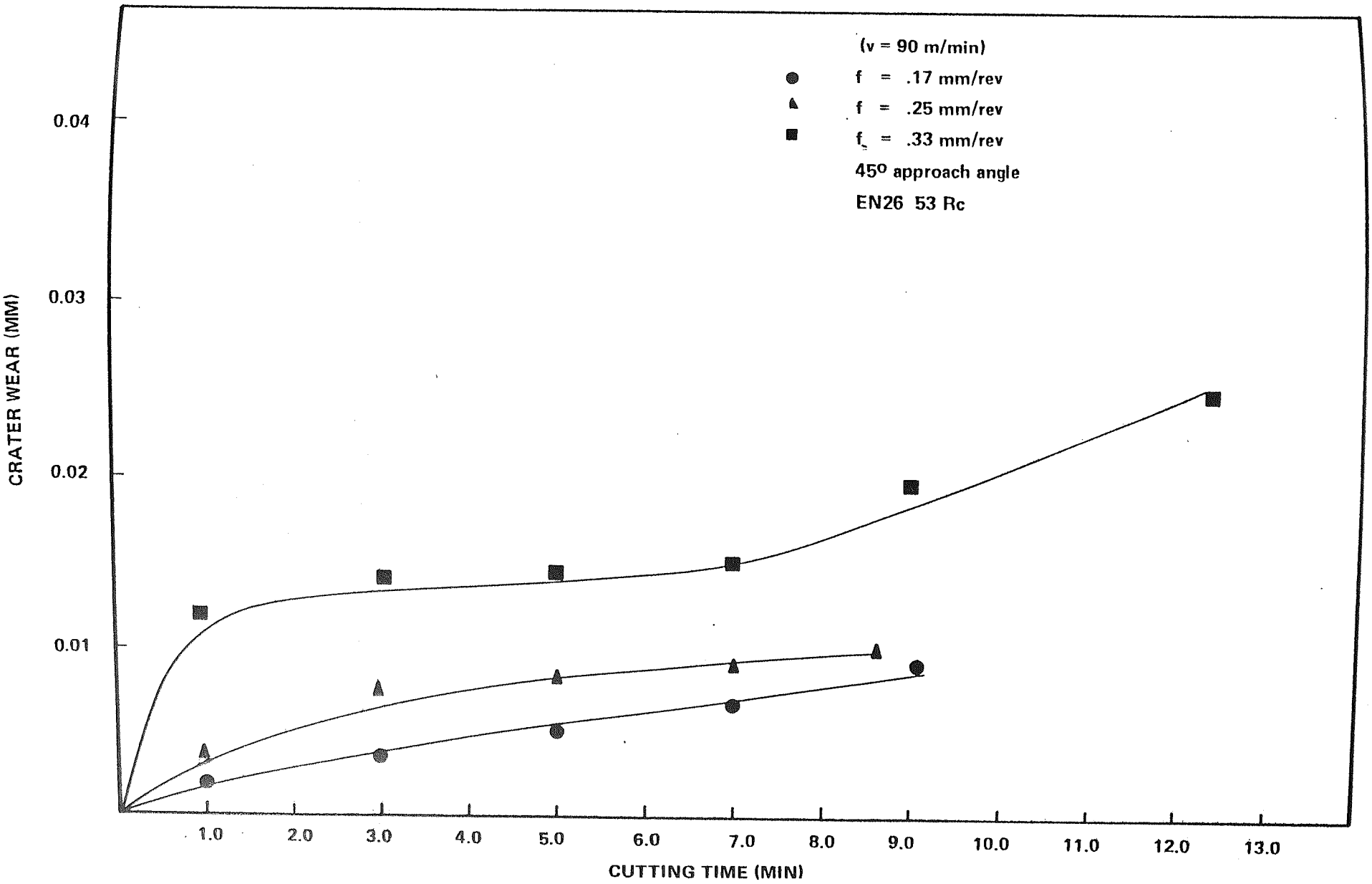

Figure 6.18 Influence of Feed Rates on Crater Wear EN26 53RC

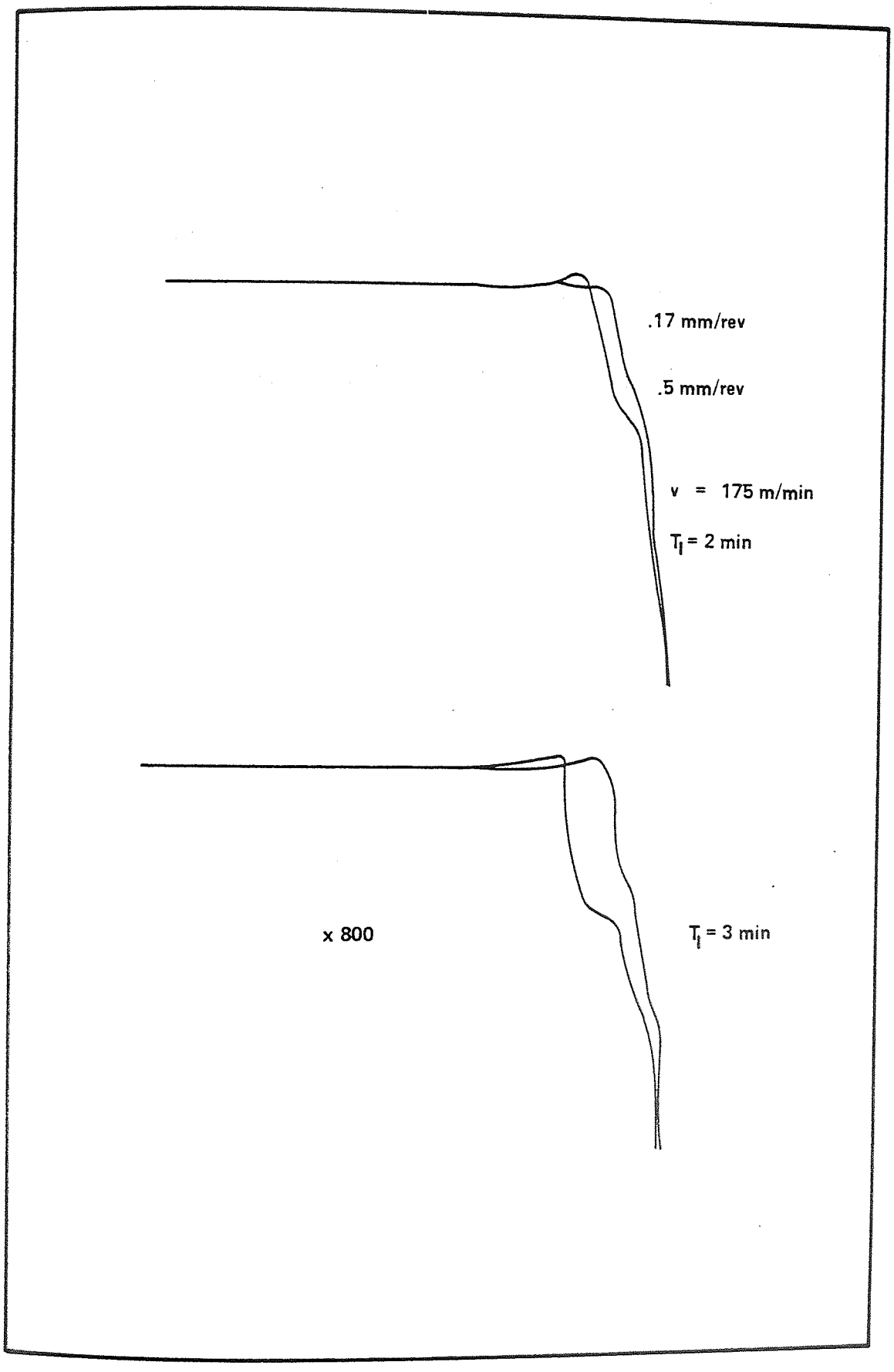

Figure 6.19 Influence of Feed Rates on Position of Crater

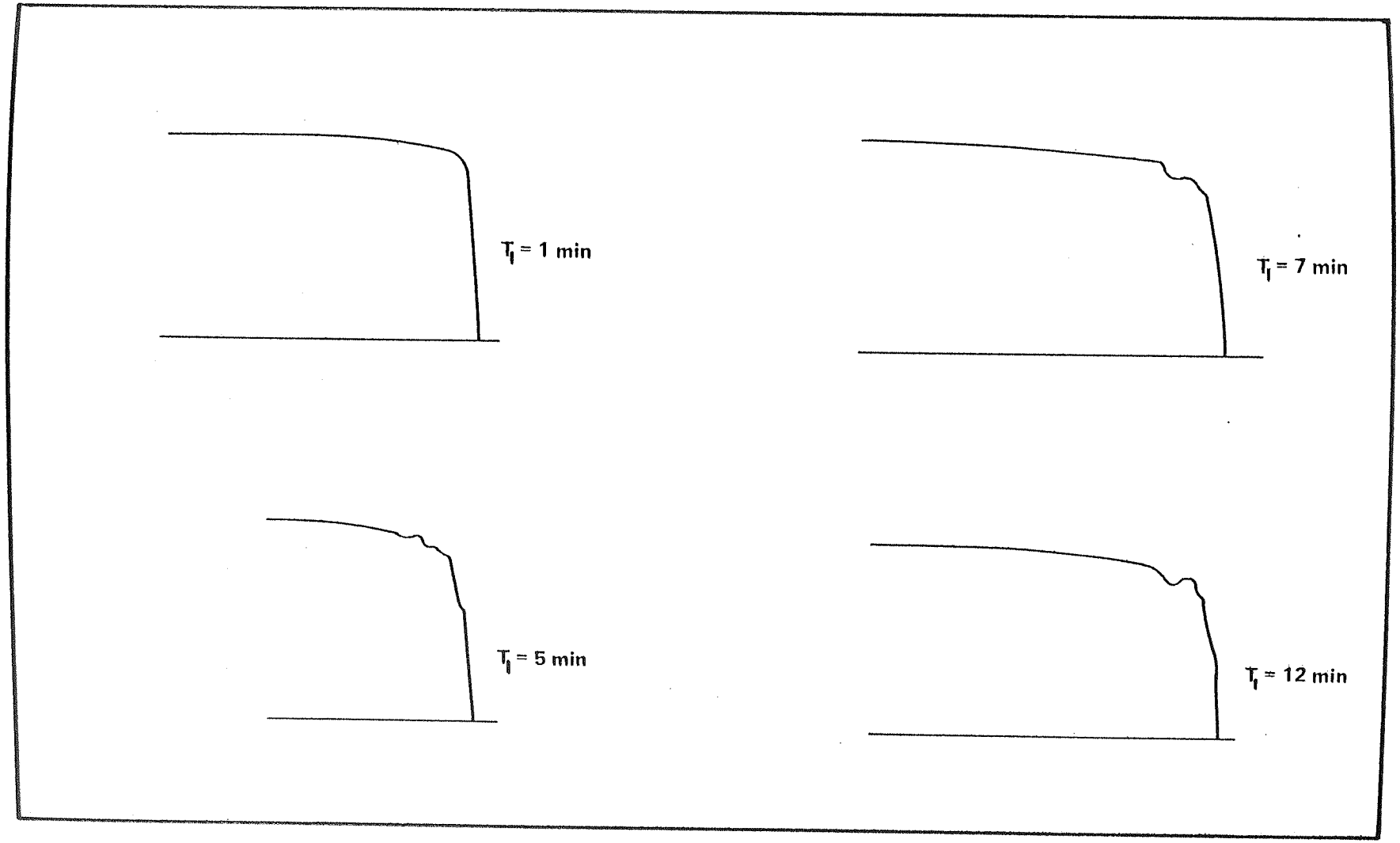

Figure 6.20 Trace of Crater Shape

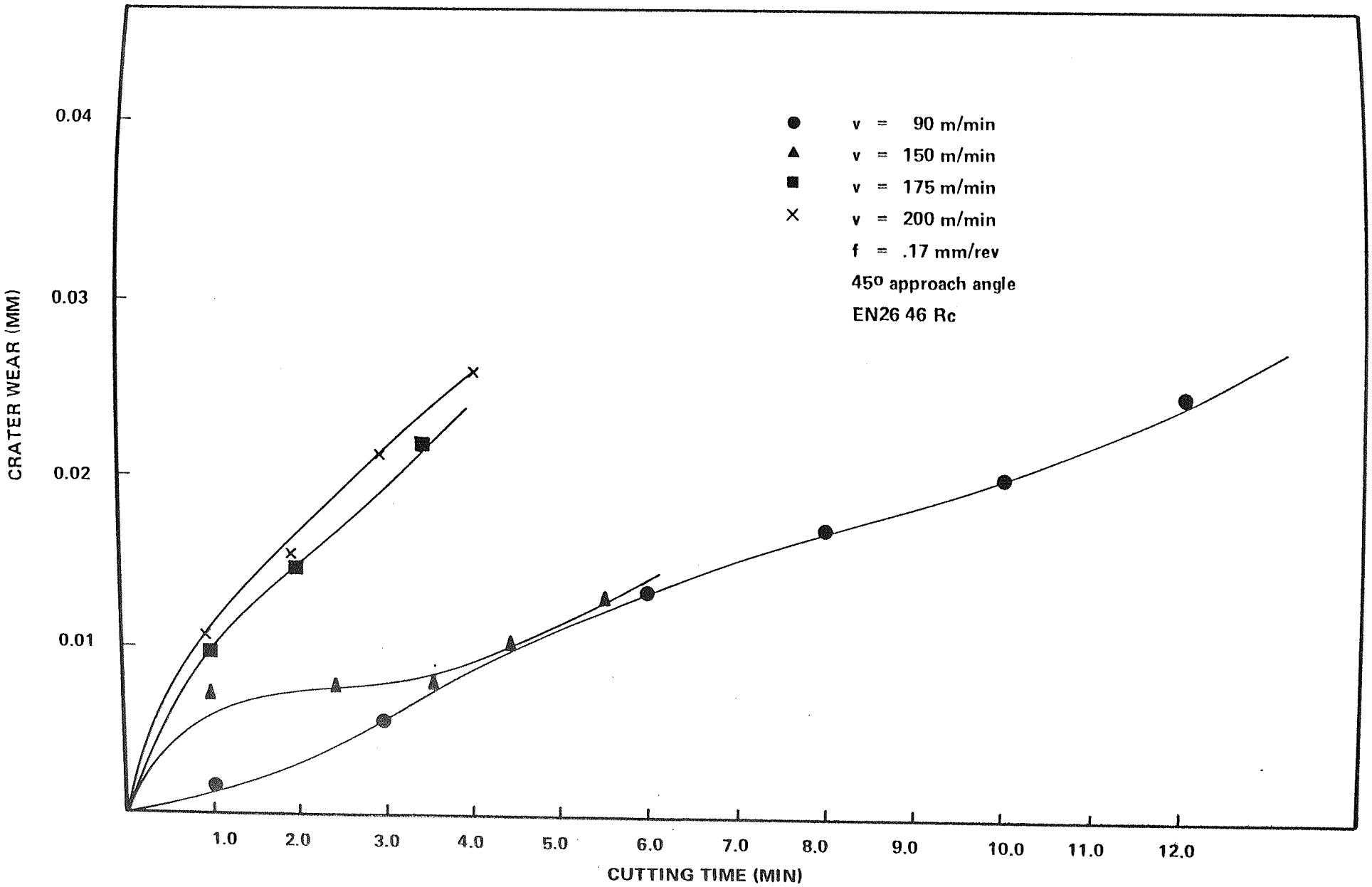

Figure 6.21 Influence of Cutting Speed on Crater Wear (EN26 46 Rc)

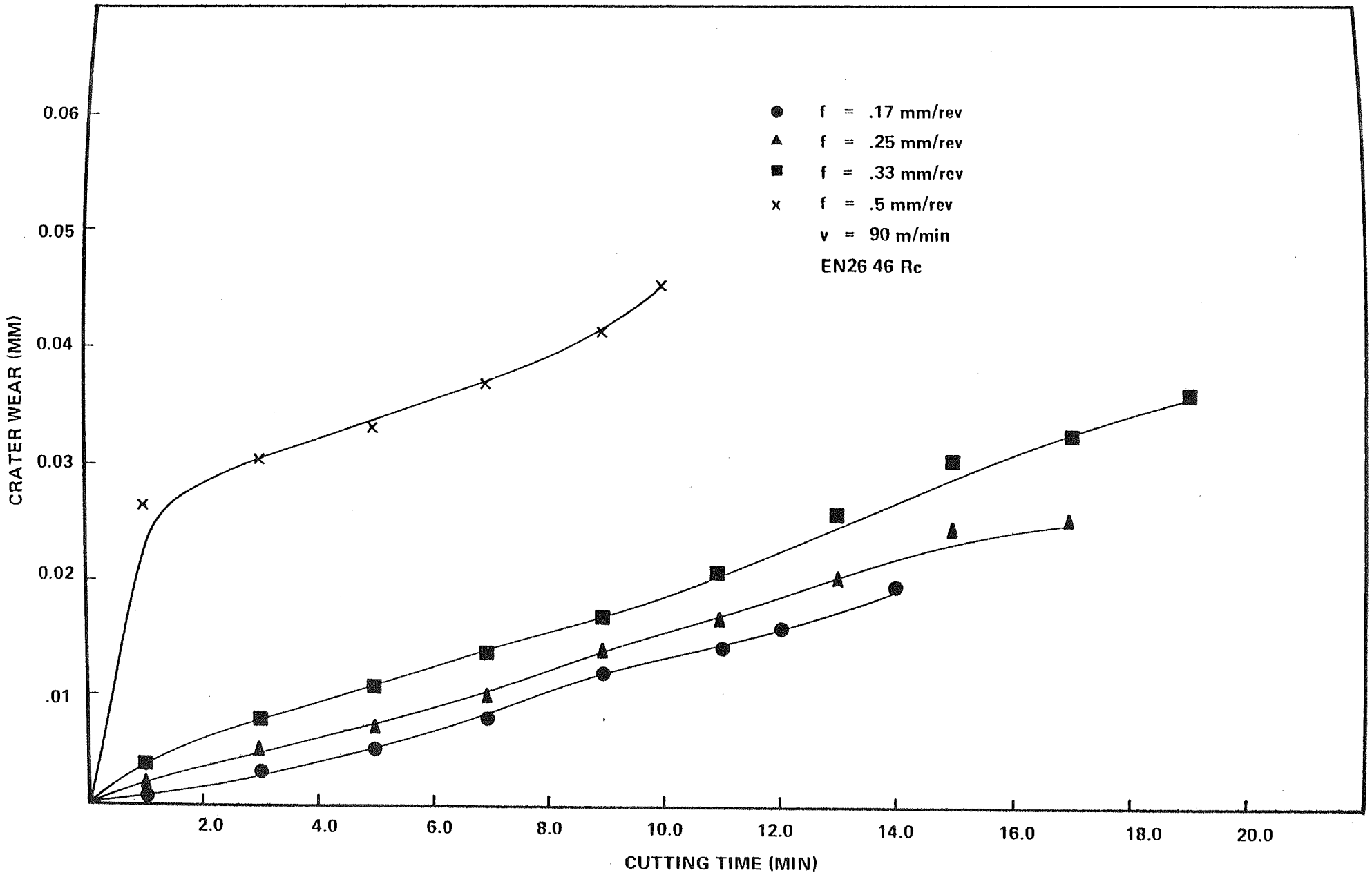

Figure 6.22 Influence of Feed Rates on Crater Wear EN26 46Rc

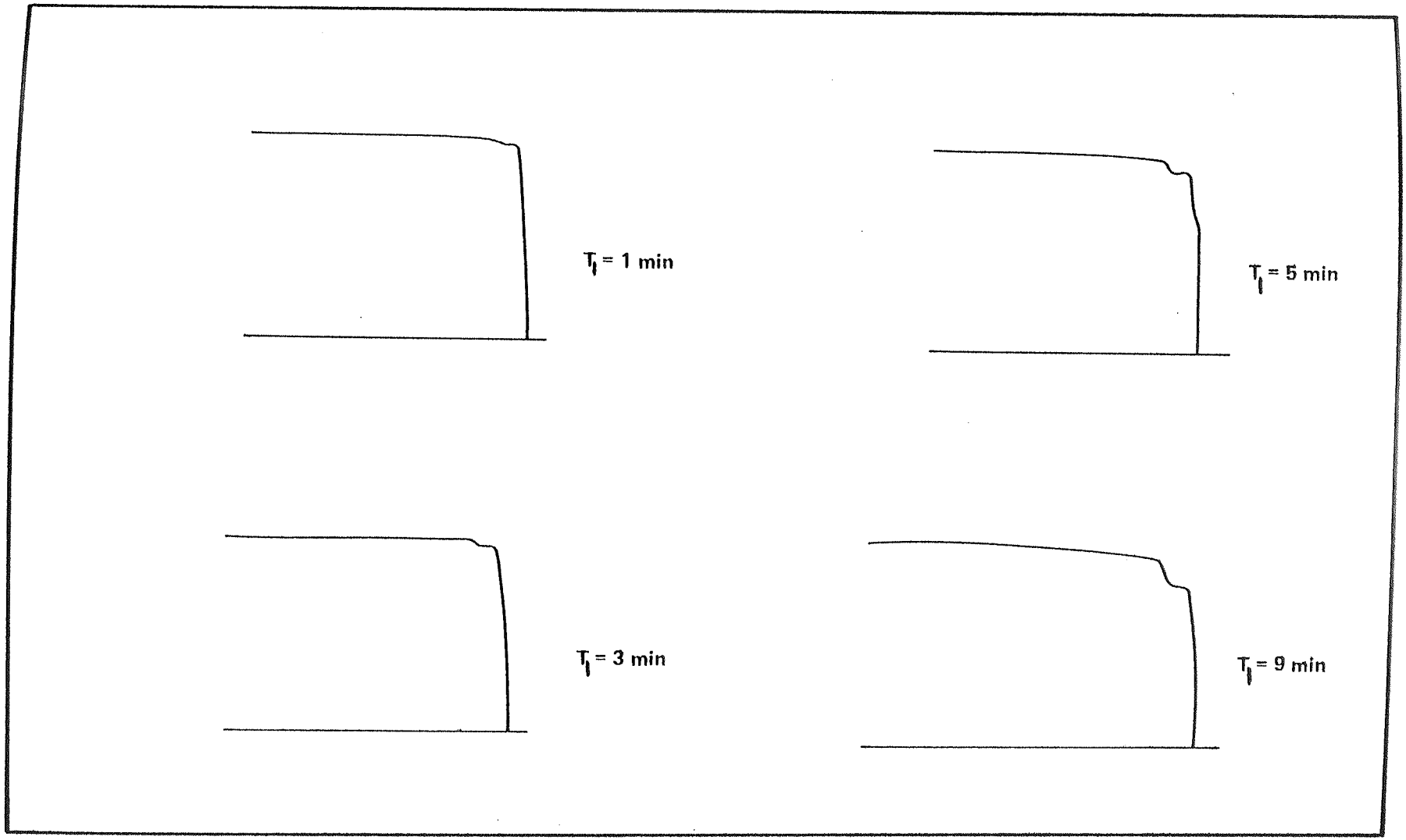

Figure 6.23a Trace of Crater Shape (v = 90 m/min, f = .25 mm/rev)

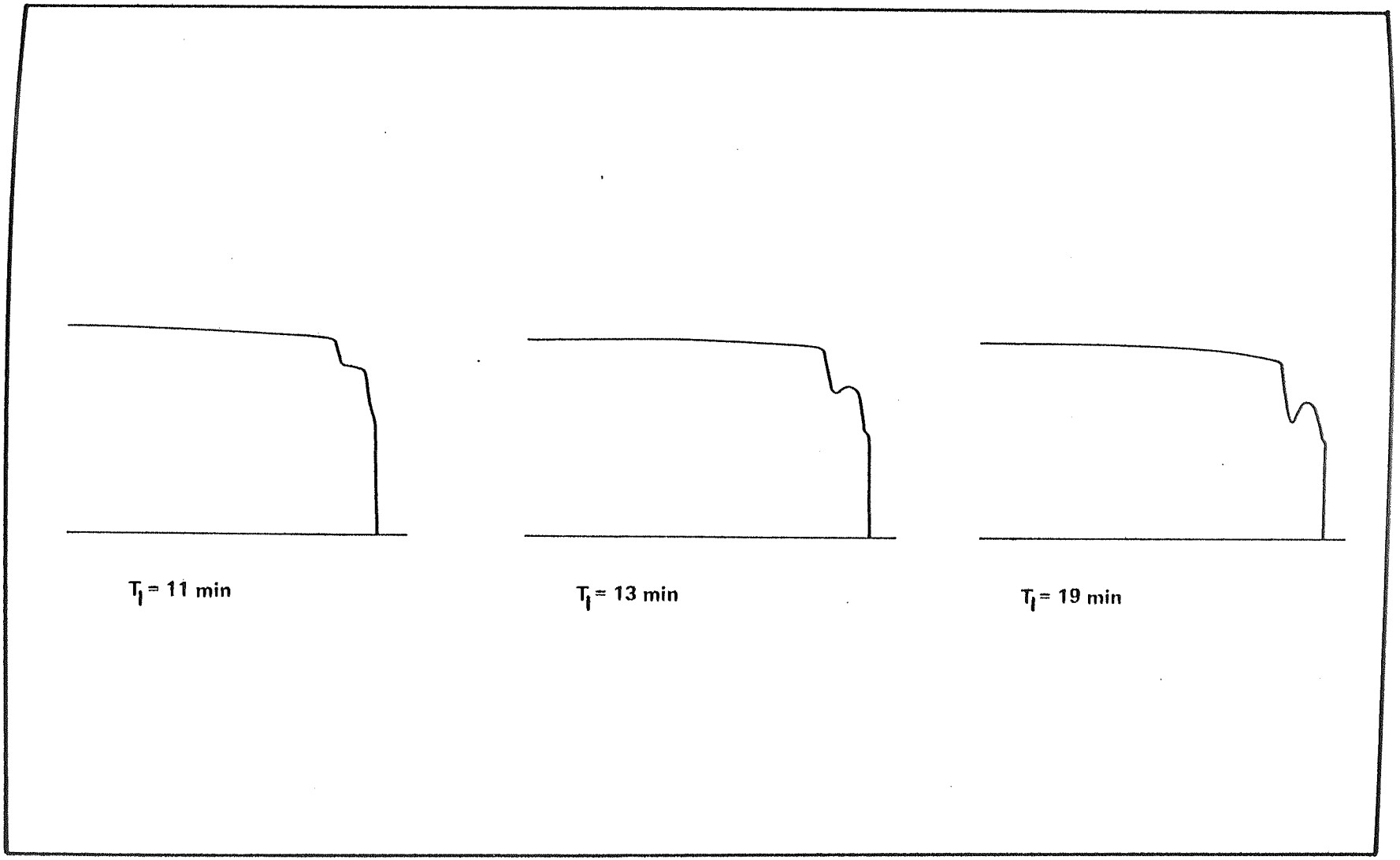

Figure 6.23b Trace of Crater Shape (v = 90 m/min, f = .25 mm/rev)

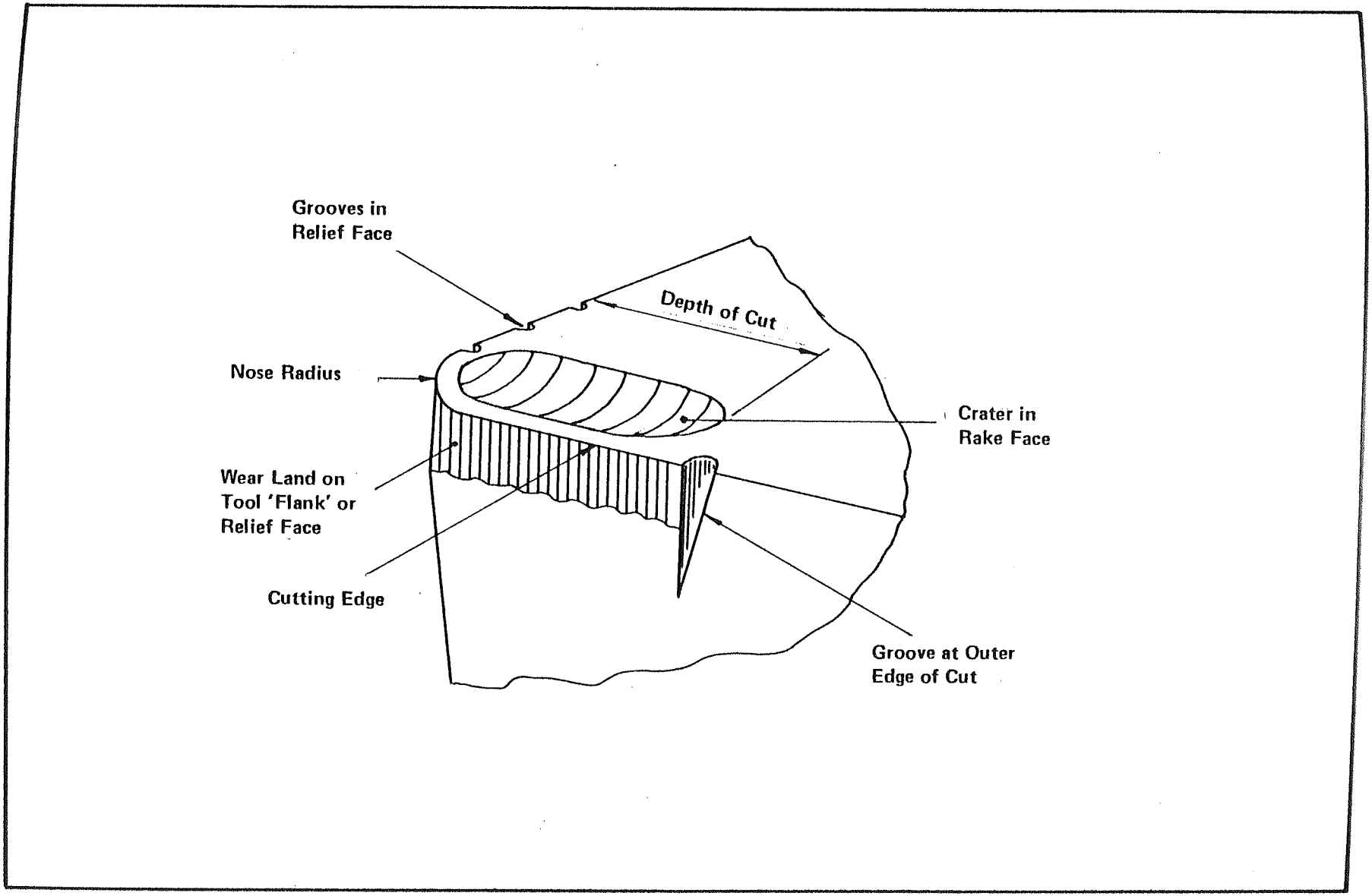

Figure 6.24 Leading and Trailing Edge Groove

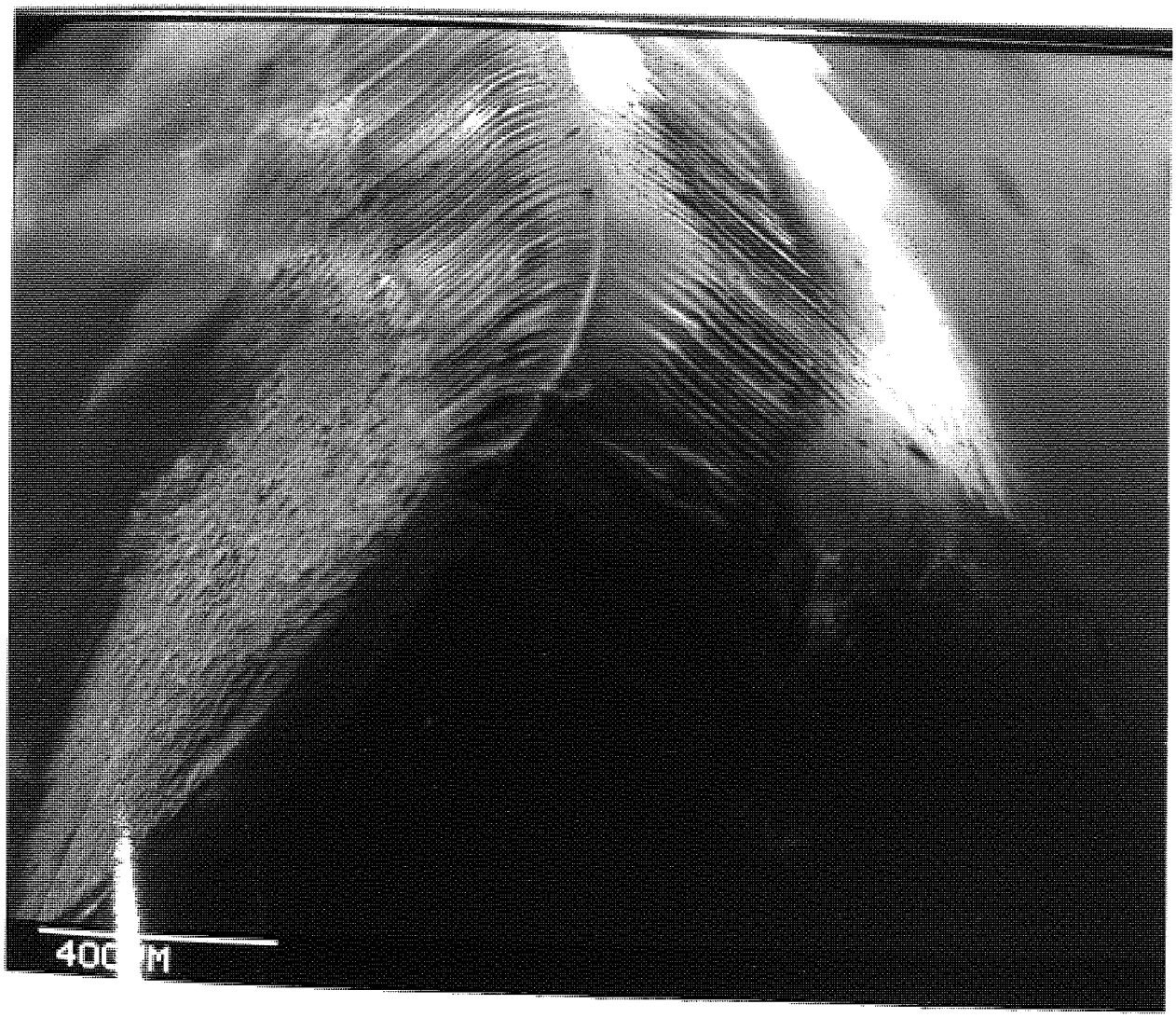

Figure 6.25 Trailing edge groove

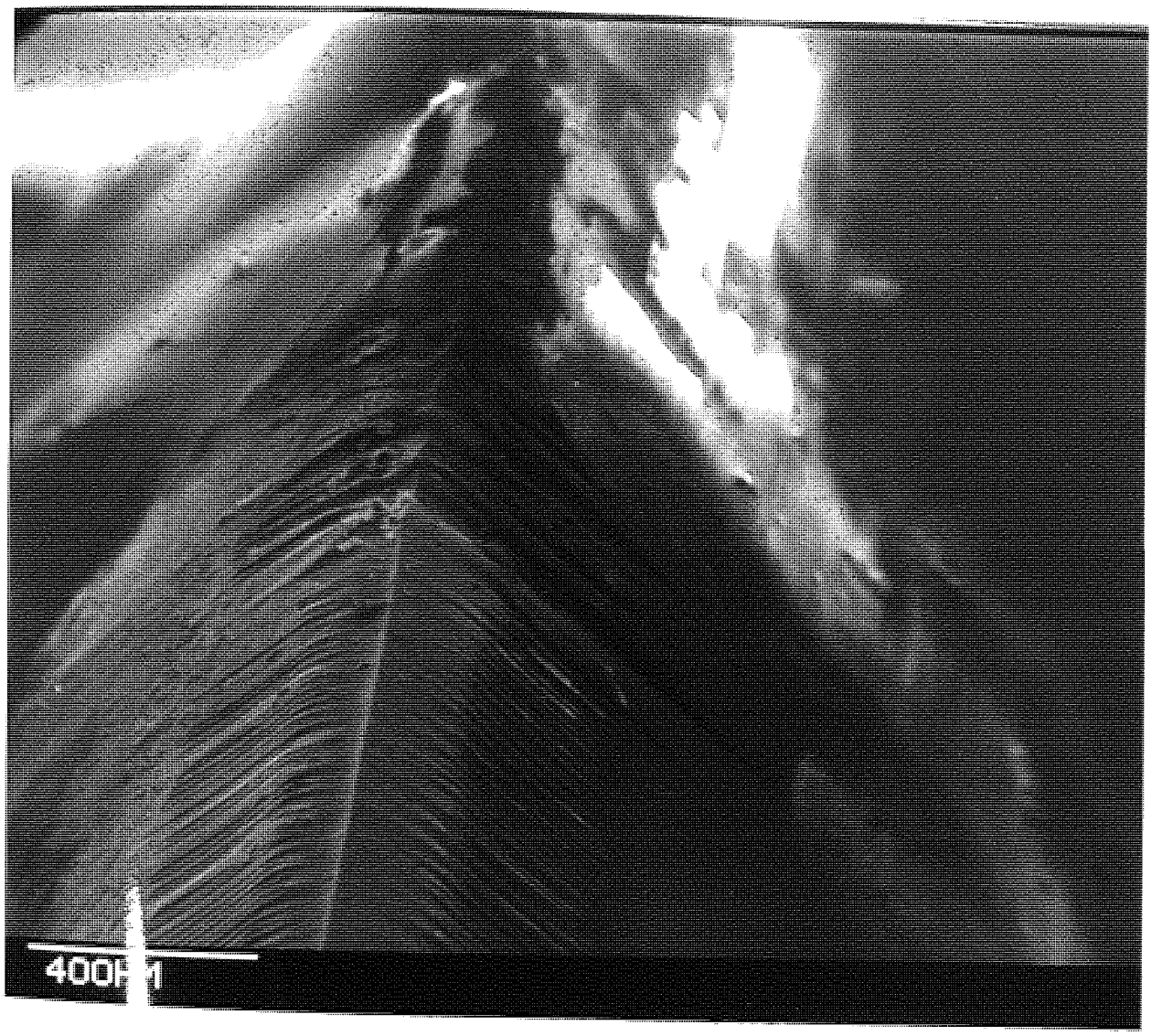

Figure 6.26 Leading edge groove

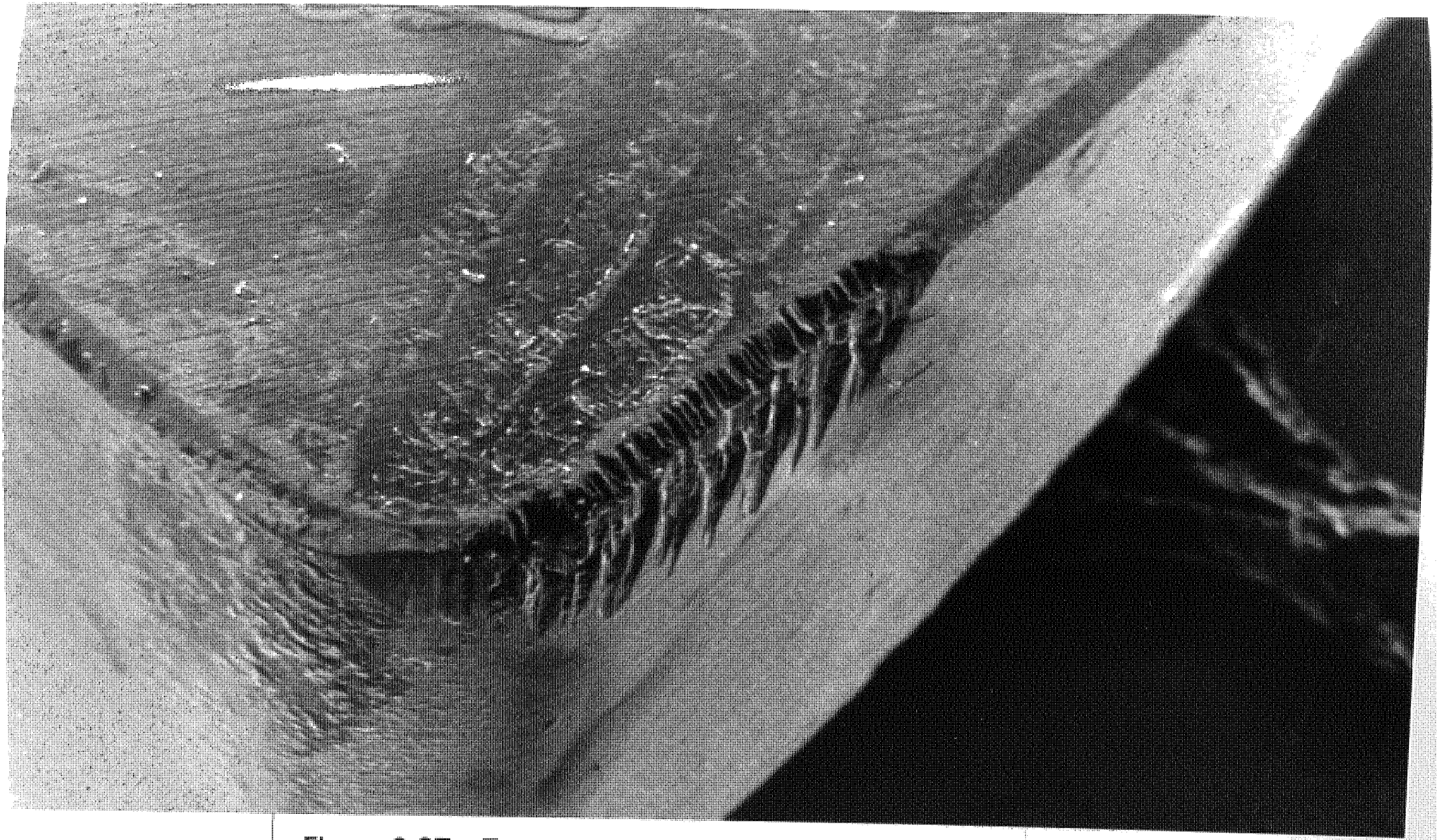

Figure 6.27 Typical wear on cutting edge (f = 0.056 mm/rev)

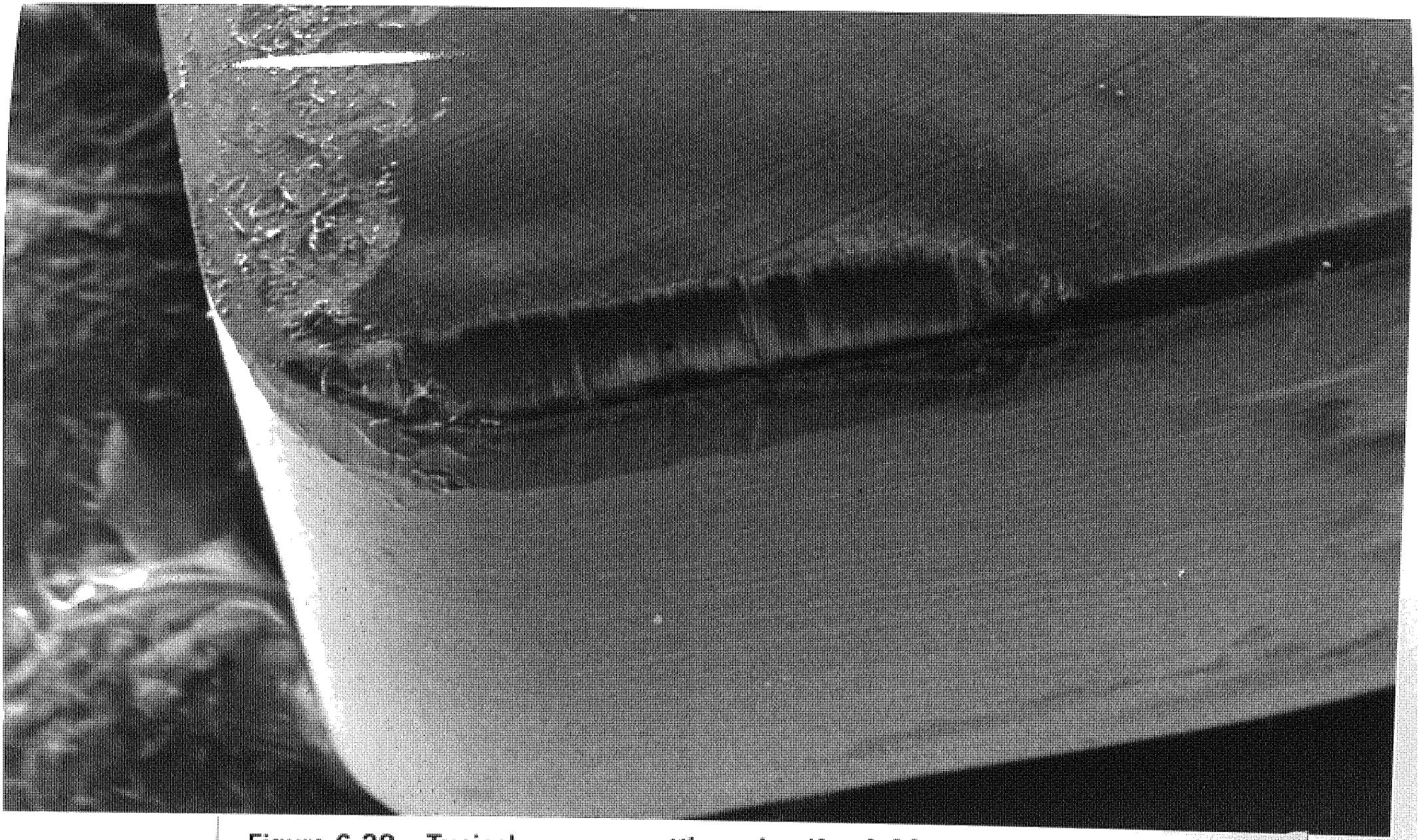

Figure 6.28 Typical wear on cutting edge (f = 0.33 mm/rev)

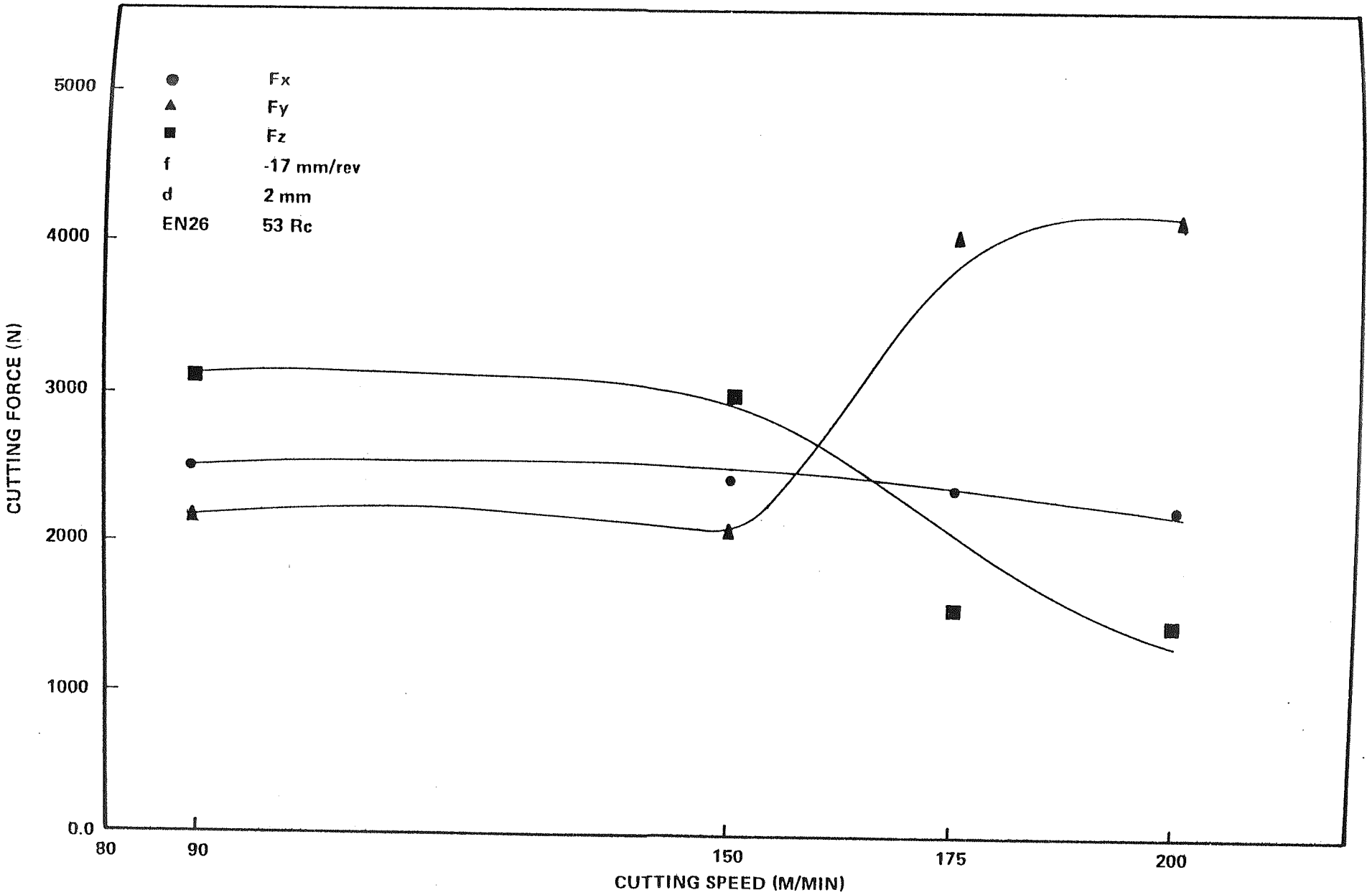

Figure 6.29 Effect of Cutting Speed on Cutting Forces (f = 0.17 mm/rev)

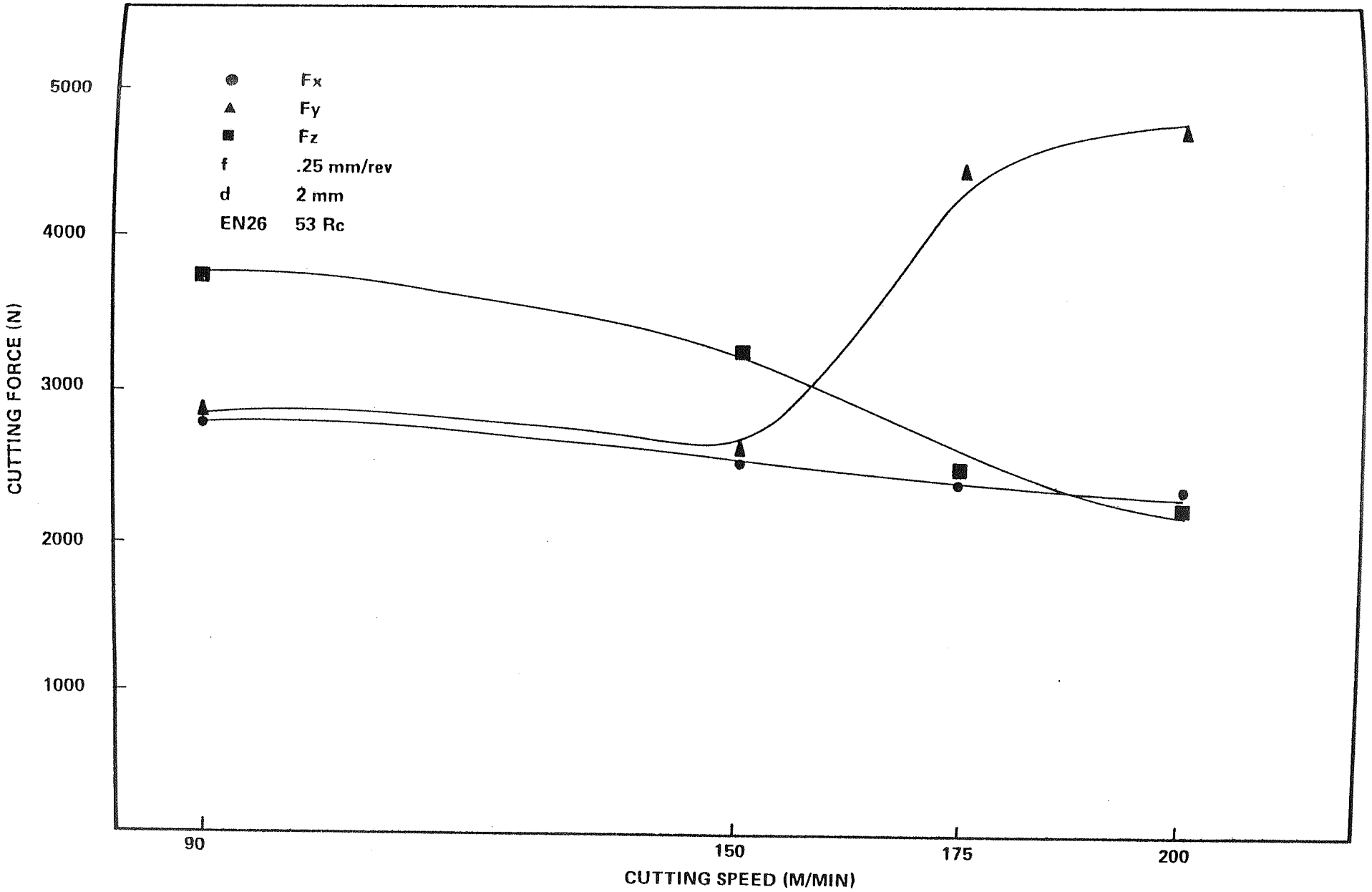

Figure 6.30 Effect of Cutting Speed on Cutting Forces (f = 0.25 mm/rev)

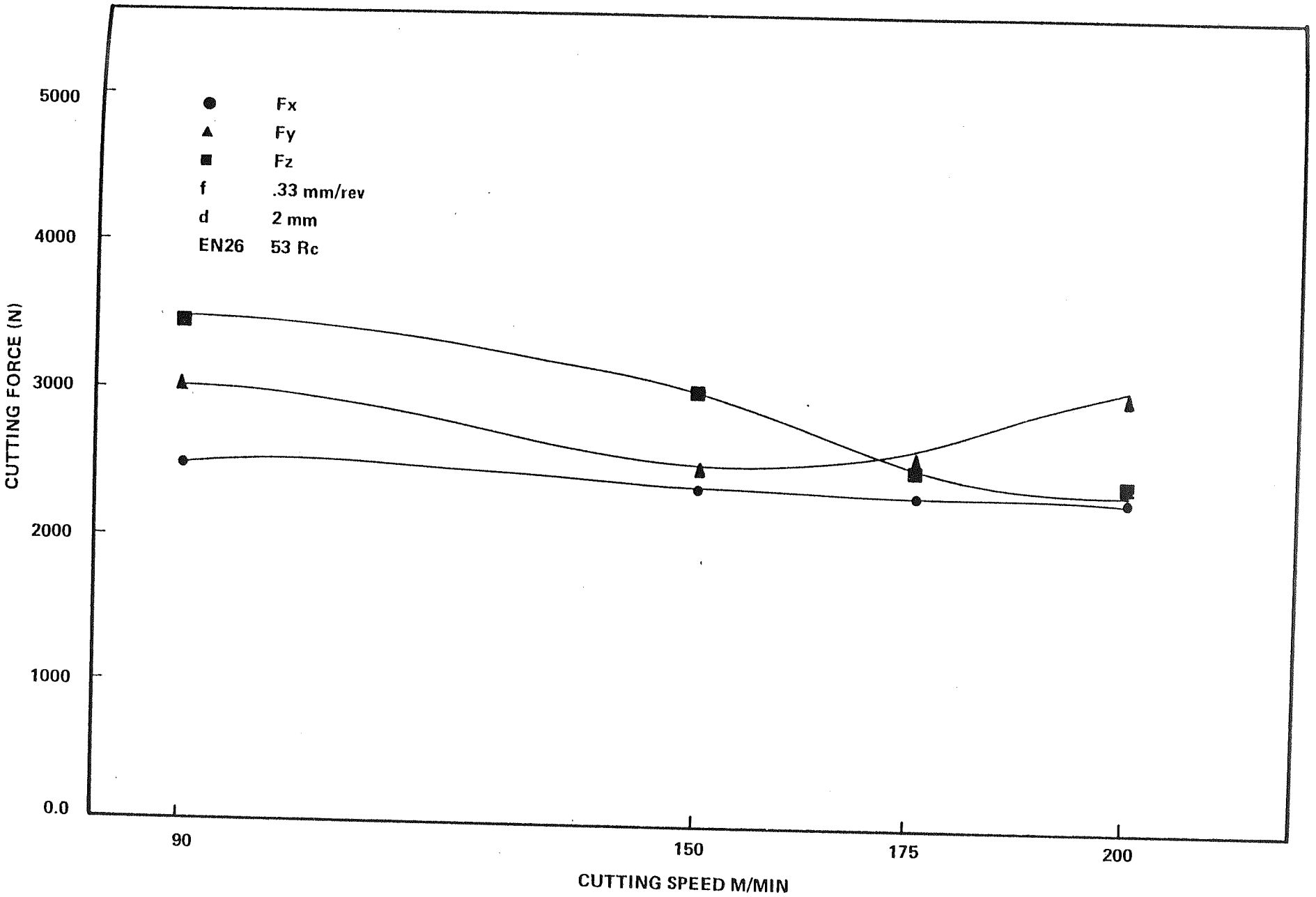

Figure 6.31 Effect of Cutting Speed on Cutting Forces (f = 0.33 mm)

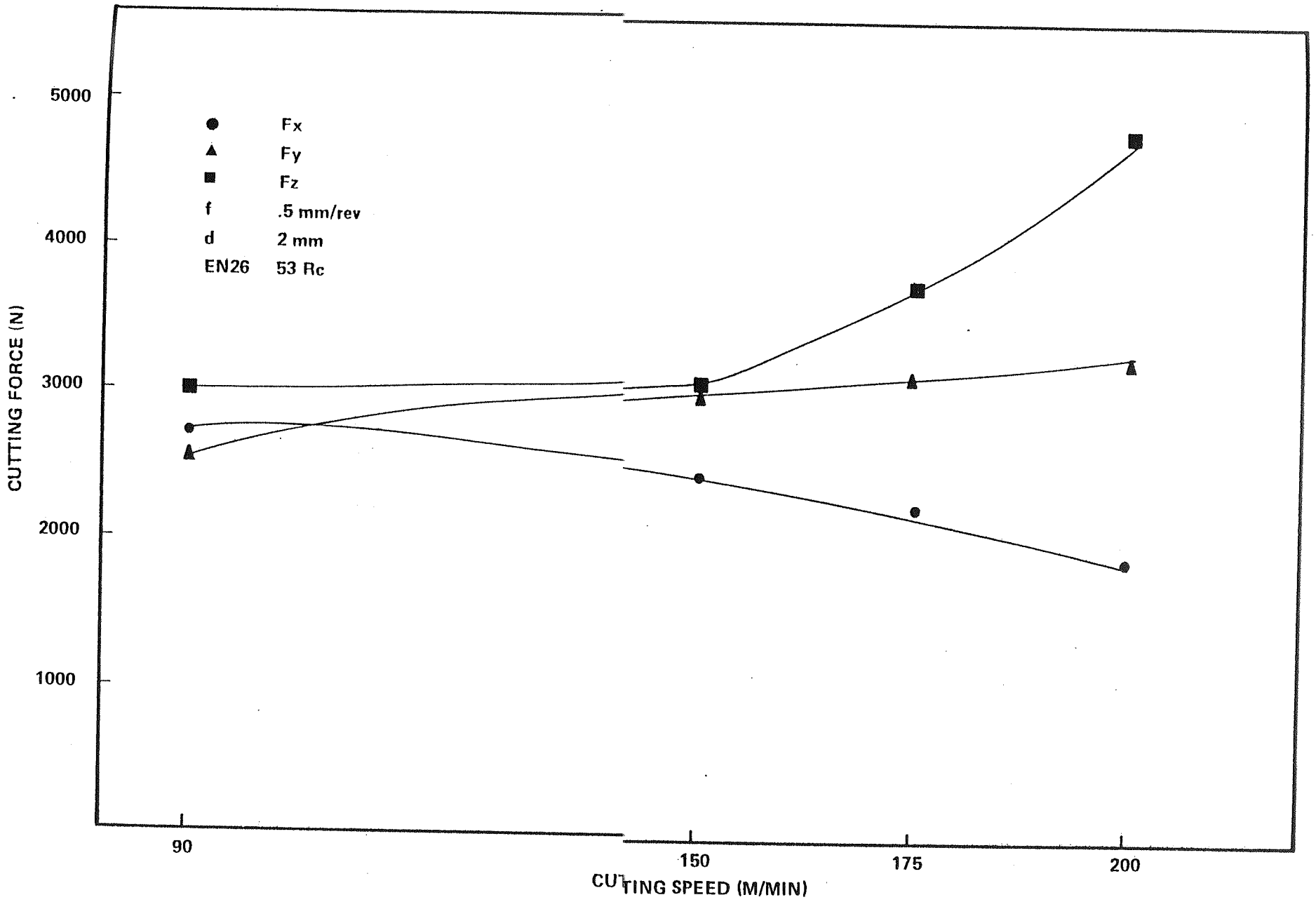

Figure 6.32 Effect of Cutting Speed on Cutting Forces (f = 0.5 mm/rev)

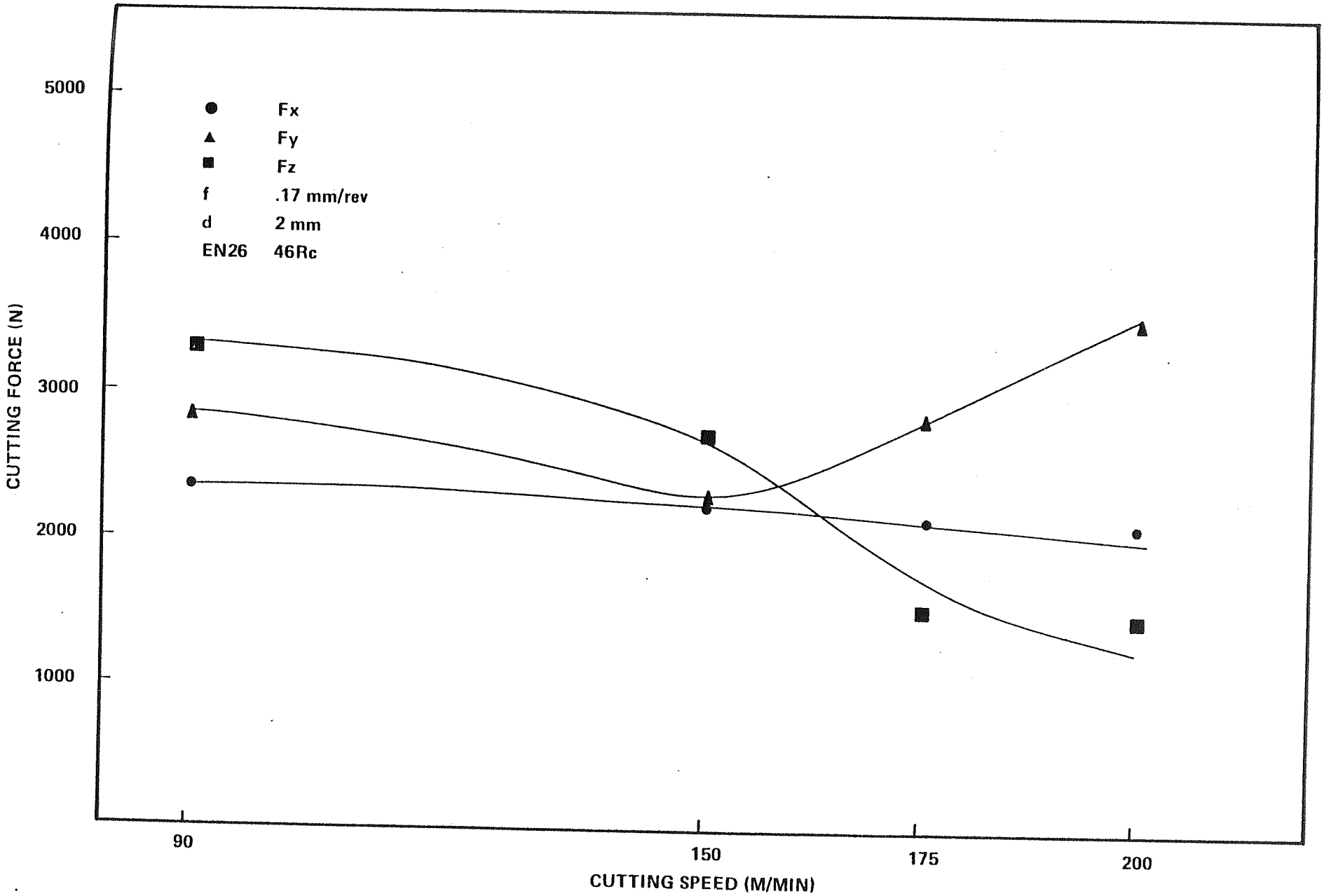

Figure 6.33 Effect of Cutting Speed on Cutting Forces (f = 0.17 mm/rev)

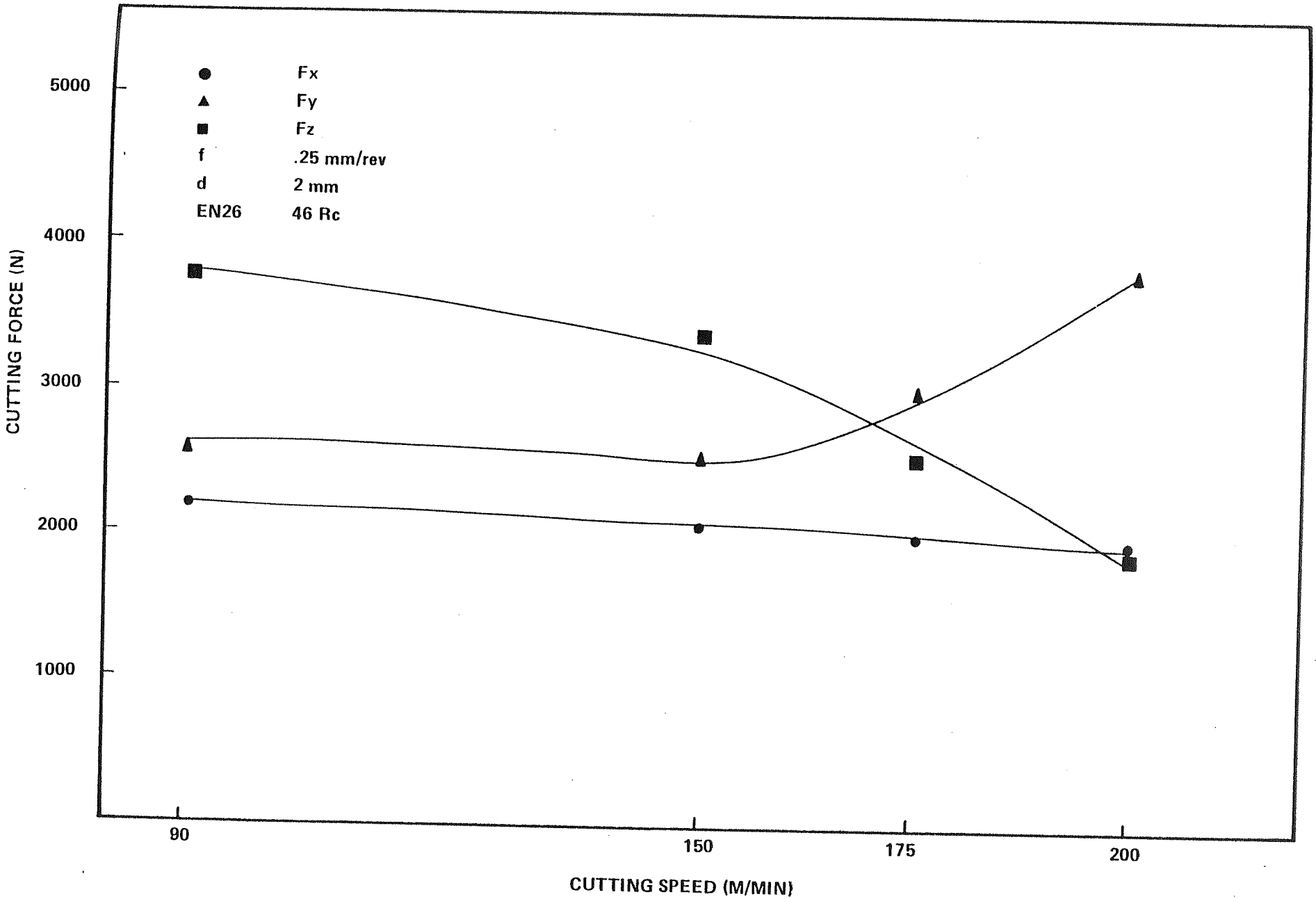

Figure 6.34 Effect of Cutting Speed on Cutting Forces (f = 0.25 mm/rev)

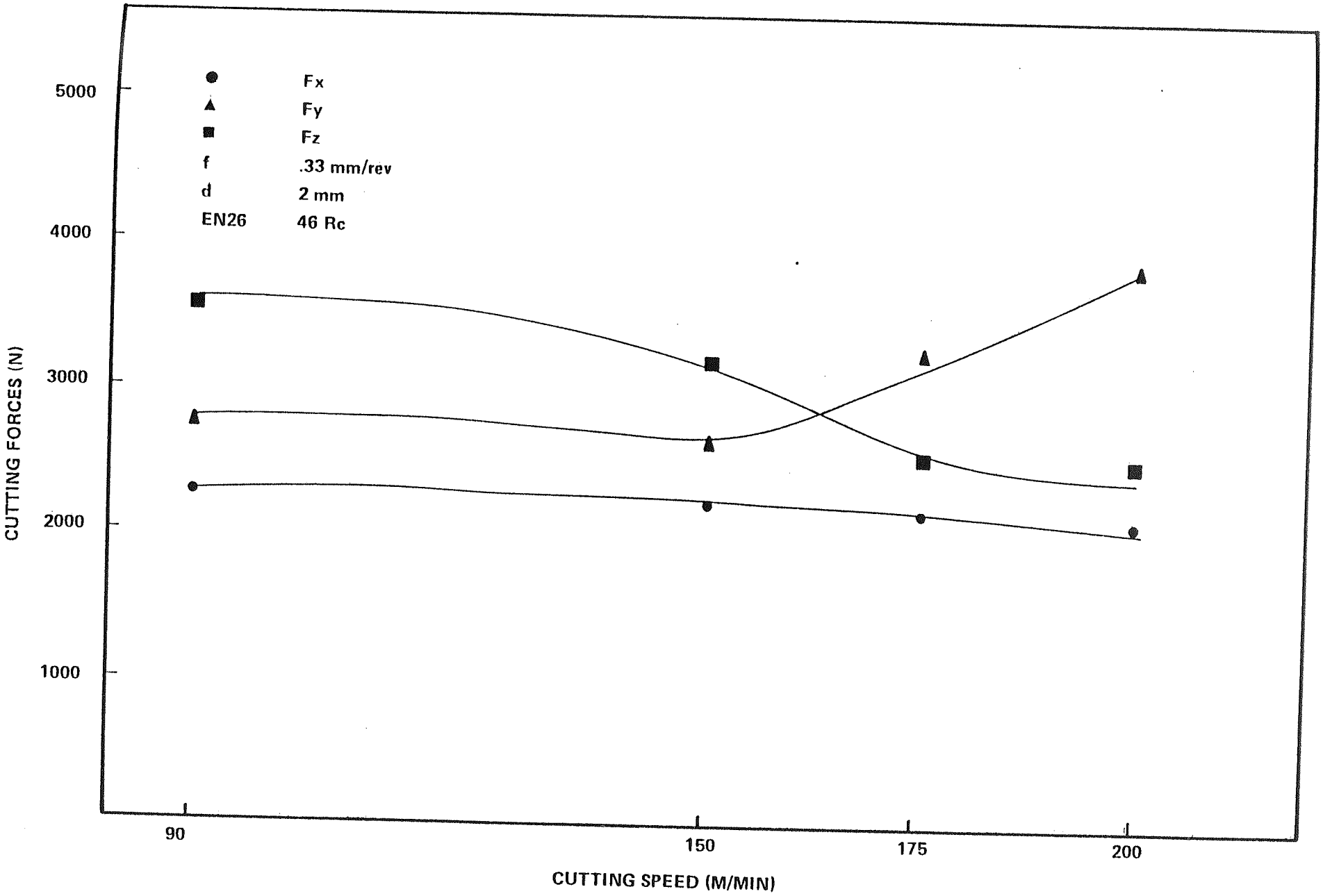

Figure 6.35 Effect of Cutting Speed on Cutting Forces (f = 0.33 mm/rev)

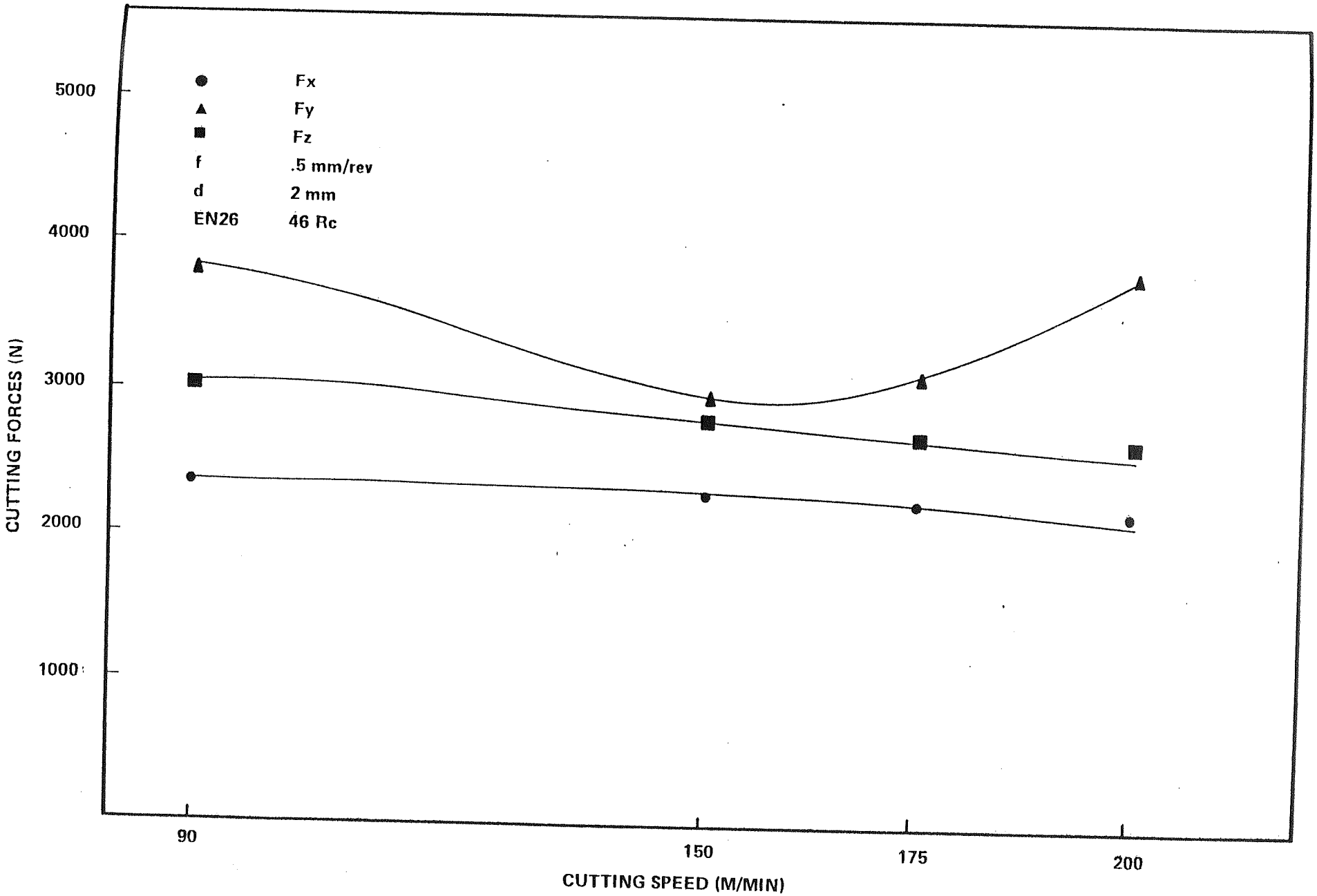

Figure 6.36 Effect of Cutting Speed on Cutting Forces (f = 0.5 mm/rev)

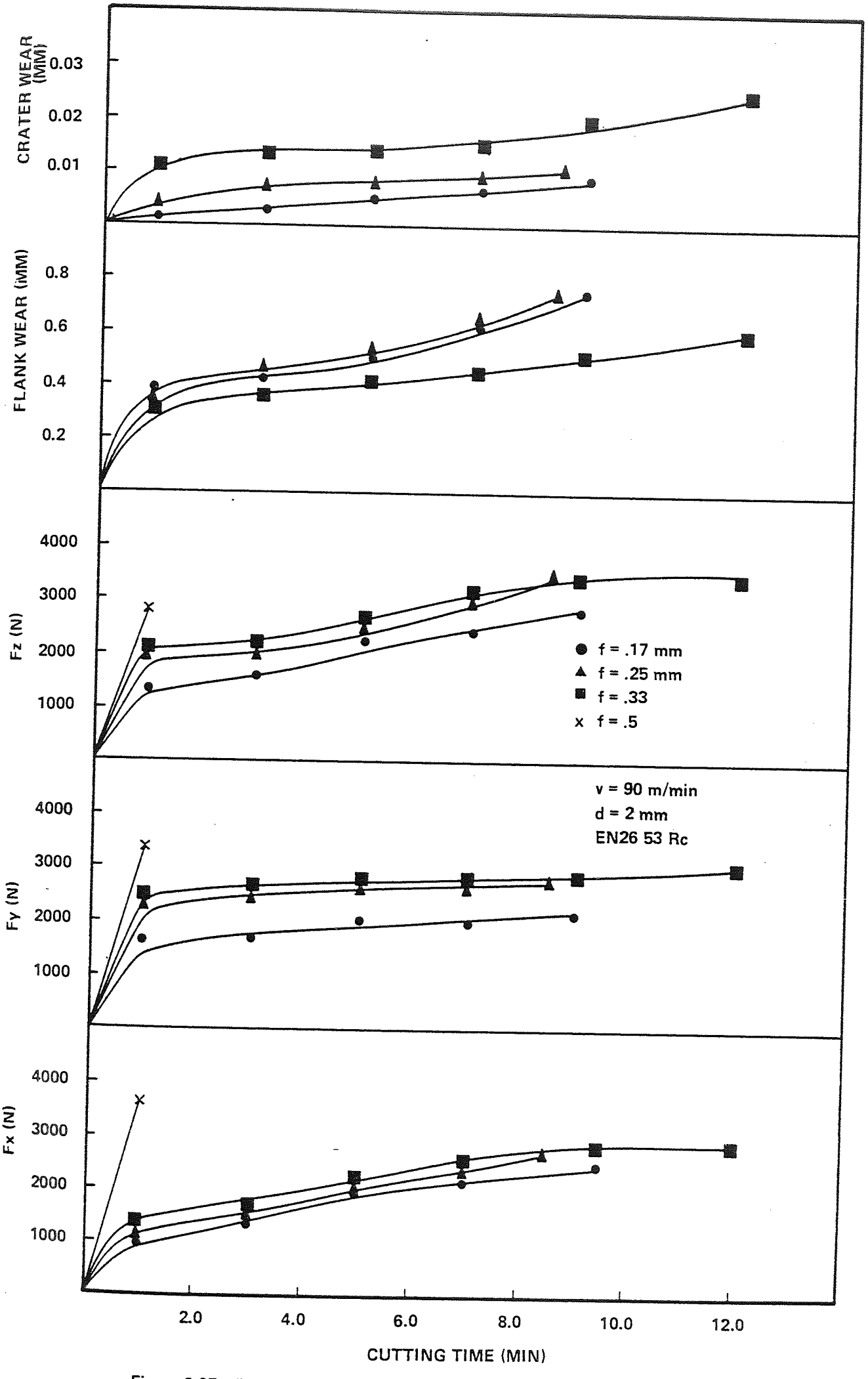

Figure 6.37 Effect of Developing Flank and Crater Wear on Cutting Forces (EN26 53Rc)

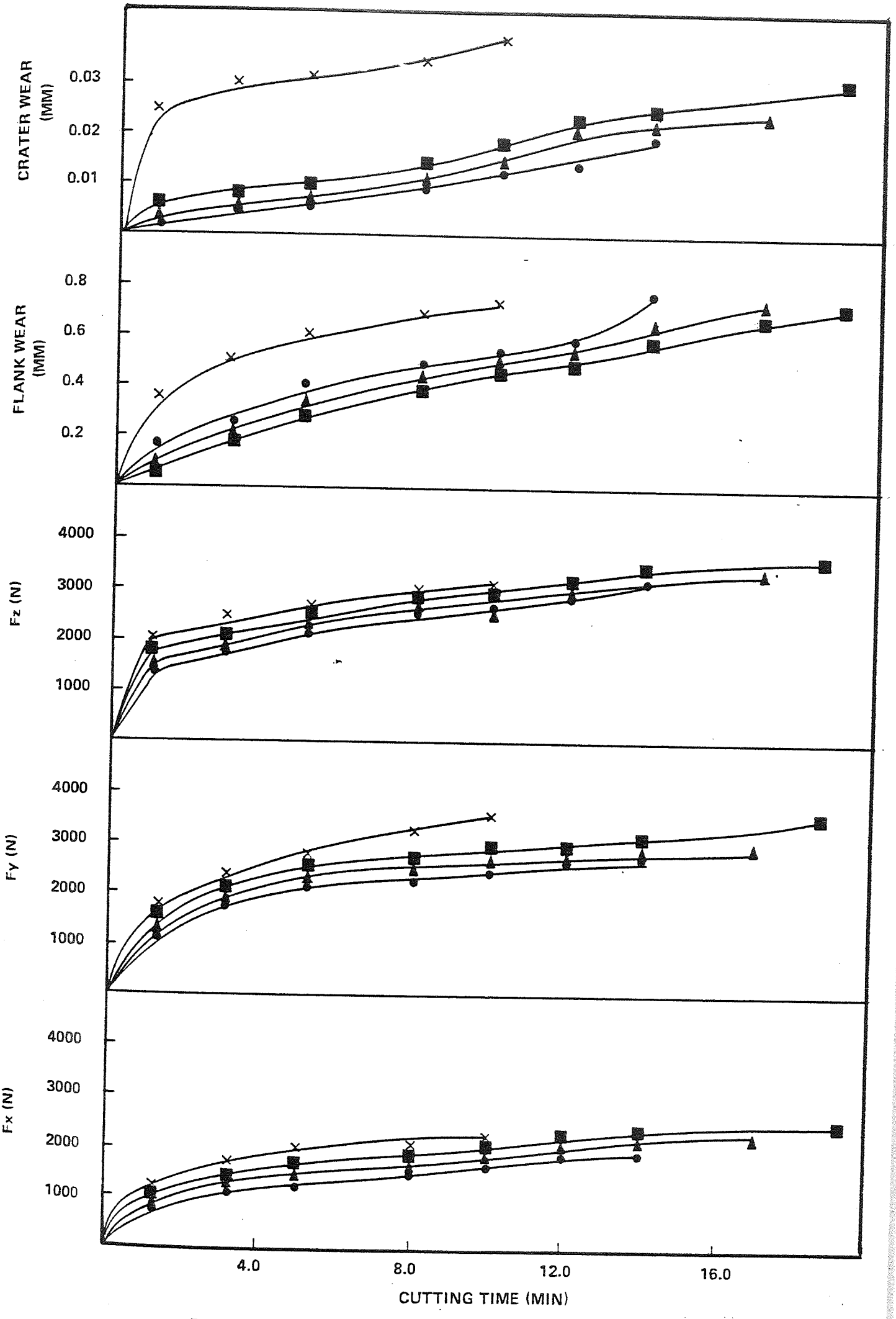

Figure 6.38 Effect of Developing Flank and Crater Wear on Cutting Forces (EN26 46Rc)

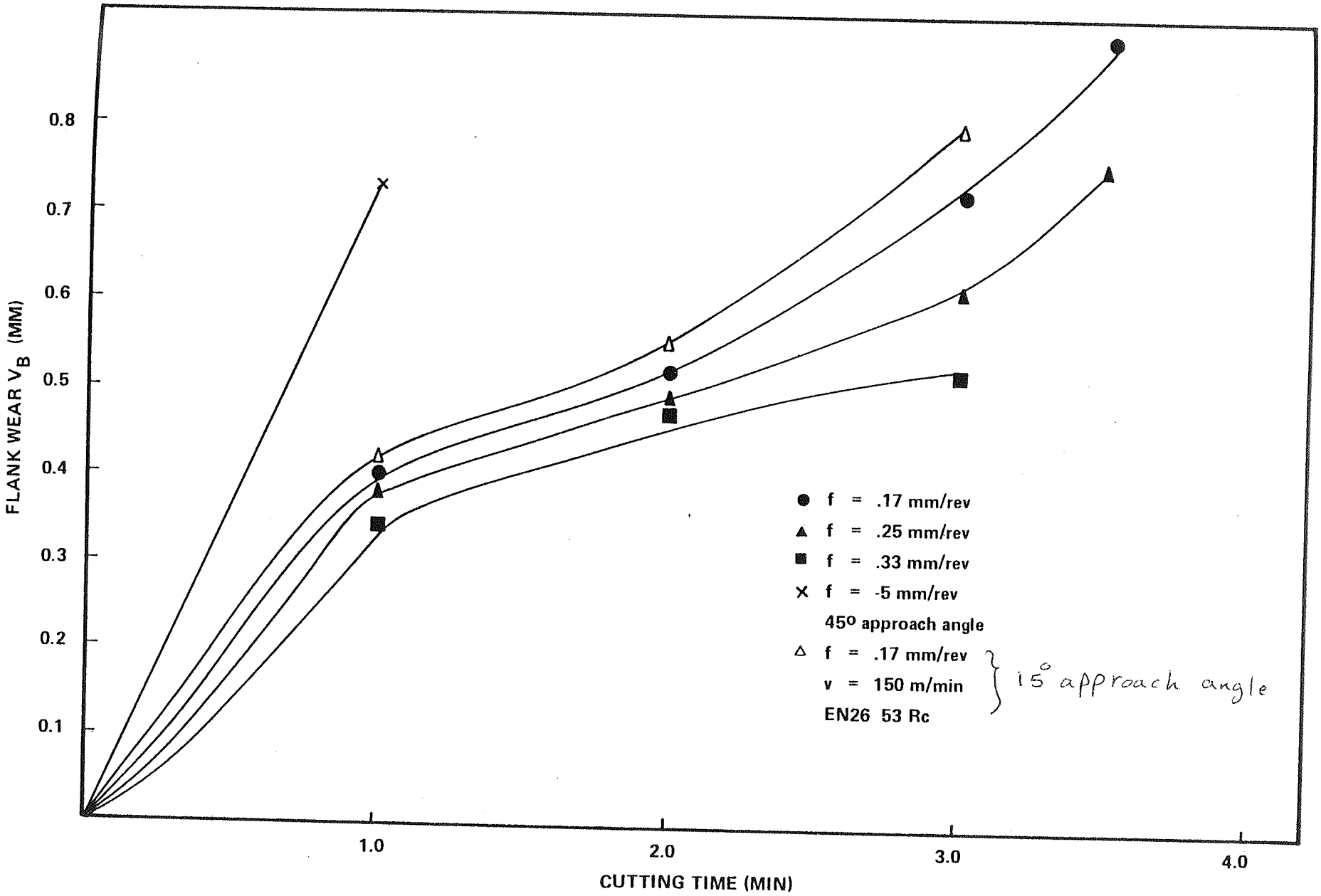

Figure 6.39 Influence of Plan Approach Angle on Flank Wear

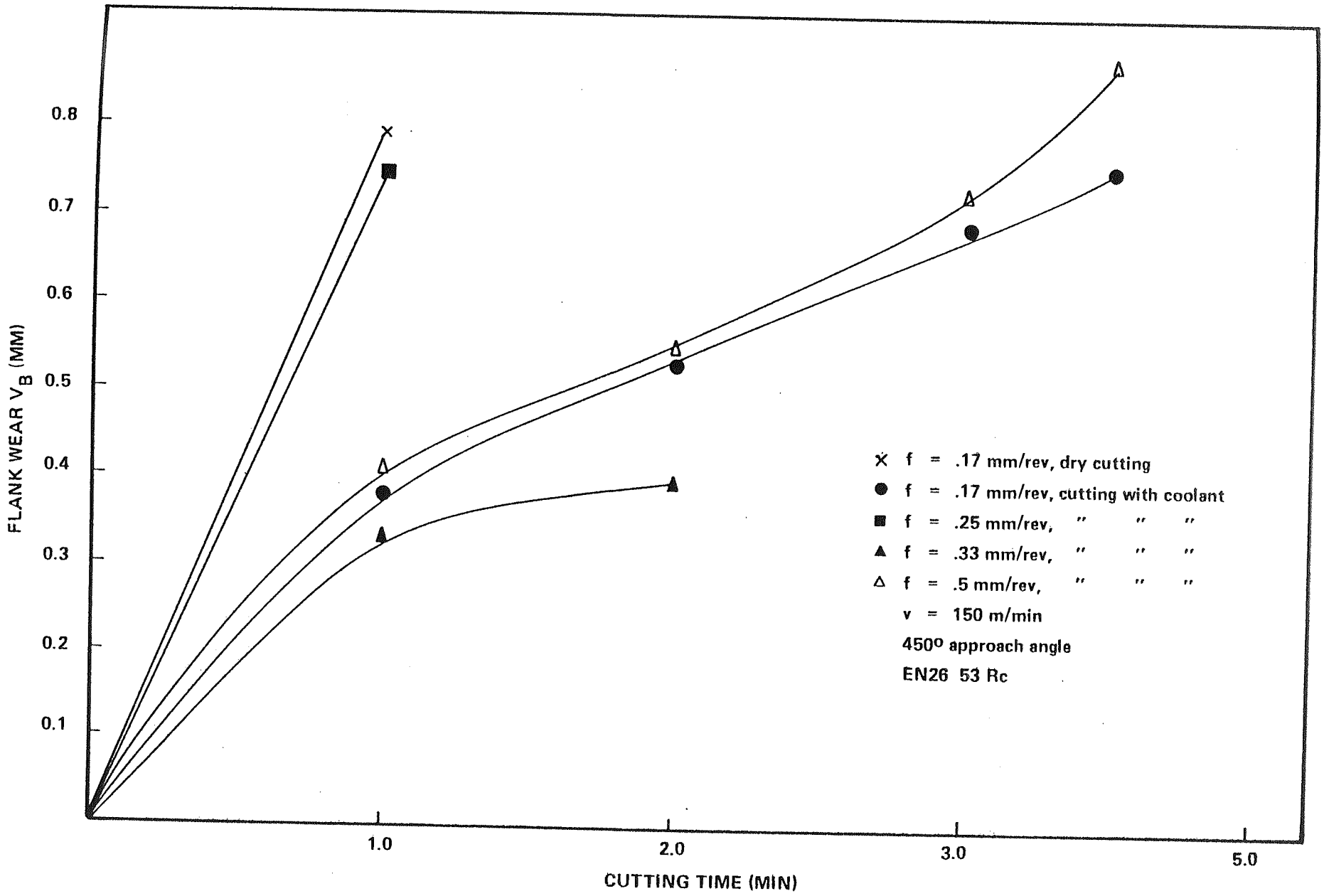

Figure 6.40 Influence of Coolant on Flank Wear EN26 53Rc

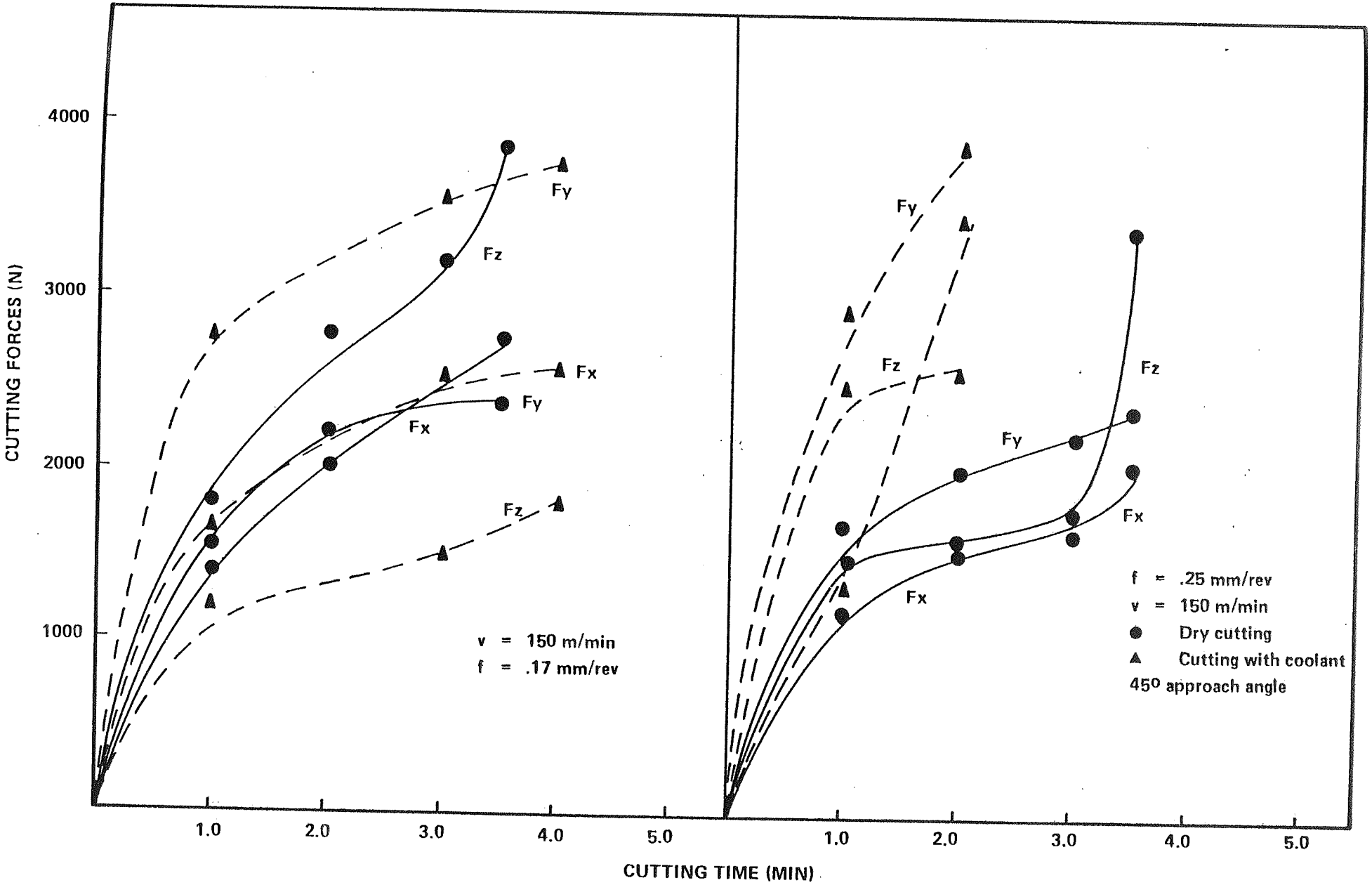

Figure 6.41 Influence of Coolant on Cutting Forces EN26 53Rc

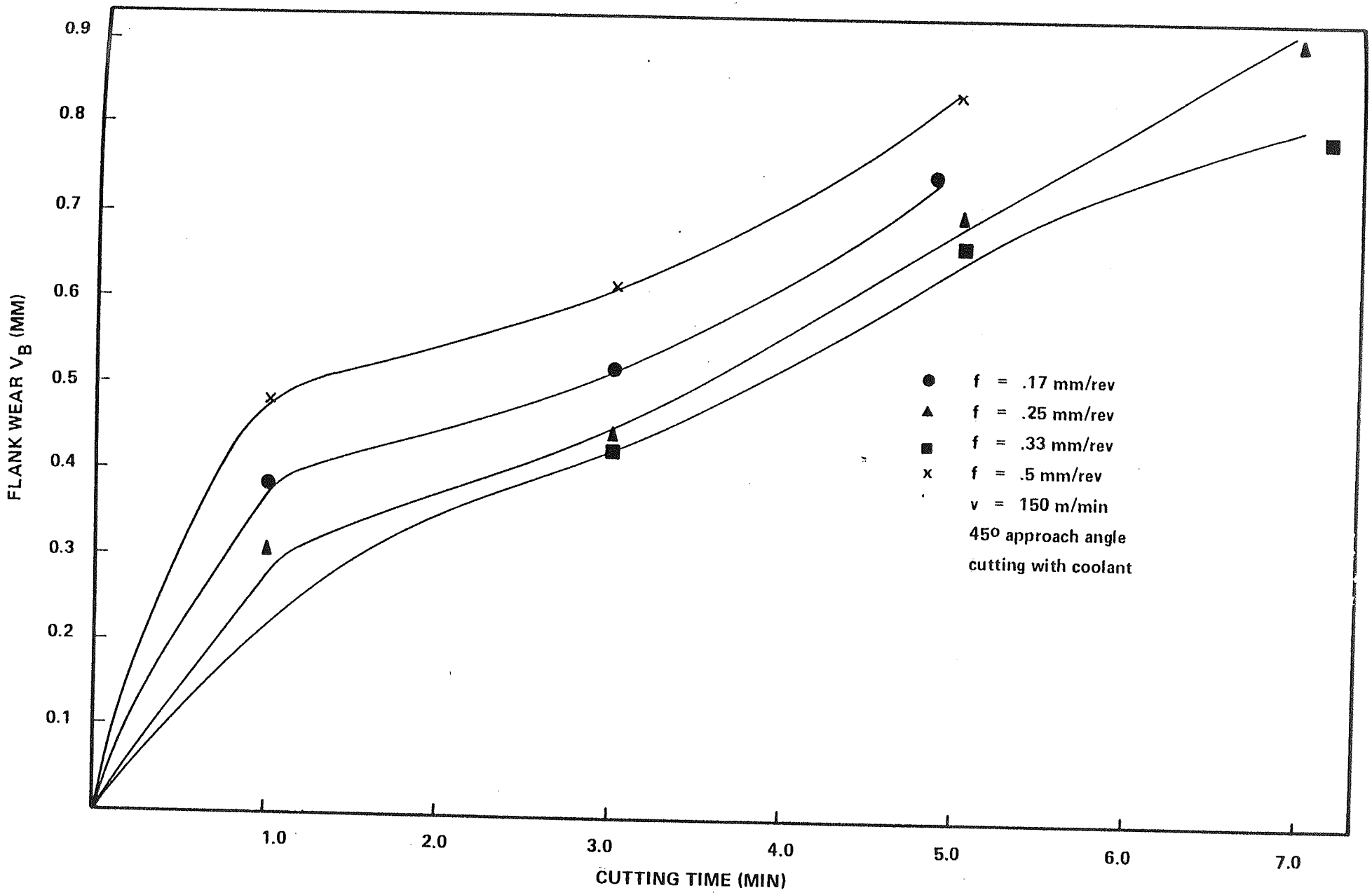

Figure 6.42 Influence of Coolant on Flank Wear (EN26 46 Rc)

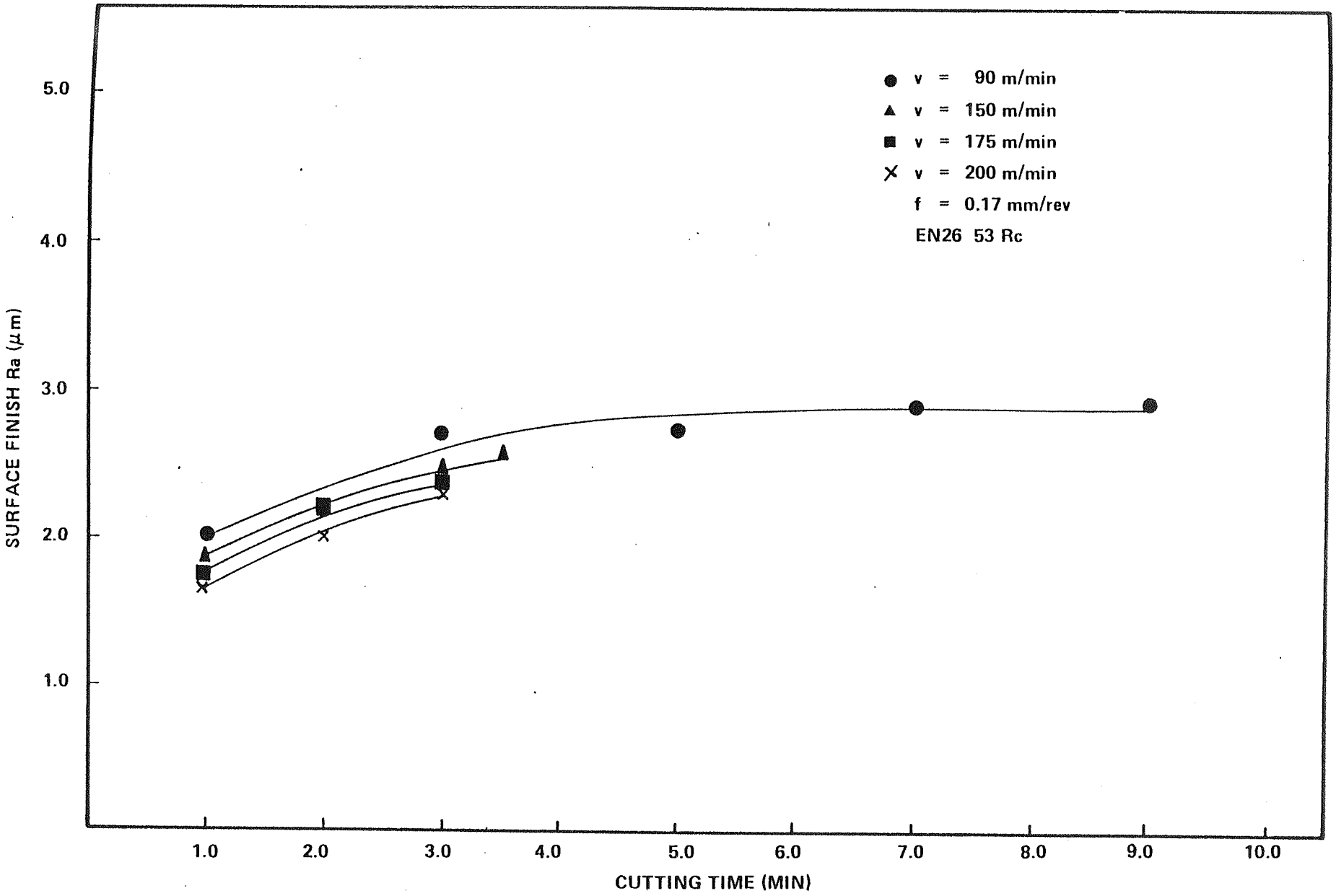

Figure 6.43 Influence of Cutting Speeds on Surface Finish

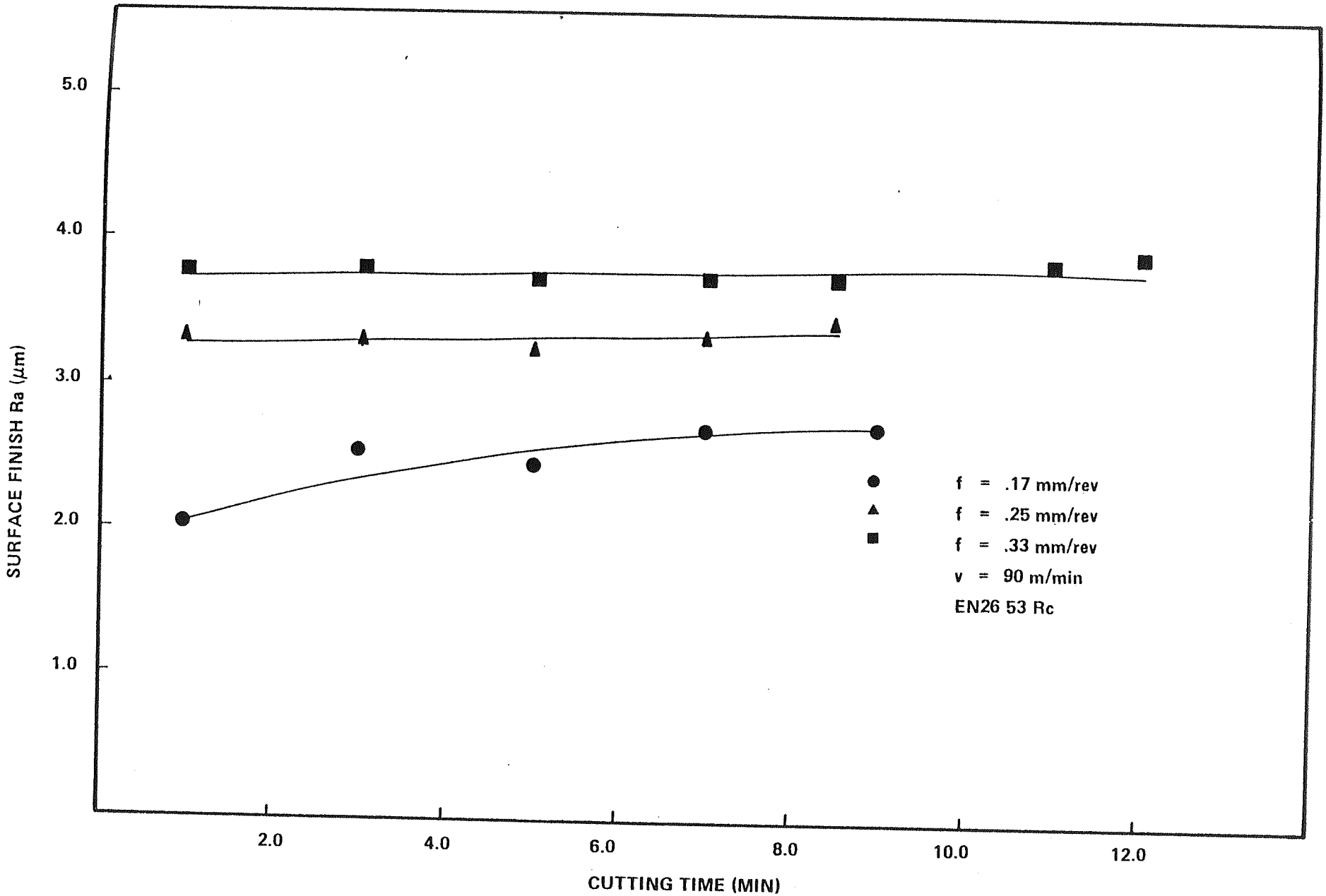

Figure 6.44 Influence of Feed Rates on Surface Finish

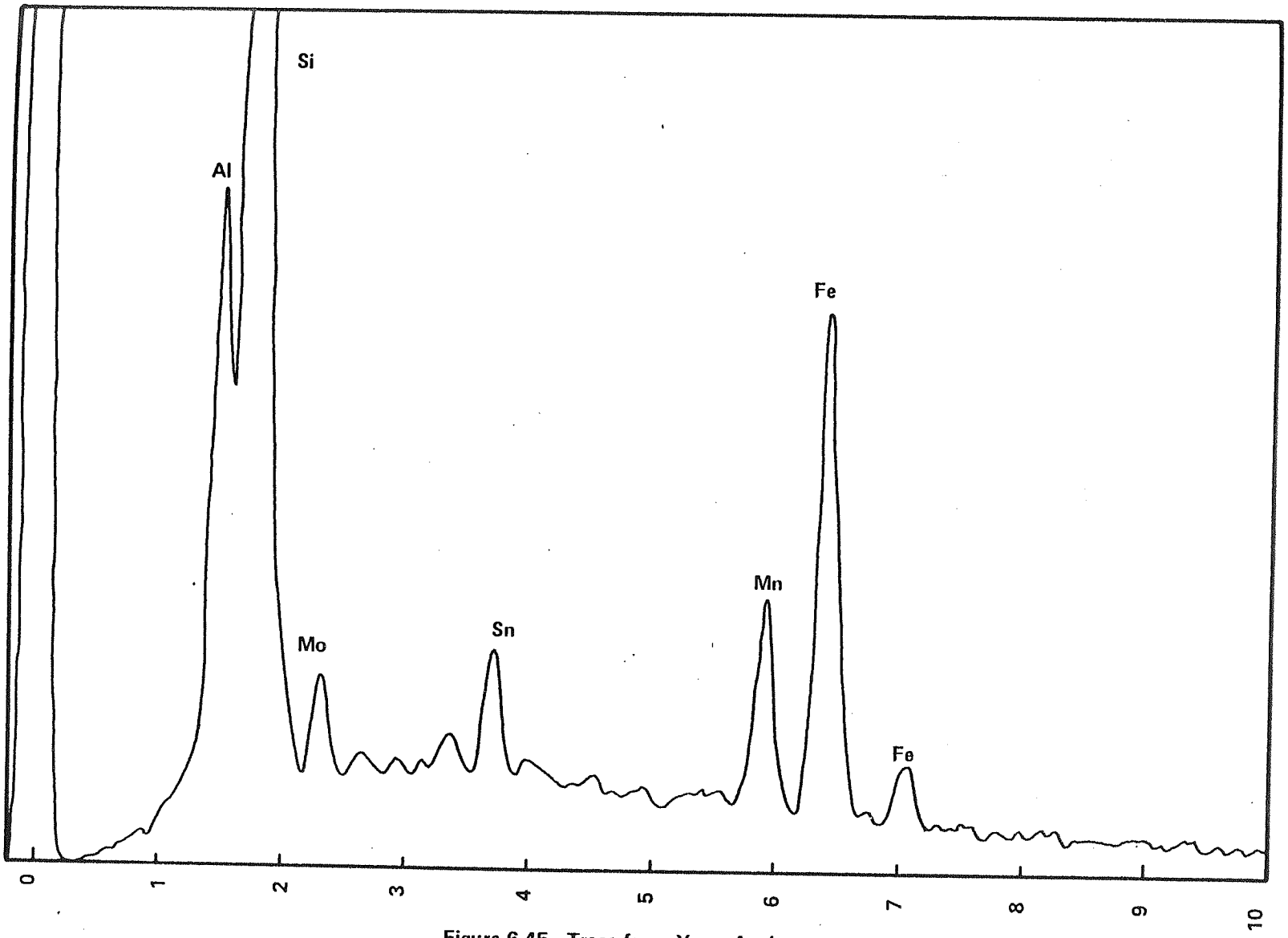

Figure 6.45 Trace from X-ray Analyser

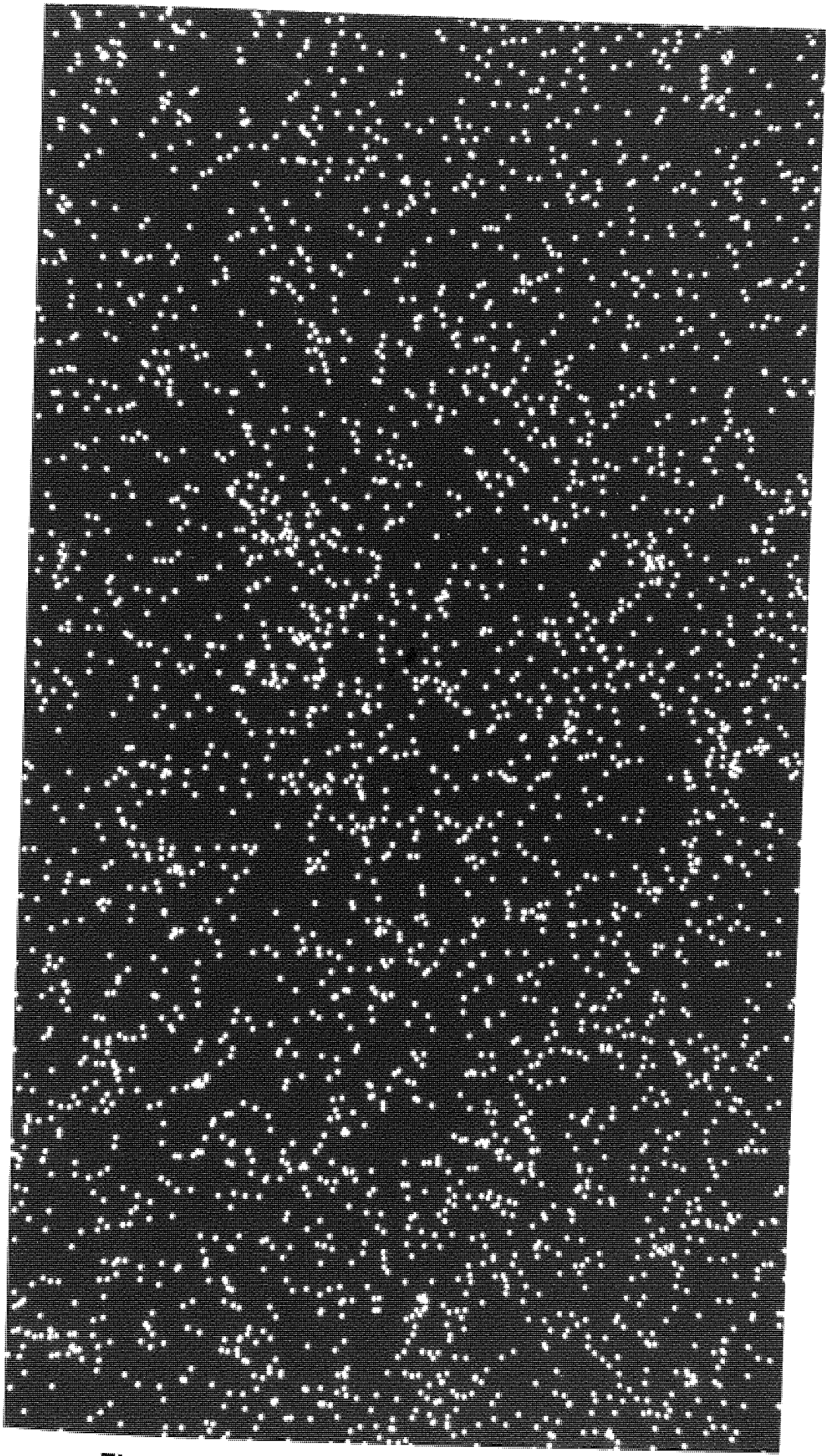

Figure 6.46a X-ray map photographs (Fe)

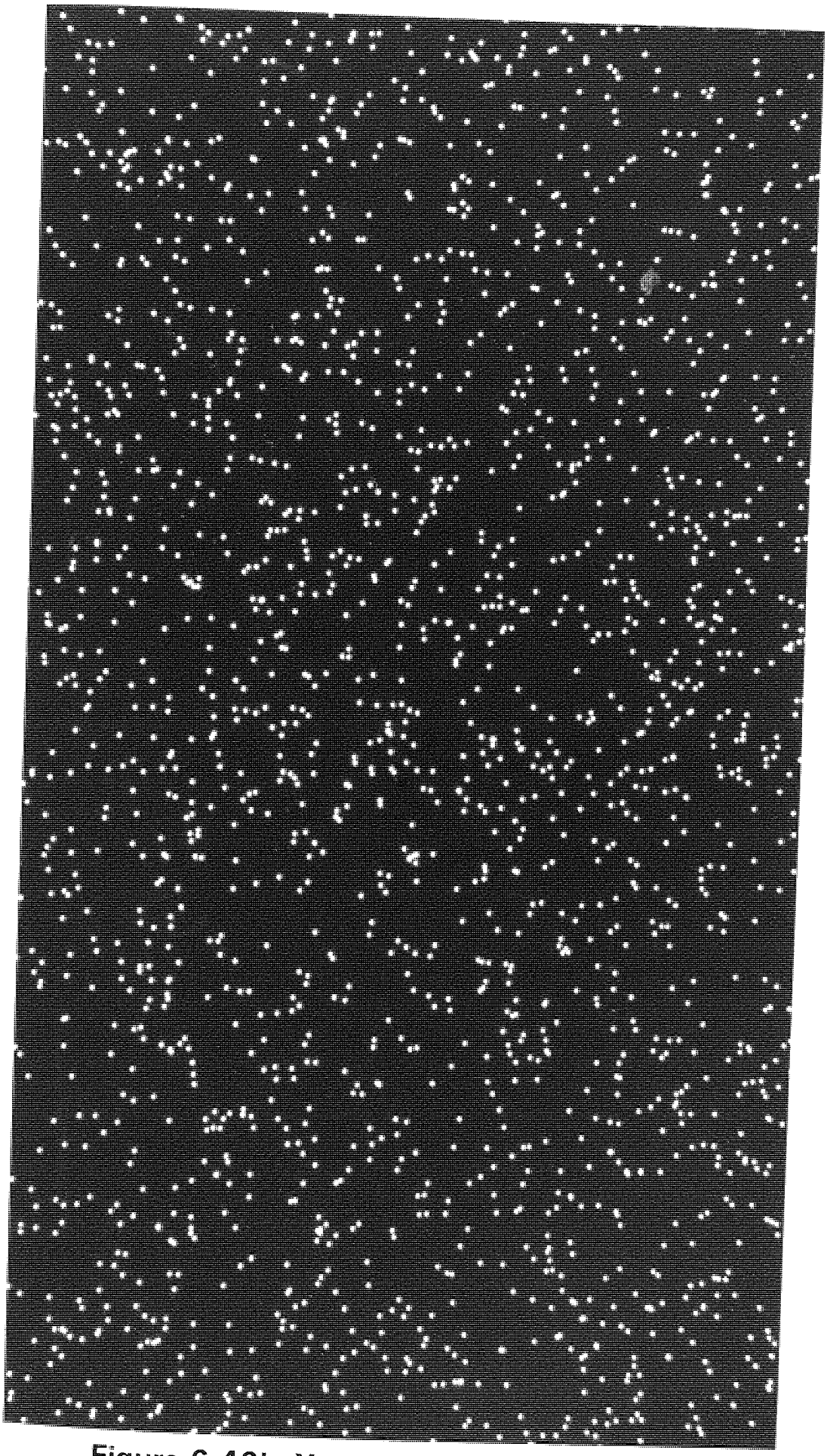

Figure 6.46b X-ray map photographs (Mn)

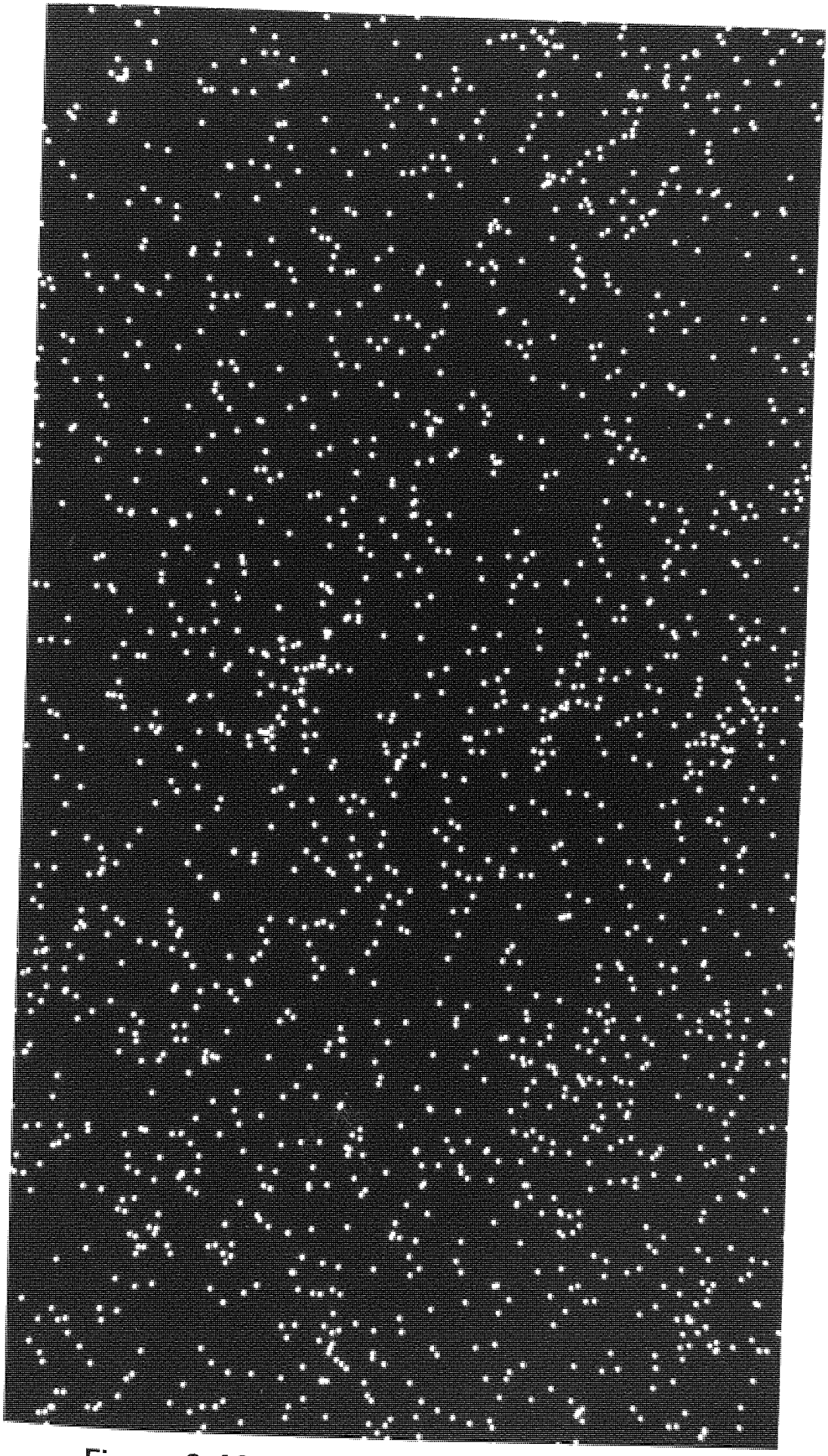

Figure 6.46c X-ray map photographs (Mo)

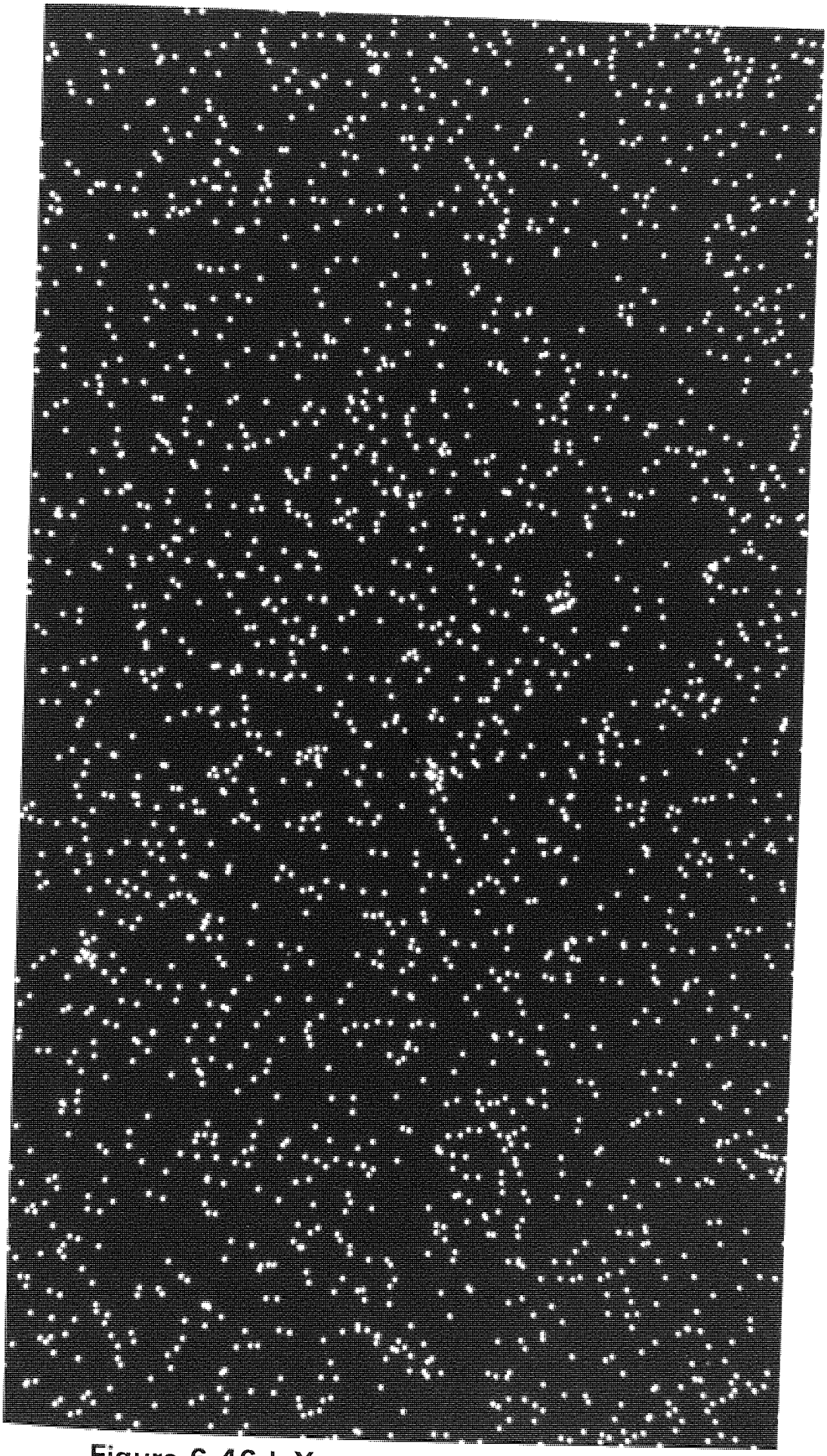

Figure 6.46d X-ray map photographs (Sn)

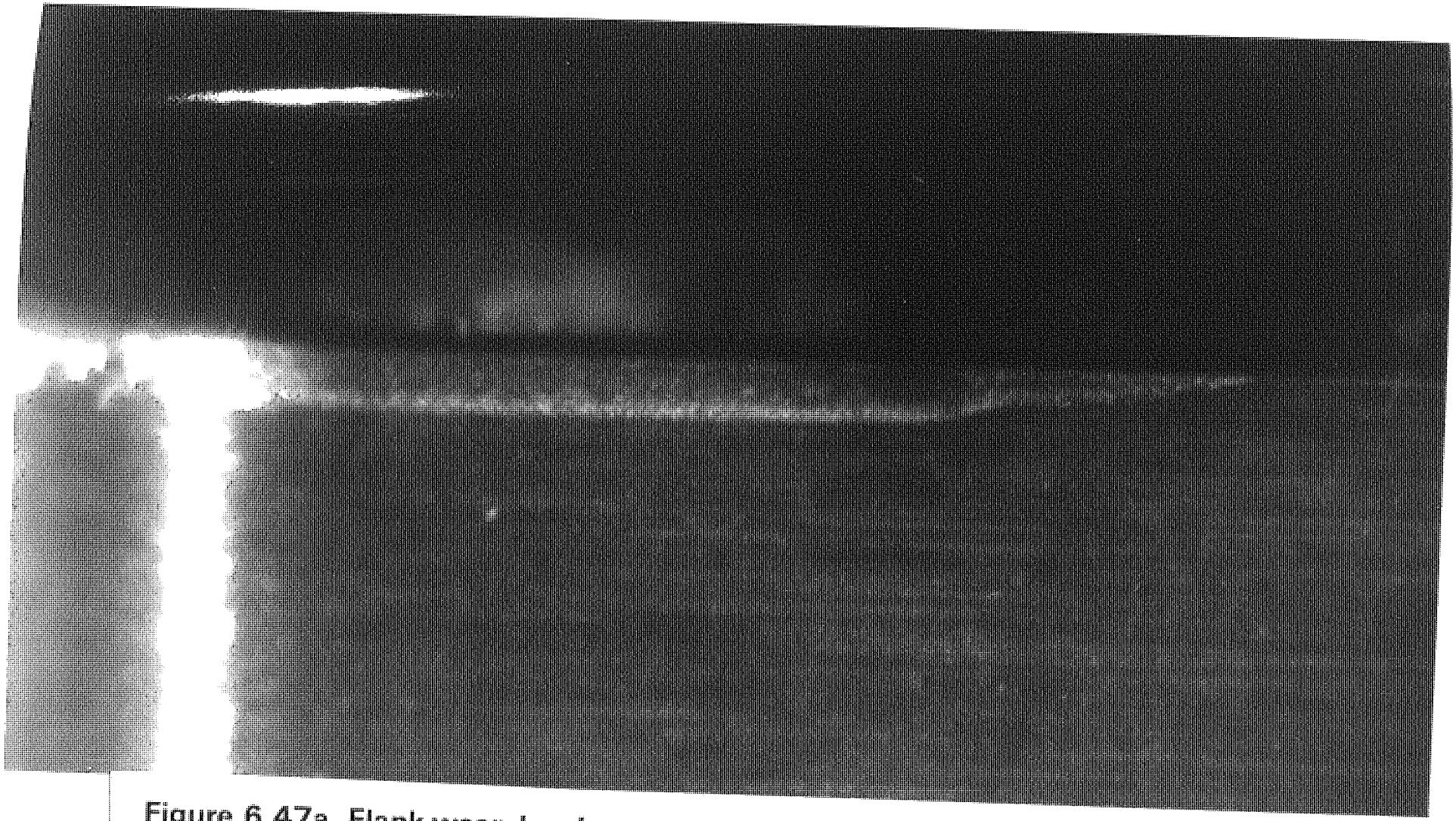

Figure 6.47a Flank wear development (TI = 3 min) f = .17mm/rev, v = 90 m/min

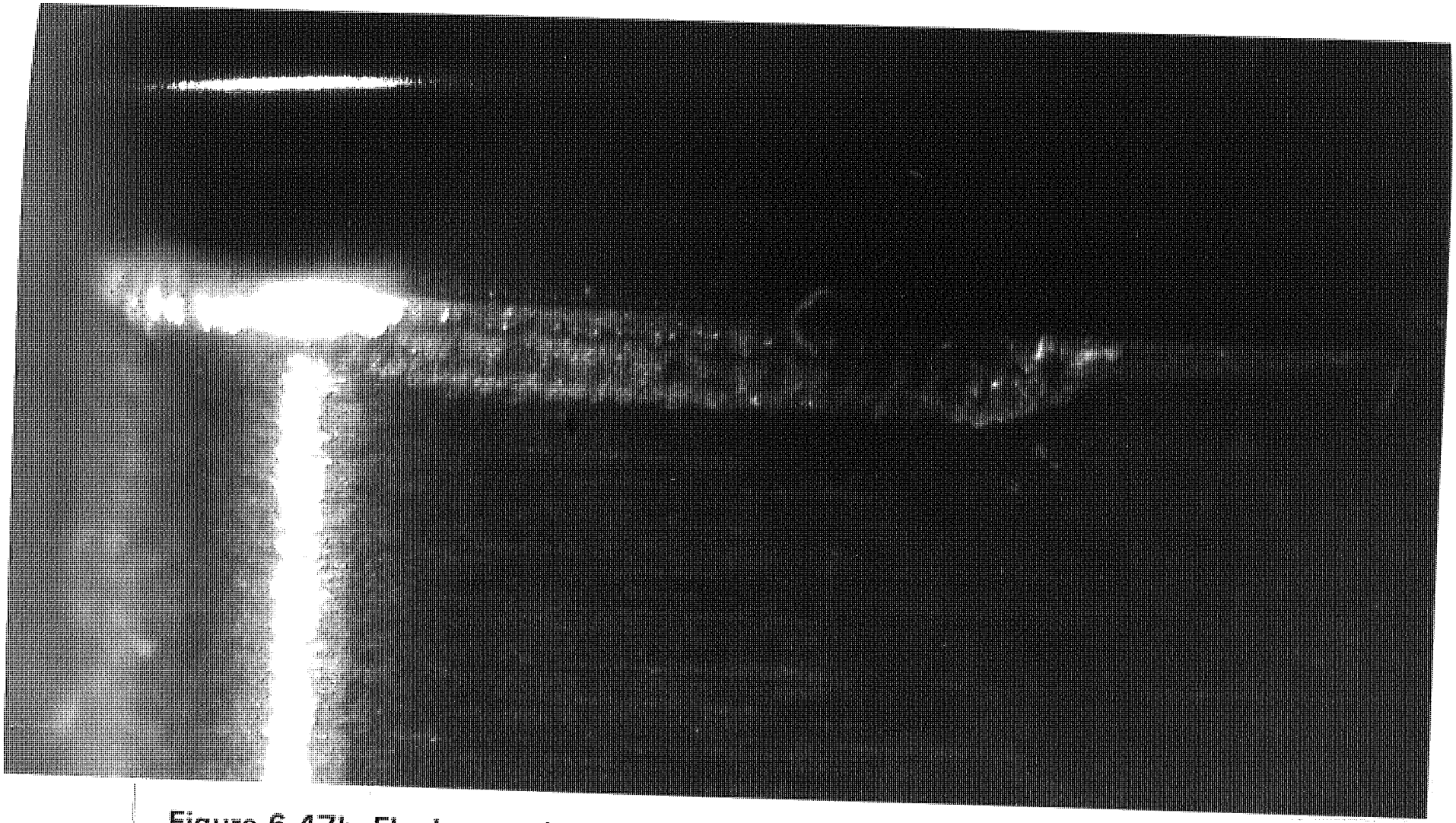

Figure 6.47b Flank wear development (Tl = 8 min) f = .17mm/rev, v = 90 m/min

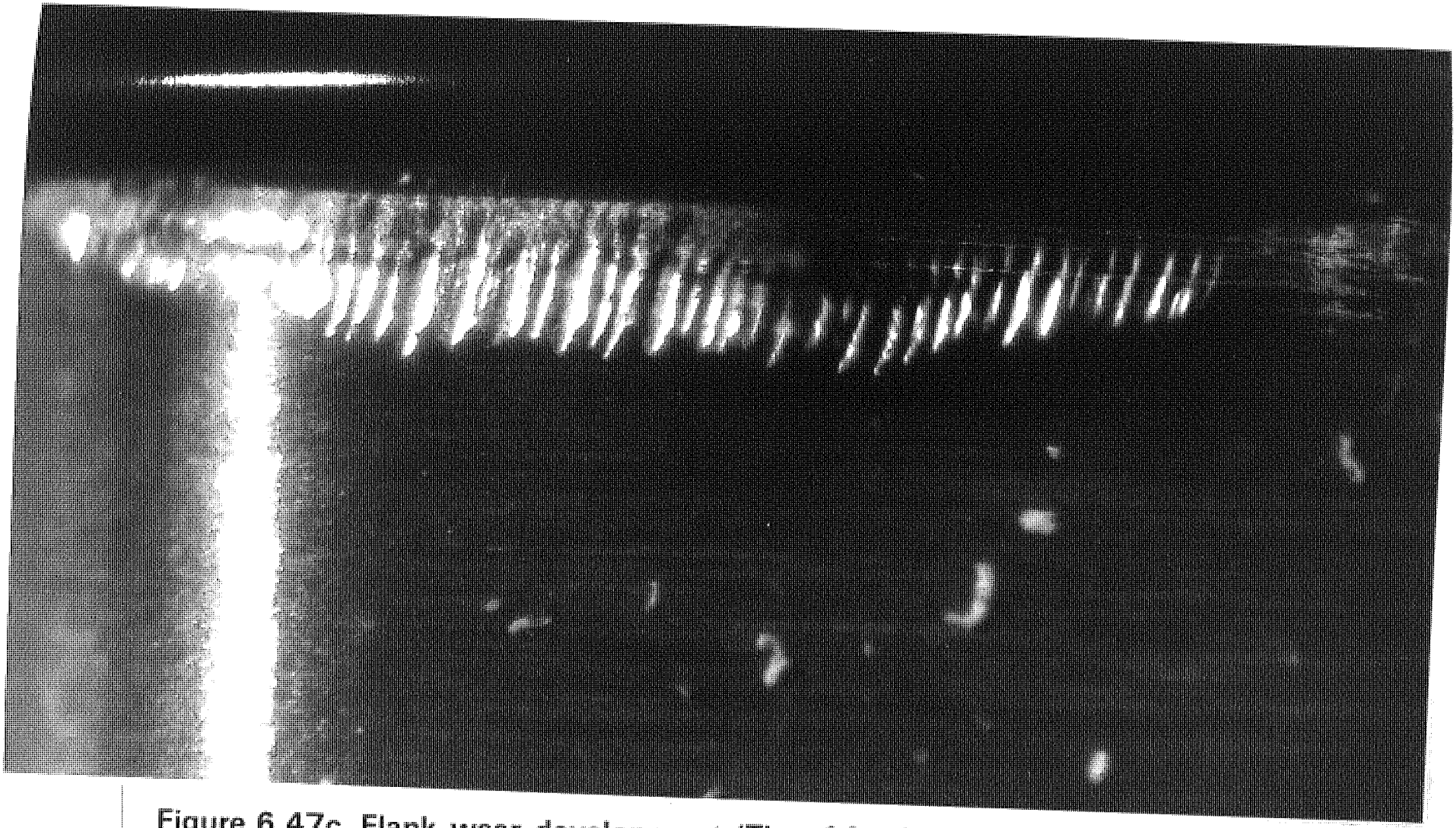

Figure 6.47c Flank wear development (TI = 14 min) f = .17mm/rev, v = 90 m/min

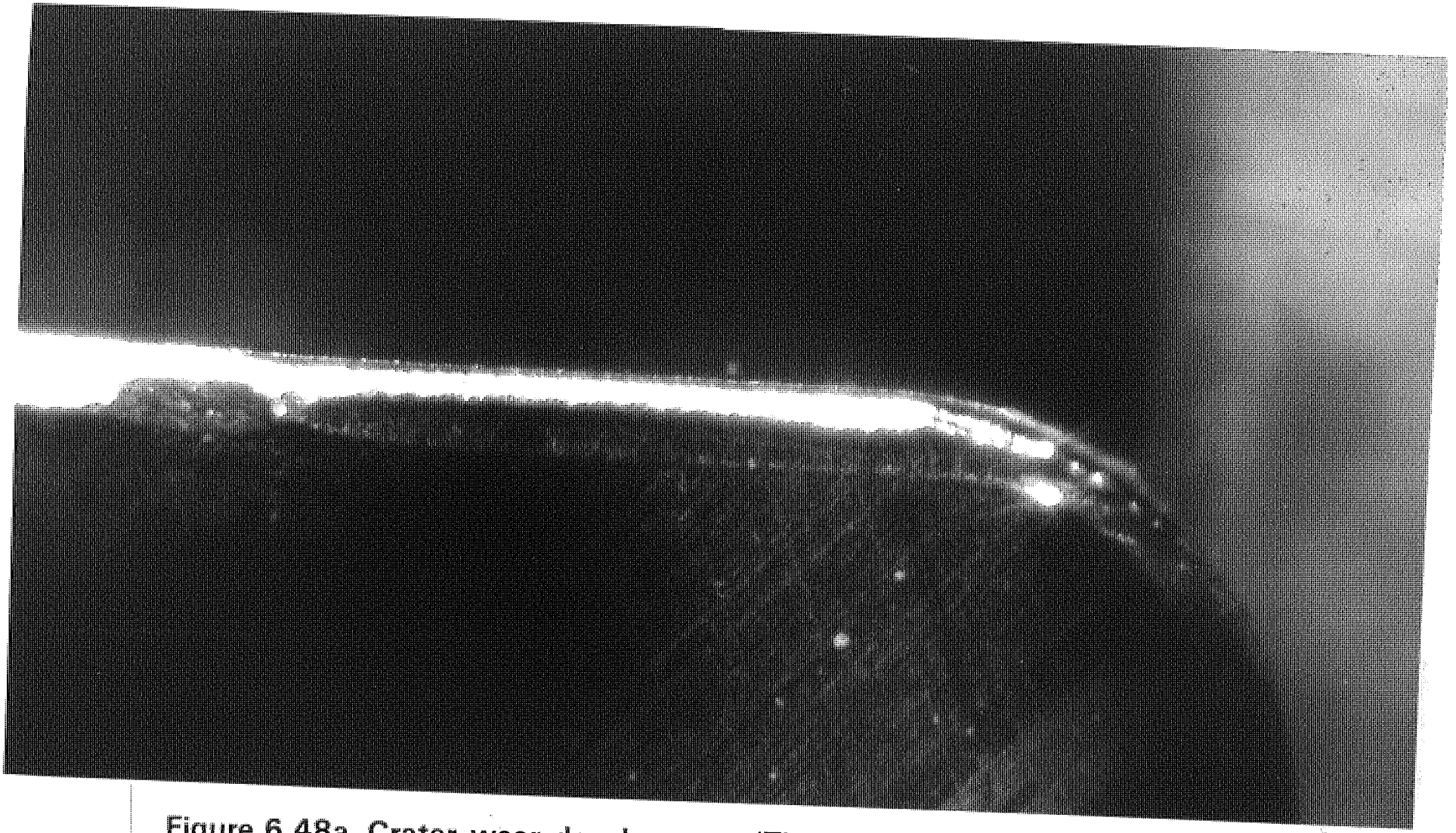

Figure 6.48a Crater wear development (TI = 3 min) f = .17mm/rev, v = 90 m/min

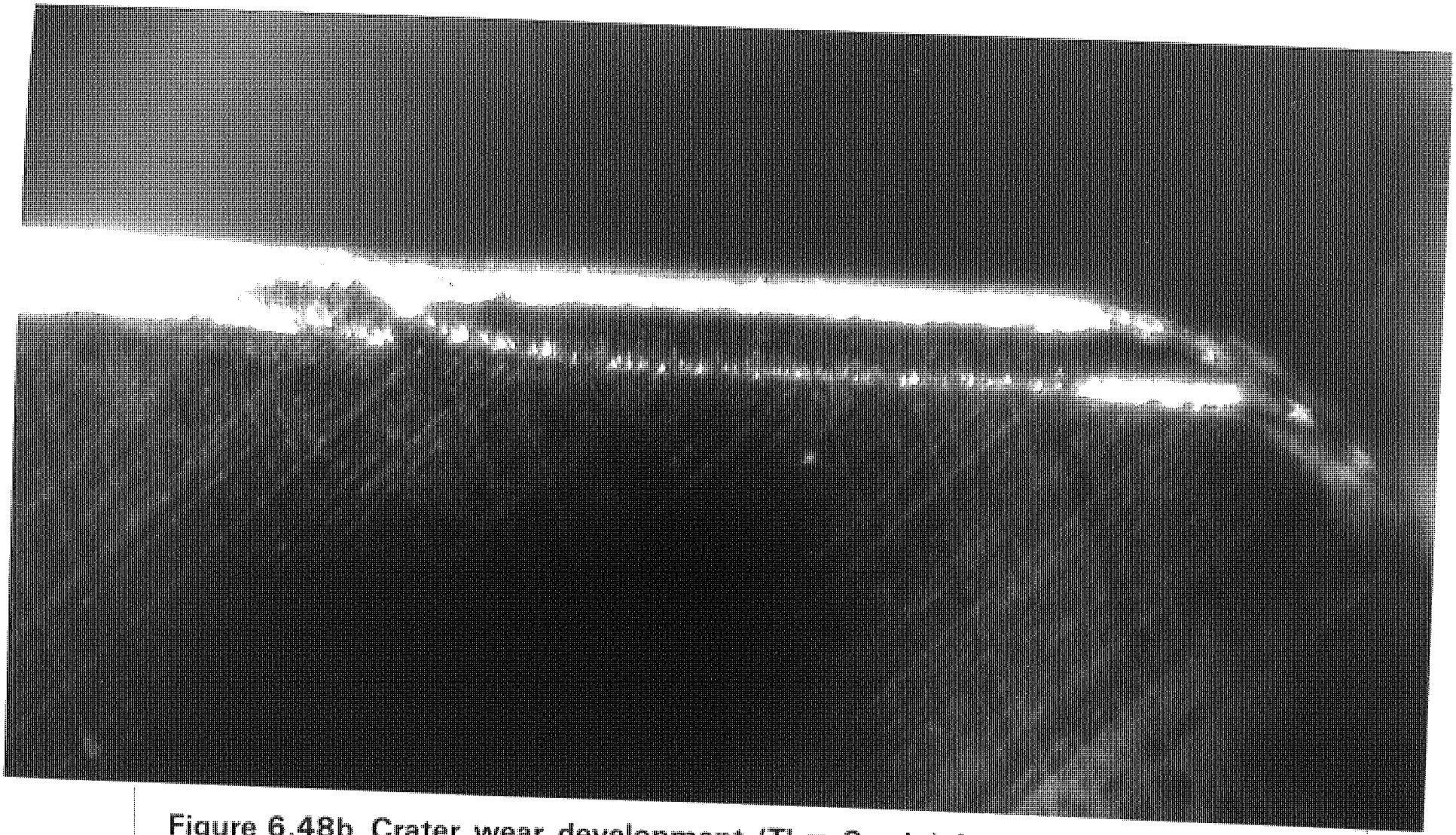

Figure 6.48b Crater wear development (TI = 8 min) f = .17mm/rev, v = 90 m/min

Figure 6.48c Crater wear development (TI = 14 min) f = .17mm/rev, v = 90 m/min

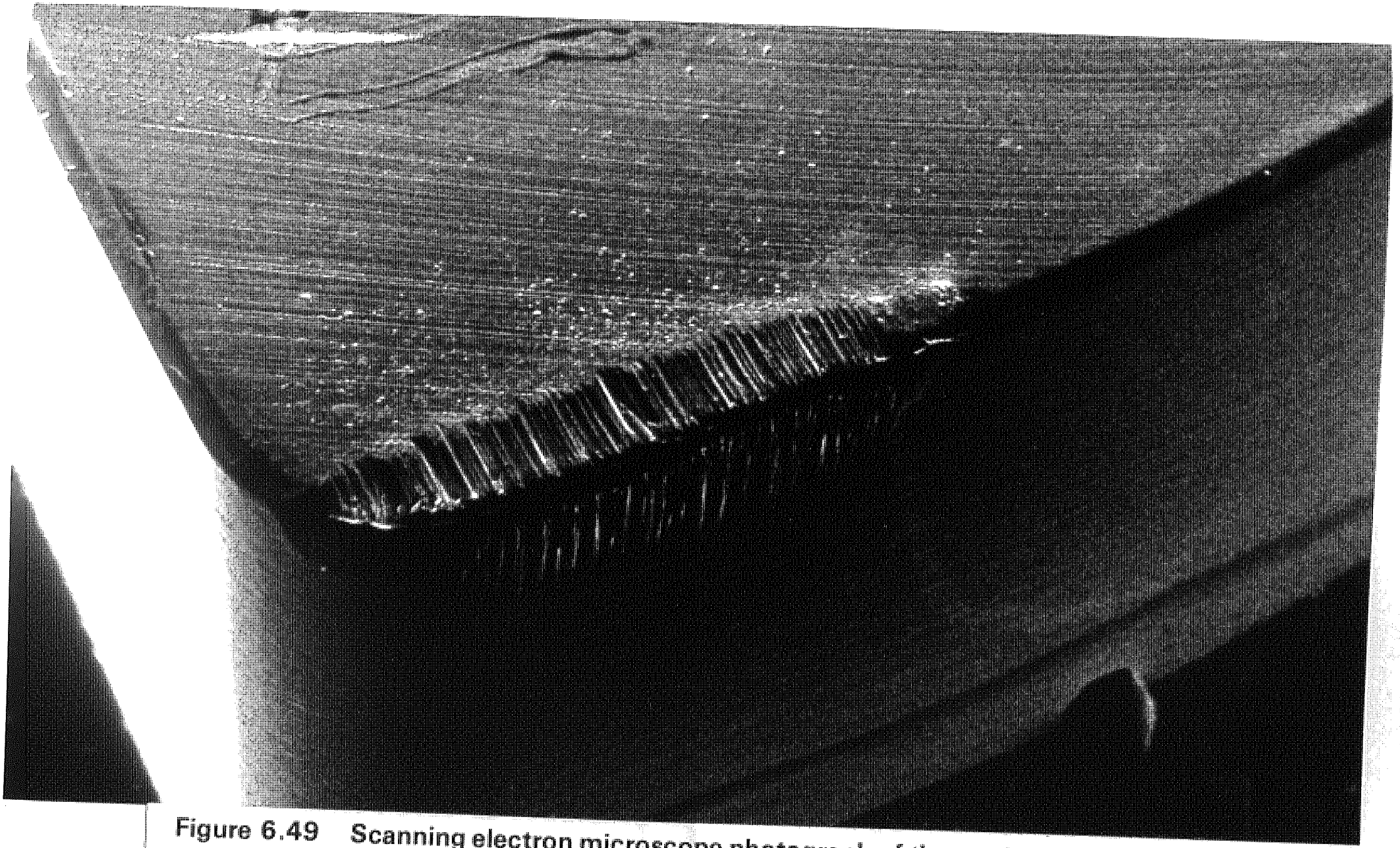

Figure 6.49 Scanning electron microscope photograph of the cutting edge of V = 90 m/min, f = .25 mm/rev

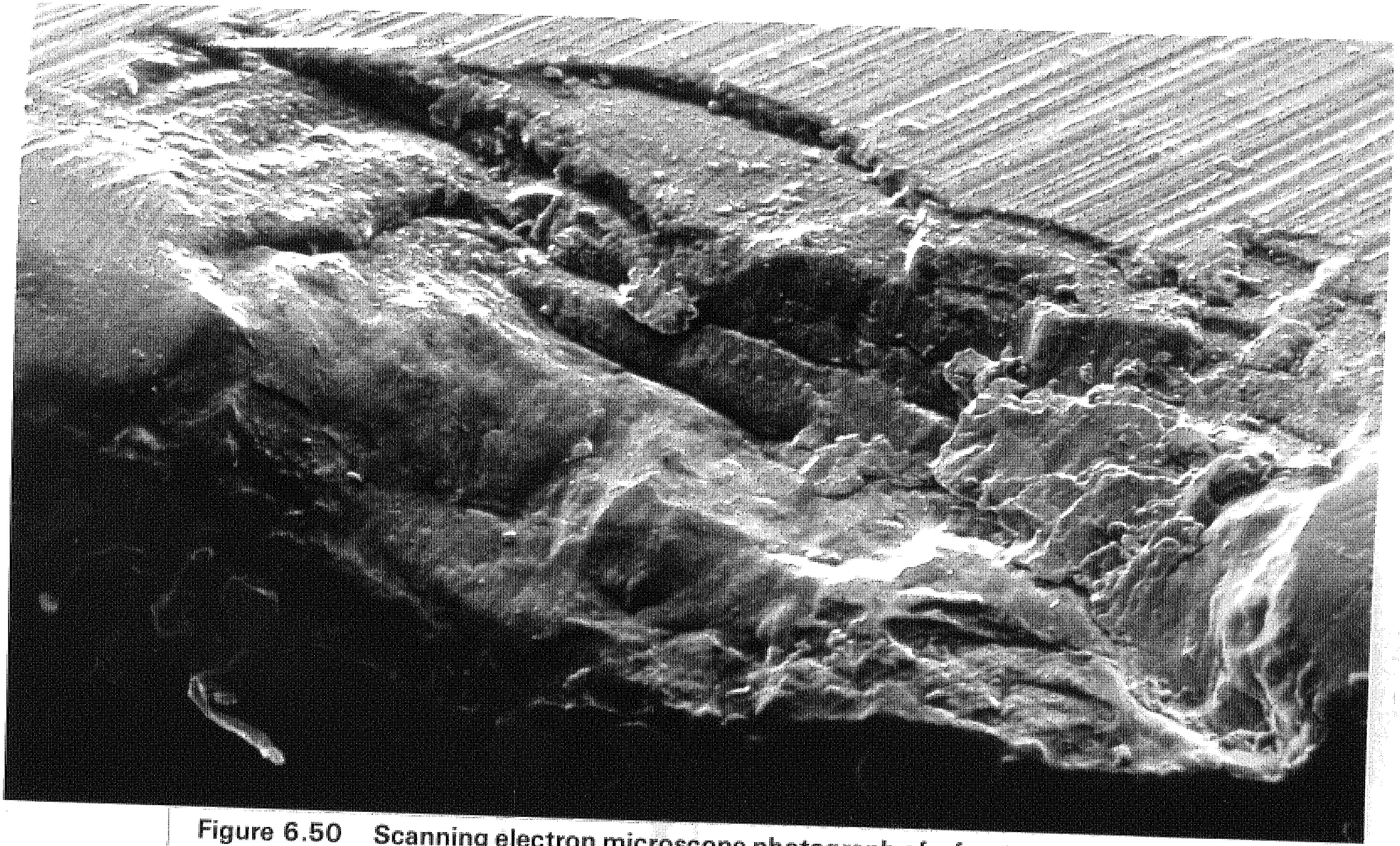

Figure 6.50 Scanning electron microscope photograph of a fracture on the rake face, V = 200 m/min, f = .33 mm/rev

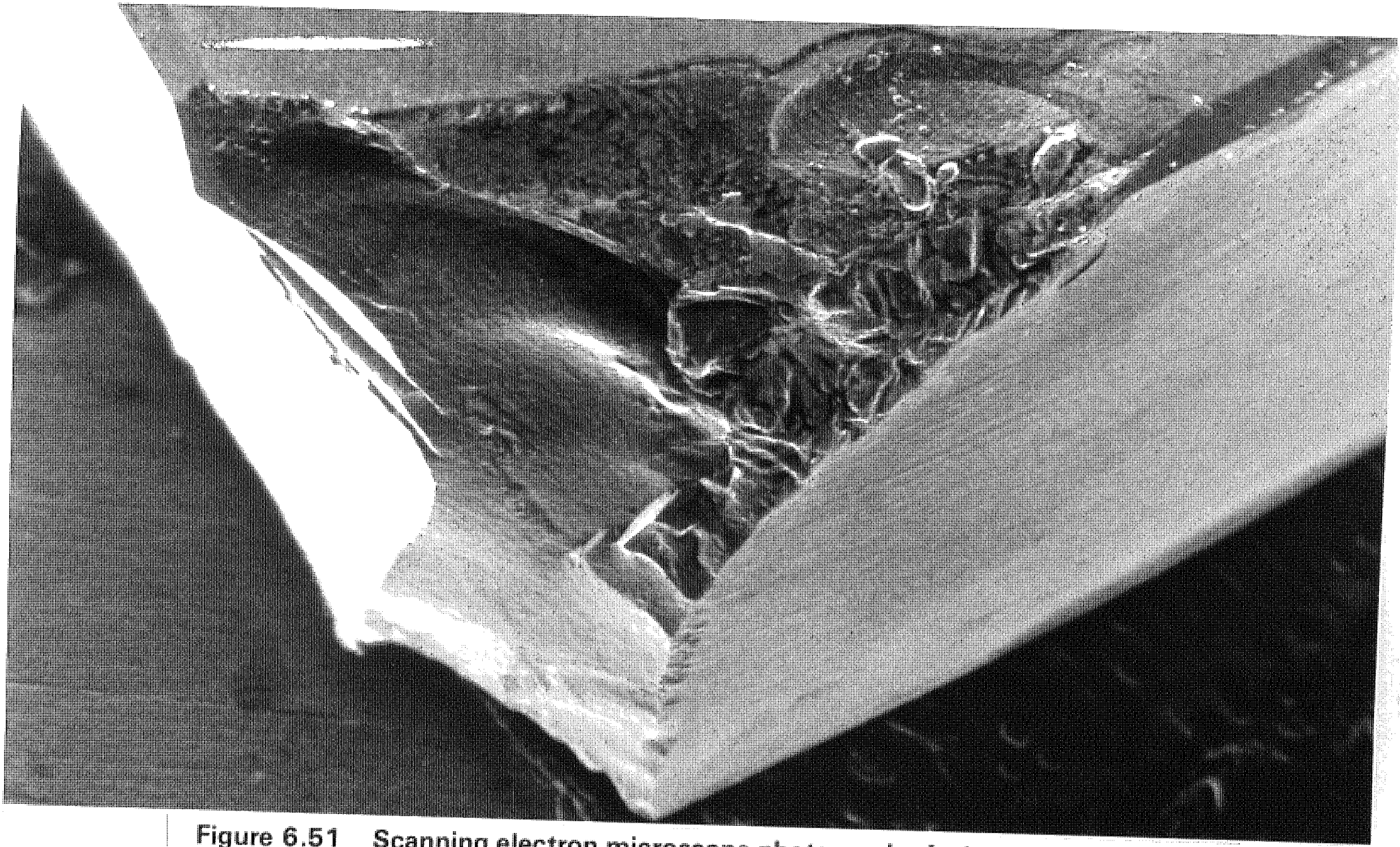

Figure 6.51 Scanning electron microscope photograph of edge crumbling, V = 400 m/min, f = -056 mm/rev

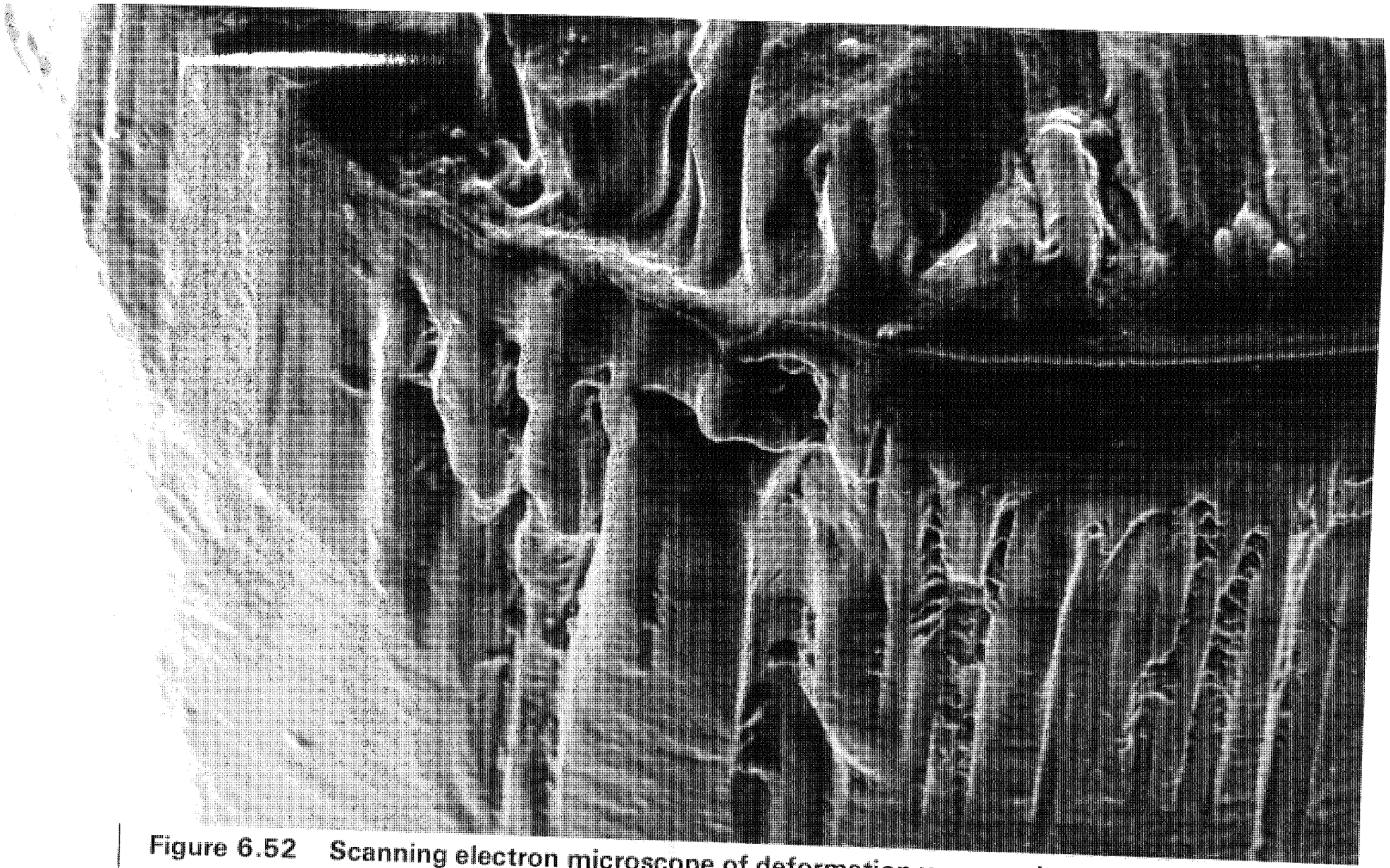

Figure 6.52 Scanning electron microscope of deformation wear on the nose of the cutting edge.

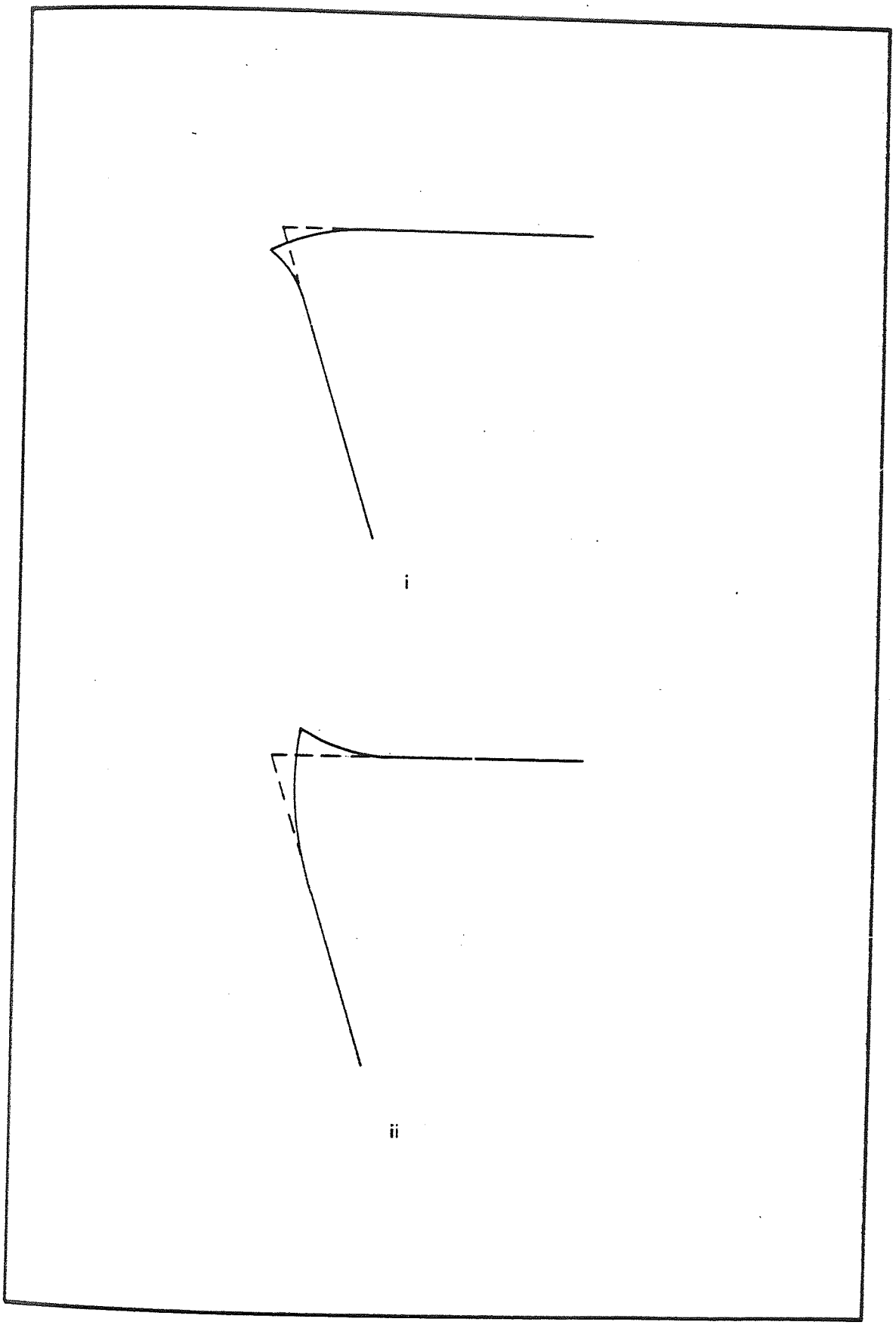

Figure 6.53 Deformation of Cutting Edge

CHAPTER SEVEN

THE USE OF A DOUBLE RAKE ANGLE ON KYON 2000 INSERTS

7.2 SURVEY OF PREVIOUS WORK ON GEOMETRY MODIFICATION

Cutting edge geometry modifications have been studied by many researchers for a number of years.

In 1922 Deleeuw[84] suggested the use of lathe tools with limited rake surface in order to facilitate chip flow. Klopstock[85] in 1925 designed the cutting tool suggested by Deleeuw, He reported that the use of such tools resulted in a minimum of compression and deformation of the chip, with a consequent reduction in tool forces, saving on power consumption, and a more favourable wear mode.

Herbert in 1928[86] suggested a compound cutting tool which combined the advantages of both obtuse and acute angle tools. The performance of double rake tools has been reported by Armitage and Schmidt[87] in milling. They suggested that using positive rake facilitated the chip flow and avoided serious chip and workpiece deformation whilst the negative rake provided a stronger cutting edge avoiding chipping and reducing wear. It was also found that the tool life increased as the land width increased up to a maximum of approximately twice the feed/revolution as compared with a conventional 12^{o} negative rake tool. Armitage and Schmidt also claimed that power requirements and temperature decreased when double rake tooling was used.

Jensen in 1958[88] presented a comparison between the cutting performance of double rake tools with both negative and positive rake carbide tools in a boring operation on hardened steel. The positive rake tools failed through chipping whilst the negative rake type increased the amount of chatter due to the lack of rigidity. A double rake tool of 30^{o} negative primary rake and 5^{o} positive secondary rake with 0.75 mm land width was selected for the same machining operation, using a wide range of feed rates.

Jensen suggested that:

1) the same tool geometry was suitable for heat treated steels and soft metals

2) the grade of carbide was unimportant although titanium grades are preferable.

3) Cutting speeds up to 194 m/min for hardened steel (42Rc) were successful.

4) tools could be stalled in cut without breakage

5) absolute rigidity of the tool and workpiece was no longer necessary.

The results of Jensen's work have been questioned by a number of authors, the argument being that tool material and edge geometry are dependent variables. Furthermore, the rigidity of the machine tool is very

important in machining operations.

Chao and Trigger[89] reported the results of an investigation on the performance of controlled or restricted contact cutting tools. They claimed a substantial reduction in power consumption, an increase in tool life, more effective utilization of cutting fluids, and improved surface finish on the machined workpiece. The cutting forces were also found to be lower with restricted contact tools. Since the frictional force on the tool top face was lower and the chips were thinner. The increase in tool life was attributed to the lower temperature at the reduced chip tool contact length.

Kibbey and Moore[90] reported results when using both carbide and ceramic tools in turning hardened tool steels (51Rc). The tests showed that the tool life increased when the negative primary angle and primary land width were increased. A negative primary rake of 30^{o}, with a land width of 0.2 mm and a 5^{o} positive secondary rake gave an increase in tool life as compared to positive rake cutting tools both for carbide finishing grades and ceramic tool materials.

Hitomi[91] carried out investigation using a 30^{o} negative primary rake and a 15^{o} to 30^{o} positive secondary rake. He studied the effect of these geometries in the development of the 'silver white chip' cutting

tool . It was found that the land forms a so called stable built-up-edge which is induced to flow out continuously along the side cutting edge and acts as an active cutting edge. The tool is claimed to reduce both the cutting temperature and cutting forces and it is also argued that tool life and surface finish are improved. The optimum feed to land width relationship was found to be ½ - ¾ of the feed.

Bagley[92] investigated the double rake tool geometries using a ceramic cutting tool material. The tool had a negative primary rake of 45° with land width being varied up to a value of 1.65 mm. Hardened tool steels (62Rc) were turned with a feed rate of .127 mm/rev and a speed of 123 m/min. It was found that the addition of the negative land strengthened the cutting edge and reduced the initial breakdown giving improved tool life compared to a positive rake tool. However, a feed rate higher than 0.127 was not possible due to the excessive temperatures and cutting forces generated. A very rigid set-up was also needed. The high ratio of land width to feed rate used in this work meant that effectively the tool was wholly negative and so any benefits could not be attributed to the use of a double rake angle.

Albrecht[93] also investigated double rake tooling when milling high strength steels. He suggested that during the milling process the stress field that develops in the cutter tooth may be such that fracture would occur

and that the nature of the stress field depended on the intensity of the initial impact and the shape of the edge on the initial impact. The tool had two different geometries, a 30^{o} negative primary rake with a 5^{o} positive secondary rake and a 0^{o} primary rake with a 25^{o} positive secondary rake. It was found that the cutting forces decreased as the land width decreased and that the minimum force value occurred at zero width. Furthermore, he reported that proper edge preparation could result in the following advantages.

- improved resistance to initial impact.
- reduced wear rate on the tool flank.
- reduced rate of increase in flank wear at high wear levels.

He also suggested that the best ratio of land width to feed was 2.4 but that in practice a 1:1 ratio would probably be used.

Zorev[94] showed that the tool behaved as a wholly negative rake tool if the land width is greater than the chip tool contact length. However, he also claimed that the chip formation process would be only marginally affected if the land width was less than the chip tool contact length. The latter finding was based on results using a low strength steel and is only applicable to this type of steel as shown by Draper [81]. It was also shown that an optimum land width to the feed ratio of 1.55 was found

when machining a steel at different levels of tensile strength and feed rate. This suggests that a single land width feed ratio is obtained for any tool work combination and cutting conditions. However this has not been confirmed by other authors and is not the result obtained in this work. The optimum land width was claimed by Zorev[26] to be around one quarter of the natural chip-tool contact length of a negative tool. The formula for optimum land width found in relation to both cutting speed and feed rate was:

$$\text{optimum land width} = \frac{f^{0.45}}{v^{0.23}}$$

However, the above expression does not take into account the workpiece material properties. Clark and Ludwing[94] concluded that the ratio of land width to feed rate should be 1:2. Furthermore, it was claimed that longer tool life was obtained from negative rake tools than positive rake tools when turning.

Braiden[95] also suggested that the land width/feed rate ratio should be a half to three-quarters. However, in the above report no tool geometry or work material were specified.

Agnew's investigation[96,97] showed that a substantial increase in tool life is obtained by:

1) Strengthening the cutting edge.

2) Directing the cutting force into the tool shank.

3) Weakening the chip.

4) Removing any obstruction to the chip flow.

A 200% increase in tool life was claimed when using cutting tools with an edge honed by tumbling in an abrasive slurry, the honed radius not exceeding 30% of the chip thickness. Agnew differentiated between a chamfer and a negative land. A chamfer was considered as having an angle of about 40^{o} to the top face of a negative rake insert and about 50^{o} to the top face of a positive rake insert giving a land angle of 45^{o}. It was claimed that this type of chamfer should be no more than 30% of the chip thickness. It is reported that there is no advantage in having a negative angle greater than 15^{o} and furthermore it is suggested that the land width should be equal to or more than the feed rate.

Agnew described three methods of edge strengthening which are:

a) Chamfering

b) Honing

c) Chamfering and honing.

These different types of edge are shown in figure (7.1) and for comparison an edge with a negative land is also shown. Agnew identified these edges by their

applications, chamfered edges are for heavy, interrupted and rough cutting conditions; honed edges are for finishing cuts and chamfered and honed edges can be used instead of chamfered tools. The honing minimises the effects of minute notches due to grinding the chamfers which would serve as initiation sites for cracks. The tools with negative lands can be coupled with any of the edges described. The recommendations for chamfered tools and tools with negative lands do not give an adequate indication why these two terms should have different meaning except the difference in the specified land angles. The recommended land angle of less than 15^{o} would probably be prone to chipping. For the chamfered tools the higher value of chamfer angle used would obviously reduce the contact length and increase the chip thickness. The ratio of chamfer width to chip thickness will be lower as compared to the case when the land angle is 15^{o}. The foregoing shows that the tools with chamfered edges and with land widths are effectively the same, and the value of the land width depends on the cutting conditions.

Lenz et al[98] used a variety of chamfer angles and land widths on two different tool materials, i.e. Tic base and WC-base carbides. An intermittent cutting operation was simulated by turning a slotted bar having a hardness of 11Rc. The tool life criteria used was to compare the number of impacts which the tools could withstand. It was also considered that the number of impacts related directly to the volume of metal removed.

Chamfering the cutting edge at the proper chamfer angle and width was found to result in a major improvement in tool life of a Tic-base tool, and in a moderate improvement in tool life for a similar grade of WC-base tool. It was suggested that a chamfer angle of -30^{o} and a land width approximately half of the feed was a good overall tool geometry for edge strengthening.

Draper[81] and Draper and Barrow[99] investigated the cutting performance of double rake angle tools. A negative land was ground on to positive rake cutting tool to simulate the change in shape due to the deformation at the cutting edge. The magnitudes of the land widths were varied in order to establish the optimum land widths for various cutting speeds, feeds, primary rake angles, work and tool materials. It was found that the land geometry used has a considerable influence on the cutting forces, chip thickness ratio, contact length and surface finish. The optimum land width was found to be dependent on the cutting speed, feed, tool and workpiece material. Furthermore, at the optimum land width, the cutting forces were found to be greater than for the pure positive tool but lower than for tools with larger than optimum land widths. However, the deformation patterns for the double rake angle tools were not investigated although it was found that the optimum land width tool gave the best tool life for a particular set of cutting conditions. It was concluded that there is no fixed relationship between the feed and land width as

was claimed by previous researchers. The land width depends on the cutting conditions used and should be established by machining experiments.

Draper also carried out a comparison between the double rake tools and restricted contact tools with particular reference to the work of Chao and Trigger[89] An explanation was provided for the performance of the various tools in terms of the average normal and shear stress values on both rake and flank faces as shown in figure (7.2)

It was found from Chao and Trigger's investigations that the average stress magnitudes on the rake face increased with a decrease in land width because it was not realised that in some instances they were working in the double contact mode region. This lead them to believe that the average stresses were increasing as discussed by Albrecht[93]. Furthermore, the shear angle relationships which are necessary to calculate the average stresses cannot be applied in the double rake contact situation due to the presence of the two rake angles and the problems involved in separating the normal and shear forces on these faces. The separation of these forces on the two rake faces along with the stress distributions will be established in the current work using a split tool dynamometer. Moreover Draper extrapolated the average and shear stresses at the rake face in the region of double contact because the cutting forces on the two faces cannot be separated as mentioned

earlier, and existing expressions such as Merchant could not cater for two rake angles. However, the extrapolation may be justified since the contact length is higher than at the optimum and hence the average stresses will be reduced. The average normal stress values on the flank are the reverse to those found on the rake face. These values were calculated using the expressions suggested by Yellowley[101,102].

$$\sigma f = C_3(1 - \sin 2\phi)$$

where C_3 is the mean shear yield strength under metal cutting conditions and ϕ is the shear angle.

Kendrick[102] studied double rake tooling when face milling a medium carbon steel. Using conventional cutting speeds and feed rates, standard positive rake and negative rake inserts were examined using up-cut and down milling after grinding a range of chamfer angles and chamfer widths on the cutting inserts. It was concluded that a significant improvement was achieved by the addition of a negative land to positive inserts for both the above two operations. Virtually any land angle improved the performance, but an optimum chamfer angle of 15^o was suggested. The cutting forces produced by the standard and modified inserts were studied, and it was reported that chamfering the inserts up to about 25^o causes only a marginal increase in the cutting forces.

Fowler[103,104] did double rake work on both carbide and coated carbide tool materials. It was found that significant improvements in the cutting performance, particularly with regard to catastrophic failure when cutting steels, were achieved by the generation of a narrow primary rake land, the width and angle of which depends upon the cutting conditions. The average chip tool interface temperature was reported to increase with an increase in the feed rate and with an increasingly negative primary rake angle at a constant land width. However, when the land width was varied for a particular set of cutting conditions, it was found that at a certain value which coincided with the optimum land width as determined from previous experiments, the temperature was minimum.

More recently Ahmmed[105] examined a double rake tool analytically using the technique of finite elements on data obtained experimentally from photoelastic machining investigations. It was claimed that the presence of a primary land has a significant effect on the stresses and deformations occurring within the tool.

7.3 EXPERIMENTAL WORK

7.3.1 Measurement of the Cutting Parameters

All cutting tests in this chapter were undertaken using a 10/30 horse-power motor Swift lathe. Cutting forces were measured using a Kistler piezo-electric 3 force dynamometer.

A universal measuring machine was used to measure the extent of flank wear, and furthermore this equipment was used to measure the contact length between the chip and the cutting edge on both the primary and secondary rake faces. Measurement of chip thickness was carried out using a clock gauge equipped with a special pointed anvil designed for this purpose. The temperature distribution on both rake face and flank face of the cutting insert was determined using the constant melting point powders technique[70]. Furthermore, cutting tests were performed using a split tool dynamometer. Measurements of the workpiece surface finish were made with portable Rank Taylor Hobson measuring equipment. The surface finish was measured for the different edge configurations used. The characteristics of the measuring equipment are described in Chapter 5.

7.3.2 Tool Edge Configuration

The definition of the geometry for the double rake tool is shown in figure (7.3). A land or chamfer is ground in the rake face at a certain angle which is called

the primary rake angle and this face of the tool is called the primary rake face. The remaining portion of the tool rake face is called the secondary rake face.

For the purpose of grinding land widths at the required angles a fixture was designed to support the insert in the required position. The Kyon 2000 ceramic inserts were ground using a special grinding machine with a diamond wheel having 400 grit size and B56 bond. After grinding, the land widths were checked by means of a universal measuring microscope.

Three levels of primary negative chamfer angle, 10^{o}, 25^{o} and 40^{o} were used together with a constant 5^{o} secondary rake angle. The land widths ranged from .1 mm up to .8 mm. The tests were carried out under both orthogonal and oblique cutting conditions.

7.3.3 Workpiece Materials

The workpiece materials used in this series of tests were:

1. EN26 alloy steel hardened to values of 53Rc and 46Rc
2. EN9
3. Cast iron grade G17.

The composition of the materials is given in Appendix II. For orthogonal cutting, tubular workpieces of outside diameter 75 mm, 3.5 $\pm$ 0.025 mm wall thickness and 230 mm in length were prepared from bar stock. For oblique machining, bars of 127 mm diameter were used.

7.4 RESULTS AND DISCUSSION

7.4.1 Workpiece Material EN26 46Rc

Figure (7.4) shows the relationship between chamfer land width and the measured variables for a variety of chamfer primary rake angles.

Lowest force values; both cutting force (F_z) and feed forces (F_x) are achieved with zero chamfer land width. Under these conditions the rake angle is 5^o positive. The introduction of a chamfer effectively provides a negative primary rake and it is not surprising therefore that for all conditions where a chamfer is used the force is higher than this base level. It is also clear from the figure that for chamfer angles of -10^o and -25^o the forces increase significantly as chamfer land width is increased to 0.4 mm but thereafter the change is marginal. At an angle of -40^o the pattern changes slightly in that a chamfer land width of 0.5 mm is reached before the forces tend to stabilise. The stabilisation of the cutting forces at a certain land width indicates that a natural contact length has been reached.

Tool/chip contact length was measured on both the secondary and/or primary rake faces of the cutting insert using a universal measuring microscope described in Chapter 5; the results for contact length shown in figure (7.4), are particularly interesting because they indicate the presence of an optimum chamfer land width for minimum contact length. An optimum position exists

for each chamfer primary rake angle. For a primary rake of -10^{o} the optimum is reached at 0.4 mm land width, while for primary rake angle -25^{o} the optimum increases slightly to 0.45 mm land width. An increase in primary rake to -40^{o} gives a higher level of 0.5 mm for the minimum contact length. These minimum contact length values closely approximate to the point at which force stabilisation occurs. The reasons for the variation in minimum contact is considered to be due to the effect of temperature variation and stress distribution on the rake face and further consideration is given to this point in Section 7.5.1 and 7.5.2.

The curves of chip thickness ratio are also shown in figure (7.4). The cutting ratio increases from that at the base case (the condition where the rake angle is 5^{o} positive i.e. zero chamfer land width) to a maximum at the same land width where the position of minimum contact length was found. After the maximum value is attained the ratio decreases (chip thickness increasing) and finally tends to stabilise when the position of natural negative contact is approached. Furthermore, it is also clear that the natural negative contact is reduced as primary rake angle becomes less negative. The use of the chip thickness ratio in the present context is particularly interesting since it is often used as a measure of the efficiency of cutting: a greater chip thickness ratio (thinner chip) indicating a more efficient chip formation process. Therefore,it

can be argued that the land width giving maximum chip thickness ratio is optimum for the tool geometry being used.

7.4.2 Workpiece Material EN26 53Rc

Orthogonal cutting tests were also performed on a workpiece material having similar composition to that reported in Section 7.4.1 but with a hardness of 53Rc. The cutting conditions for this series of tests were similar to those used for material having hardness of 46Rc (V = 33 m/min and f = .25 mm/rev). The influence of land width on both the tangential force and feed force are shown in figure (7.5). It is seen from these graphs that there is a similar trend in the behaviour of the cutting forces with increasing land width to that reported for the softer material. As expected the cutting forces produced are somewhat higher because of the higher hardness. The lowest cutting forces values are obtained with zero chamfer land width. It is also clear from the figure that the higher hardness value had the effect of displacing the point of force stabilisation to a higher land width value. For primary rake angles of -10^{o} and -25^{o} the forces are increased significantly as land width is increased up to 0.5 mm, and then tend to level off. A land width of 0.6 mm is reached before the forces approach stabilisation when a primary rake angle of -40^{o} is used.

The variation in contact length and chip thickness ratio are again similar to that observed for a workpiece material with a hardness of 46Rc. The only significant difference is that the minimum contact length is slightly greater e.g. 0.6 mm compared to 0.5 mm for a -40^{o} primary rake angle tool. Once again the point of minimum contact length corresponds to the maximum chip thickness ratio indicating an optimum condition.

7.4.3 Workpiece Material EN9

Cutting tests were carried out using annealed EN9 as a workpiece material to investigate the behaviour of a relatively soft material. In this case a cutting speed of 75 m/min and a feed rate of .25 mm/rev were used. The plots of the cutting force F_z and the feed force F_x with respect to chamfer land width for a variety of primary rake angles are shown in figure (7.6). It is seen from this figure that similar force patterns are obtained to those of hardened steel. As expected the cutting forces are less in this case since the workpiece material used was in the annealed condition.

The pattern of contact length and chip thickness variation with changes in land width is rather different from that obtained with hardened EN26. Minimum contact length is apparently consistent at 0.6 mm for all values of primary rake angle and is equal to the land width at this point. The variation in chip thickness ratio is

much less pronounced and the influence of primary rake angle is less significant.

When machining a relatively soft material chip formation is much easier to achieve than when a hardened material is used. Consequently changes in tool geometry will be expected to have less significance and although there is an optimum land width for minimum contact length its use is less critical than it is for more onerous cutting conditions.

7.4.4 Workpiece Material Cast Iron G.17

When cutting a brittle material such as cast iron the chip formation will be different from that obtained for alloy steels. Accordingly a similar set of tests were carried out and the results are shown in figure (7.7) The workpiece material was machined orthogonally at a cutting speed of 100 m/min and a feed rate of .25 mm/rev. From figure (7.7) it is evident that as land width increases the cutting force increases up to a certain land width and thereafter the forces again tend to stabilise.

When machining cast iron it is generally expected that a small discontinuous chip will be produced with relatively low cutting forces and this is evident from the cutting test conducted. Due to the discontinuous nature of the chip it was not possible in this series

of tests to measure the chip thickness. However, contact length measurements were made and the results are presented in figure (7.7). The results reveal similar trends to those obtained for other materials and a minimum contact of 0.4 mm was observed for primary rake angle -10^{o}, while the minimum values for the higher primary rake angles of -25^{o} and -40^{o} were somewhat higher.

The implication of these results is that the concept of a minimum contact length, corresponding to a particular value of land width, is consistent for a range of workpiece materials. The fact that the material characteristics can be very different does not change the basic argument that an optimum land width exists and that this width is a function of primary rake angle.

7.5 TEMPERATURE, STRESS AND CHIP FORMATION

7.5.1 Temperature Distribution

As mentioned in the literature review in Chapter 2, the temperature produced during the cutting operation is one of the most important factors affecting the tool performance. It was decided, therefore, that in order to give a clearer explanation of the improvements brought about by double rake tools, temperature measurements would be made. Maximum information was expected from measurements of temperature distribution within the cutting tool insert for a range of tool geometries. No reference to temperature distribution when using double rake tools could be found in the literature.

The cutting tests were performed under orthogonal conditions at a cutting speed of 33 m/min and a feed rate of .17 mm/rev. EN26 having a hardness of 46Rc was used as a workpiece material. The tools had a primary rake angle of -25^{o} and a secondary rake of $+5^{o}$ together with three levels of chamfer land width of 0.3 mm, 0.45mm and 0.7 mm.

The technique used for measurement of temperature distribution in this work was the constant melting powder technique. An example of the divided surface observed under the microscope is shown in figure (7.8). White spots in the photographs found on the surface away from the cutting edge are unmelted powders. The surface consists of two zones, that is, a melted zone and an unmelted zone, and the boundary line between the two zones is clearly discernable from the photographs. The dotted line describes the equitemperature line for the melting point of the powder used. By using different powders having different melting points (see Table 7.1), the temperature distribution within the tool can be obtained by superimposing these equitemperature lines on the tool cross section.

The isotherm maps and temperature distributions on rake and flank faces obtained are shown in figures (7.9, 7.10 and 7.11) for the different land widths investigated. The temperature distribution along the rake and flank faces were obtained by plotting the

Table (7.1) Powders and respective melting points used in temperature investigation.

Name of powder	Chemical symbol	Melting point ^{o}C
lead sulphate	$PbSO_4$	1170
lead sulfide	PbS	1114
potassium magnesium sulfate	$K_2SO_4.2MgSO_4$	927
sodium chloride	NaCl	801
potassium chloride	KCl	776
cadmium chloride	CdCl	568
lead chloride	$PbCl_2$	501
Tin	Sn	232.1

temperatures at the points where the equitemperature lines intersect the rake face and flank face, respectively. It is clear from the figures that the temperature distribution within the tool is different for the three types of tool configuration. At 0.3 mm chamfer land width the contact length, as indicated in figure (7.12) is 0.475 mm and is therefore much greater than the chamfer width. In this situation both primary and secondary rake angles are significant. The high contact length will lead to high friction energy and therefore a high shear strain is required to form the chip[106]. A similar effect is seen (figure (7.11)) at the longest chamfer land width because although contact is now restricted to the primary rake the length of contact is higher than the optimum value. With a chamfer width of 0.45 mm the contact length falls close to its optimum value giving good cutting conditions, lowest friction energy, lowest shear strain and consequently the minimum recorded temperatures. It is interesting to mention in this context that with the above mentioned geometry, no melting was observed at the cutting edge when powder of higher than 927^{o}C melting point was used. The temperature pattern obtained with the optimum geometry results in a better performance from the tool.

Authors[81,103] who have used the tool work thermo-couple method to measure average temperatures have recorded an initial decrease in temperature followed by an increase as tool geometry is changed to give increased contact length. These results confirm such a temperature

variation.

Furthermore, in recent work on thermal stresses carried out by Ahmmed[105], it was found that as temperature increases in the cutting operation the level of thermal stress also increases, particularly close to the cutting edge. An increase in thermal stress would be expected to increase the likelihood of thermally induced cracking at the tool point. The tool geometry used by Ahmmed was different from the one used in this investigation but it is believed that the thermal stresses would act in a similar way and would therefore be expected to have an effect on cutting tool performance.

Moreover, it would appear also from the figures that the maximum temperatures were shifted away from the cutting edge and this can be related to the tool wear as discussed by Hoshi[107] and Usui[108]. These workers concluded that the wear form varied from that of conventional tools in that:

1. the crater shifts away from the cutting edge as cutting proceeds,

2. the crater begins near the end of the primary contact length and grows on to the secondary rake face and

3. the crater on a double rake tool is considerably smaller when compared with the crater obtained

with a conventional tool under similar cutting conditions.

The second finding correlates the region of maximum temperature with the region where the cratering starts and is given in favour of the better performance of double rake tools. Furthermore, the constant melting point technique used in this work also gave an explanation of what is happening along the flank face of the tool. It is clear from the figures that a better temperature distribution was obtained when double rake tool is used. The graphs also reveal that a lower temperature is observed, along the flank face with the optimum geometry.

7.5.2 Stress Measurements

From the literature review and the experimental results in Sections 7.2 and 7.4.1-7.4.4, it is seen that the cutting forces, contact length and chip thickness are readily measurable parameters. These cutting parameters may be studied in order to assess the behaviour of tools with various edge geometries. However, in order to gain a better understanding of the detailed stress distribution on the cutting edge a split tool dynamometer[25] was used. Data on stress distribution for single rake tools has been reported[23,24] but there is no literature available on stress distribution with double rake tools.

7.5.2.1 The Split-Tool Dynamometer

The design features of the split-tool dynamometer are described in detail in Chapter 5. Its working principles are given here.

As the name implies, this type of dynamometer uses a cutting tool which is not a solid whole. It comprises two tool inserts suitably ground to a typical configuration shown in figure (7.13). The dynamometer is designed in such a way as to make only one of the tool components force sensitive, and therefore the dynamometer measures only part of the cutting force. Different cutting geometries are ground on the cutting insert;

and by varying the position of the gap (G) (see figure (7.13)) a different portion of the cutting forces will be measured. Stress distributions can then be calculated from the measurements of $(F_z, F_x L_1)_n$ and $(G)_n$. From figure (7.14) is seen that the point at which $(F_{n+1} - F_n)_z$ or $(F_{n+1} - F_n)_x$ acts is given by M_n where

$$M_n = \frac{1}{2}\left[(L_1+G)_{n+1} + (L_1+G)_n\right]$$

Then if W is the width of cut,

$$\sigma_n = \frac{(F_{n+1} - F_n)_z}{W\left[(L_1+G)_{n+1} - (L_1+G)_n\right]}$$

$$\tau_n = \frac{(F_{n+1} - F_n)_x}{W\left[(L_1+G)_{n+1} - (L_1+G)_n\right]}$$

However, in order to simplify the calculation of the stresses, a graphical relationships are drawn between both F_z, F_x and the value $(L_1 + G)$, and then the values of σ_n and τ_n can be calculated by choosing regular intervals of the term $(L_1 + G)_{n+1} - (L_1 + G)_n$. The gap between the two parts of the tool tip is very important and has to be maintained at 0.076 ± 0.025 mm using a high power microscope in situ.

The split tool dynamometer was built onto a Kistler piezo electric turning dynamometer as shown in figure (7.15) and accurate results were only achieved if great care was taken with tool setting. The major experimental

limitation was that because the gap position influenced the length 'L_1' and hence the strength of the front section of the split tool it proved impossible to obtain a force reading nearer than 0.142 mm to the cutting edge.

7.5.2.2 Tool Material

Kyon 2000 ceramic inserts (12.7, 12.7, 4.76 mm) were used. These standard inserts were modified so that the cutting test were performed on a cutting tool having chamfer land widths of .3, .45 and .7 mm with a constant primary rake angle -25^{o} and secondary rake angle of $+5^{o}$ The land width L_1 of each front and back tip was checked, together with the angles, using a universal measuring microscope described in Chapter (5). The tool set-up is shown in figure (7.15).

7.5.2.3 Workpiece Material

The material used in these series of tests was tubular EN9. The preparation of this material was described in Chapter 5. Material in the hardened condition was also tried, but no useful results could be obtained because of the high force developed during the cutting operations.

7.5.2.4 Analysis of Split Tool Dynamometer Data

It is possible to calculate both the normal stress and shear stress distributions from pairs of measured values of F_z, F_x and G. However, smoothing out of the measurable data was done by plotting F_z, F_x against $(L_1 + G)$. The above relationships are shown in figures (7.16, 7.17 and 7.18). From each group σ_n and τ_n were calculated using an interval of 0.5 mm between successive lengths of $(L_1 + G)$. In some cases the last value of $(L_1 + G)$ would be less than 0.5 mm from the previous one.

It is seen from the graphs that similar trends were obtained for all the three different geometry tests. For a land width of .3 mm there is a large force acting on the secondary as well as the primary rake and because secondary rake is positive it is likely that large forces acting in this area will lead to tool failure. At .45 and .7 mm land width the forces are confined to the negative primary rake but they are significantly higher at the larger land width. Hence best performance would be expected at .45 mm land width. It is noticeable from the graphs that the forces near the cutting edge are maximum, while moving away from the cutting edge they tend to decrease to minimum values as the chip leaves the rake face.

However, as shown from the figures, no attempt was made to join the curves to the "zeroland" results

(those cutting test obtained using a solid tool) so as to obtain the stress distributions all the way to the cutting edge.

7.5.2.5 Normal Stress Distributions

The results of the normal stress distributions obtained while machining EN9 are shown in figure (7.19). It can be seen from the figure that the level of compressive stress increases as the land width is increased from 0.3 mm (case of double rake contact) to 0.45 mm (case where optimum contact occurred). However, a further increase in land width up to 0.7 mm, causes a decrease in compressive stress. Furthermore, the results indicate that the stress distribution on the primary rake face is high compared to that on the secondary rake face. This is because the primary rake face is the major part of the tool as far as contact length is concerned. Moreover, it would appear from the graphs that similar trends are obtained where the stress values are maximum near the cutting edge and reduce to minimum values when the chip leaves the rake face of the tool.

Similar relationships were suggested by Draper and Barrow[99] where it was not possible to measure the stresses on the double rake tooling since the forces need to be apportioned on the primary and secondary faces. Ahmmed[105] more recently carried out an

investigation on double rake tooling performance using a photoelastic model. He reported as shown in figure (7.20) that a neutral axis exists (when n=0) between the regions of compressive and tensile stresses. Furthermore results on different geometries indicate that this axis moves away from the cutting edge as the land width increases up to an optimum condition, and thereafter the axis begins to get closer to the point where the land width ends. This movement of the neutral axis away from the cutting edge indicates that the tool rake face is under a high compressive stress outside the tool chip contact length which is not the case with the standard tool. The above findings confirm the results obtained here under actual metal cutting operations.

It may be concluded that by using double rake tool a higher compressive stress is produced which is more favourable for a tool material lacking toughness.

7.5.2.6 Shear Stress Distributions

Figure(7.21) shows the shear stress distributions along the rake face of the cutting insert for the tests carried out. Again as shown from the figures similar trends were obtained for the different geometries. Although no stress values were obtained at the cutting edge, due to limitations of the split dynamometer technique , the graphs reveal that maximum values are found to be near the cutting edge and the tendency of the

stresses to reduce to minimum values as the chip leaves the rake face of the tool. It is also seen that when the land width of the cutting insert increases the shear stress at the cutting edge increases. This is expected since the area under the curves is proportional to the frictional forces. Furthermore, it was found that under all the cutting conditions used, there was no indication that a constant shear stress value could be obtained near the cutting edge, as suggested by Zorev[26]. These results confirm the findings of Kudo[23] and others.

It is interesting to note that the results obtained by Ahmmed[105] using the photoelastic technique confirm the results obtained in this work.

7.5.3 The Chip Formation Process

The role which tool-chip contact length plays in affecting chip formation has been studied by many investigators. As shown from the results presented in Section 7.4 a reduction in tool chip contact length when double rake tooling is used can bring about a reduction in chip thickness, lower and better distribution of cutting temperature, better stress distributions and an increase in the tool life.

Examination of the photomicrographs produced by Fowler et al[103] and reproduced in figure (7.22) shows the formation of a compressed area of workpiece material

called a "dead zone" on the missing part (the chamfer) of the cutting edge over which the chip must shear. Figure (7.22) reveals typical chip formations for various land widths which were obtained with TiN coated double rake tools. It is seen that as the optimum contact is approached, figure (7.22), the chip thickness becomes unstable giving a saw-tooth upper surface chip. Returning to the controlled contact, the chip becomes stable.

Furthermore, as the chip formation process is basically considered a shearing process these results indicate a condition where the chip is produced with less strain. Therefore, it may be suggested that the shear angle developed when using double rake tools has the tendency of increasing initially when the contact is on both primary and secondary faces and as the controlled contact is reached, it decreases. Results to confirm this are shown in figures (7.23) and (7.24) where an experimental shear angle-chamfer land width relationship is presented for EN26 and EN9 materials respectively. The shear angle is calculated using the following formula[81]:

$$\tan\phi = \frac{t1/t2 \cdot \cos\alpha_2}{1 - t1/t2\left[\sin\alpha_2 - f/t1 \sin(\alpha_1+\alpha_2)\right]}$$

It may be concluded,therefore, that although the type of the tool used in this investigation was different from that used by Fowler[103], the generally expected mode of chip formation as defined by Fowler would apply.

7.6 PRACTICAL CUTTING TESTS WITH KYON 2000 DOUBLE RAKE TOOLS

7.6.1 The Influence of Geometry Modification on Tool Life

It is clear from the orthogonal cutting test results that there is a definite point for each of the materials used at which the tool geometry is optimum. These results agree with the findings of Draper[81] for carbide and Fowler[104] for coated carbide as discussed in the literature survey in Section 7.2. The optimum contact length found for the investigations carried out using Kyon 2000 ceramic cutting tool is shown to be highly dependent on the workpiece material and cutting conditions. The performance of the tool at this position can be considered to be optimum, because the chip thickness ratio (t_1/t_2) is maximum at that point compared to all the other land widths used. In order to verify that the expected optimum tool geometry would give optimum tool life, a limited series of tool life tests was carried out. The primary rake land width was varied and oblique cutting condition were used as being more representative of practical operations. For these tests a fixed primary rake angle of -25^{o} was chosen. The tests were carried out at a cutting speed of 150 m/min, a feed rate of .25 mm/rev, and a depth of cut of 2 mm and with a 45^{o} side cutting edge angle. The workpiece material used was EN26 having a hardness of 46Rc.

Tool life is defined in these series of tests as the time taken for the flank wear to reach 0.75 mm.

The results of the above series of tests are shown in figures (7.25) and (7.26). From figure (7.25) it can be seen that tool life increases to a maximum with an increase in land width followed by a decrease and a tendency to level off at higher land widths. By comparison of these results with figure (7.4) obtained under similar conditions, but for orthogonal cutting, it is clear that the maximum tool life value is obtained when the land width is equal to the optimum as defined by the maximum chip thickness ratio.

Figure (7.26) shows the flank wear-cutting time relationship. It is noticeable from the graphs that as the land width was increased from .2 mm to .45 mm, the wear on the cutting edge was reduced. However, a further increase in land width resulted in an acceleration of the flank wear of the cutting insert. It is also evident that the tool wear curves are similar to the typical wear curve shown in figure (6.1)

It can be concluded from these tests that the increase in tool life brought about by an increase in the land width from .2 mm to .45 mm may be attributed to the increase in strength and resistance of the cutting insert to failure. However, further increase in land width beyond the optimum value of 0.45 mm resulted

in a reduction in tool life which is due to the increase in temperature caused by the increase in frictional energy and shear strain since the contact length showed an increase after the optimum land width position.

7.6.2 Effect of Geometry Modification on Surface Finish

During the tool life study cutting tests reported in Section 7.6.1, the surface finish of the workpiece was monitored. Results of the measurements with respect to land width variation are shown in figure 7.27. It is seen from the figure that the improvement in surface finish follows similar trends to that found for the contact length in orthogonal cutting tests (see figure (7.4)). The improvement in surface finish can therefore be considered to be due to the influence of the tool wear progress during machining when the land width was altered, a finding substantiated by Enahoro in a study of factors affecting surface finish[109].

7.7 CHAPTER CLOSURE

In this chapter, edge geometry has been modified to give a double rake, negative/positive combination, and results were reported for a range of workpiece materials. Significant improvements in the cutting performance were achieved. The results are explained by the study of cutting parameters; cutting forces, chip thickness ratio, chip contact lengths, temperature distribution and chip formation. The stress distributions proposed by other researchers have been investigated only for single rake tools, but the current work has established the stress distributions for double rake geometries. Optimum geometry was shown to depend on both workpiece material and cutting conditions.

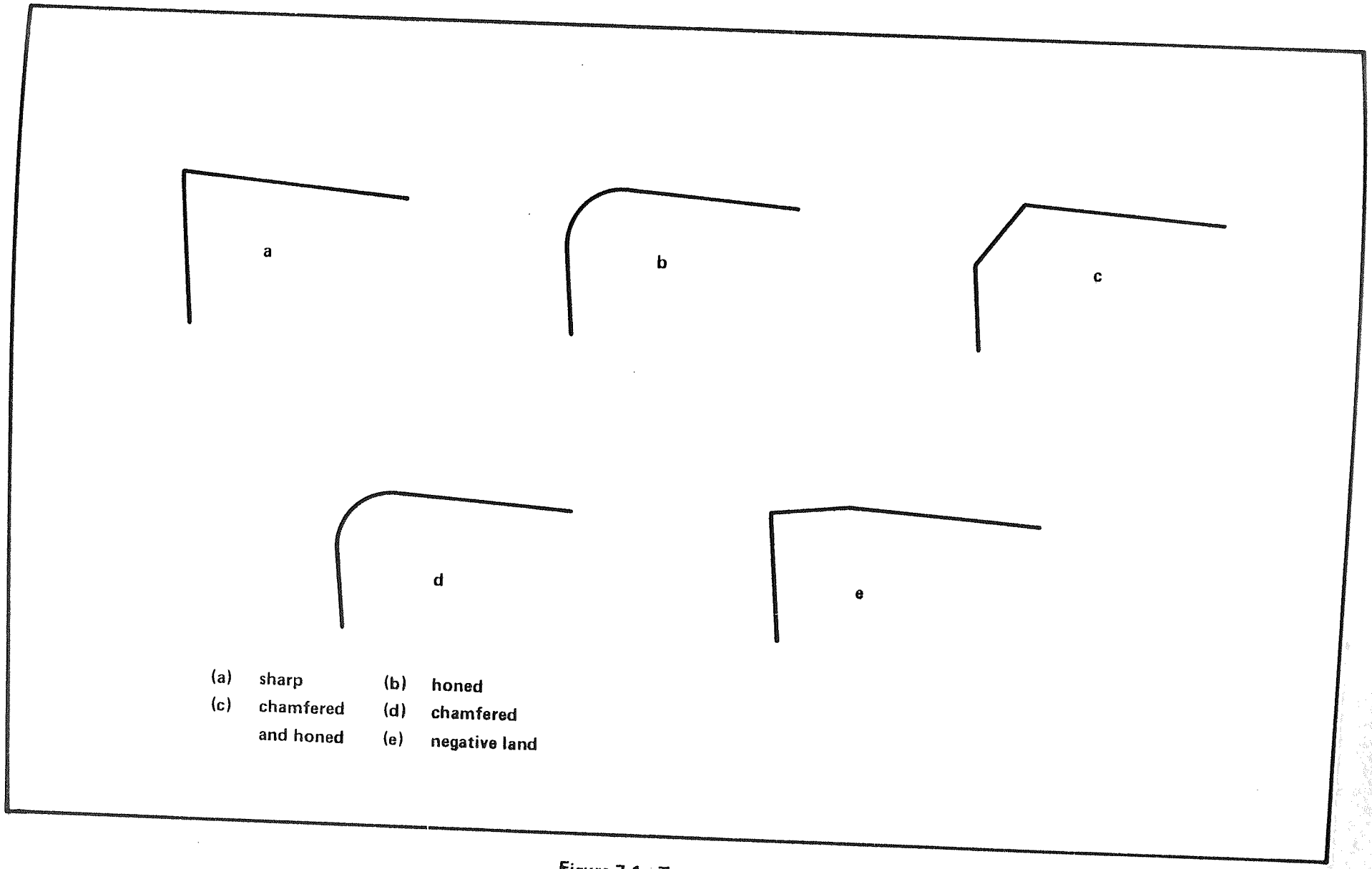

(a) sharp
(b) honed
(c) chamfered and honed
(d) chamfered
(e) negative land

Figure 7.1 Types of Edge

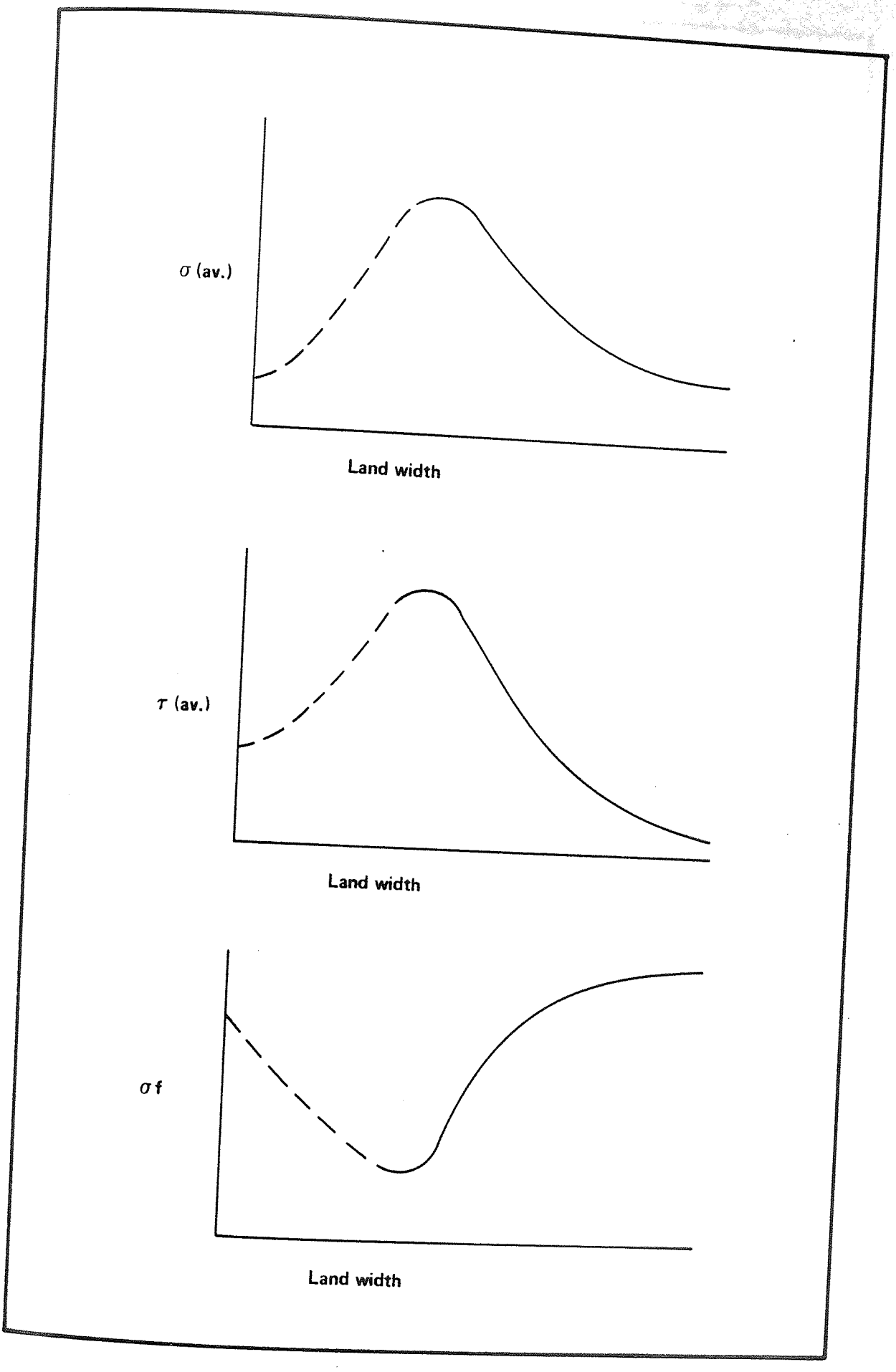

Figure 7.2 Average Stress Plots

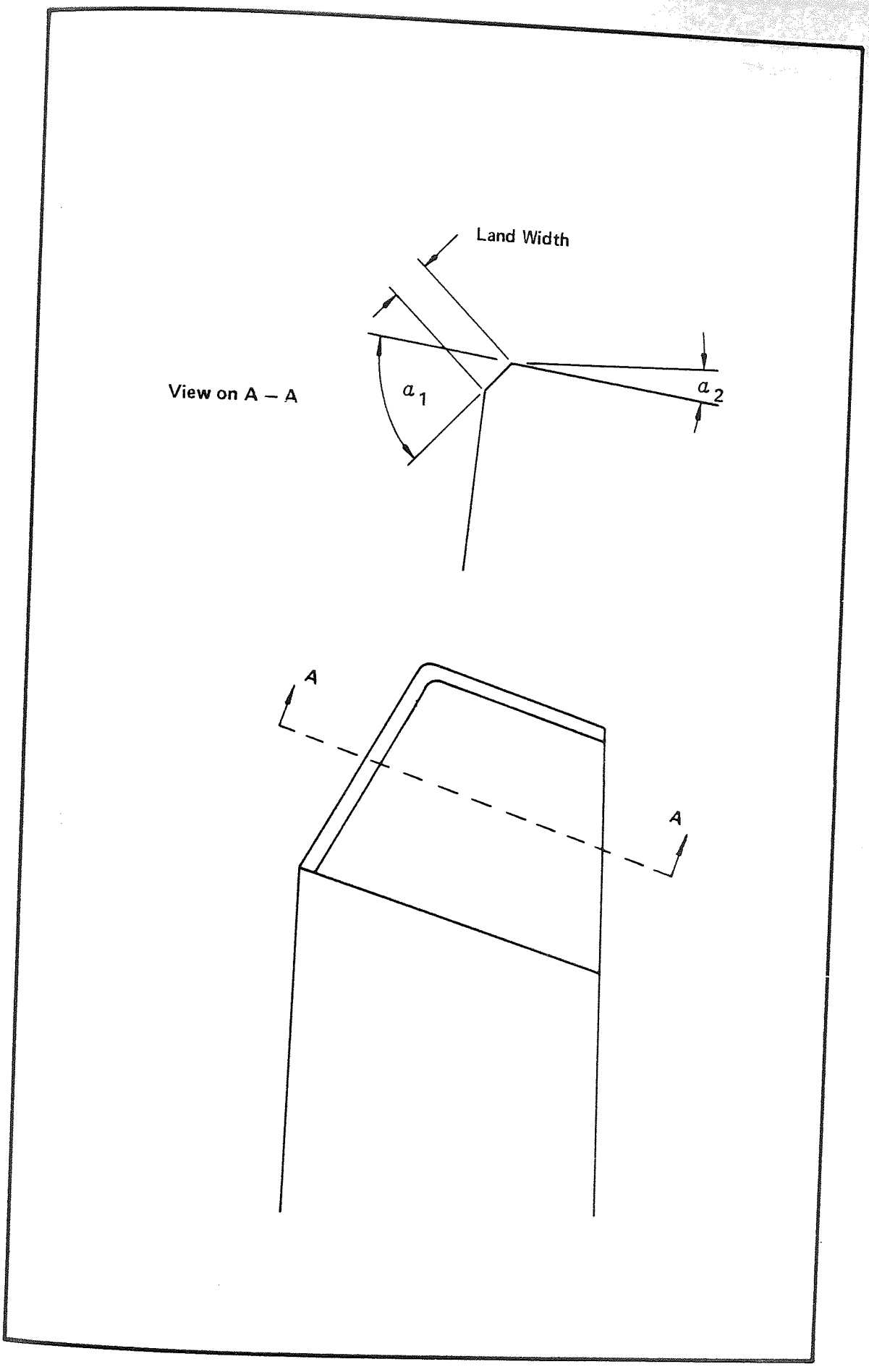

Figure 7.3 Double Rake Geometry

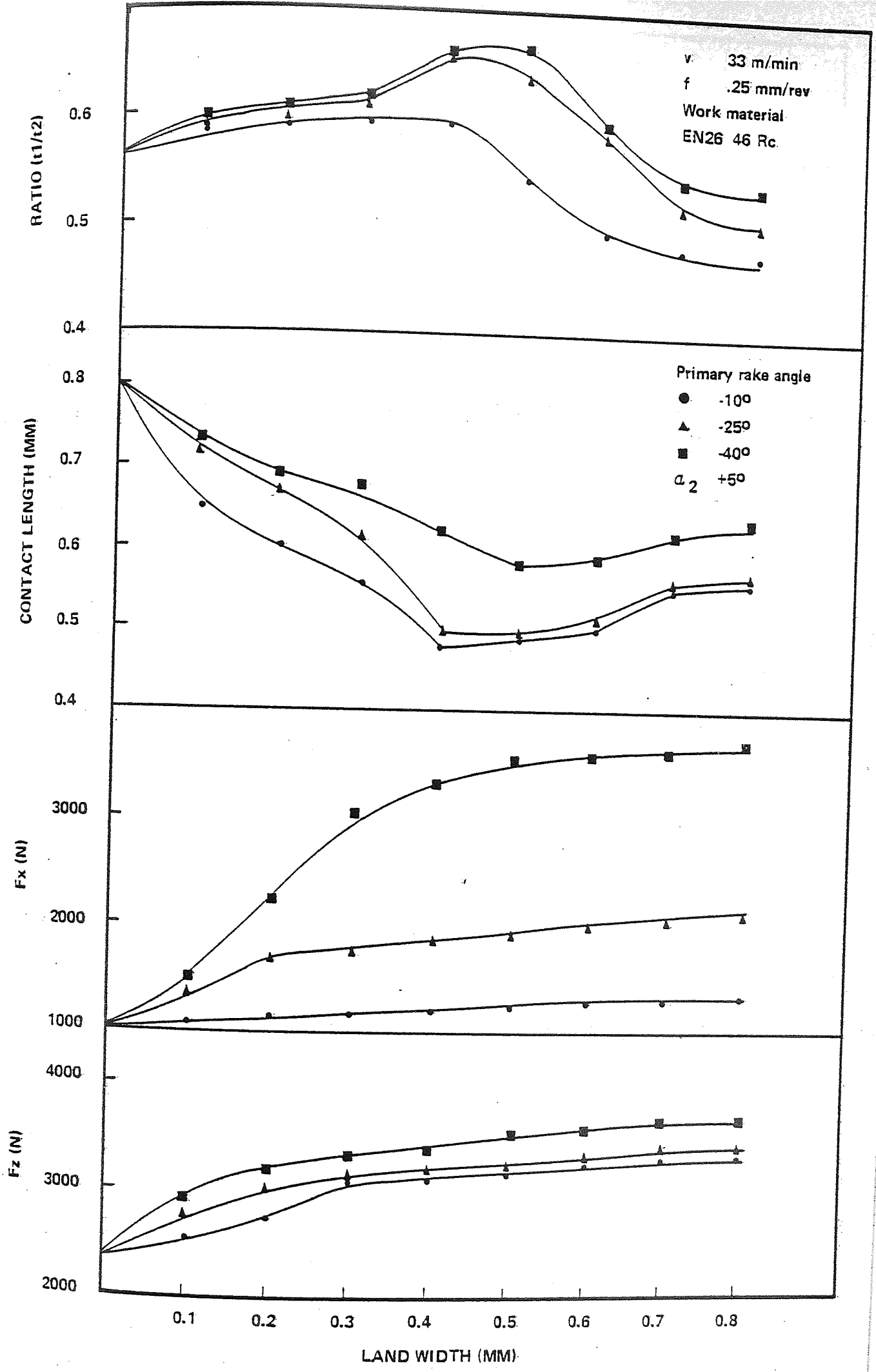

Figure 7.4 Effect of Land Width on Cutting Parameters at Various Land Angles

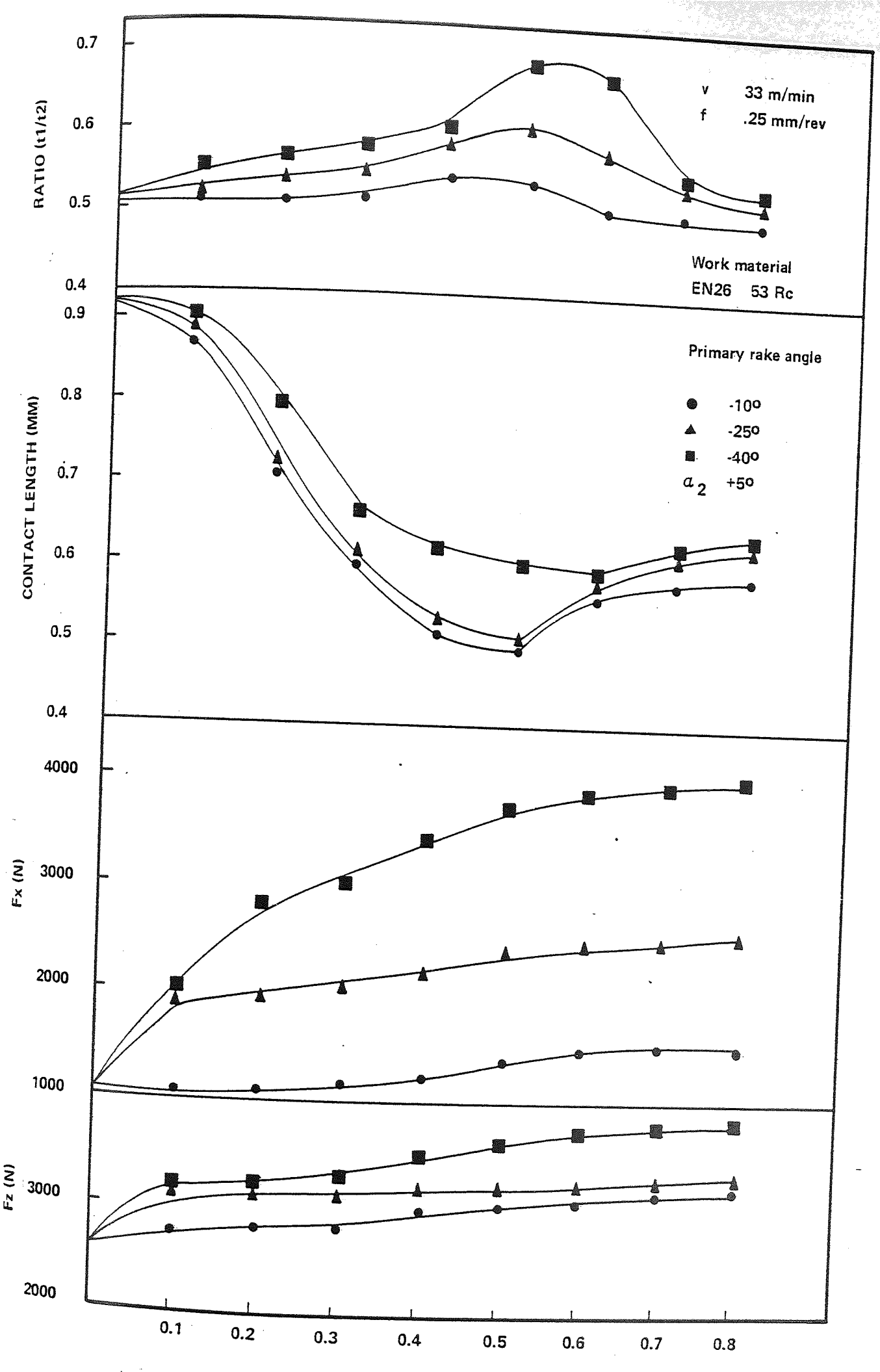

Figure 7.5 Effect of Land Width on Cutting Parameters at Various Land Angles

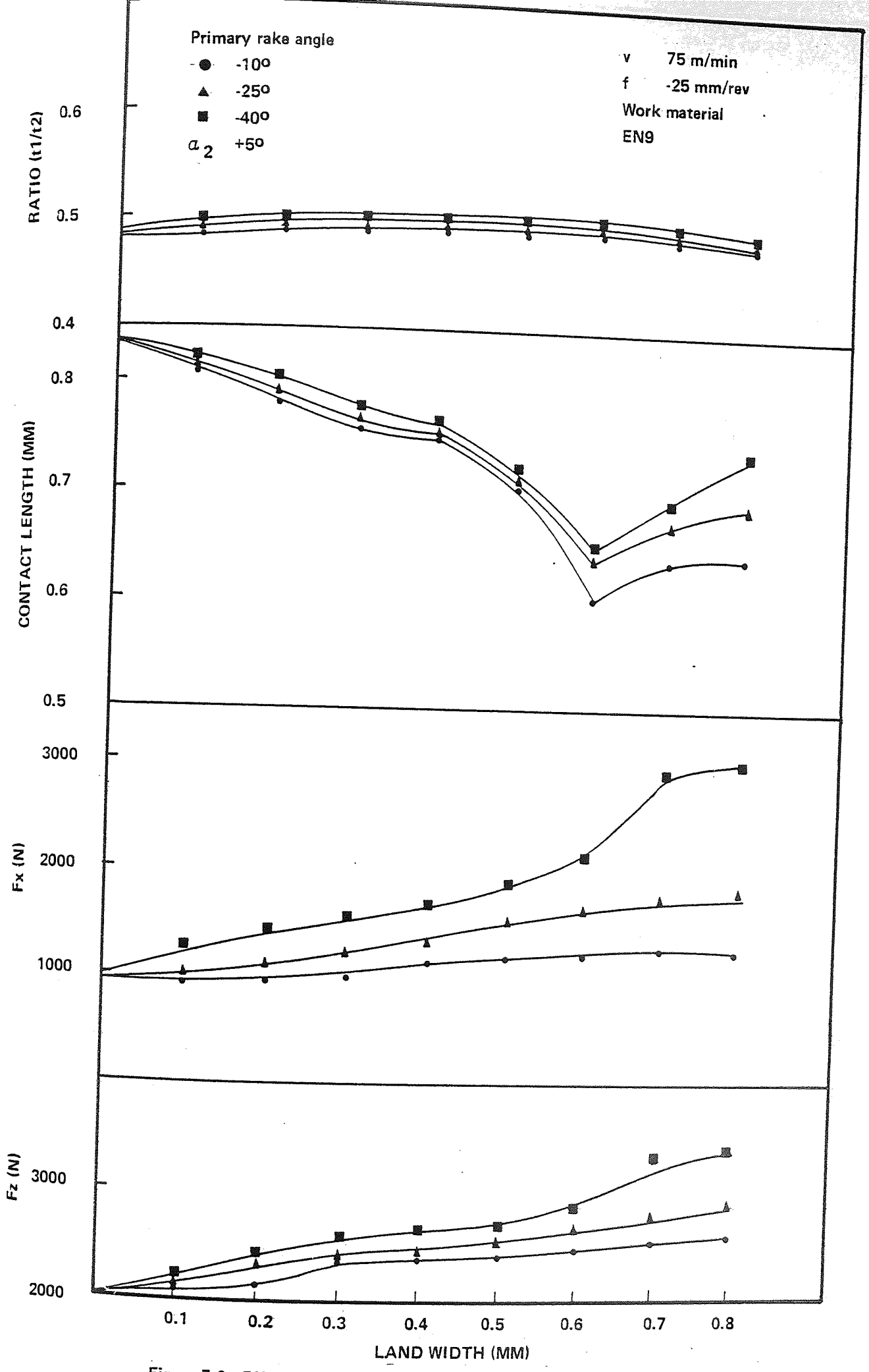

Figure 7.6 Effect of Land Width on Cutting Parameters at Various Land Angles

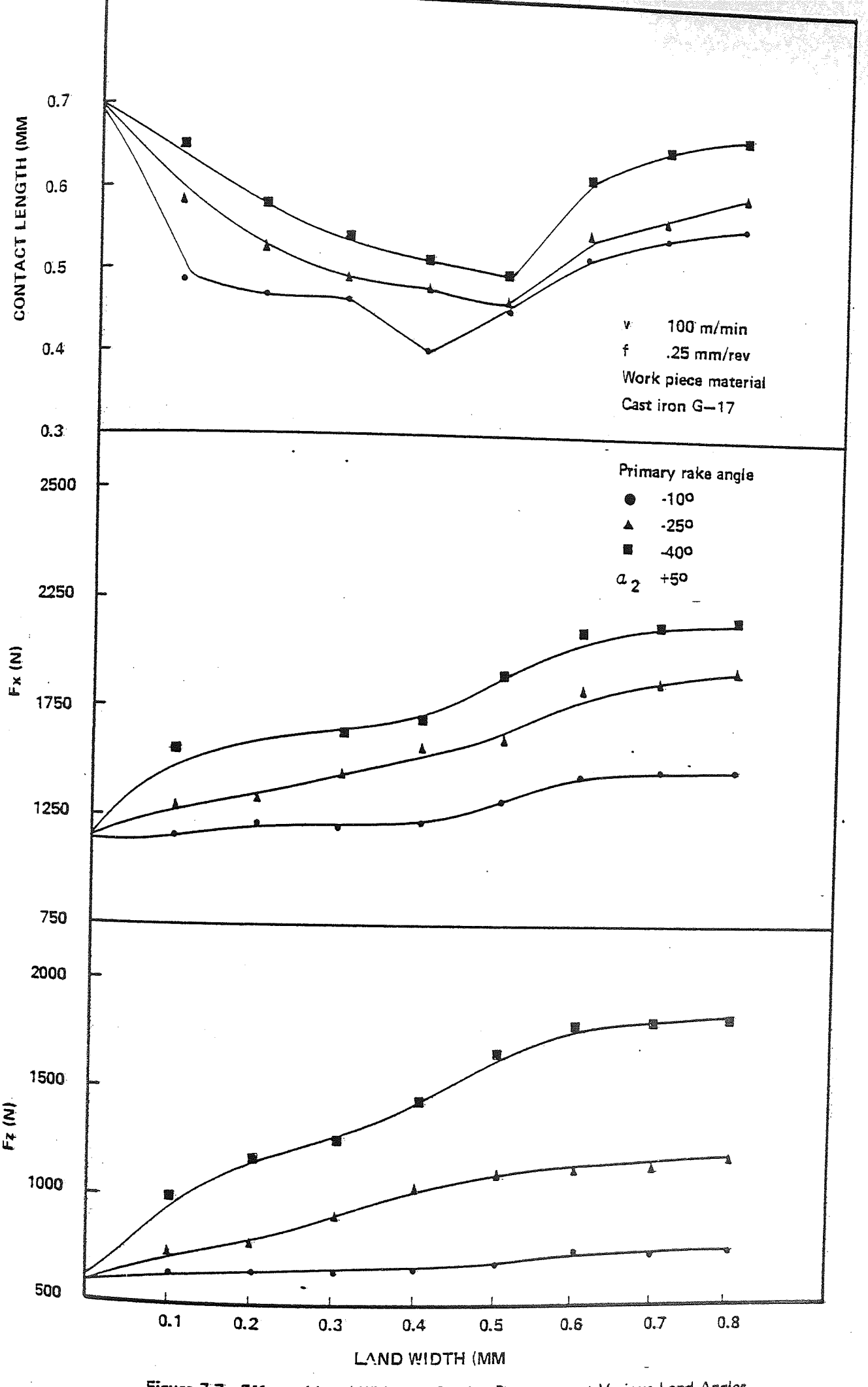

Figure 7.7 Effect of Land Width on Cutting Parameters at Various Land Angles

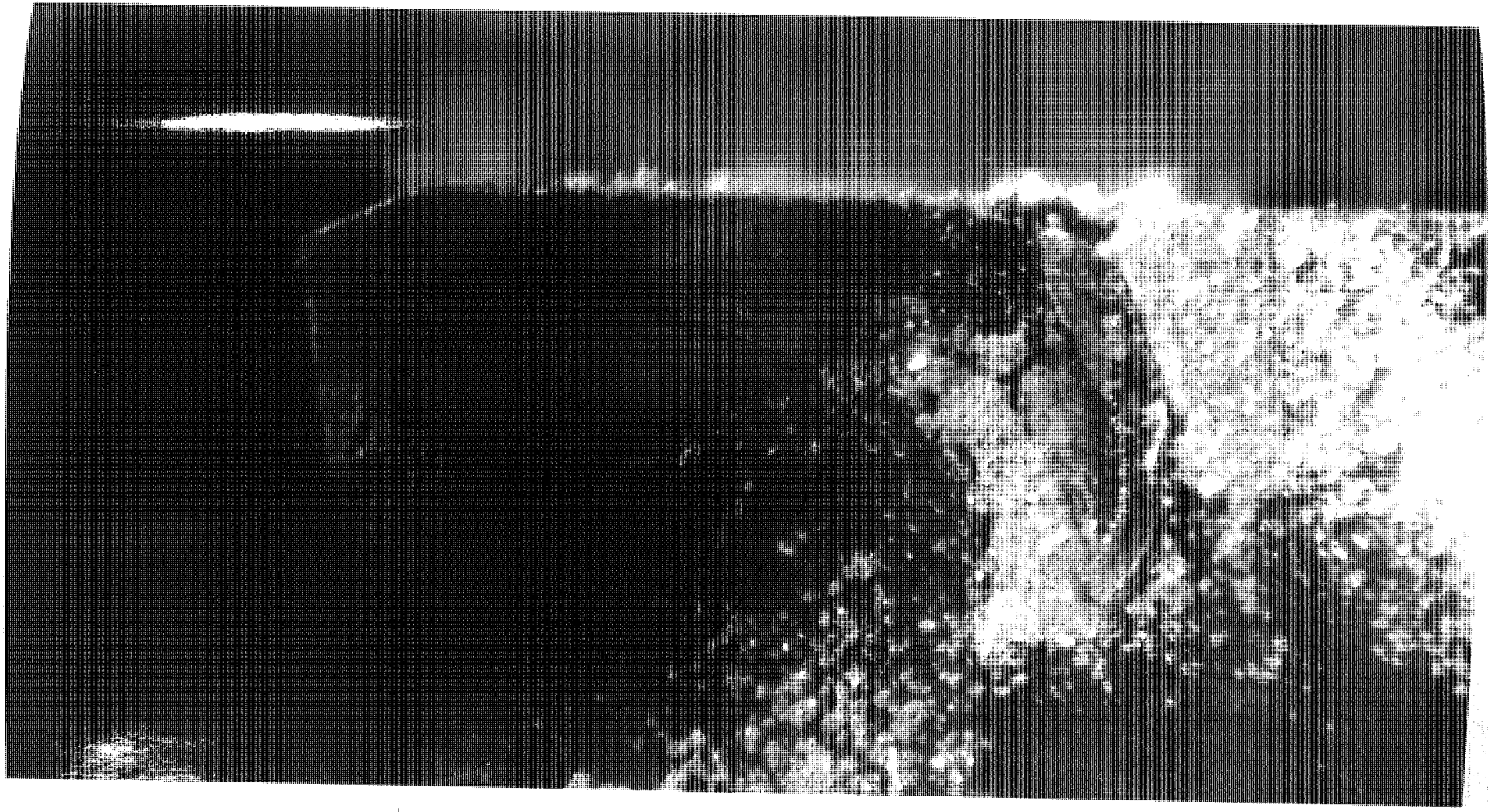

Figure 7.8 Views of divided surface

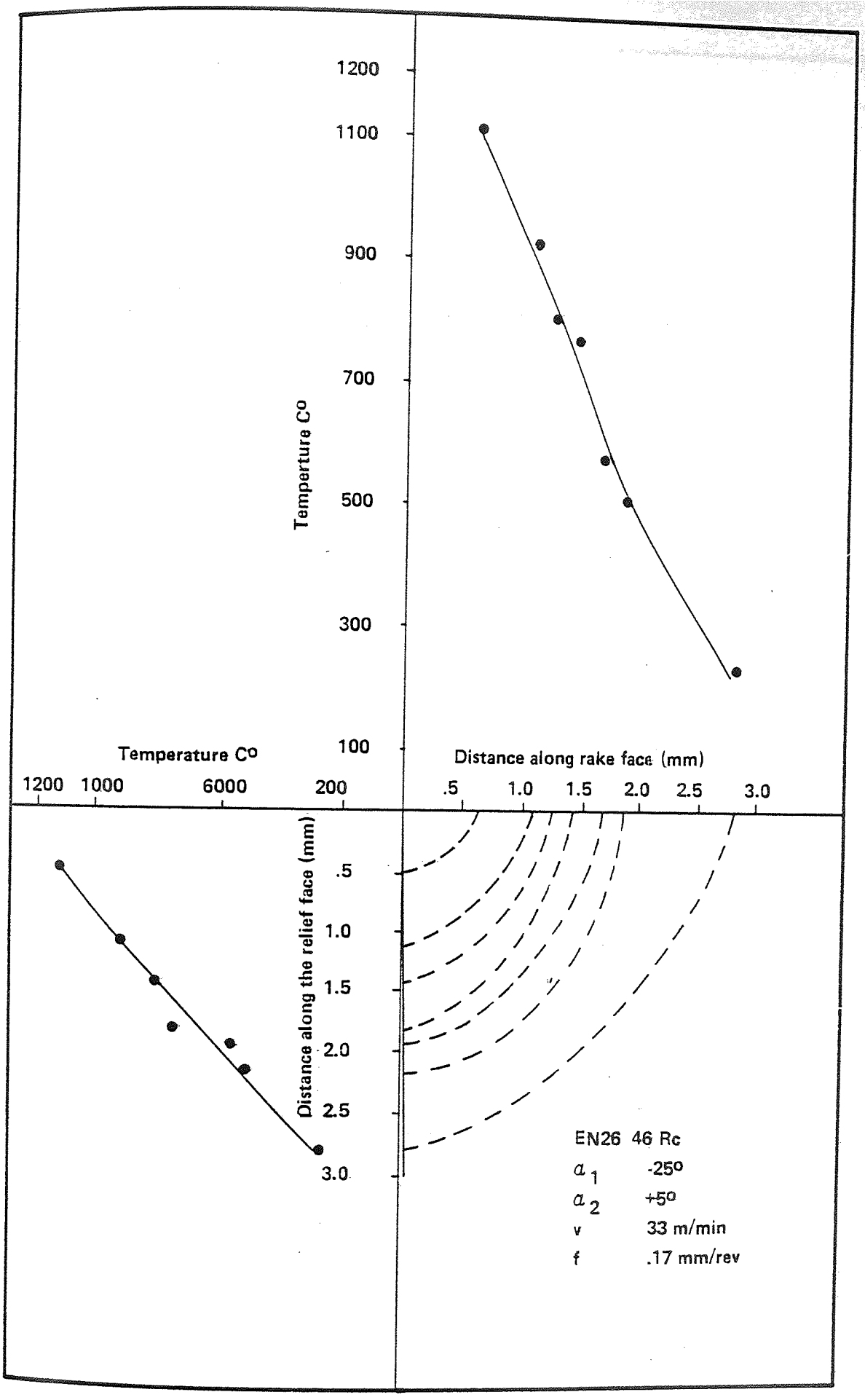

Figure 7.9 Effect of Land Width on Temperature Distribution (.3 mm Land Width)

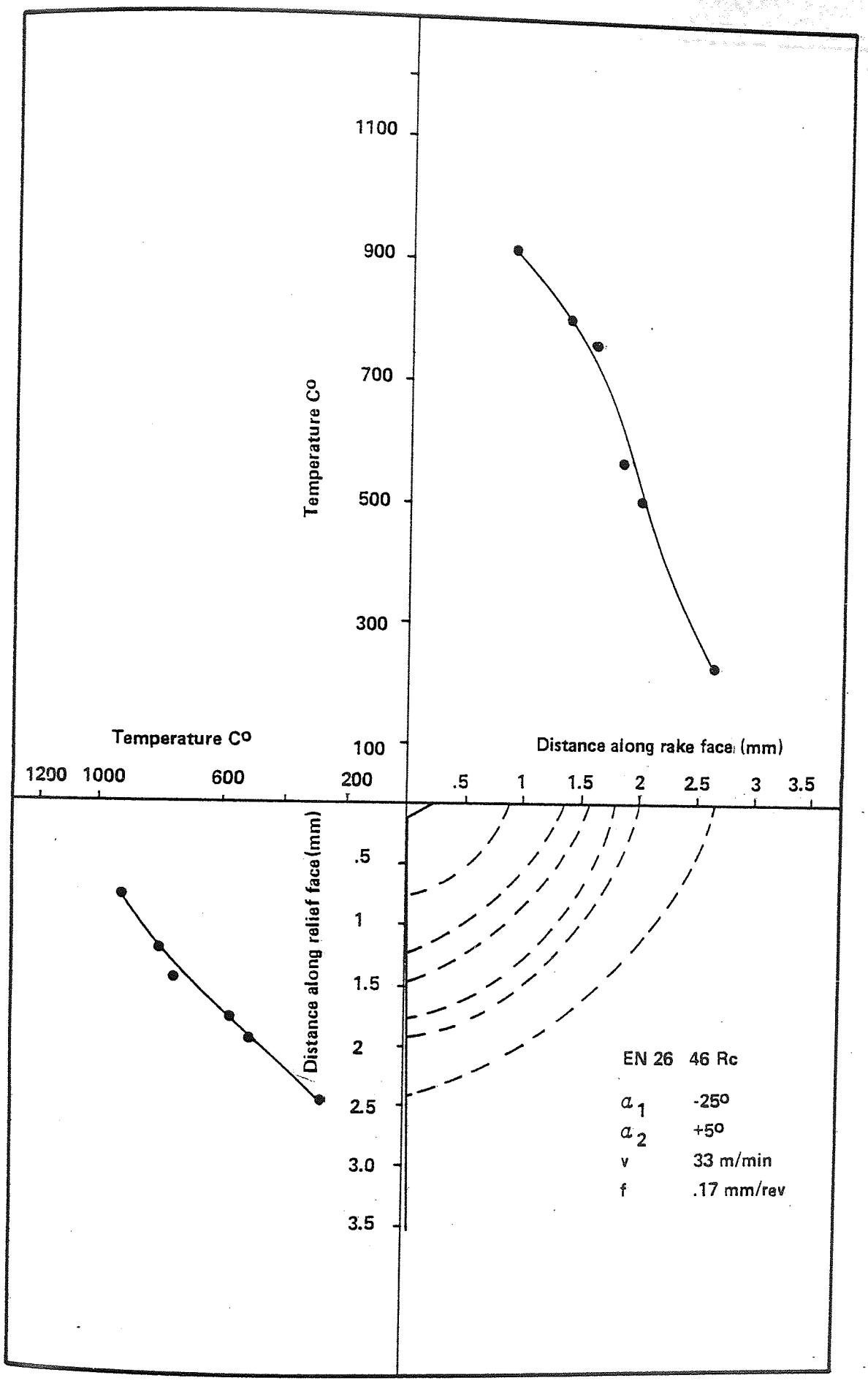

Figure 7.10 Effect of Land Width on Temperature Distribution (.45 mm Land Width)

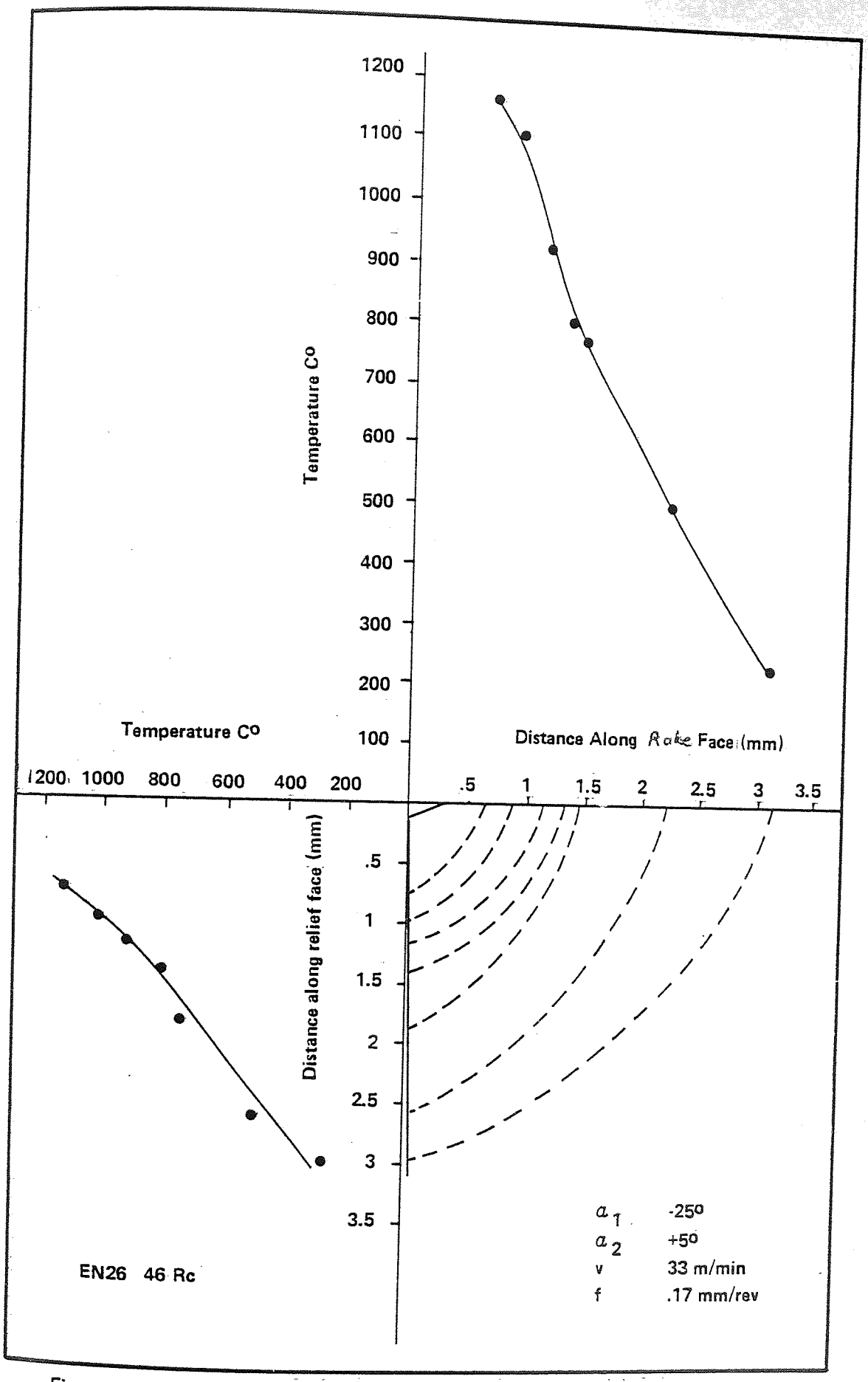

Figure 7.11 Effect of Land Width on Temperature Distribution (.7 mm Land Width)

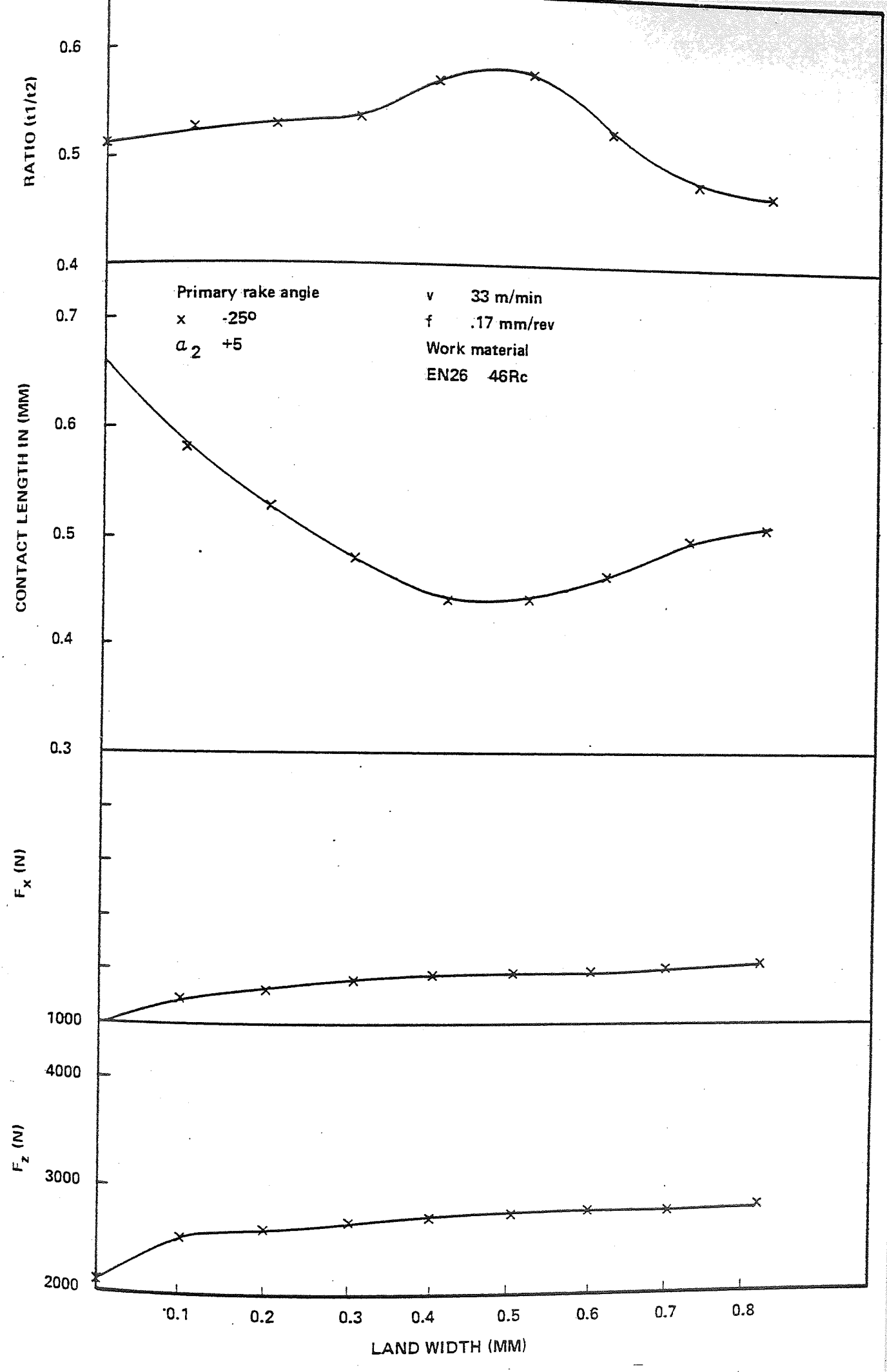

Figure 7.12 Effect of Land Width on Cutting Parameter (f = .17 mm/rev)

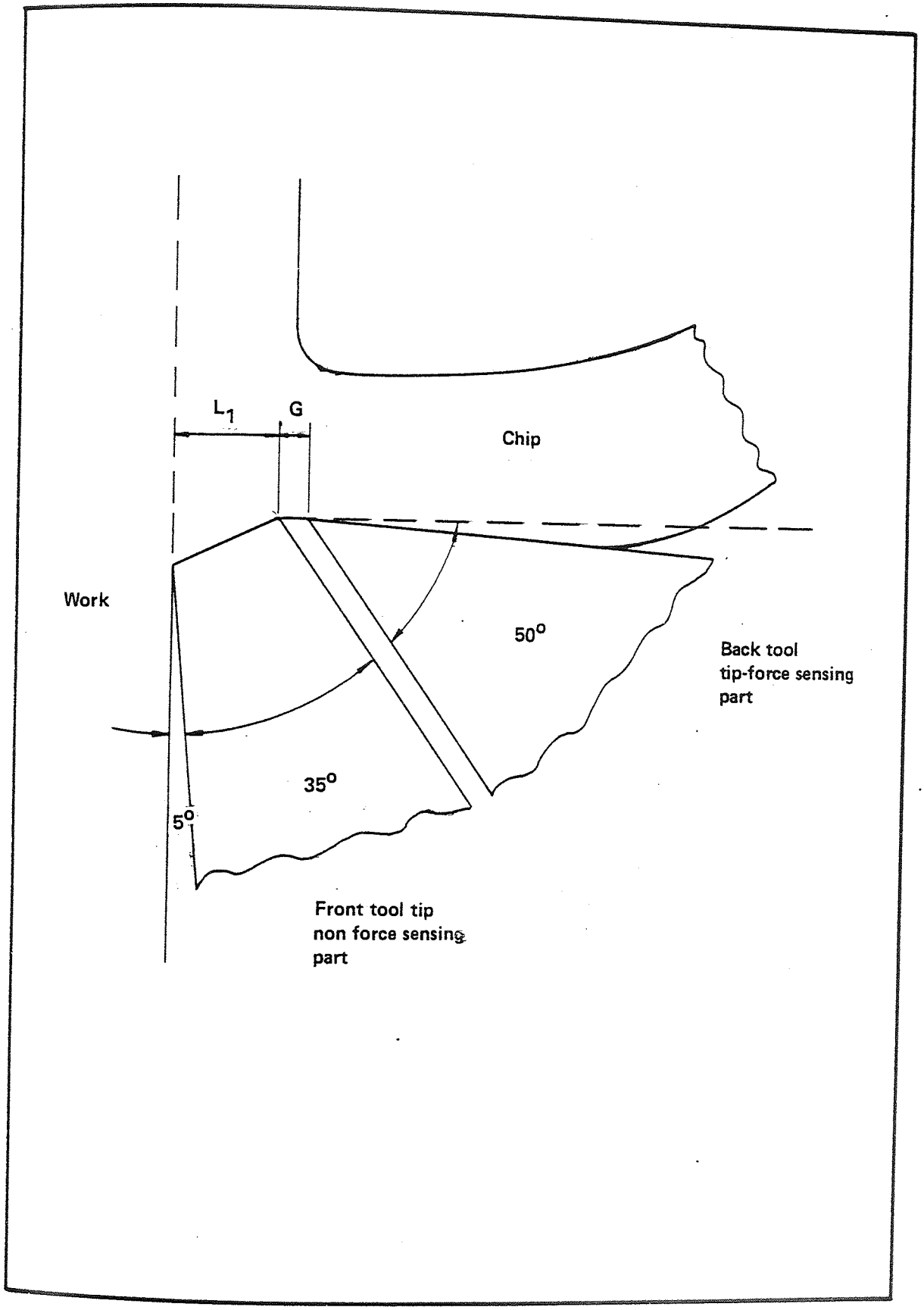

Figure 7.13 The Split Tool Principle

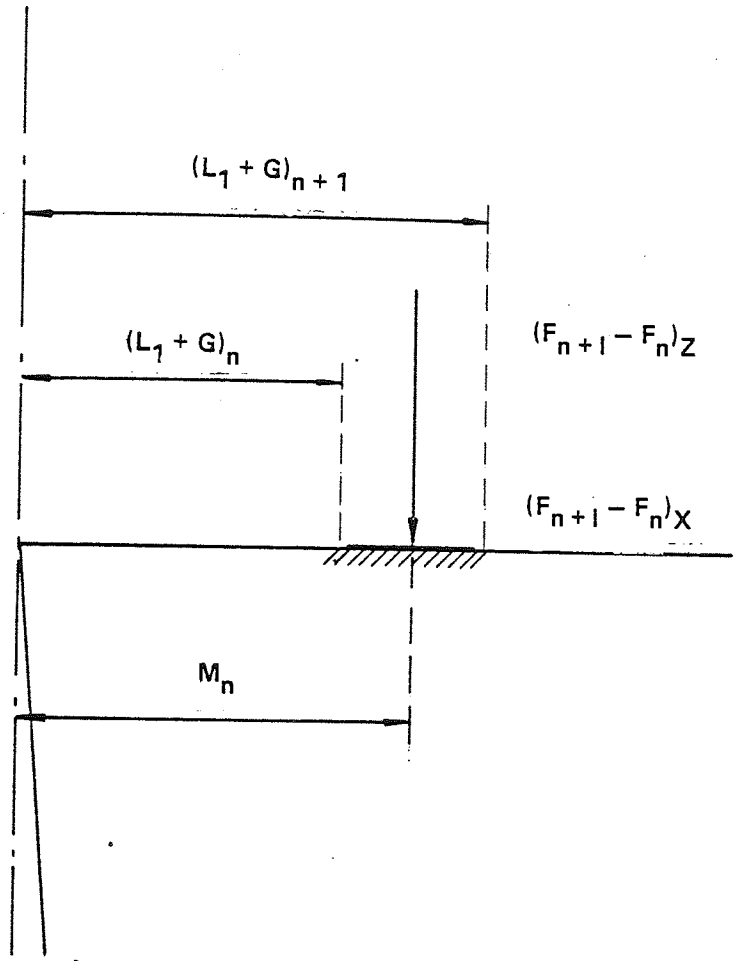

Figure 7.14 Stress Calculations

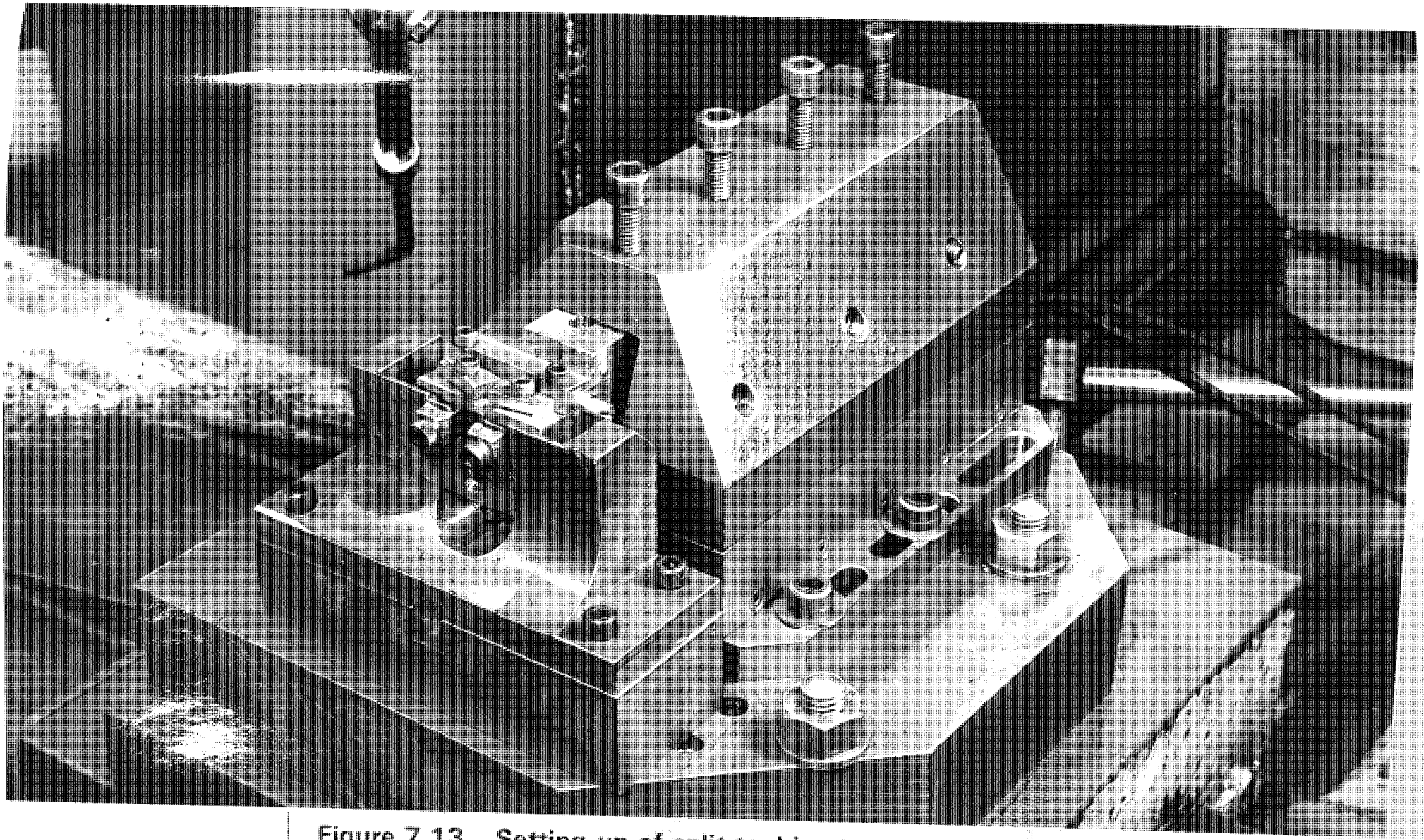

Figure 7.13 Setting-up of split tool in stress measurement

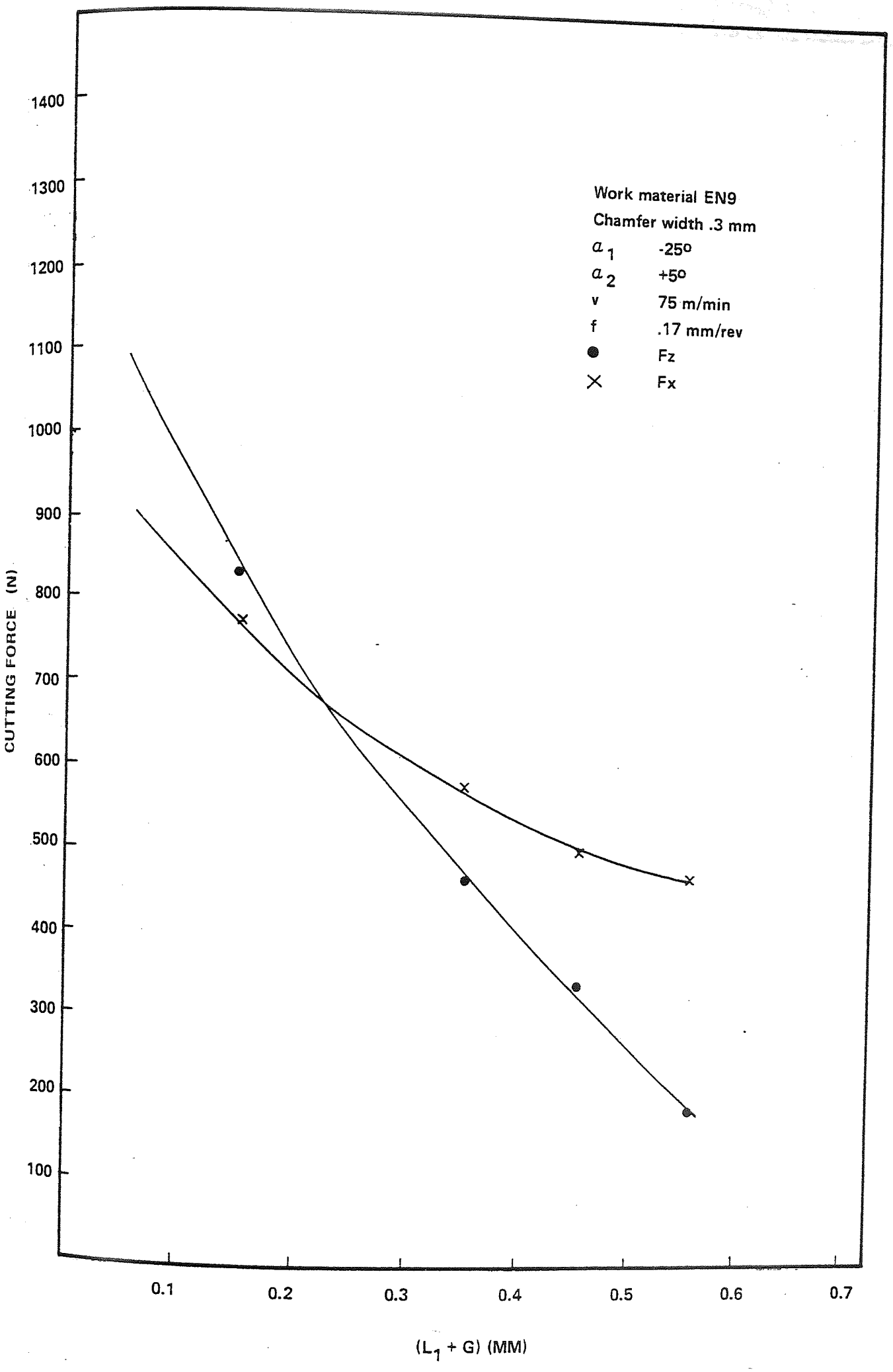

Figure 7.16 Distribution of Forces along the Rake Face (Land width .3 mm)

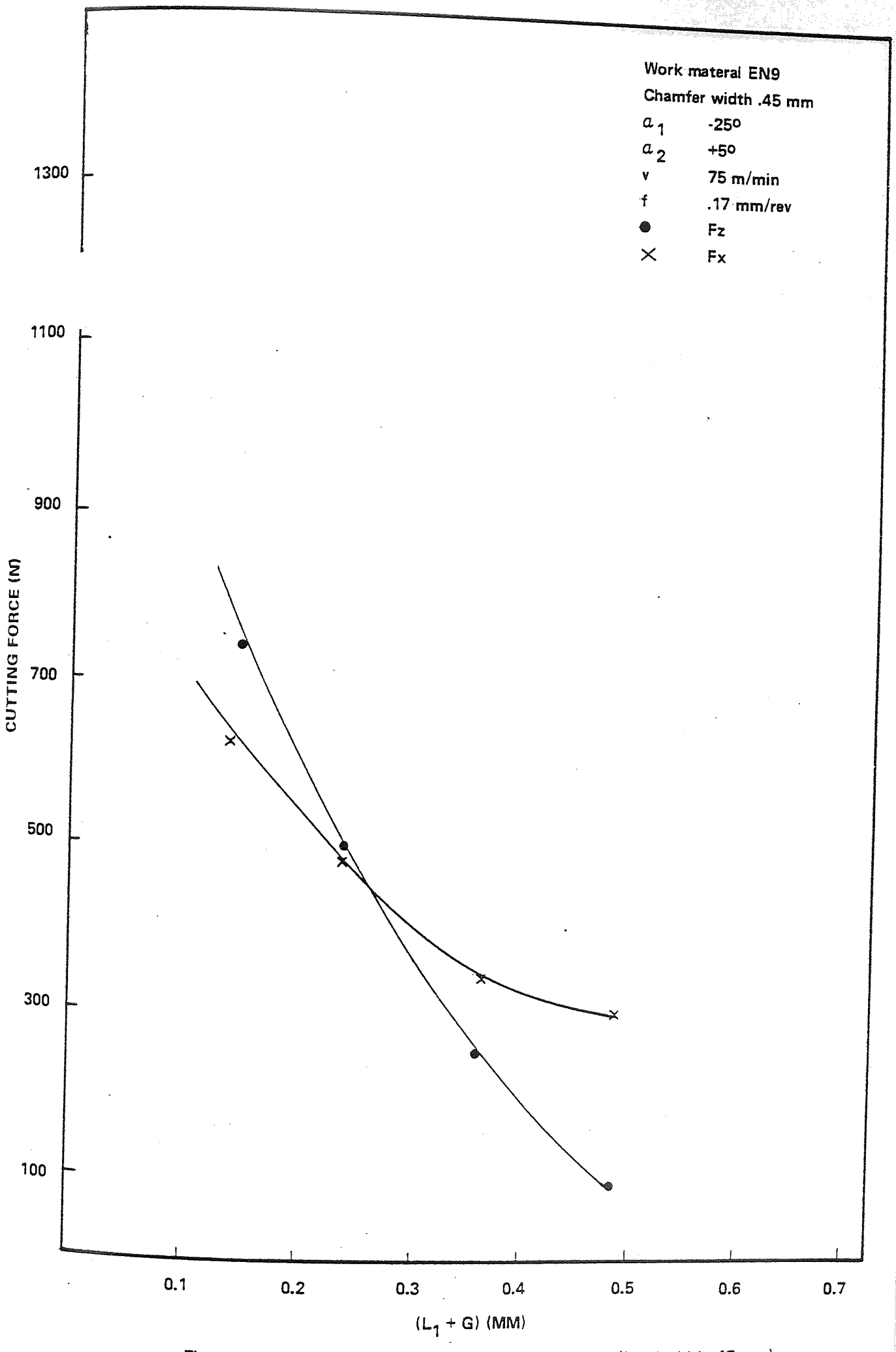

Figure 7.17 Distribution of Forces along the Rake Face (Land width .45 mm)

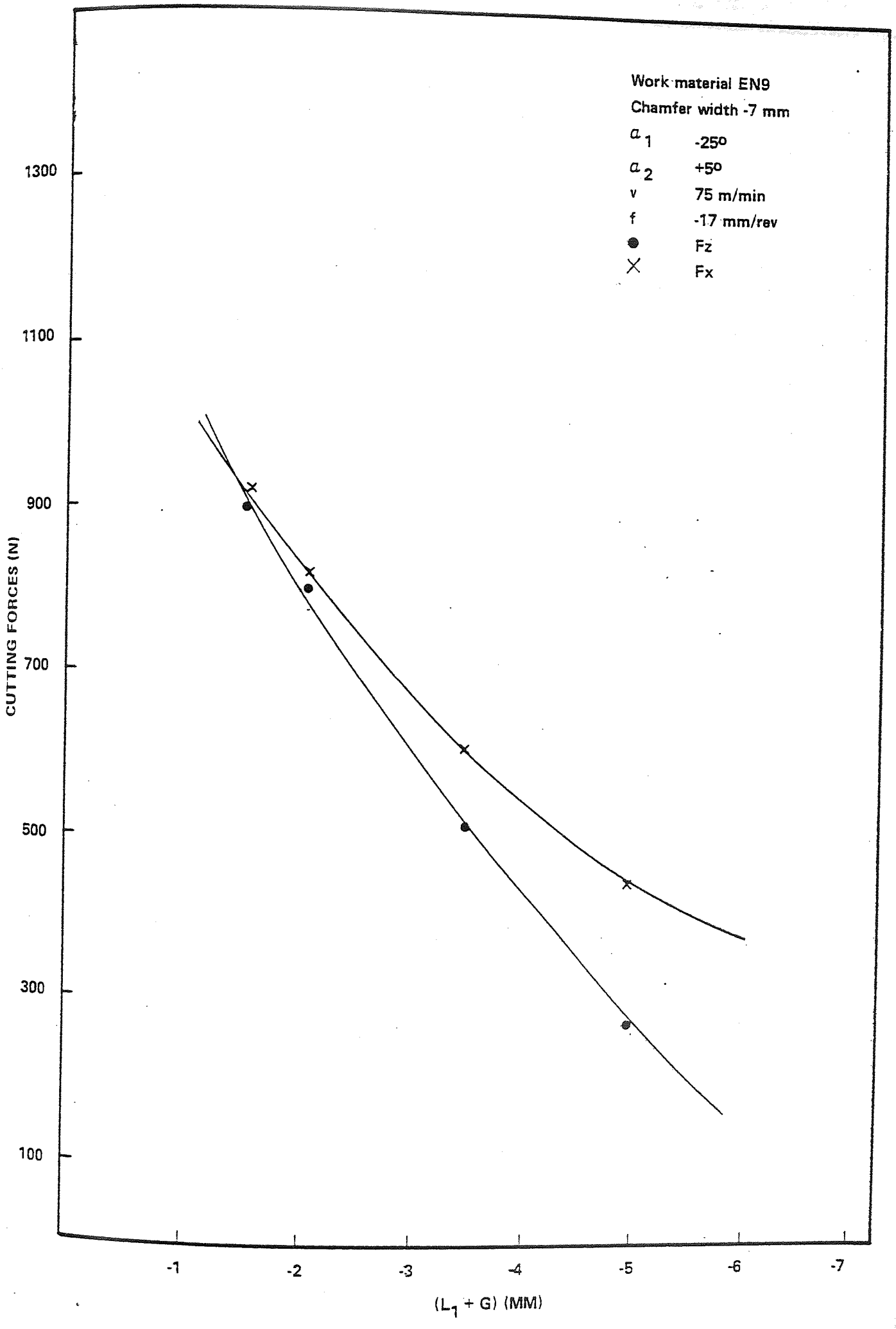

Figure 7.18 Distribution of Forces along the Rake Face (Land width -7mm)

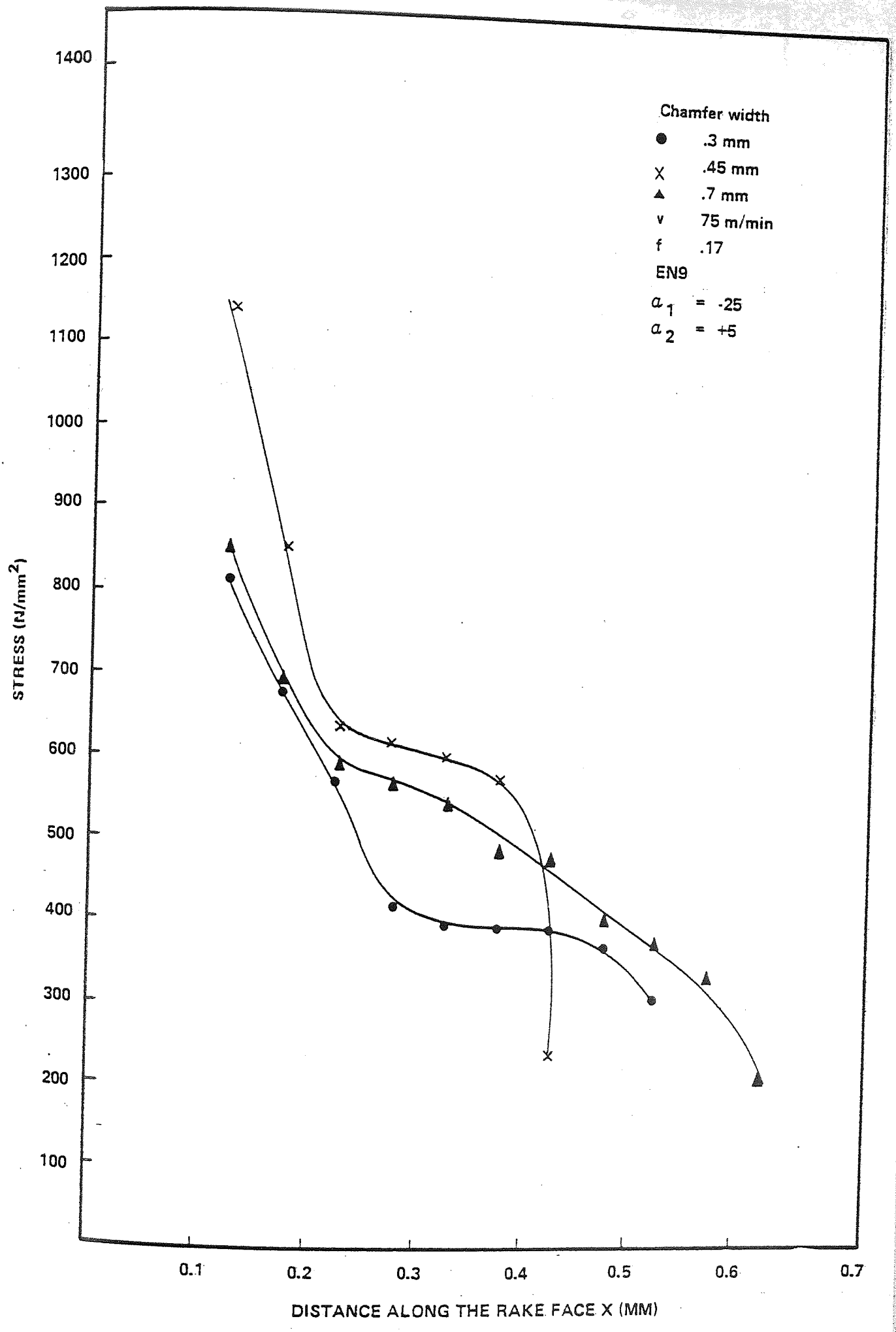

Figure 7.19 Normal Stress Distributions along the Rake Face

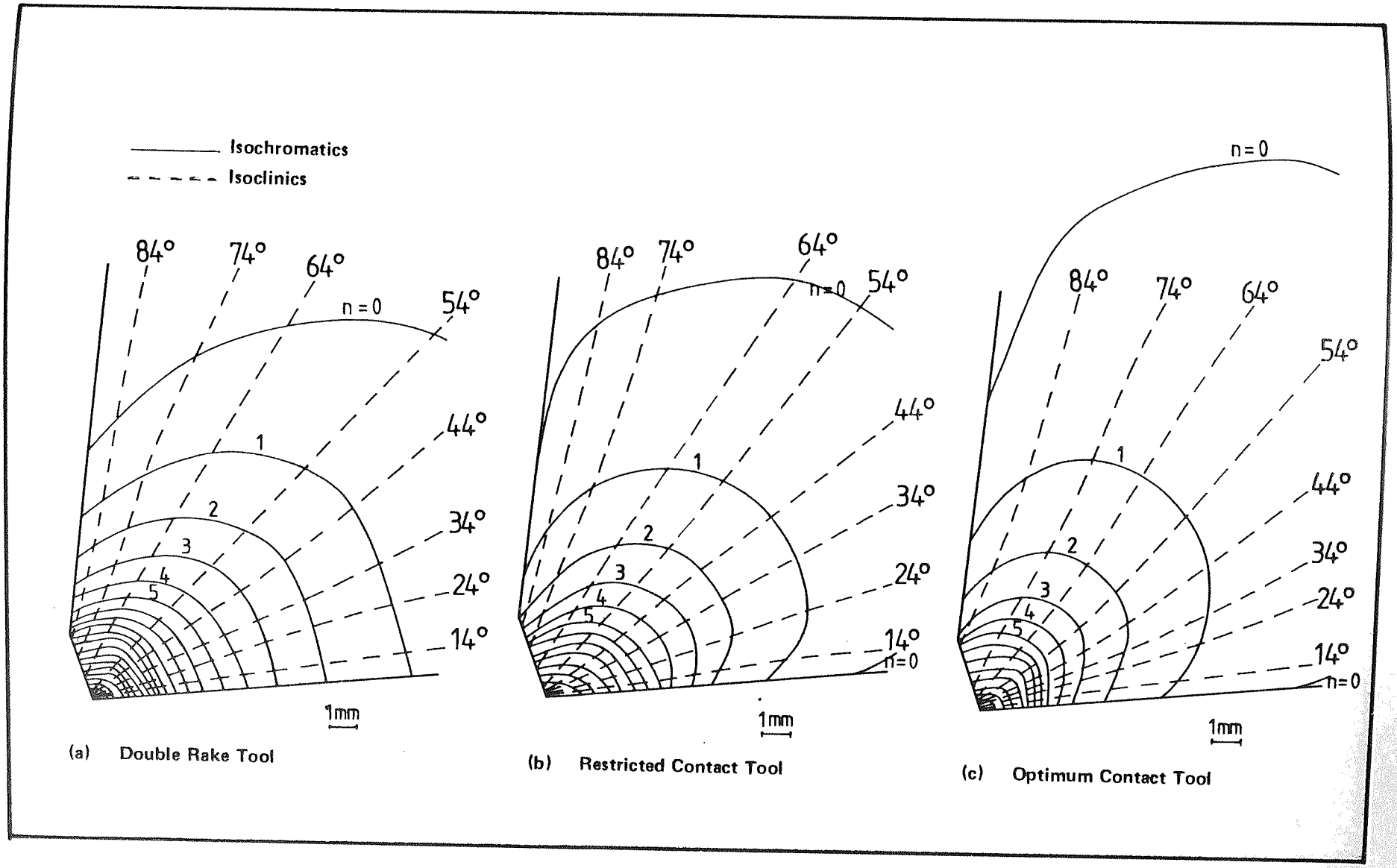

Figure 7.20 Isochromatics and Isoclinics for Photoelastic Double Rake Tool

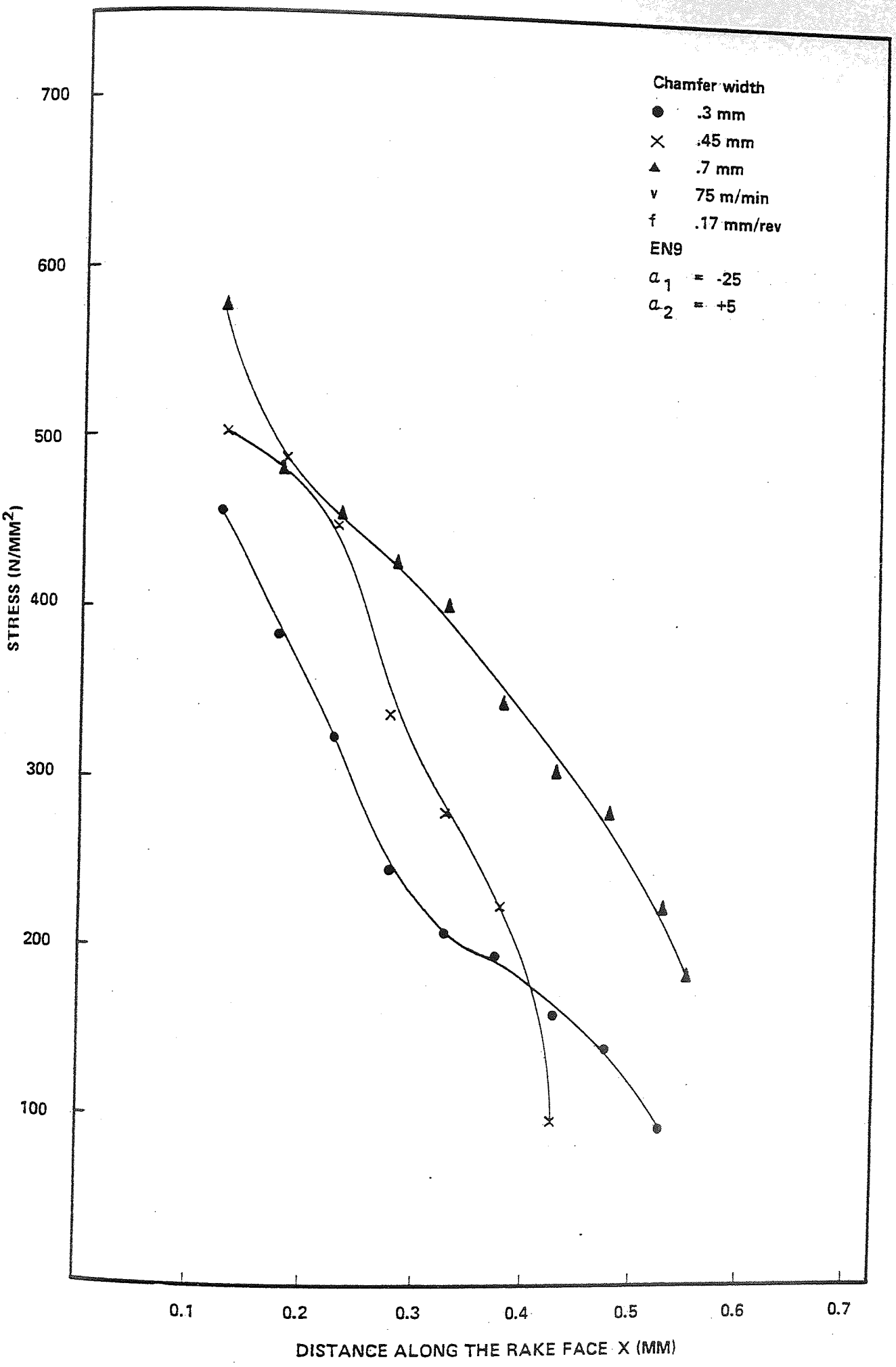

Figure 7.21 Shear Stress Distributions Along the Rake Face

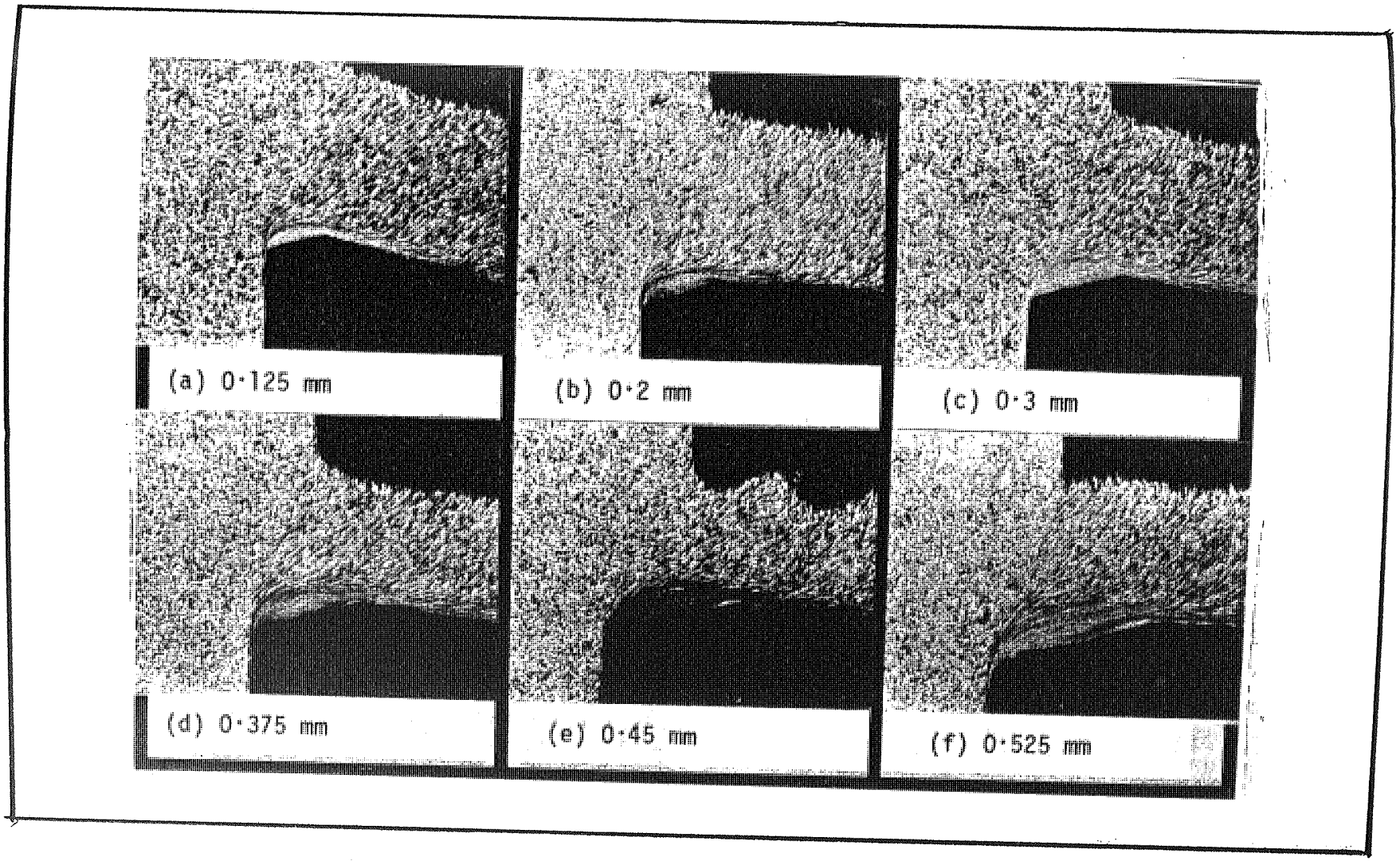

Figure 7.22 Chip Formation for various Land Widths with TIN coated modified Geometry Tools

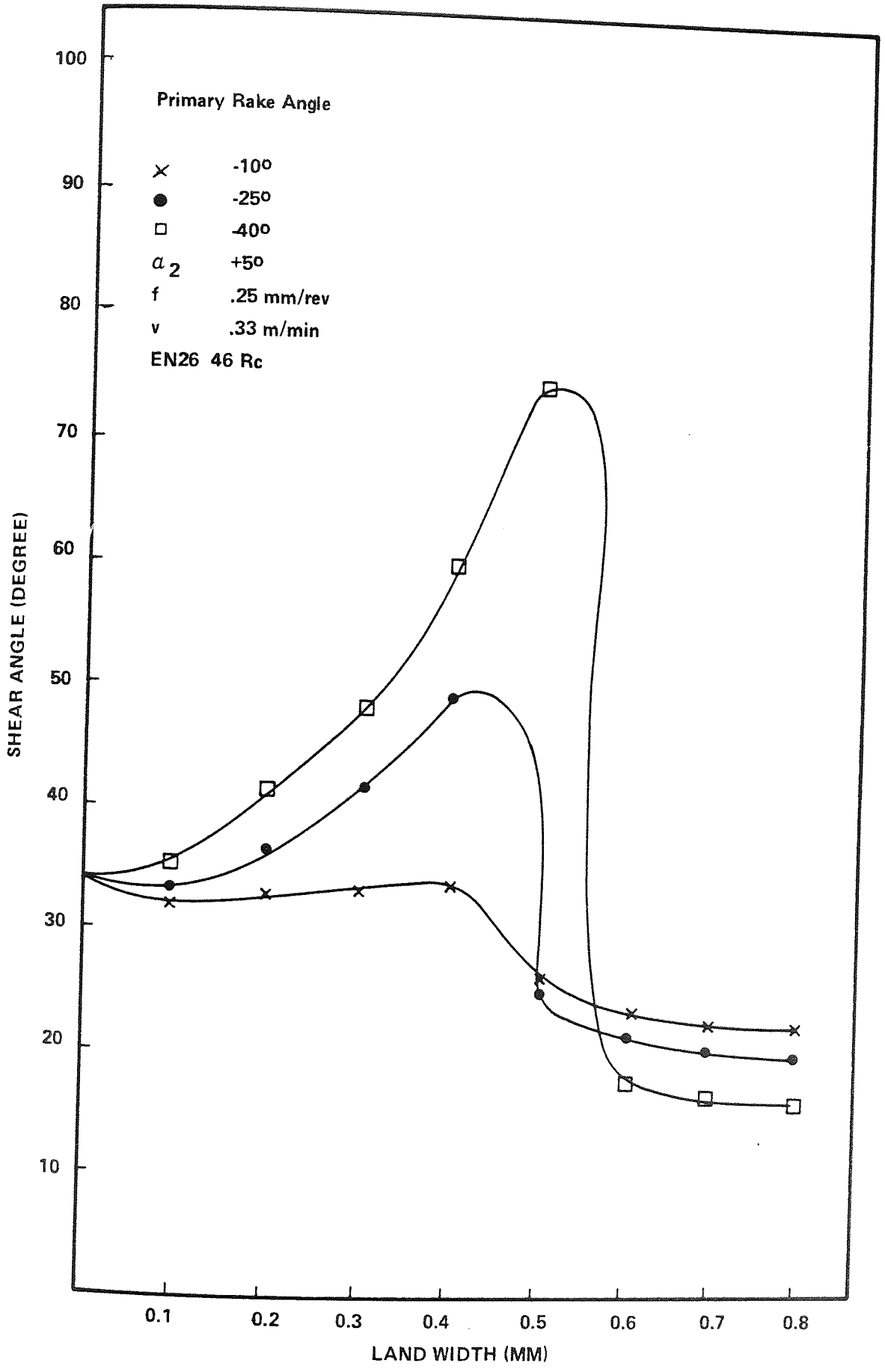

Figure 7.23 Influence of Land Width on Shear Angle (Material EN26)

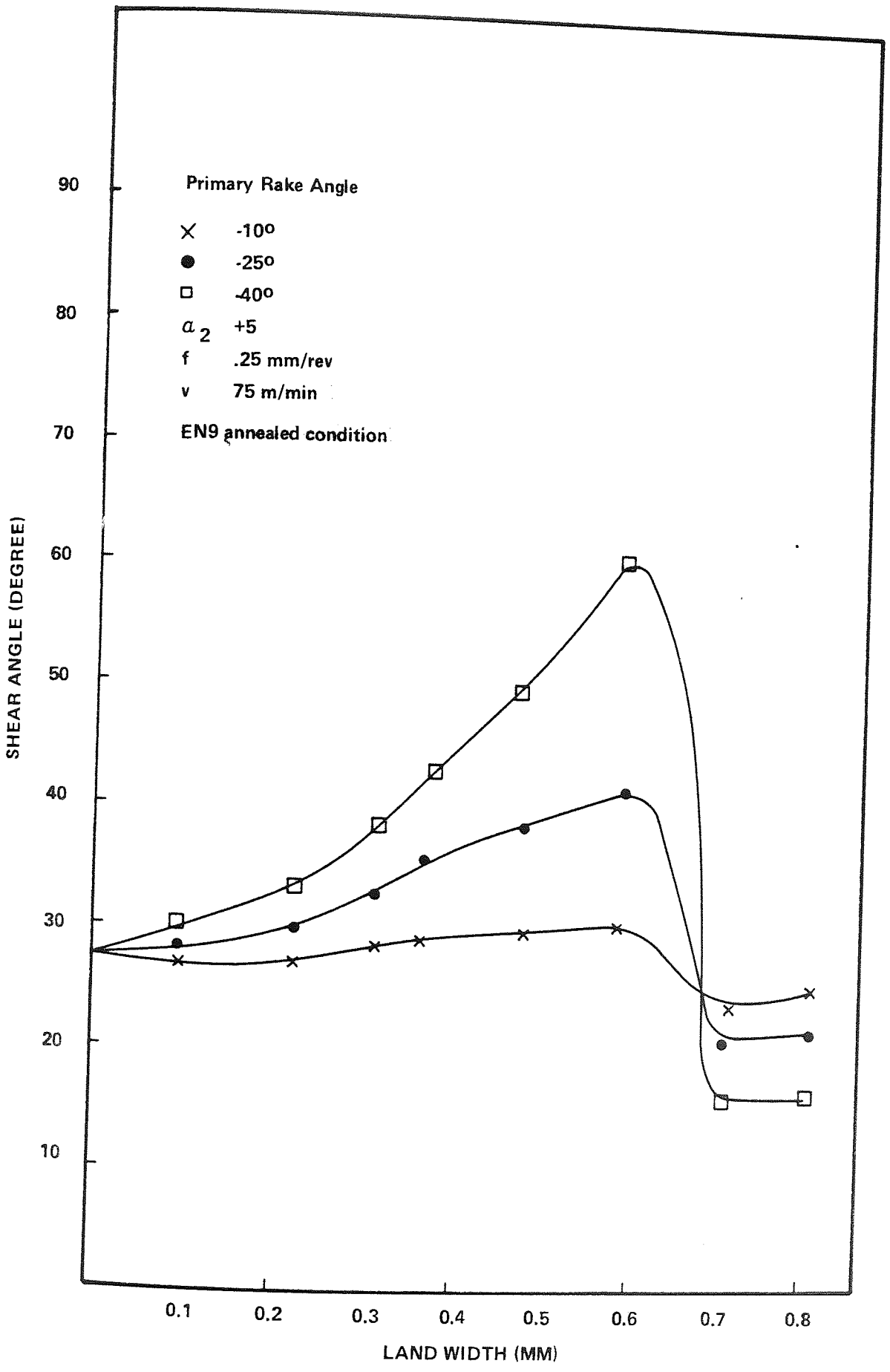

Figure 7.24 Influence of Land Width on Shear Angle (Material EN9)

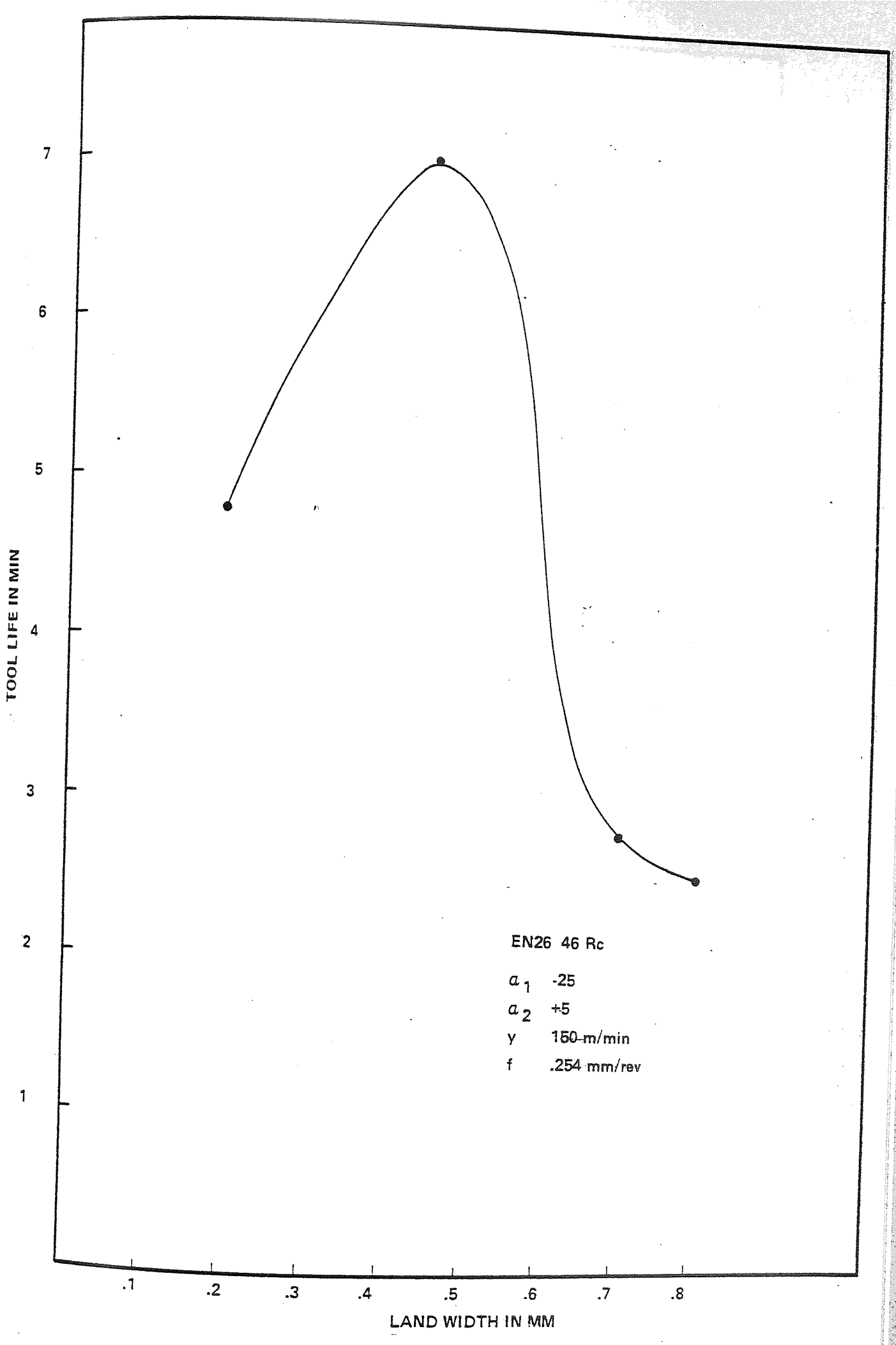

Figure 7.25 The Influence of Chamfer Land Width on Tool Life (Double Rake Tool)

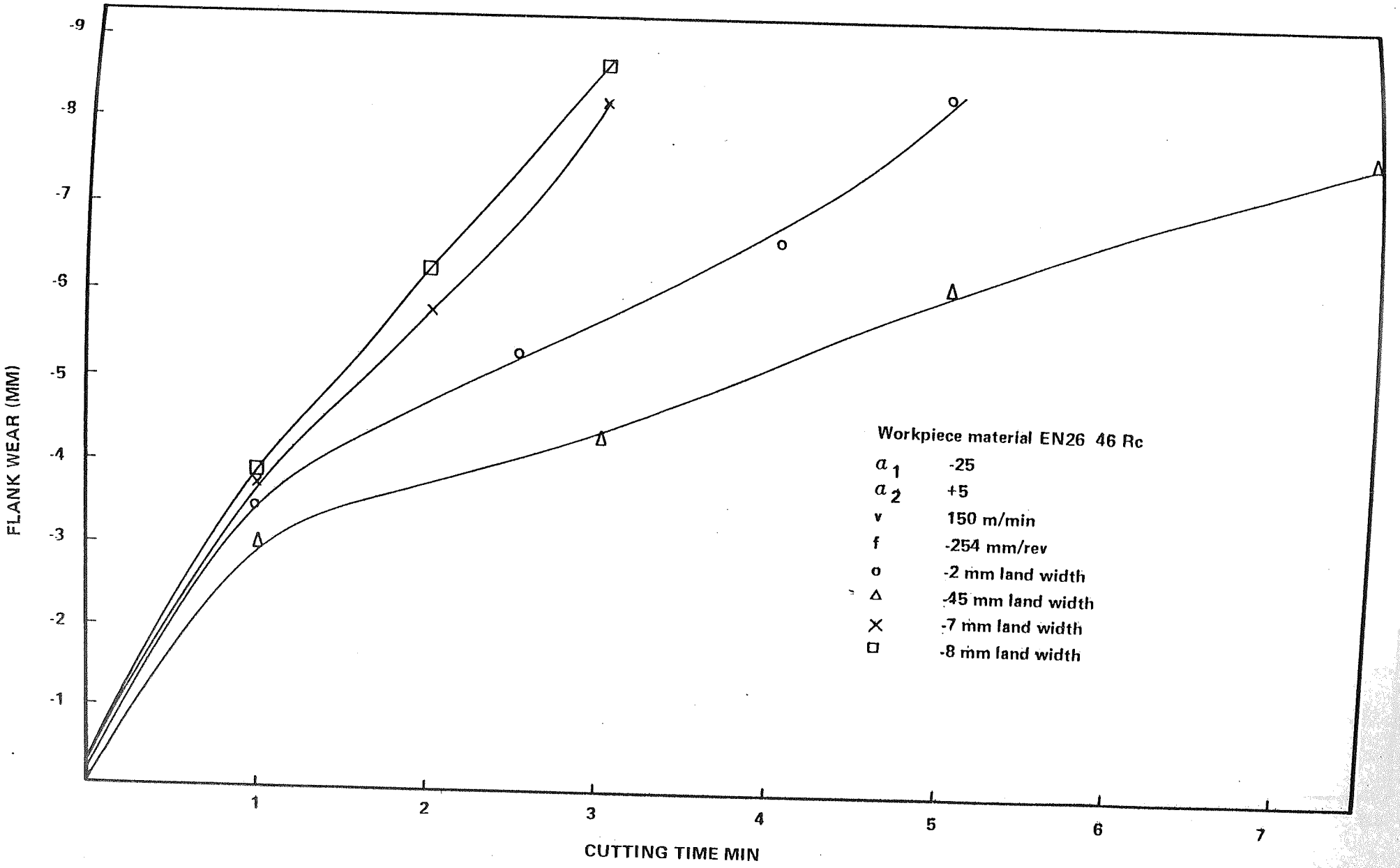

Figure 7.26 Influence of Land Width on Flank Wear (Double Rake Tool)

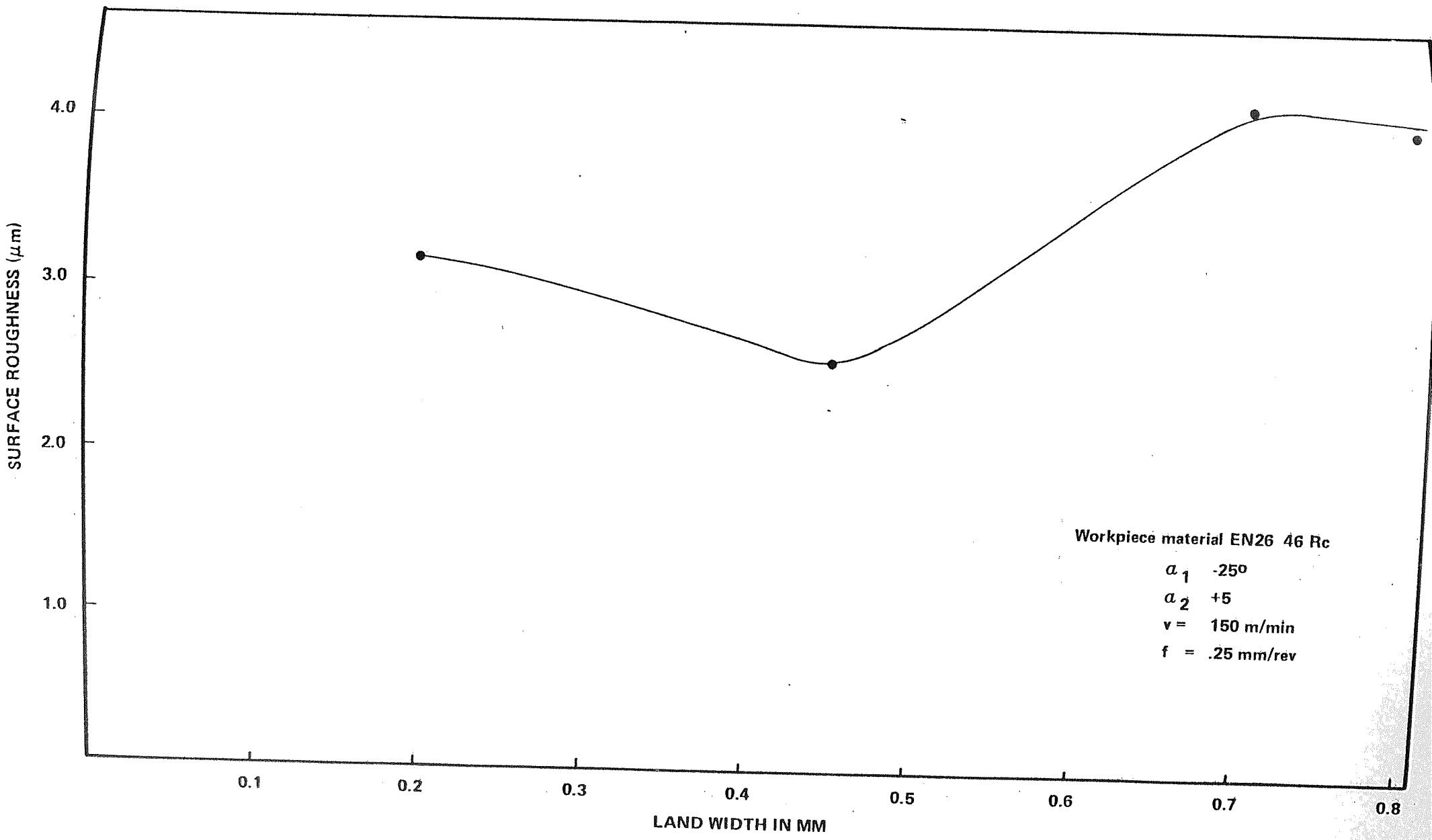

Figure 7.27 Effect of Land Width on Surface Roughness (Double Rake Tools)

CHAPTER EIGHT

THE INFLUENCE OF EDGE CHAMFER DIMENSIONS ON CUTTING PERFORMANCE

8.1 INTRODUCTION

As mentioned in Chapter 7, it is generally recognised that in the metal cutting process, tool material and edge geometry are dependent variables and major differences in tool performance can be obtained by modifying edge geometry. However, although geometry modification has been studied by many researchers, it seems from Section 7.2 and as stated by Draper and Barrow[99] that the conclusions drawn from these investigations are largely inconclusive and often contradictory. Therefore, there appears to be a need for optimum geometry to be established for each combination of tool, workpiece and cutting conditions.

Moreover, it has been shown from the results of the cutting tests discussed in Chapter 6 that although the standard geometry of Kyon 2000 inserts can be used in machining a hardened steel,catastrophic edge breakdown is obtained under certain cutting conditions. The reasons for this are discussed in Section 6.14. The purpose of the chapter is to examine the effects of modifications to the edge geometry by generation of a series of chamfer angles and chamfer widths on the cutting edge. The commercially available standard tool edge geometry for Kyon 2000 was chosen on the basis of its similarity to the edge geometry used for carbide tools. The following results indicate that better tool performance can be obtained if a different edge geometry is used.

8.2 EXPERIMENTAL DESIGN

The aim of the tests was to compare two types of cutting tool insert; the commercially available one and the modified geometry inserts.

Oblique cutting tests were performed using a single negative rake tooling geometry. The criteria of tool failure was exactly similar to those used in both Chapters 6 and 7. i.e. 0.75 mm flank wear.

8.2.1 Factors Selection

It is necessary to study the response of the standard geometry and the new design geometries to the variation of (i) feed rate, (ii) chamfer width and (iii) chamfer angle as these are likely to be the variables with a major influence on the cutting insert performance. However, limitations to these variables may be imposed by the available range of feeds in the test lathe and by the accuracy that the grinding machine can be set to produce the cutting configuration. The definition of chamfer configuration used is shown in figure (8.1).

8.2.2 Statistical Design of Experiments

In designing the experimental work in this chapter the following objectives were considered:

- Design the experiments in order that statistical analysis can be exercised with the data collected.
- Plan statistically the experimental sequence and the combination of factors for each experiment
- Investigate the difference (if any) between the conventional and the new cutting insert design when feed rates, chamfer angles and chamfer width are varied.
- Make the series of experiments as economical as possible.

The advantages of statistical design of experiments have been emphasized by many authors[110,111]. As a matter of efficiency, a three way classification with interaction factorial design experiment was used in the present investigation.

An appropriate model is:

$$Y_{ijk} = \mu + \tau_i + B_j + q_k + (\tau B)_{ij} + (\tau q)_{ik} + (Bq)_{jk} + (\tau Bq)_{ijk} + e_{ijk} \quad \ldots\ldots\ldots \quad 1$$

Four levels of both feed rate and chamfer width were used together with three levels of chamfer angle, and the complete tests plan can be seen in Table (8.1). The cutting speed used for this series of experiments was 150 m/min with a depth of cut of 2 mm while the approach angle was maintained at 45^{o} throughout the tests.

Presentation chamfer angle	Chamfer width mm	Feed rate mm/rev			
		.17	.25	.33	.5
-10^{o}	.2				
	.3				
	.5				
	1				
-15^{o}	.2				
	.3				
	.5				
	1				
-25^{o}	.2				
	.3				
	.5				
	1				

TABLE (8.1)

(Test plan of the geometry modification)

8.2.3 Equipment

The lathe, the wear measuring equipment, the force measuring dynamometer and the accompanying electronic devices were exactly similar to those used in Chapters 6 and 7 and have already been described in Chapter 5. Furthermore, the modified insert was mounted on a tool holder which is similar to the one used in Chapter 6.

8.2.4 Material

The material used in this series of tests was hardened high strength alloy steel EN26. The level of hardness was 53RC.

8.3 RESULTS AND DISCUSSIONS

8.3.1 Flank Wear

As mentioned at the beginning of this chapter, the aim was to compare the performance of the conventional standard cutting insert and the modified new design geometry which were done on the basis of the tool wear testing. However, the cutting forces variation due to the new design were monitored with all the cutting inserts tested and will be discussed later in Section 8.3.4.

Results of the flank wear-time relationships are shown in figures (8.2-8.7). Figures (8.2-8.4) show the results for a variety of chamfer widths and chamfer angles when a feed rate of .17 mm/rev and cutting speed of 150 m/min are used. It can be seen from the above three figures that there is an immediate detectable difference between the wear profiles referring to the new design geometries and it is clear from the figures of all the chamfer angles tested that the .3 mm chamfer width gave the best performance of the cutting inserts. It is particularly interesting to note that at a chamfer angle of -25^{o} the standard chamfer length of 0.2 mm gave very unsatisfactory results.

Figures (8.5-8.7) show similar relations to the above, but for feed rate of .25 mm/rev, and again the

graphs reveal that .3 mm chamfer width proved to be the best geometry for the work material used. It is also evident from the above mentioned graphs that increasing the chamfer width from .2 mm to .3 mm gave a significant improvement in the tool performance,while above .3 mm the tool broke under all conditions except for a chamfer angle of -25^{o}. Even at -25^{o} tool breakage occurred when the chamfer length was increased to 1mm.

8.3.2 Correlation Between Tool Life, Chamfer Width and Chamfer Angle

The influence of chamfer width at different levels of chamfer angle is shown in figure 8.8 and 8.9. The results in figure (8.8) were obtained at a cutting speed of 150 m/min and feed rate of 0.17 mm/rev. In these tests the tool life is defined as the time taken for the flank wear to reach 0.75 mm.

The results in figure (8.8) indicate that there is an optimum chamfer width at which tool life is a maximum for each chamfer angle used. Moreover, tool life also varies with chamfer angle and the maximum tool life was obtained with a chamfer angle of -15^{o} and chamfer width of 0.3 mm.

Modifications to the tool edge geometry gave 100% improvement in tool life when compared with the conventional available standard geometry when machining

EN26 in the hardened condition. Figure (8.9) shows similar relations to those obtained in figure (8.8) but for a feed rate of .25 mm/rev, and again the improvement in tool life of the cutting insert due to the new design geometry can be easily detected. The optimum chamfer width which gave a maximum tool life was also .3 mm, and as with the cases in figure (8.8) the maximum tool life point varies with chamfer angle. However, further extensions of chamfer width above .3 mm resulted in a considerable reduction in tool life and in some cases the cutting insert was broken off. For comparison purposes a test was carried out with zero chamfer width (i.e. the presentation rake angle was 5^{o}negative) and the tool only survived for 1-2 minutes when using similar cutting conditions to those used in figures (8.8) and (8.9).

It is worth mentioning that with the optimum cutting insert geometry of 0.3 mm chamfer width and -15^{o} chamfer angle the cutting process continued up to 14 minutes cutting time and the tool showed no breakage with acceptable surface finish.

Further discussions on the reasons for the improvement obtained in tool life are included in Section 8.3.4.

8.3.3 The Effect of Feed Rate

The influence of feed rate on the tool life of the cutting inserts are shown in figures (8.10-8.12) for a

variety of chamfer widths and chamfer angles including the geometry specified for the conventional insert.

As shown from the curves, the general trends reveal that as the feed rate increases the tool life decreases. However, in one case (chamfer width .2 mm and chamfer angle -25^{o}) the tool life was increased as the feed rate increased up to .33 mm/rev and then decreased as feed was further increased. The reasons for the above phenomenum were discussed in Section 6.3.

Figure (8.10) shows the results for chamfer angle -10^{o}; and it is clear from the figure the .3 mm chamfer width gave the optimum condition among the chamfer widths tested, and it is also evident that the tool life obtained with .3 mm chamfer width is better than the values obtained when using the conventional geometry at a feed rate of .17 mm/rev and .25 mm/rev.

Similar results were obtained in figures (8.11) and (8.12) where the chamfer angle used was -15^{o} and -25^{o} respectively, and again .3 mm chamfer width proved to be the optimum. The maximum tool life obtained, which gave 100% improvement compared with the conventional cutting tool geometry, was for the combination of .3 mm chamfer width and -15^{o} chamfer angle. The effect of feed rate can be explained as follows. When using a small feed rate (for specified volume of material to be removed) the surface area separated is expected to be less than

the surface area of separation when a coarse feed is used. In both cases the same volume of metal will be removed; but the coarse feed will result in a lower total energy consumption. Furthermore, on small feed rates there is a minimum deformation in the workpiece and chip. For this reason the cutting force is assumed to be directly proportional to the area of the surface of separation and to the volume of metal removed. If it was possible to separate the chips from the workpiece in one plane only, i.e. without disturbing the adjacent layers in the material, the increase in the cutting forces with increase in the feed rate would be very small and would coincide with the increase in the area of the surface of separation.

However, besides separation of the material planes, compression, bending, friction and other phenomena occur in a metal-cutting operation and the effects of these phenomena can be observed as deformation.

Since this deformation in the chip and in adjacent layers of the workpiece is proportional to the feed, the tool forces become greater with increasing feed rate and this was evident from the measured cutting force carried out during the tests(87).

8.3.4 The Influence of the New Design Configuration on the Cutting Forces.

The strengthening effect obtained by properly chamfering the cutting edge of Kyon 2000 ceramic insert puts an entirely different perspective on these materials as a substantial improvement in tool life was obtained(112) as shown in Section 8.3.2. It is likely that the cutting forces play an important role in this improvement, and therefore, it is intended here to consider the cutting force occurring during machining.

Table (8.2) is a typical set of force data obtained at a cutting condition of V=150 m/min and f=.17 mm/rev, and figure (8.13) shows the direction of the resultant cutting force of both feed force and main cutting force with respect to the cutting edge. With the normal standard chamfer width of 0.2 mm the force is higher than at higher chamfer widths and furthermore, the angle of inclination of the force is much less. An increase in chamfer width to 0.3 mm gives a substantial reduction in force combined with a large increase in angle of inclination. A further increase to 0.5 mm land width increases the force but is compensated by an increased angle so that from figure (8.8) it is clear that there is little difference in tool life between 0.3 and 0.5 mm chamfer width with a chamfer angle of 25^{o}. At a chamfer width of 1 mm the force remains the same, but the inclination reduces and so does the resulting tool life.

Tables (8.3) and (8.4) present the force data when chamfer angles of -10^{o} and -15^{o} were used with similar cutting conditions applied to the previous mentioned case. Figures (8.14) and (8.15) show the direction of the resultant cutting forces for the data in Tables 8.3 and 8.4.

It is noticeable from both Tables 8.3 and 8.4 that changing the chamfer width has an influence on both the resultant cutting force and its inclination with respect to the cutting edge. The modification of tool edge configuration brought about a condition where all the resultant cutting forces were less than the resultant cutting force value obtained when the standard geometry was used. In addition all the directions of these resultant cutting forces were inclined as shown in figures (8.14) and (8.15). The angles which the cutting forces make to the tool shank is higher than that for a standard tool. Furthermore, similar phenomena is obtained when .25 mm/rev feed rate had been used.

It would appear therefore that the new design of the proper chamfer angle and chamfer width combination has an influence on both the value and the direction of the resultant cutting force acting on the cutting edges. The correct chamfer configuration redirects the cutting force into the tool shank, thereby minimising any components tending to cause tensile bending stresses, in which a brittle material such as Kyon 2000 ceramic

Table (8.2) Cutting forces for modified Geometry Tools (chamfer angle -25°)

Chamfer width (mm)	Cutting force (N)	Feed force (N)	Radial force (N)	Resultant force R (N)	Inclination angle (C)
.2	3800	2650	2250	4632	36°
.3	2200	2825	2775	3580	52°
.5	1950	3100	4400	3662	57°
1	2100	3000	4750	3661	54°

Table (8.3) Cutting forces for modified Geometry Tools (chamfer angle -10°)

Chamfer width (mm)	Cutting force (N)	Feed force (N)	Radial force (N)	Resultant force R (N)	Inclination angle (C)
.2	1850	2275	3625	2932	51°
.3	1775	3750	5000	4149	65°
.5	1650	3000	4100	3424	61°
1	1950	3850	5350	4316	63°

Table (8.4) Cutting forces for modified Geometry Tools (chamfer angle -15°)

Chamfer width (mm)	Cutting force (N)	Feed force (N)	Radial force (N)	Resultant force R (N)	Inclination angle (C)
.2	1800	2200	3375	2842	51°
.3	1550	3050	5300	3421	63°
.5	1675	3150	5950	3567	62°
1	1900	4200	5950	4609	66°

f = .17 mm/rev

V = 150 m/min

insert is relatively weak. Redirecting the cutting force into the tool would have the effect of increasing the compressive components[98], which Kyon 2000 tools are particularly well suited to withstand as mentioned in Chapter 4.

8.3.5 Surface Finish

Surface finish is largely a geometrically determined parameter, depending on the nature of the tool edge in contact with the workpiece, and their relative movements. This can be seen from figure (8.16) where measurements of the variation of surface finish with cutting time for the land widths used in the tool life tests at a -25^{o} chamfer angle. It can be seen from the above figure that a substantial improvement in surface finish is brought about by the new design suggested. Similar results were reported by other authors[81,113]; and this is attributed to the better tool wear performance obtained with geometry modification.

8.3.6 Statistical Analysis

In order to test the model suggested in Section 8.2.2 and the significance of each variable in the experiment an analysis of variance has been carried out on the experimental results which were obtained for tool life of the insert, main cutting force F_Z, radial force F_Y, feed force F_X.

The results of the tests of the tool life which is shown in Table 8.5 will be considered in this section in some detail.

Chamfer angle in degree	Chamfer width in mm	Feed rate mm/rev .17	.25	.33	.5
-10^{o}	.2	5	3.3	4.5	1
	.3	5.5	4.5	1	.25
	.5	5	2	.166	.166
	1	4.75	1	.25	.083
-15^{o}	.2	5	3.75	.33	.166
	.3	7.5	7	.33	.166
	.5	6.6	1	.25	.166
	1	6.3	.166	.166	.166
-25^{o}	.2	3.125	3.5	4.75	1
	.3	7	6.5	.75	.166
	.5	6.75	3.5	1	.166
	1	5.3	1	1	.166

Table (8.5) Tool life results in minutes for modified geometry

Referring to Table (8.5) and in order to calculate the variance ratio of each variable in the experiment and its interaction, the following variance estimate mean square were calculated as follows(82):

Total sum of square of the treatments = μ = 616.794

Mean sum of squares (M.S.S) = $\frac{Y^2}{abc}$ = 316.608 2

The sum of squares due to chamfer angle

$$\tau_{s.s.} = \frac{\Sigma\, Yi^2..}{bc} - M.S.S. \qquad \ldots\ldots\ldots 3$$

$$= \frac{5097.342}{16} - 316.608$$

$$= 1.976$$

The sum of squares due to feed rate

$$B_{s.s.} = \frac{\Sigma Y^2.j.}{ac} - M.S.S. \qquad \ldots\ldots\ldots 4$$

$$= \frac{6209.296}{12} - 316.608$$

$$= 200.833$$

The sum of squares due to chamfer width

$$q_{s.s.} = \frac{\Sigma Y^2..k}{ab} - M.S.S. \qquad \ldots\ldots\ldots 5$$

$$q_{s.s.} = \frac{4041.742}{12} - 316.608$$

$$= 20.203$$

The sum of squares due to the interaction between chamfer angle and feed rate

$$(\tau B)_{s.s.} = \frac{\Sigma Y^2 ij.}{c} - \frac{\Sigma Yi^2..}{bc} - \frac{\Sigma Y.^2 j.}{ac} - \frac{Y^2...}{abc} \quad \ldots\ldots\ldots 6$$

$$= \frac{2113.428}{4} - 318.583 - 517.441 + 316.608$$

$$= 8.941$$

The sum of squares due to the interaction between chamfer angle and chamfer width

$$(\tau q)_{s.s.} = \frac{\Sigma Yi^2.k}{b} - \frac{\Sigma Yi^2..}{bc} - \frac{\Sigma Y^2..k}{abc} \quad \ldots\ldots\ldots 7$$

$$= \frac{1376.645}{4} - 318.583 - 336.811 + 316.608$$

$$= 5.375$$

The sum of squares due to the interaction between feed rate and chamfer width

$$(Bq)_{s.s.} = \frac{\Sigma Y^2.jk}{a} - \frac{\Sigma Y^2.j.}{ac} - \frac{\Sigma Y^2..k}{ab} + \frac{Y^2...}{abc} \quad \ldots 8$$

$$= \frac{1764.193}{3} - 517.441 - 336.811 + 316.608$$

$$= 50.42$$

The sum of squares due to the interaction between chamfer angle, feed rate and chamfer width which can be considered the residual between the above three variables is:

$$(\tau Bq)_{s.s.} = \frac{\Sigma Y^2 ijk}{l} - \frac{\Sigma Yi^2.k}{b} - \frac{\Sigma Y^2 ij}{c} - \frac{\Sigma Y^2.jk}{a}$$

$$+ \frac{\Sigma Yi^2..}{bc} + \frac{\Sigma Y^2.j.}{ac} + \frac{\Sigma Y^2..k}{ab} - \frac{Y^2..}{abc} \quad \ldots\ldots 9$$

$$= 616.794 - 344.161 - 528.357 - 588.064 +$$
$$318.583 + 517.441 + 336.811 - 316.608$$

$$= 12.439$$

In Table (8.6) a complete analysis of variance of all factors or variables and their interaction is presented. Proceeding in a similar way as for the modified new design geometry; the analysis of variance of the main cutting force, radial force, and feed force, the effects of the different factors and their interactions were computed and presented in Tables 8.7, 8.8 and 8.9 respectively.

For the range of the test factors used the analysis of variance of the tool life of Table 8.6 reveals that the effect of feed rate is highly significant at 1% and 5% levels. The effect of chamfer width is highly significant at 1% and 5% levels. The analysis also shows that the interaction between chamfer width and feed rate are also highly significant at 1% and 5% levels, whilst the interaction between the chamfer angle and feed rate are only significant at 10%.

The results of the cutting forces variance analysis are summarised in Table (8.10). Regarding the main cutting force statistical analysis; it is noticeable from the table that the chamfer width is highly significant followed by the chamfer angle and finally by the feed rate. The radial force shows a dependency on the feed rate and the interaction between the factors investigated. This can be explained on the basis that when cutting starts, the tool geometry has no effect on the radial force but once the cutting edge deteriorates the interaction between the factors investigated has a great influence on the radial force and this proved to be true from the cutting tests performed. However, surprisingly the effect of the factors investigated do not reveal significance at the feed force statistical analysis, with the exception of feed rate which is the only factor significant. This might be taken, on a purely statistical basis, as meaning that the cutting performance of the insert is independent of the factors tested (except for feed rate). However, this is not true

as is evident from the cutting test carried out. The reason of this result could be that the levels of the factors were chosen in a way which was not suitable for feed force statistical analysis.

The above analysis of the cutting insert tests performance reveals that the expectation built upon the hypothesis of better cutting edge wear performance, with a new cutting edge geometry were achieved. It is shown in figures(8.8) and (8.9) that approximately 100% improvement in tool life over the standard conventional cutting insert were attained.

Table (8.6) Analysis of Variance (Refer to Table 8.5)

Tool life results of modified new design geometry

Source	Sum of Square S.S	Degree of Freedom	Variance Estimate Mean Square	Variance Ratio	
Treatments	616.794	48			
Mean S.S	316.608	1			
τ	1.976	2	0.9879	1.429	n.s
B	200.833	3	66.941	96.875	***
q	20.203	3	6.7343	9.745	***
τB	8.941	6	1.4901	2.1564	*
τq	5.375	6	0.89	1.296	n.s
Bq	50.42	9	5.602	8.107	xxx
Residual	12.439	18	0.691		

*** Significant at 1% and 5% levels

* Significant at 10% level

n.s Not significant at 1% and 5% (non significant)

Table (8.7) Analysis of Variance of Main cutting force results of modified new design geometry

Source	Sum of Square S.S	Degree of Freedom	Variance Estimate Mean Square	Variance Ratio	
Treatments	327178750	48			
Mean S.S	300500208.3	1			
τ	9613229.2	2	4806614.6	14.818	***
B	4934479.2	3	1644826.4	5.071	*
q	302309895.8	3	100769965.2	310.647	***
τB	1834895.8	6	305815.967	.943	n.s
τq	938750	6	156458.334	.483	n.s
Bq	1708541.6	9	189837.956	.586	n.s
Residual	5838961.4	18	324386.745		

*** Significant at 1% and 5% levels

* Significant at 1% and 5% levels

n.s Not significant at 1% and 5% levels (non significant)

Table (8.8) Analysis of Variance of Radial force results of modified new design geometry

Source	Sum of Square S.S	Degree of Freedom	Variance Estimate Mean Square	Variance Ratio	
Treatments	63251225	48			
Mean S.S	577789708.3	1			
τ	42712	2	21356	.0608	n.s
B	16547956.2	3	5515985.4	15.689	***
q	2005331.2	3	668443.7333	1.901	n.s
τB	7465554.7	6	1244259.116	3.539	***
τq	6234617.2	6	1039102.866	2.956	***
Bq	16097579.3	9	1788619.922	5.088	***
Residual	6328766.7	18	351598.15		

*** Significant at level 1% and 5%

n.s Not significant at 1% and 5% levels (Non-significant)

Table (8.9) Analysis of Variance of Feed force results of modified new design geometry

Source	Sum of Square S.S	Degree of Freedom	Variance Estimate Mean Square	Variance Ratio	
Treatments	291819100	48			
Mean S.S	268.474×10^6	1			
τ	570845.9	2	285422.95	1.225	n.s
B	9901312.5	3	3300437.5	14.158	***
q	1110454.2	3	370151.4	1.588	n.s
τB	1989012.5	6	331502.084	1.422	n.s
τq	1709395.8	6	284899.3	1.222	n.s
Bq	3767058.3	9	418562.034	1.796	n.s
Residual	4196229.2	18	233123.845		

*** Significant at 1% and 5% levels

n.s Not significant at 1% and 5% levels (Non-significant)

Table (8.10)

TABLE ; REPRESENT (A.O.V.) EFFECT OF VARIABLE ON EXPERIMENT

RESPONSE	Feed	Chamfer Angle	Chamfer Width	Interaction between Chamfer Angle & Chamfer Width	Interaction between Chamfer Angle & Feed	Interaction between Chamfer Width & Feed
TOOL LIFE Y	***	n.s	**	*	*	**
FEED FORCE Fx	**	n.s	n.s	n.s	n.s	n.s
RADIAL FORCE Fy	**	n.s	n.s	*	*	*
MAIN CUTTING FORCE Fz	*	**	***	n.s	n.s	n.s

*** very highly significant

** highly significant

* significant

n.s not significant

8.4 CHAPTER CLOUSRE

In this chapter a new tool geometry is suggested. A major improvement in the cutting performance was found in comparison with standard conventional available cutting inserts. The geometry modification rotates the resultant cutting force vector in such a manner that the tool edge stresses becomes more compressive and consequently more favourable to a material lacking toughness.

Results of the variance analysis showed that feed rate, chamfer angle and chamfer width have influenced the performance of the tools.

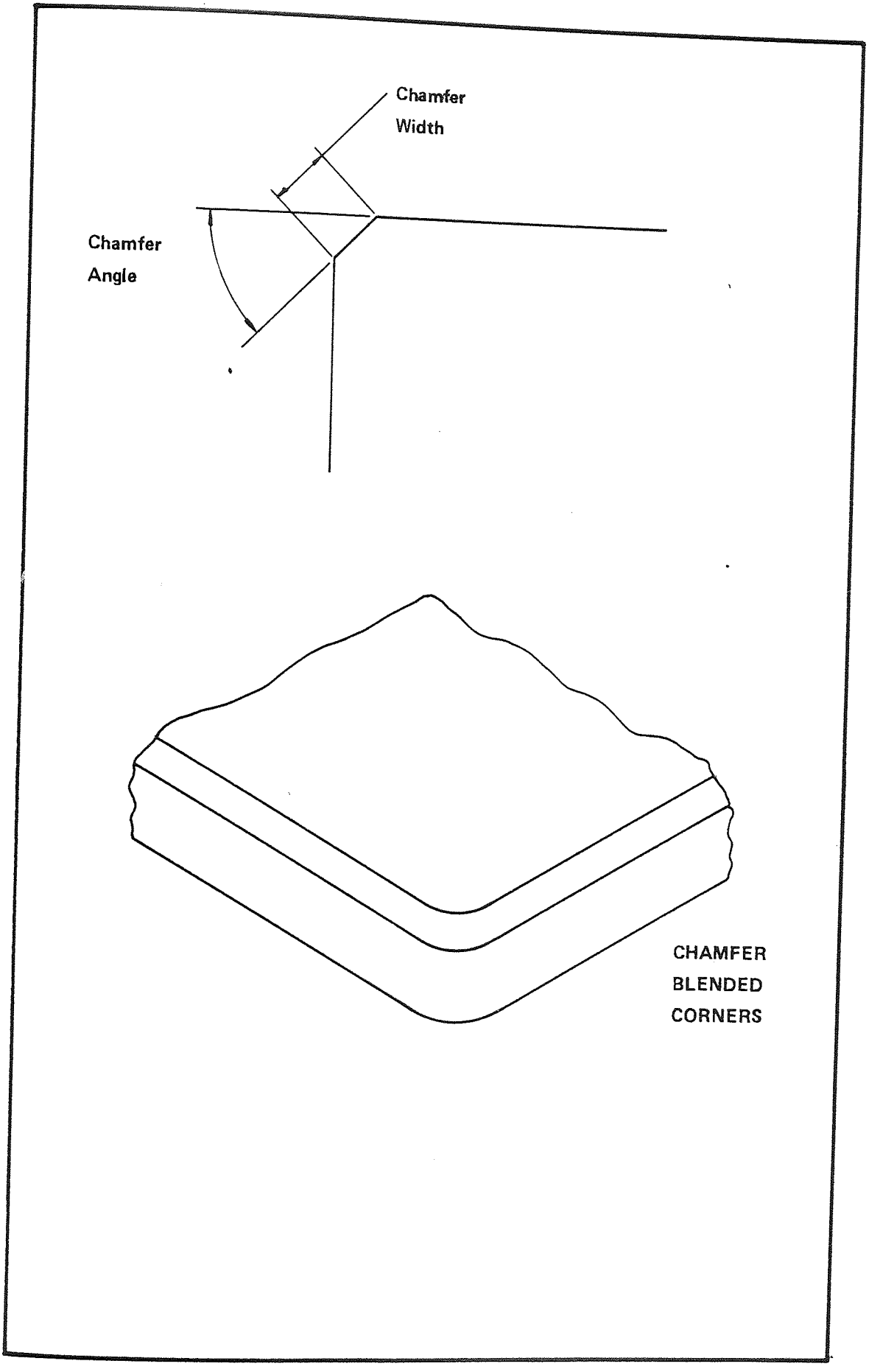

Figure 8.1 Negative Cutting Tool with Chamfer Configuration

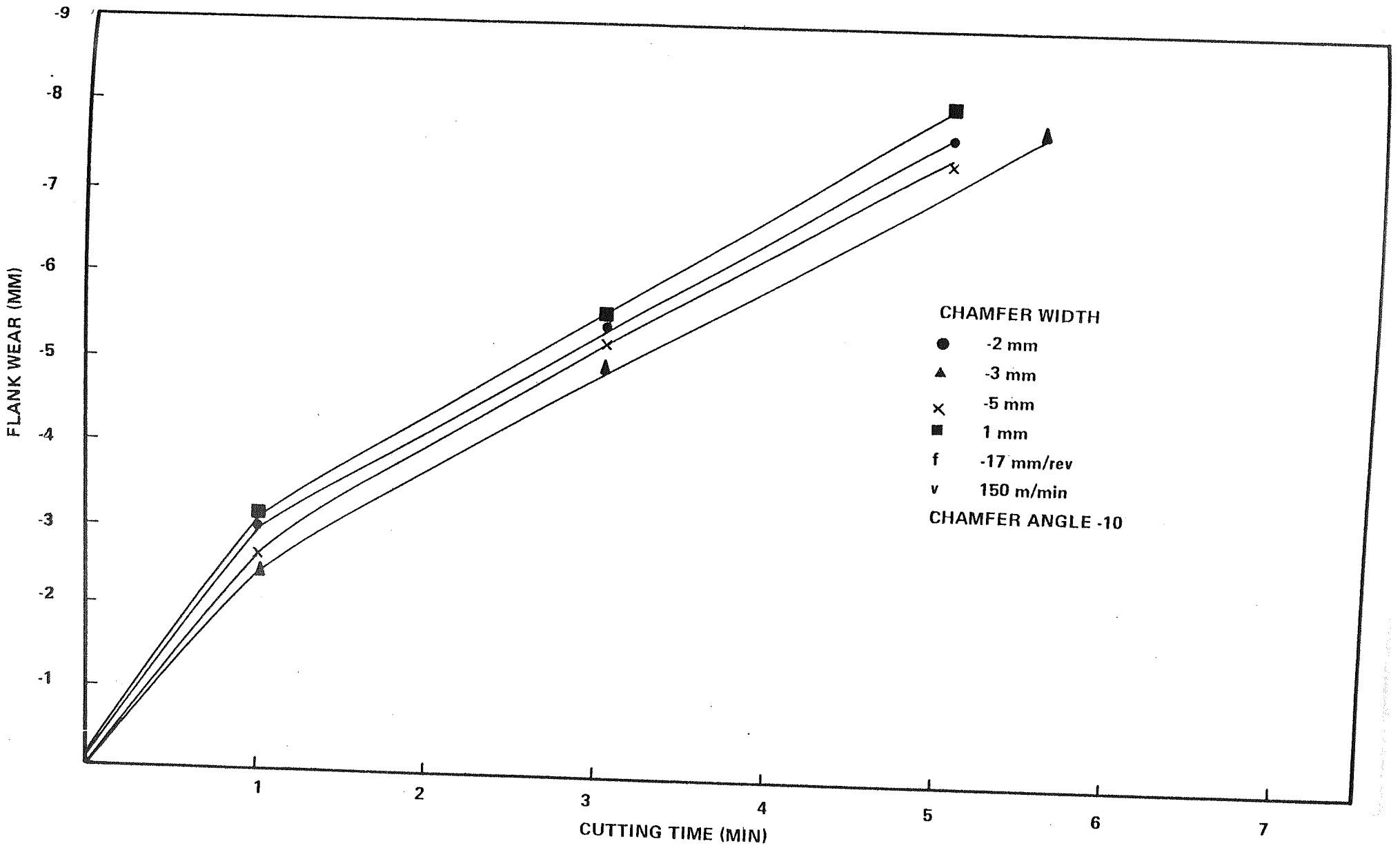

Figure 8.2 Influence of Chamfer Width on Flank Wear (Chamfer angle -10°, f = .17 mm/rev)

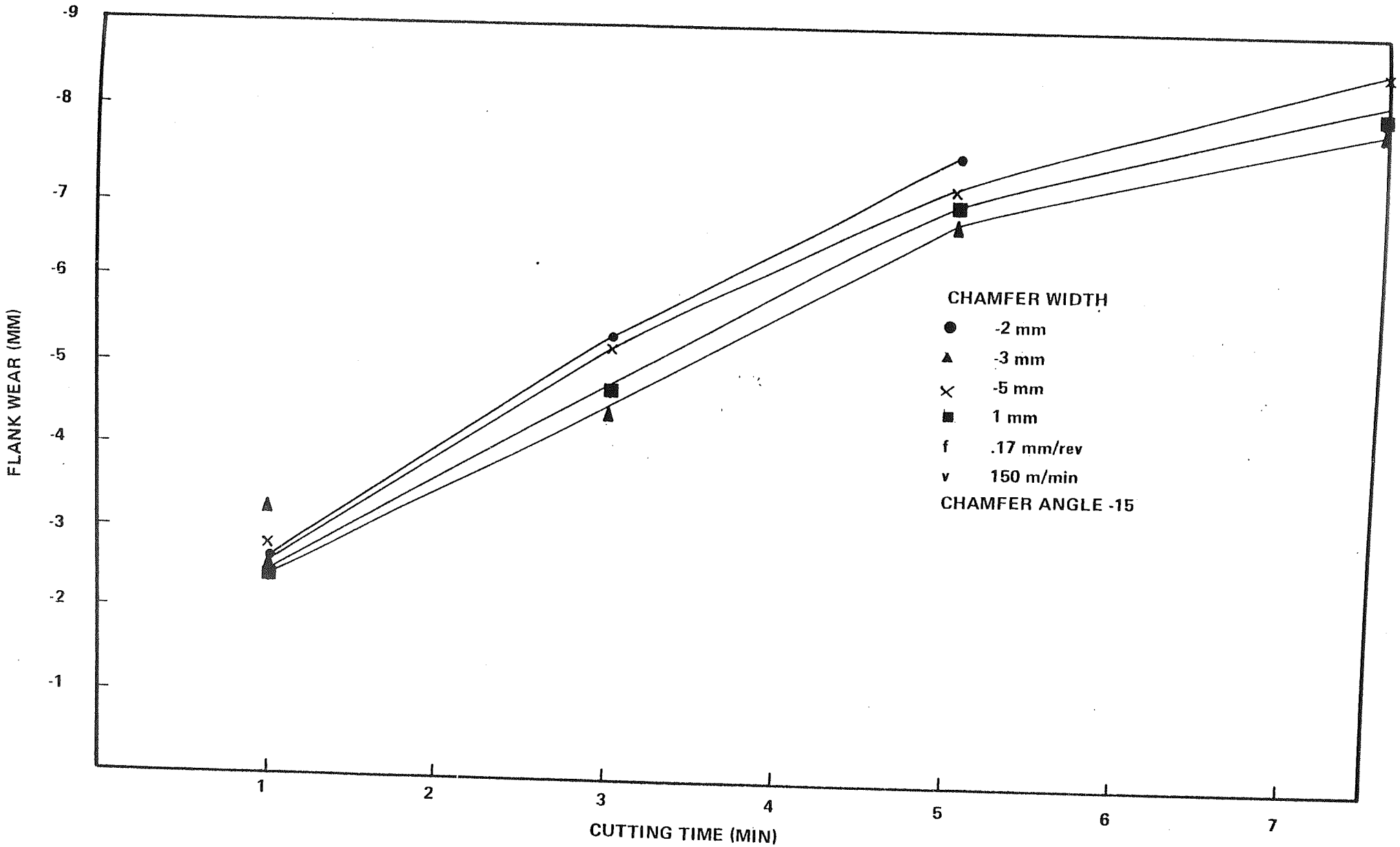

Figure 8.3 Influence of Chamfer Width on Flank Wear (Chamfer Angle -15°, f = .17mm/rev)

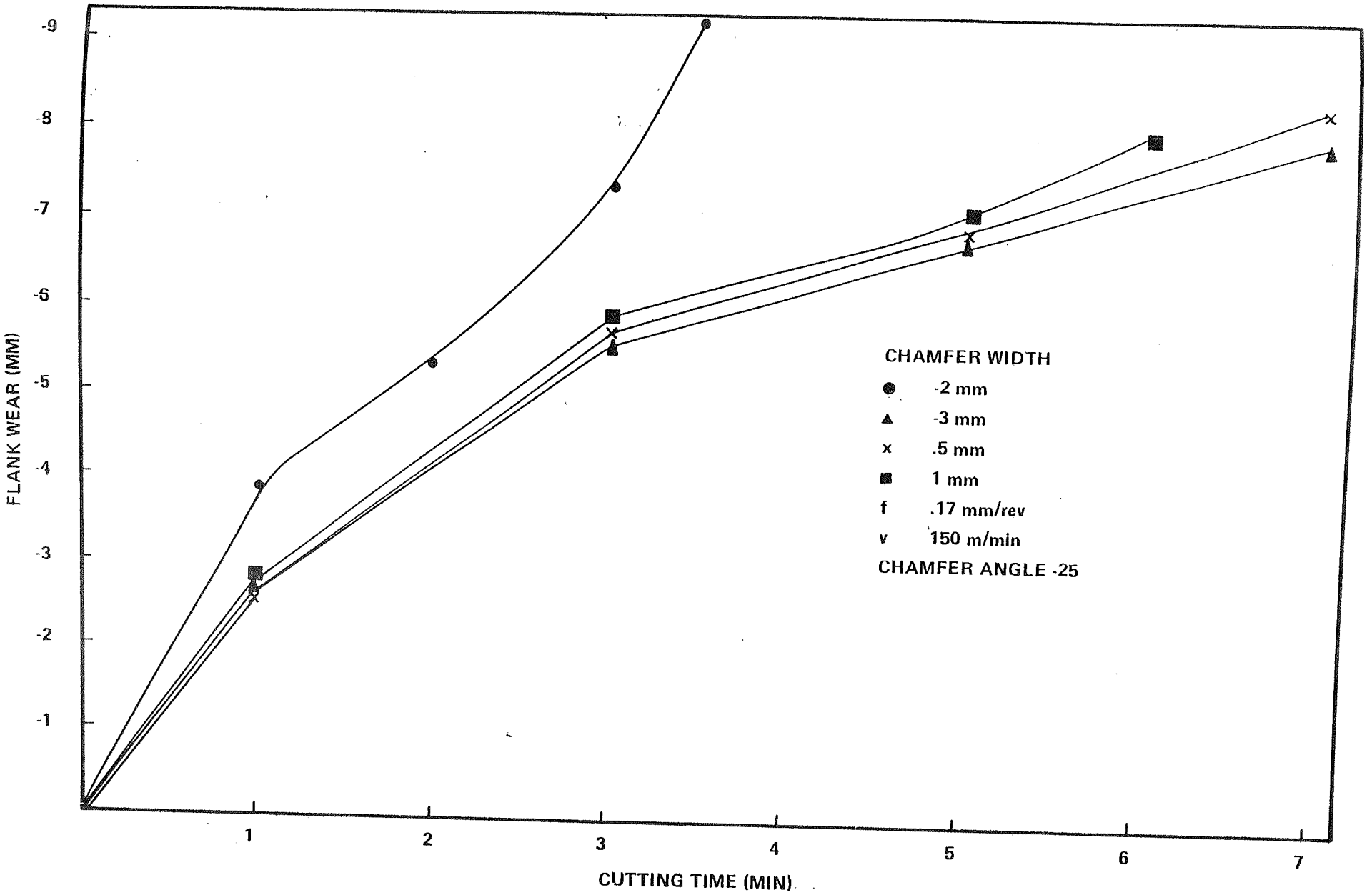

Figure 8.4 Influence of Chamfer Width on Flnak Wear (Chamfer Angle -25°, f = .17 mm/rev)

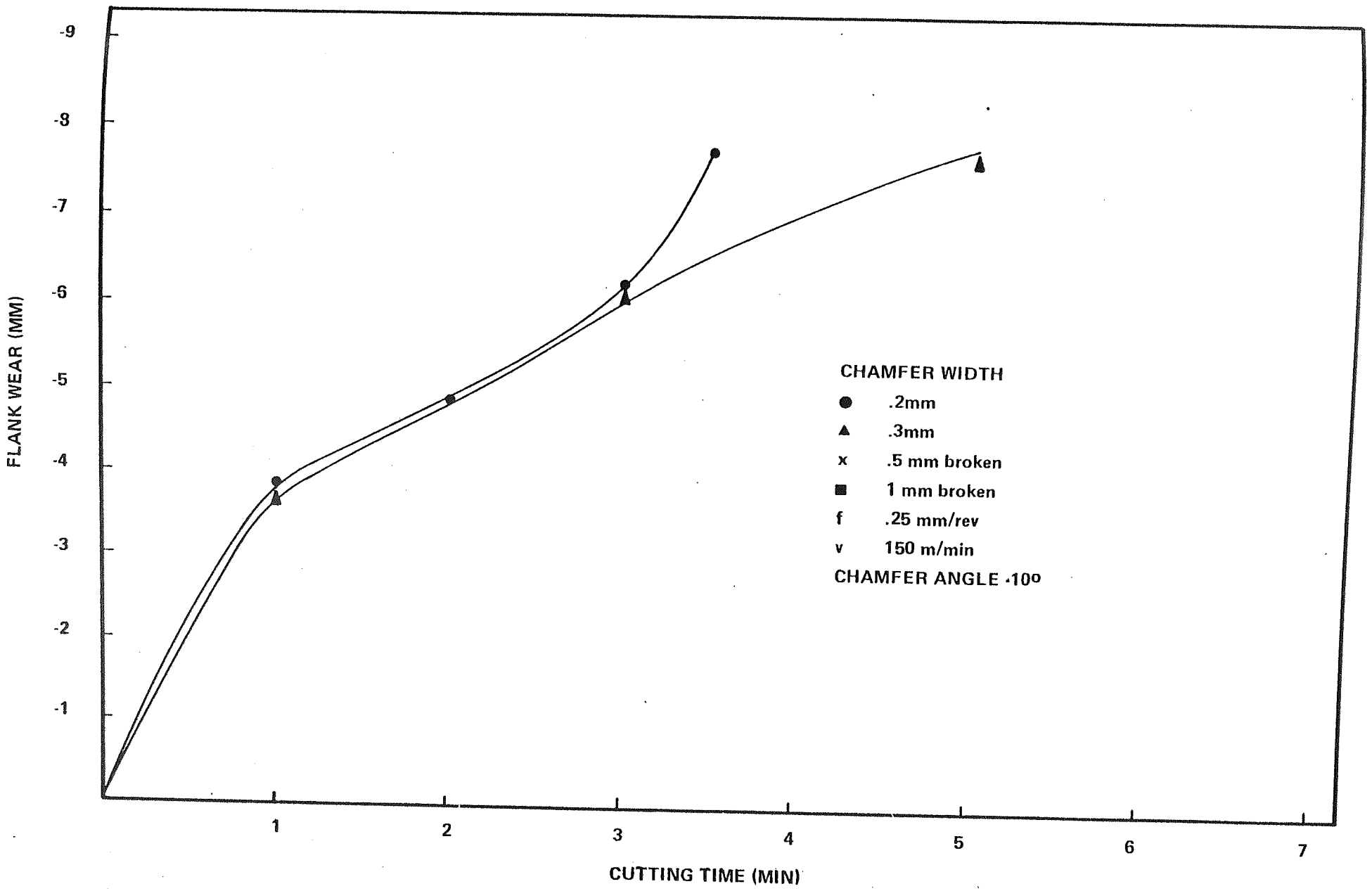

Figure 8.5 Influence of Chamfer Width on Flank Wear (Chamfer Angle -10°, f = .25 mm/rev)

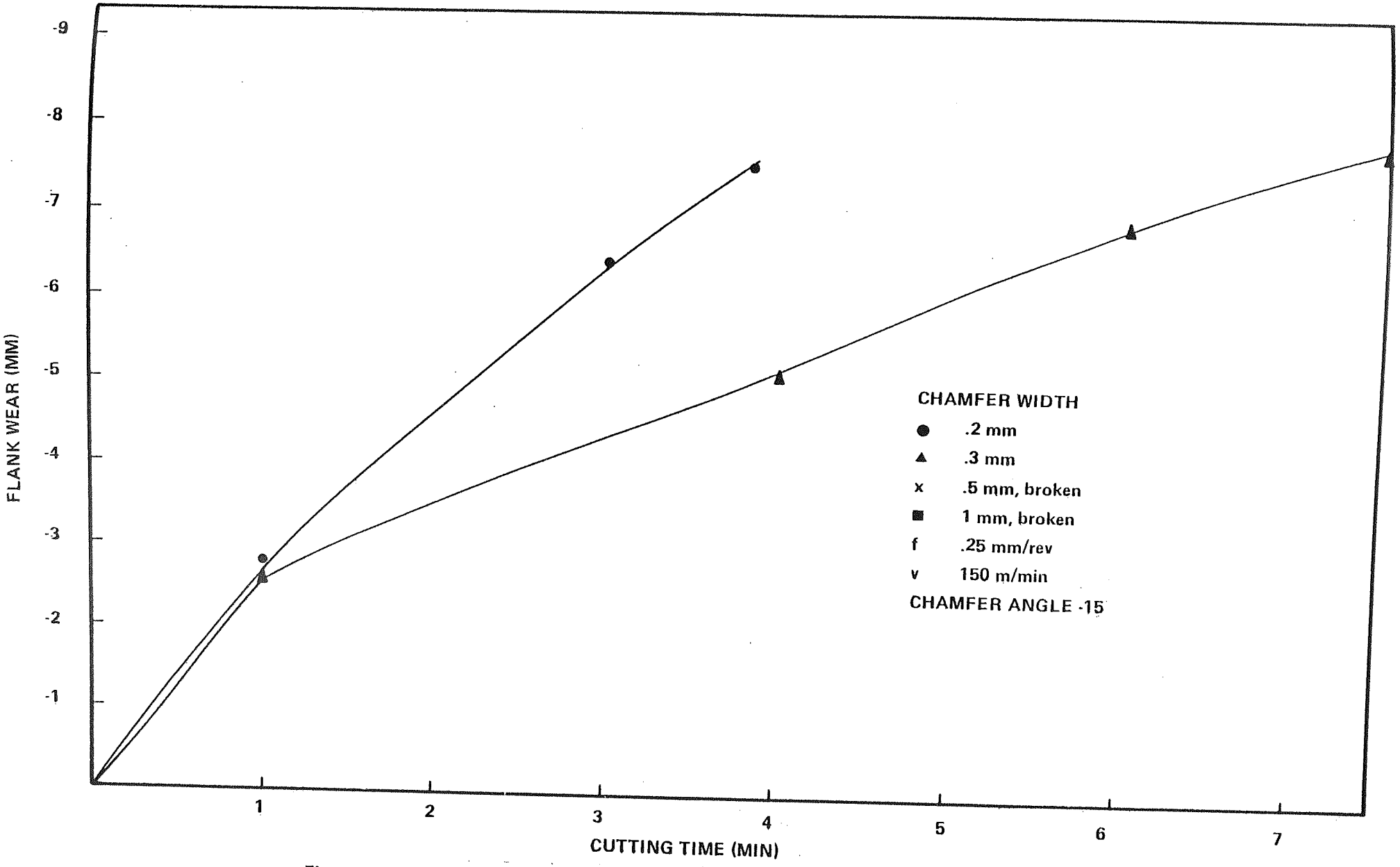

Figure 8.6 Influence of Chamfer Width on Flank Wear (Chamfer Angle -15°, f = .25 mm/rev)

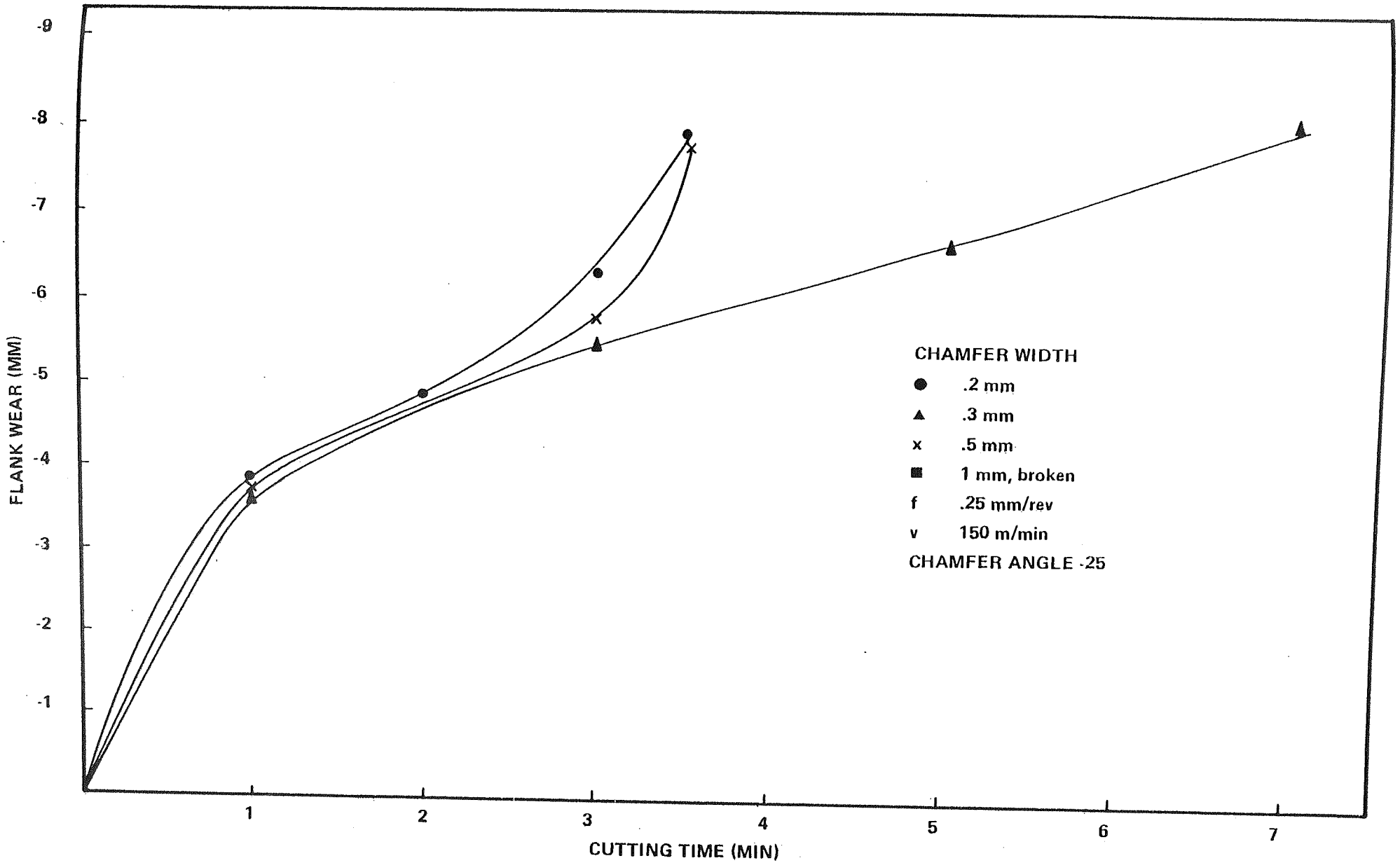

Figure 8.7 Influence of Chamfer Width on Flank Wear (Chamfer Angle -25°, f = .25 mm/rev)

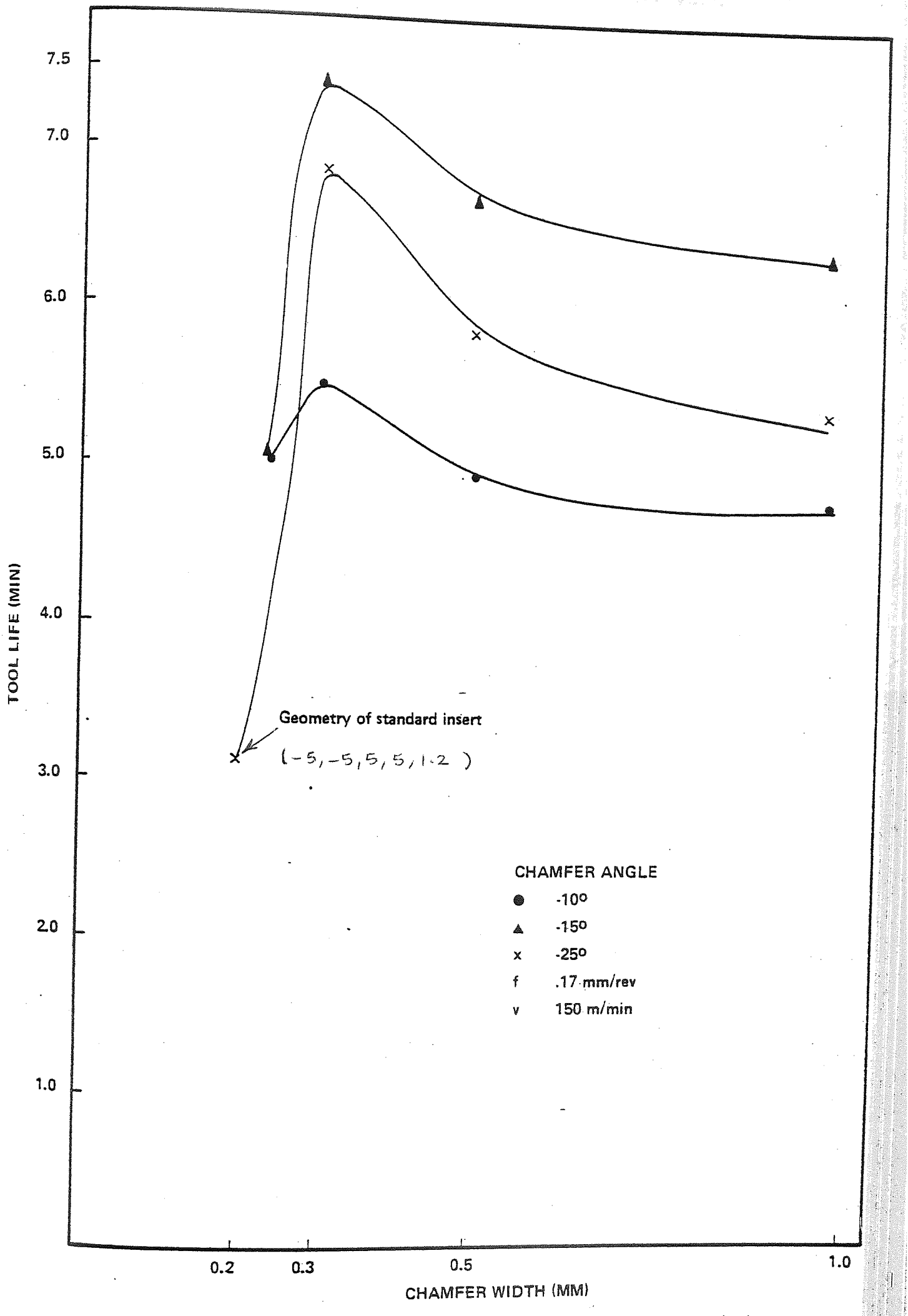

Figure 8.8 Influence of Tool Geometry Modification on Tool Life (f = .17 mm/rev)

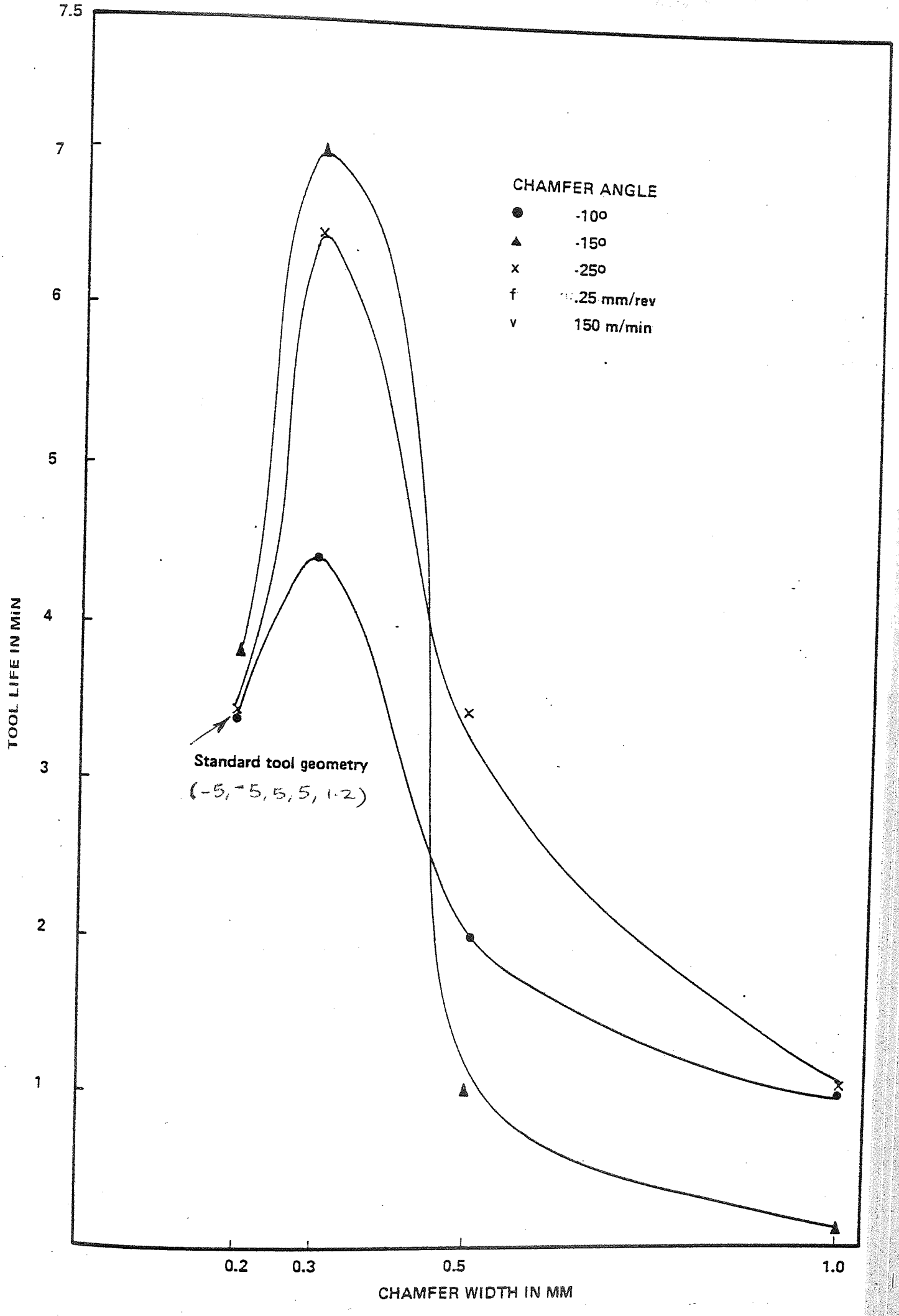

Figure 8.9 Influence of Tool Geometry Modification on Tool Life (f = .25 mm/rev)

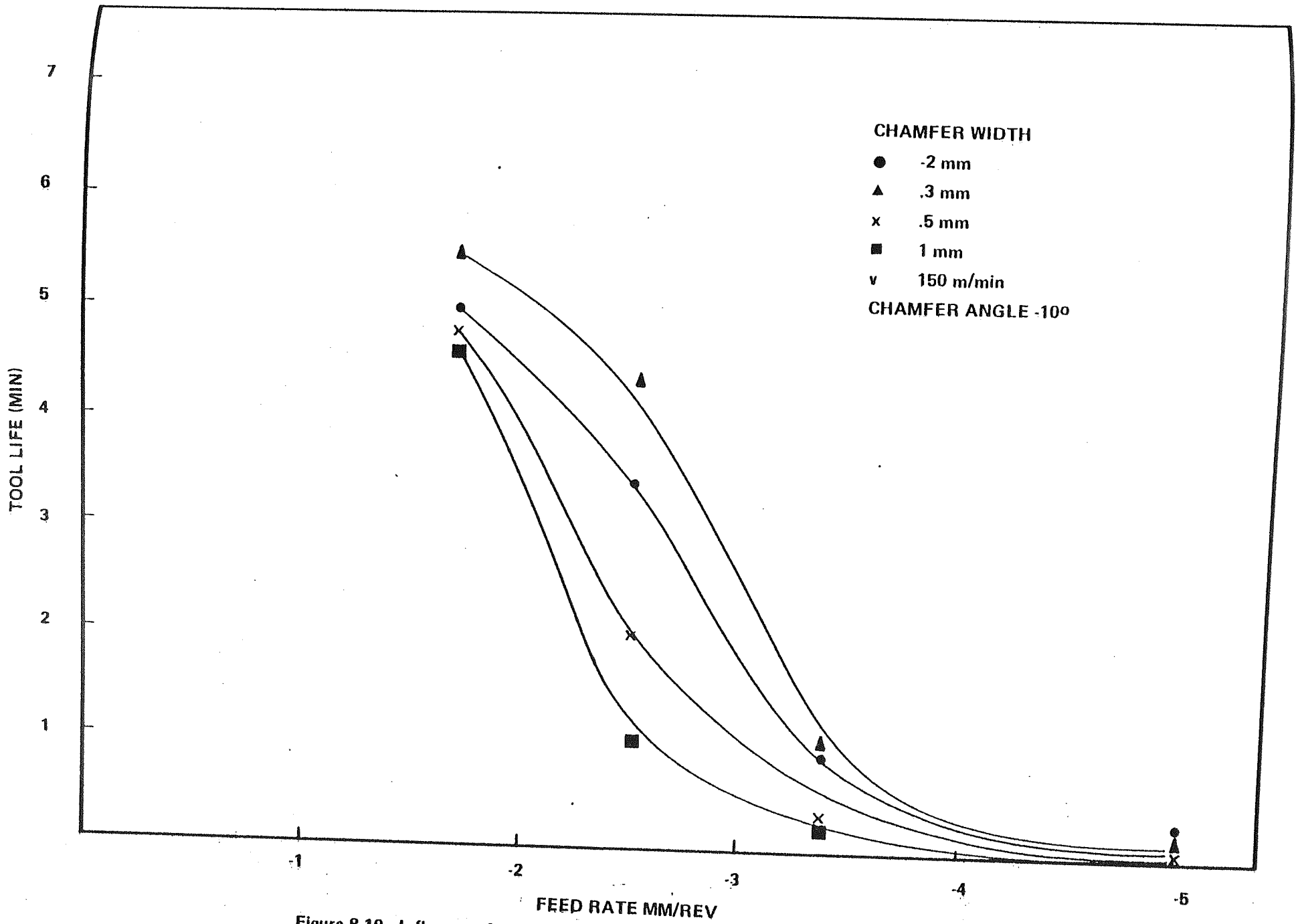

Figure 8.10 Influence of Feed Rate on Geometry Modification (Chamfer Angle -10°)

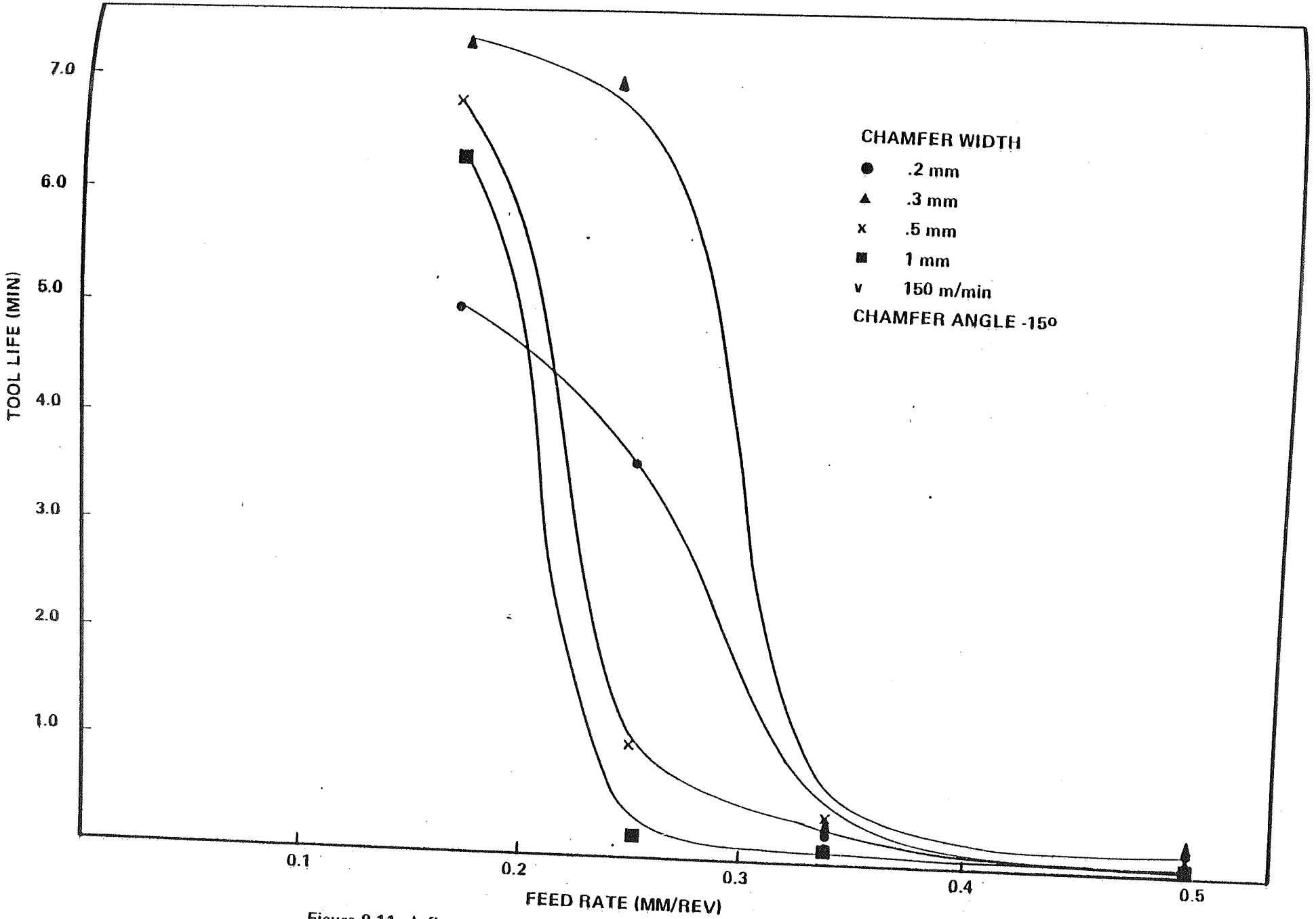

Figure 8.11 Influence of Feed Rate on geometry Modification (Chamfer angle -15°)

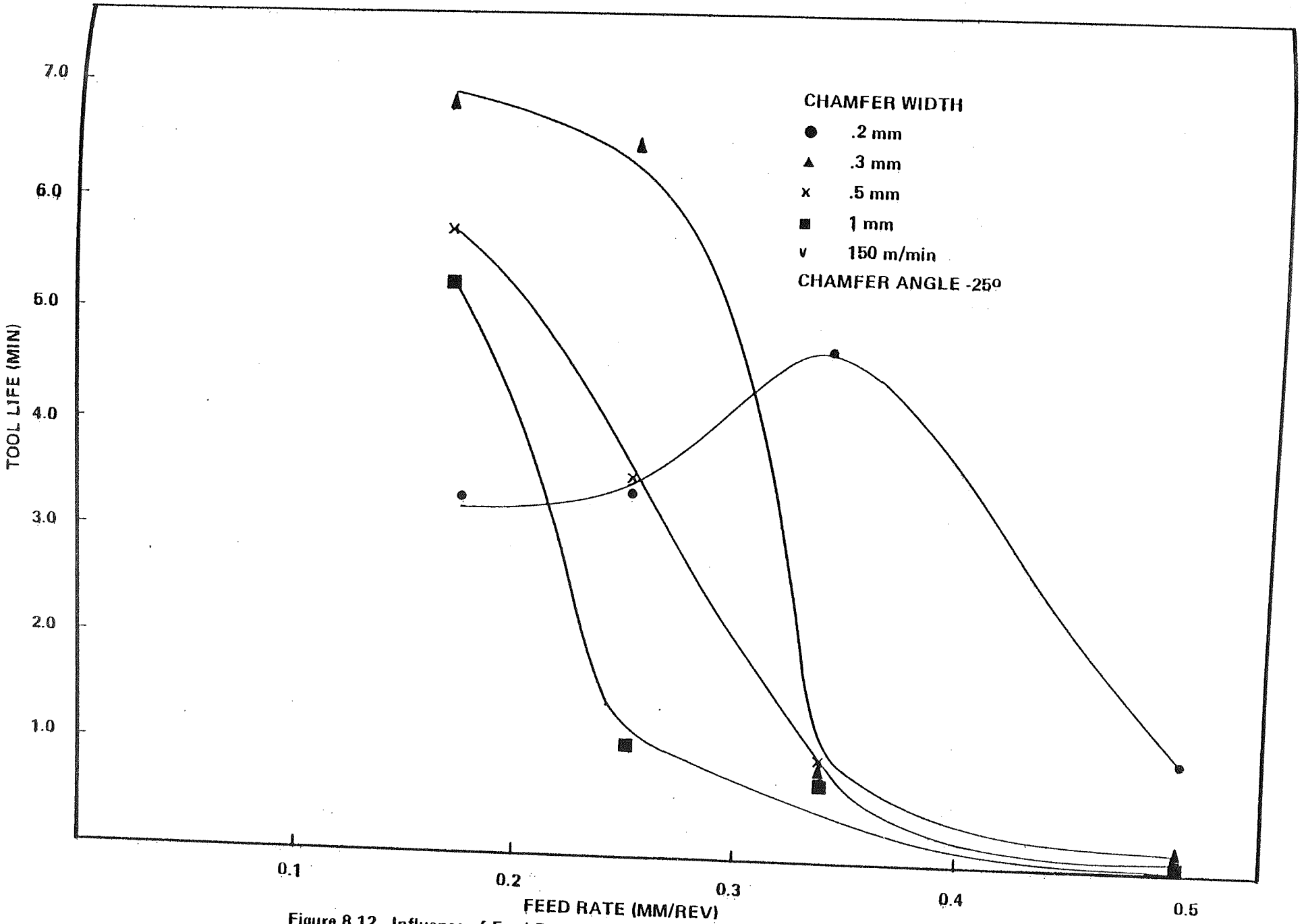

Figure 8.12 Influence of Feed Rate on Geometry Modification (Chamfer Angle -25°)

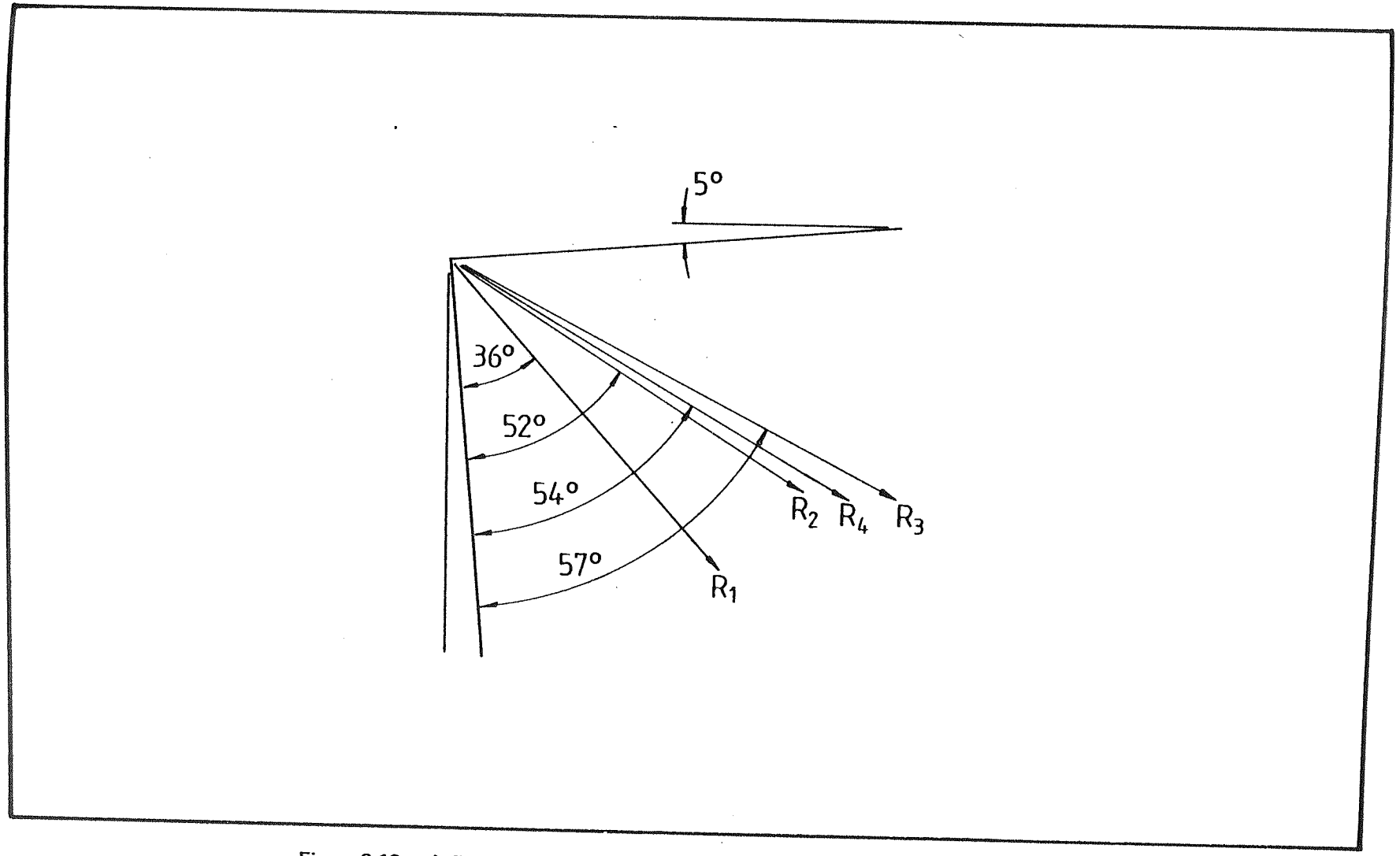

Figure 8.13 Influence of Tool Geometry Modification on Direction of Resultant Cutting Force (Chamfer angle -25°)

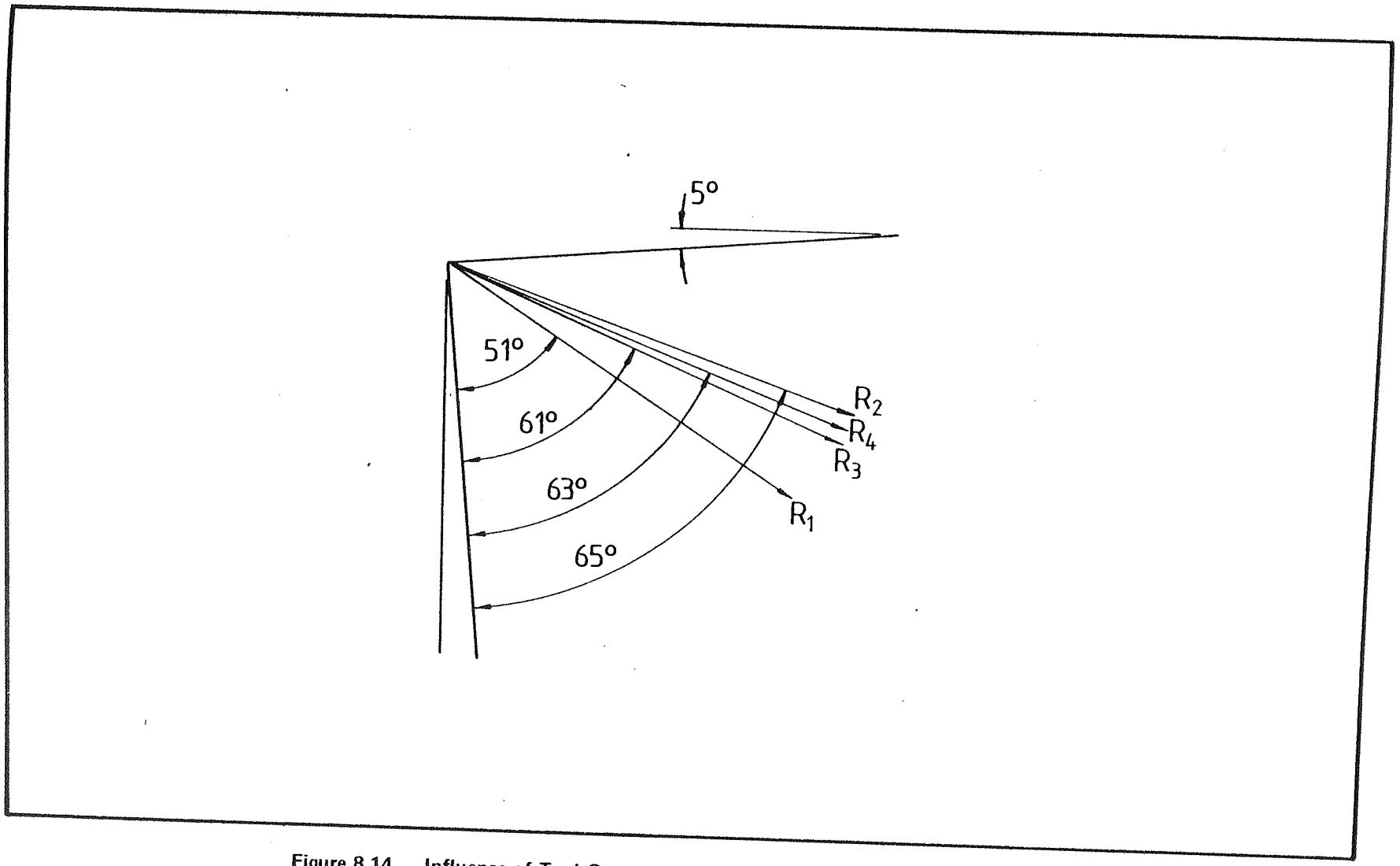

Figure 8.14 Influence of Tool Geometry Modification on Direction of Resultant Cutting Force (Chamfer angle -10°)

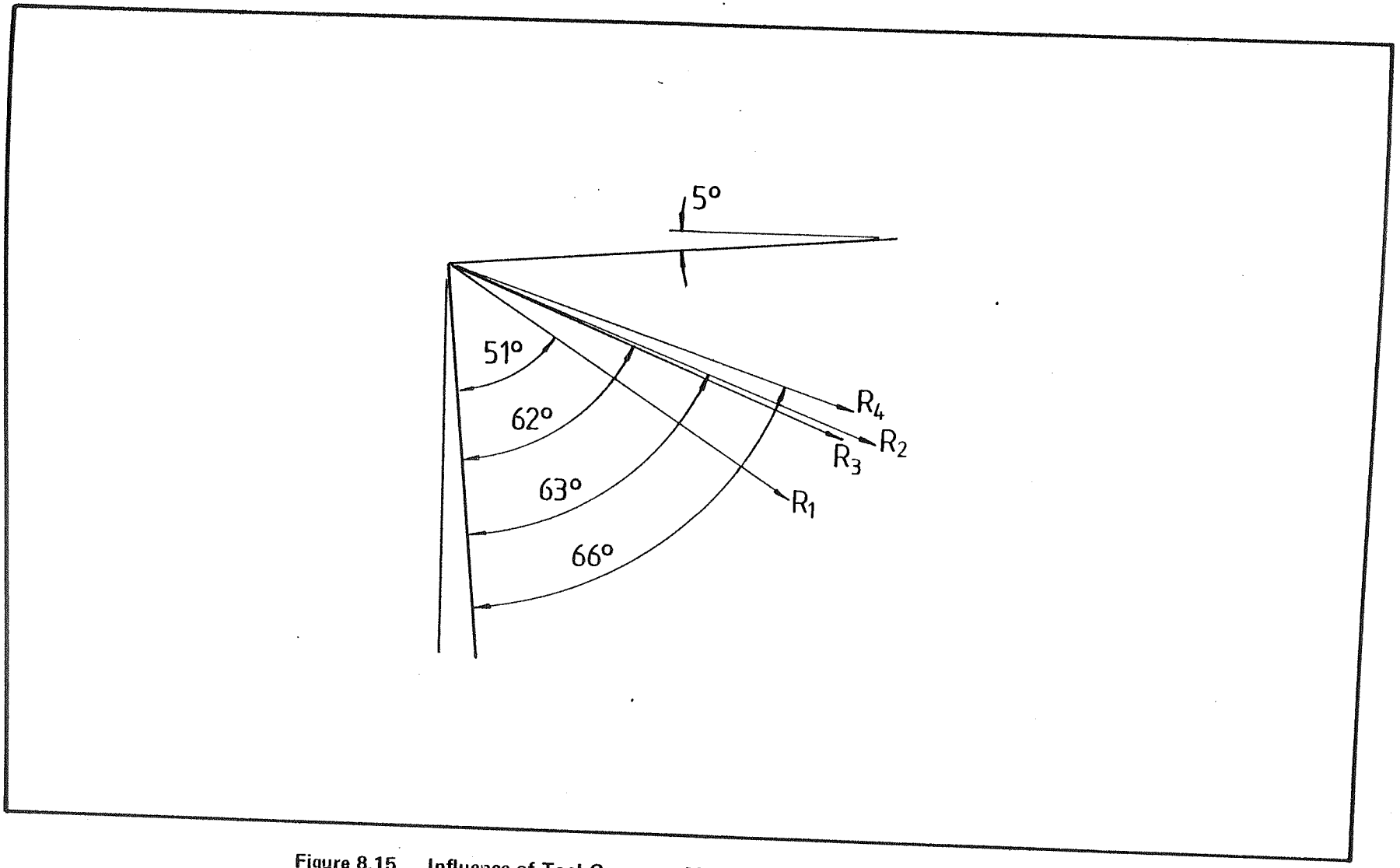

Figure 8.15 Influence of Tool Geometry Modification on Direction of Resultant Cutting Force (Chamfer angle -15°)

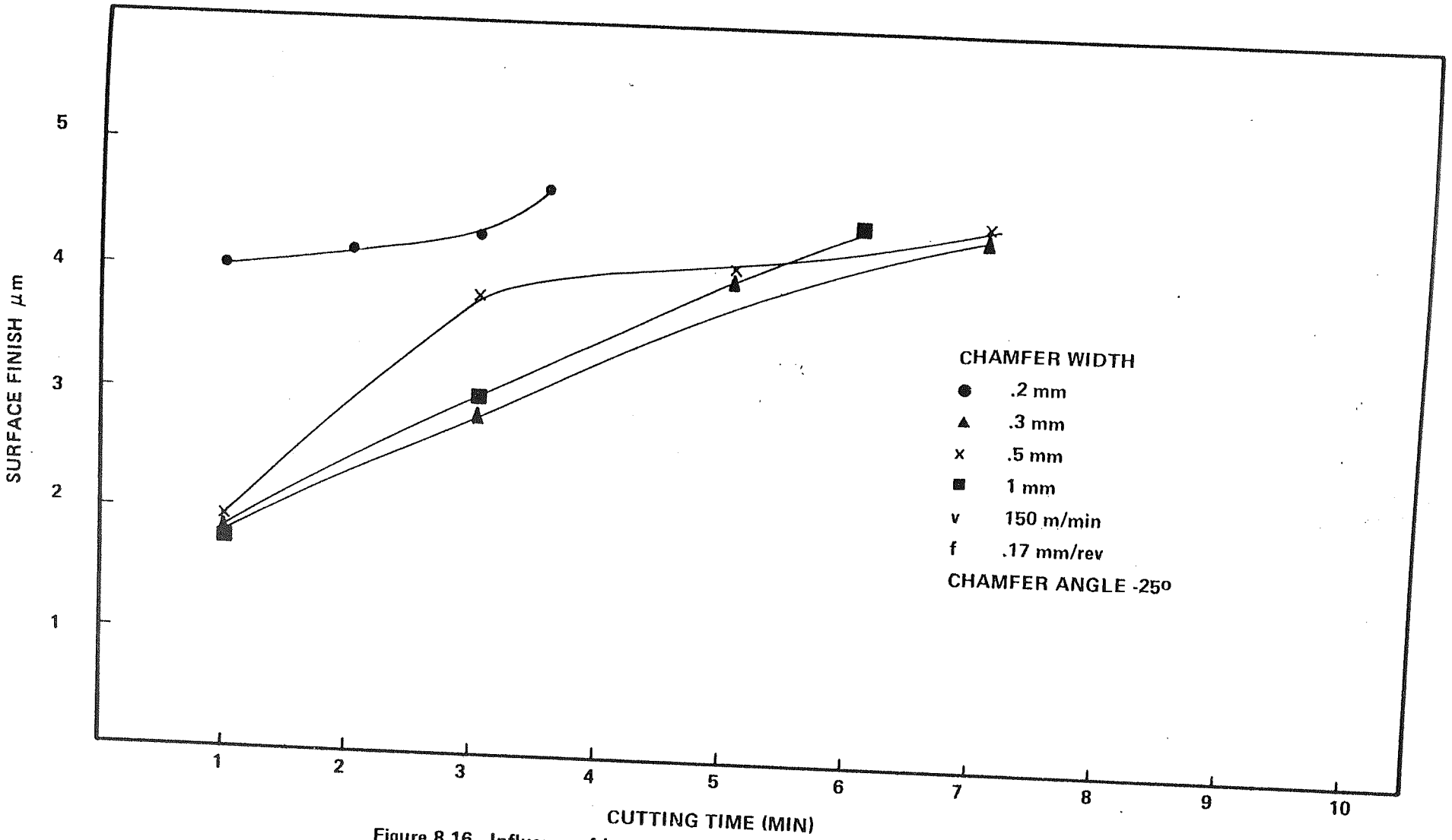

Figure 8.16 Influence of Land Width on Surface Finish (Single Rake Tool)

CHAPTER NINE

CONCLUSIONS AND SUGGESTIONS FOR FURTHER WORK

1) It is possible to machine hardened EN26 high strength alloy steel with Kyon 2000 cutting tools. Correct selection of speeds and feed rates are necessary in this application.

2) Using a cutting fluid gives no advantages and may lead to premature edge breakage due to the development of high force levels.

3) A reduction in tool wear rate is obtained when a large plan approach angle is used, and therefore, large plan approach angles are recommended, particularly for high feed rates.

4) The tool wear rate on the cutting edge shows a dependency on the hardness of the work material being machined.

5) The selected feed rate is very important. Increasing the feed rate up to a certain level gives a substantial reduction in tool wear and consequently increases in the tool life.

6) The higher temperatures generated by increasing the cutting speed reduce the secondary shear strength of the workpiece material and consequently the cutting forces are lower.

7) Four main modes of failure occur when machining a hardened steel with Kyon 2000 ceramic

(a) flank and crater wear

(b) grooving wear

(c) deformation wear and

(d) brittle failure

8) Using the SPSS package,a good correlation is obtained between predicted and actual tool life

9) The double rake tool edge geometry which combines both negative and positive conditions, results in a significant improvement in the cutting performance.

10) The optimum land width for a double rake tool occurs at a position where the contact length is minimum and the chip thickness ratio is maximum.

11) The measured cutting forces obtained when using double rake tools increases as land width increases up to the optimum land width position, and thereafter, they tend to stabilise as the natural contact length is approached.

12) The calculated shear angle has a tendency to increase to a maximum value when the contact is on both primary and secondary faces. This condition coincides with the optimum land width position. The shear angle decreases when the contact takes place on the primary rake only

13. The trend of shear angle-land width relationships are similar to the chip thickness ratio relationships.

14) The temperature on the cutting tool reaches a minimum value at the optimum land width. Above and below this position, the temperature increases.

15) The maximum temperature recorded moves further away from the cutting edge when a double rake tool is used.

16) The level of normal stress distribution at the rake face varies with tool geometry. The maximum values occur when optimum land geometry is used.

17) The maximum value of the normal stress, which coincides with the optimum position of land width, gives better tool performance since the cutting edge is placed under a higher compressive stress and this is more favourable for Kyon 2000 ceramic.

18) The shear stress distribution near the cutting edge is not a constant as has been suggested by some authors.

19) The edge preparation normally used for carbide tools is not the most appropriate for Kyon 2000 in machining hardened alloy steel. An increase in chamfer width to 0.3 mm and a reduction in chamfer angle to 15^{o} can increase tool life by over 100% compared with a commercial insert.

20) The geometry modification rotates the resultant cutting force vector in such a manner that the tool edge stresses become more compressive and consequently more favourable to material lacking toughness.

21) A significant improvement in surface finish is obtained with the modified tool geometry.

22) The variance analysis indicated that the feed rate, chamfer width and chamfer angle highly influence the cutting performance.

1) More work needs to be done to reduce grooving wear. Possibilities include machining in a special environment such as nitrogen and using an extremely rigid machine tool.

2) A further investigation of the possibility of using sialon ceramic tool in intermittent cutting would be useful.

3) With regard to the modified edge geometries further work could establish;

   i) the suitability of using sialon ceramic for the machining of stainless steel and rock materials,

   ii) the optimum land shape on the tool e.g. intersected, blended, symmetrical, asymmetrical, etc.

   iii) the effect of chip breakers.

4) A study of triple rake geometry to determine whether or not further tool life improvements can be obtained would be beneficial.

APPENDICES

APPENDIX I

```
## Pdn    0    3199-AFL                TERMINAL: 65                6 JUN 83 12:29:49                ###### V003 ###
```

```
1STATISTICAL PACKAGE FOR THE SOCIAL SCIENCES  ---  BATCH SYSTEM                6 JUN 83 12:25:38        PAGE     1
  --- U N I V E R S I T Y   O F   V E R M O N T   S P S S ---
 SPSS FOR HARRIS/(VULCAN 10A OR VOS 1.1), RELEASE 9.1, MAY 1, 1982
0                          CURRENT DOCUMENTATION FOR THE SPSS BATCH SYSTEM
 ORDER FROM MCGRAW-HILL:   SPSS, 2ND ED. (PRINCIPAL TEXT)       ORDER FROM SPSS INC.:  SPSS STATISTICAL ALGORITHMS
                           SPSS UPDATE 7-9 (USE W/SPSS, 2ND FOR REL. 7, 8, 9)        KEYWORDS: THE SPSS INC. NEWSLETTER
                           SPSS POCKET GUIDE, RELEASE 9
                           SPSS PRIMER (BRIEF INTRO TO SPSS)
-DEFAULT SPACE ALLOCATION..      ALLOWS FOR..     62 TRANSFORMATIONS
 WORKSPACE      10948 DBLWORDS                    250 RECODE VALUES + LAG VARIABLES
 TRANSPACE       1563 DBLWORDS                   1001 IF/COMPUTE OPERATIONS
```

```
                    1 NUMBERD          YES
                    2 RUN NAME          TOOL LIFE REGR
                    3 FILE NAME        REGR
                    4 VARIABLE LIST     T,D,DV,DFV
                    5 INPUT MEDIUM     CARD
                    6 INPUT FORMAT     FREEFIELD
                    7 N OF CASES            16
                    8 VAR LABELS        T TOOL LIFE/
                    9                   D FEED RATE/
                   10                   DV CUTTING SPEED/
                   11                   DFV  INTERACTION FEED RATE AND CUTTING SPEED/
                   12 REGRESSION          VARIABLE=T,D,DV,DFV/
                   13                     REGRESSION=T WITH D,DV,DFV (1)/
                   14 OPTIONS          1
                   15 STATISTICS       2


  ***** REGRESSION PROBLEM REQUIRES      84 DBLEWORDS WORKSPACE, NOT INCLUDING RESIDUALS *****
```

```
1TOOL LIFE REGR                                                6 JUN 83 12:25:38        PAGE     2
  --- U N I V E R S I T Y   O F   V E R M O N T   S P S S ---

 SPSS NOW CONTAINS A NEW REGRESSION PROCEDURE.
 SEE CHAPTER 3, PAGES 94-121 OF THE SPSS RELEASE 7-9 UPDATE MANUAL.
 NEW REGRESSION WILL REPLACE THIS (OLD) REGRESSION PROCEDURE IN THE NEXT RELEASE.

 TO AVOID PRINTING THIS TEXT, SPECIFY OPTION 20.

 NEW REGRESSION CONTAINS MANY NEW FEATURES, INCLUDING

 - TRUE STEPWISE SELECTION
 - BACKWARD EXCLUSION
 - REGRESSION THROUGH THE ORIGIN
 - MEAN SUBSTITUTION OFMISSING DATA
 - INTERNAL SELECTION FOR CROSS-VALIDATION
 - MANY TYPES OF RESIDUALS, PREDICTED VALUES, AND DISTANCE MEASURES
 - HISTOGRAMS, NORMAL PROBABILITY PLOTS AND OUTLIER TABLES OF RESIDUALS
```

```
REGRESSION      VARIABLES = A TO E/
                REGRESSION = A WITH B,C(2) D,E(1)/
```

```
    NEW REGRESSION  VARIABLES = A TO E/
                    DEPENDENT = A/ENTER B,C/FORWARD D,E/

SAME REQUEST, ABBREVIATED FORM:
    NEW REGRESSION  VAR A TO E/
                    DEP A/ENT B,C/FOR D,E/
```

```
REGRESSION      VARIABLES = A, C, E TO P, R, T TO Z/
                REGRESSION = A (999,3.84,.2)
                           WITH C TO Z/
```

```
    NEW REGRESSION  VAR = A, C, E TO P, R, T TO Z/
                    CRITERIA =  FIN(3.84) TOLERANCE(.2)/
                    DEP = A/STEPWISE/

(THE USER HAS SPECIFIED TRUE STEPWISE IN NEW REGRESSION.)
```

```
REGRESSION      VARIABLES = A TO E/
                REGRESSION = A WITH B TO E RESIDS=0/
OPTIONS         2,11,12
STATISTICS      1,2,4,5,6
```

```
    NEW REGRESSION  VARIABLES = A TO E/MISSING = PAIRWISE/
                    DESCRIPTIVE = MEAN STDDEV COR/
                    DEP = A/STEPWISE/
                    RESIDUALS/CASEWISE = ALL/
                    SCATTER = (*RESID,*PRED)/SAVE = RESID PRED/

DEFAULT CASEWISE PLOT IS OF OUTLIERS ONLY:  CASEWISE/
SCATTERPLOTS OF ANY VAR IN EQUATION:  SCATTER = (A,*RESID)/
```

16 READ INPUT DATA

FILE REGR (CREATED 6 JUN 83 12:25:38)

VARIABLE	MEAN	STANDARD DEV	CASES
T	7.5938	4.9446	16
D	0.3125	0.1261	16
DV	153.7500	42.1703	16
DFV	48.0469	24.0078	16

FILE REGR (CREATED 6 JUN 83 12:25:38)

0* M U L T I P L E R E G R E S S I O N * * * * * * * * * * * * * * * VARIABLE LIST 1
REGRESSION LIST 1

DEPENDENT VARIABLE.. T TOOL LIFE

OVARIABLE(S) ENTERED ON STEP NUMBER 1.. DV CUTTING SPEED

OMULTIPLE R	0.84307	ANALYSIS OF VARIANCE	DF	SUM OF SQUARES	MEAN SQUARE	F
R SQUARE	0.71076	REGRESSION	1.	260.66016	260.66016	34.4027
ADJUSTED R SQUARE	0.69010	RESIDUAL	14.	106.07422	7.57673	
STANDARD ERROR	2.75259					

---------- VARIABLES IN THE EQUATION ----------

VARIABLE	B	BETA	STD ERROR B	F
DV	-0.9885192E-01	-0.84307	0.01685	34.403
(CONSTANT)	22.79223			

---------- VARIABLES NOT IN THE EQUATION ----------

VARIABLE	BETA IN	PARTIAL	TOLERANCE	F
D	-0.16607	-0.30878	1.00000	1.37
DFV	-0.15994	-0.24858	0.69869	0.85

0VARIABLE(S) ENTERED ON STEP NUMBER 2.. D FEED RATE

0MULTIPLE R	0.85927	ANALYSIS OF VARIANCE	DF	SUM OF SQUARES	MEAN SQUARE	F
R SQUARE	0.73834	REGRESSION	2.	270.77386	135.38693	18.3411
ADJUSTED R SQUARE	0.69808	RESIDUAL	13.	95.96052	7.38158	
STANDARD ERROR	2.71691					

VARIABLES IN THE EQUATION

VARIABLE	B	BETA	STD ERROR B	F
DV	-0.98851925-01	-0.84307	0.01663	35.312
D	-6.569217	-0.16607	5.56094	1.370
(CONSTANT)	24.82636			

VARIABLES NOT IN THE EQUATION

VARIABLE	BETA IN	PARTIAL	TOLERANCE	F
DFV	0.48686	0.20420	0.04603	0.52

0VARIABLE(S) ENTERED ON STEP NUMBER 3.. DFV INTERACTION FEED RATE AND CUTTING SPEED

0MULTIPLE R	0.86559	ANALYSIS OF VARIANCE	DF	SUM OF SQUARES	MEAN SQUARE	F
R SQUARE	0.74925	REGRESSION	3.	274.77525	91.59175	11.9520
ADJUSTED R SQUARE	0.68656	RESIDUAL	12.	91.95913	7.66326	
STANDARD ERROR	2.76826					

VARIABLES IN THE EQUATION

VARIABLE	B	BETA	STD ERROR B	F
DV	-0.1301875	-1.11031	0.04656	7.818
D	-21.92630	-0.55939	22.07508	0.987
DFV	0.1002737	0.48686	0.13877	0.522
(CONSTANT)	29.64420			

VARIABLES NOT IN THE EQUATION

VARIABLE	BETA IN	PARTIAL	TOLERANCE	F

MAXIMUM STEP REACHED
0STATISTICS WHICH CANNOT BE COMPUTED ARE PRINTED AS ALL NINES.

--- U N I V E R S I T Y O F V E R M O N T S P S S ---

FILE REGR (CREATED 6 JUN 83 12:25:38)

0* M U L T I P L E R E G R E S S I O N * * * * * * * * * * * * * VARIABLE LIST 1
REGRESSION LIST 1

DEPENDENT VARIABLE.. T TOOL LIFE

0 SUMMARY TABLE

VARIABLE		MULTIPLE R	R SQUARE	RSQ CHANGE	SIMPLE R	B	BETA
DV	CUTTING SPEED	0.84307	0.71076	0.71076	0.84307	-0.1301875	-1.11031
D	FEED RATE	0.85927	0.73834	0.02758	0.16607	-21.92630	-0.55939
DFV	INTERACTION FEED RATE AND CUTTING SPEED	0.86559	0.74925	0.01091	0.57452	0.1002737	0.48686
(CONSTANT)						29.64420	

--- U N I V E R S I T Y O F V E R M O N T S P S S ---

0CPU TIME REQUIRED.. 0.94 SECONDS
ELAPSED WALL TIME.. 5 SECONDS

(CROSS GENERATED)

FORMAT ERRORS IN INPUT
12 CORRECT RECORDS READ
0 ERRORS DETECTED

Pdm 8 3197-AF1 TERMINAL: 65 6 JUN 83 12:31:39 No of Pages 4 ****** V003 ***

```
************************************************************************************************************************************
************************************************************************************************************************************
**********                                                                                                       ****************
** Pdn    8   3177 AH           TERMINAL  57                6 JUN 83 12:55:41                                     ****** V003 ***
**********                                                                                                       ****************
************************************************************************************************************************************
************************************************************************************************************************************
************************************************************************************************************************************

                                                                          6 JUN 83 12:52:39          PAGE     1
1STATISTICAL PACKAGE FOR THE SOCIAL SCIENCES  ---  BATCH SYSTEM.
 --- U N I V E R S I T Y   O F   V E R M O N T   S P S S ---
SPSS FOR HARRIS/(VULCAN 10A OR VOS 1.1), RELEASE 9.1, MAY 1, 1982
                                   CURRENT DOCUMENTATION FOR THE SPSS BATCH SYSTEM
0                                                                 ORDER FROM SPSS INC.:    SPSS STATISTICAL ALGORITHMS
 ORDER FROM MCGRAW-HILL:   SPSS, 2ND ED. (PRINCIPAL TEXT)                                  KEYWORDS: THE SPSS INC. NEWSLETTER
                           SPSS UPDATE 7-9 (USE W/SPSS,2ND FOR REL. 7, 8, 9)
                           SPSS POCKET GUIDE, RELEASE 9
                           SPSS PRIMER (BRIEF INTRO TO SPSS)
-DEFAULT SPACE ALLOCATION .      ALLOWS FOR..    62 TRANSFORMATIONS
 WORKSPACE      10948 DBLWORDS                  250 RECODE VALUES + LAG VARIABLES
 TRANSPACE       1563 DBLWORDS                 1001 IF/COMPUTE OPERATIONS

                1 NUMBERD            YES
                2 RUN NAME           TOOL LIFE REGR
                3 FILE NAME          REGR
                4 VARIABLE LIST       T,D,DV,DFV
                5 INPUT MEDIUM       CARD
                6 INPUT FORMAT       FREEFIELD
                7 N OF CASES              16
                8 VAR LABELS          T TOOL LIFE/
                9                     D FEED RATE/
               10                     DV CUTTING SPEED/
               11                     DFV  INTERACTION FEED RATE AND CUTTING SPEED/
               12 REGRESSION            VARIABLE=T,D,DV,DFV/
               13                       REGRESSION=T WITH D,DV,DFV (1)/
               14 OPTIONS              1
               15 STATISTICS         2

 ***** REGRESSION PROBLEM REQUIRES      84 DBLEWORDS WORKSPACE, NOT INCLUDING RESIDUALS *****

                                                                          6 JUN 83 12:52:39          PAGE     2
1TOOL LIFE REGR
 --- U N I V E R S I T Y   O F   V E R M O N T   S P S S ---

 SPSS NOW CONTAINS A NEW REGRESSION PROCEDURE.
 SEE CHAPTER 3, PAGES 94-121 OF THE SPSS RELEASE 7-9 UPDATE MANUAL.
 NEW REGRESSION WILL REPLACE THIS (OLD) REGRESSION PROCEDURE IN THE NEXT RELEASE.

 TO AVOID PRINTING THIS TEXT, SPECIFY OPTION 20.

 NEW REGRESSION CONTAINS MANY NEW FEATURES, INCLUDING

 - TRUE STEPWISE SELECTION
 - BACKWARD EXCLUSION
 - REGRESSION THROUGH THE ORIGIN
 - MEAN SUBSTITUTION OFMISSING DATA
 - INTERNAL SELECTION FOR CROSS-VALIDATION
 - MANY TYPES OF RESIDUALS, PREDICTED VALUES, AND DISTANCE MEASURES
 - HISTOGRAMS, NORMAL PROBABILITY PLOTS AND OUTLIER TABLES OF RESIDUALS
```

```
REGRESSION      VARIABLES = A TO E/
                REGRESSION = A WITH B,C(3) D,E(1)/
```

```
    NEW REGRESSION  VARIABLES = A TO E/
                    DEPENDENT = A/ENTER B,C/FORWARD D,E/

SAME REQUEST, ABBREVIATED FORM:
    NEW REGRESSION  VAR A TO E/
                    DEP A/ENT B,C/FOR D,E/
```

```
REGRESSION      VARIABLES = A, C, E TO P, R, T TO Z/
                REGRESSION = A (999,3.84,.2)
                        WITH C TO Z/
```

```
    NEW REGRESSION  VAR = A, C, E TO P, R, T TO Z/
                    CRITERIA = FIN(3.84) TOLERANCE(.2)/
                    DEP = A/STEPWISE/

(THE USER HAS SPECIFIED TRUE STEPWISE IN NEW REGRESSION.)
```

```
REGRESSION      VARIABLES = A TO E/
                REGRESSION = A WITH B TO E RESIDS=0/
OPTIONS         2,11,12
STATISTICS      1,2,4,5,6
```

```
    NEW REGRESSION  VARIABLES = A TO E/MISSING = PAIRWISE/
                    DESCRIPTIVE = MEAN STDDEV COR/
                    DEP = A/STEPWISE/
                    RESIDUALS/CASEWISE = ALL/
                    SCATTER = (*RESID,*PRED)/SAVE = RESID PRED/

DEFAULT CASEWISE PLOT IS OF OUTLIERS ONLY:  CASEWISE/
SCATTERPLOTS OF ANY VAR IN EQUATION:  SCATTER = (A,*RESID)/
```

16 READ INPUT DATA

1TOOL LIFE REGR
---- U N I V E R S I T Y O F V E R M O N T S P S S ---
FILE REGR (CREATED 6 JUN 83 12:52:39)

VARIABLE	MEAN	STANDARD DEV	CASES
T	3.0837	3.6071	16
D	0.3125	0.1261	16
DV	153.7500	42.1703	16
DFV	48.0462	24.0079	16

1TOOL LIFE REGR
---- U N I V E R S I T Y O F V E R M O N T S P S S ---
FILE REGR (CREATED 6 JUN 83 12:52:39)
0* M U L T I P L E R E G R E S S I O N * * * * * * * * * * * * * * VARIABLE LIST 1
REGRESSION LIST 1

DEPENDENT VARIABLE.. T TOOL LIFE
0VARIABLE(S) ENTERED ON STEP NUMBER 1.. DV CUTTING SPEED

0MULTIPLE R	0.73946
R SQUARE	0.54680
ADJUSTED R SQUARE	0.51443
STANDARD ERROR	2.51354

ANALYSIS OF VARIANCE	DF	SUM OF SQUARES	MEAN SQUARE	F
REGRESSION	1.	106.71896	106.71896	16.8916
RESIDUAL	14.	88.45002	6.31786	

---------- VARIABLES IN THE EQUATION ----------

VARIABLE	B	BETA	STD ERROR B	F
DV	-0.6325117E-01	-0.73946	0.01539	16.892
(CONSTANT)	12.80862			

---------- VARIABLES NOT IN THE EQUATION ----------

VARIABLE	BETA IN	PARTIAL	TOLERANCE	F
D	-0.39434	-0.58577	1.00000	6.79
DFV	-0.38275	-0.47524	0.69871	3.79

* *

OVARIABLE(S) ENTERED ON STEP NUMBER [illegible] D FEED RATE

			ANALYSIS OF VARIANCE	DF	SUM OF SQUARES	MEAN SQUARE	F
OMULTIPLE R	[illegible]		REGRESSION	2.	137.06852	68.53426	15.3345
R SQUARE	[illegible]		RESIDUAL	13.	58.10045	4.46927	
ADJUSTED R SQUARE	[illegible]						
STANDARD ERROR	[illegible]						

------------------ VARIABLES IN THE EQUATION ------------------

VARIABLE	B	BETA	STD ERROR B	F
DV	-0.6325117E-01	-0.73946	0.01294	23.878
D	-11.27567	-0.39434	4.32705	6.791
(CONSTANT)	16.3[illegible]			

------------- VARIABLES NOT IN THE EQUATION -------------

VARIABLE	BETA IN	PARTIAL	TOLERANCE	F
DFV	1.11120	0.43696	0.04603	2.83

* *

OVARIABLE(S) ENTERED ON STEP NUMBER 3.. DFV INTERACTION FEED RATE AND CUTTING SPEED

			ANALYSIS OF VARIANCE	DF	SUM OF SQUARES	MEAN SQUARE	F
OMULTIPLE R	0.87129		REGRESSION	3.	148.16186	49.38729	12.6076
R SQUARE	0.75915		RESIDUAL	12.	47.00712	3.91726	
ADJUSTED R SQUARE	0.69893						
STANDARD ERROR	1.97921						

------------------ VARIABLES IN THE EQUATION ------------------

VARIABLE	B	BETA	STD ERROR B	F
DV	-0.1154231	-1.34940	0.03329	12.024
D	-36.94556	-1.29206	15.78265	5.480
DFV	0.1669545	1.11120	0.09921	2.832
(CONSTANT)	24.35400			

------------- VARIABLES NOT IN THE EQUATION -------------

VARIABLE	BETA IN	PARTIAL	TOLERANCE	F

MAXIMUM STEP REACHED

OSTATISTICS WHICH CANNOT BE COMPUTED ARE PRINTED AS ALL NINES.

1TOOL LIFE REGR 6 JUN 83 12:52:39 PAGE 5

--- U N I V E R S I T Y O F V E R M O N T S P S S ---

FILE REGR (CREATED 6 JUN 83 12:52:39)

0* * * * * * * * * * * * * * * * * * * M U L T I P L E R E G R E S S I O N * * * * * * * * * * * * * VARIABLE LIST 1
REGRESSION LIST 1

DEPENDENT VARIABLE.. T TOOL LIFE

0

SUMMARY TABLE

VARIABLE		MULTIPLE R	R SQUARE	RSQ CHANGE	SIMPLE R	B	BETA
DV	CUTTING SPEED	0.73946	0.54680	0.54680	0.73946	-0.1154231	-1.34940
D	FEED RATE	0.83804	0.70231	0.15550	0.39434	-36.94556	-1.29206
DFV	INTERACTION FEED RATE AND CUTTING SPEED	0.87129	0.75915	0.05684	0.67332	0.1669545	1.11120
(CONSTANT)						24.35400	

1TOOL LIFE REGR 6 JUN 83 12:52:39 PAGE 6

--- U N I V E R S I T Y O F V E R M O N T S P S S ---

OCPU TIME REQUIRED.. 0.95 SECONDS

ELAPSED WALL TIME.. 4 SECONDS

```
1               17 FINISH          (SPSS GENERATED)
            NORMAL END OF SPSS RUN.
             17 COMMAND RECORDS READ
              0 ERRORS DETECTED

** Pdn    8    3199 AFL          TERMINAL: 57          6 JUN 83 12:57:27          No of Pages       4          ****** V003 ***
```

```
## Pdn     0    3199-AFI                TERMINAL: 75          17 MAY 83 12:02:18                    ###### V003 ###
```

```
1 1STATISTICAL PACKAGE FOR THE SOCIAL SCIENCES  ---  BATCH SYSTEM              17 MAY 83 11:59:58        PAGE     1
2    --- U N I V E R S I T Y   O F   V E R M O N T   S P S S ---
3  SPSS FOR HARRIS/(VULCAN 10A OR VOS 1.1), RELEASE 9.1, MAY 1, 1982
4 0                          CURRENT DOCUMENTATION FOR THE SPSS BATCH SYSTEM
5  ORDER FROM MCGRAW-HILL:  SPSS, 2ND ED. (PRINCIPAL TEXT)       ORDER FROM SPSS INC.:  SPSS STATISTICAL ALGORITHMS
6                           SPSS UPDATE 7-9 (USE W/SPSS,2ND FOR REL. 7, 8, 9)           KEYWORDS: THE SPSS INC. NEWSLETTER
7                           SPSS POCKET GUIDE, RELEASE 9
8                           SPSS PRIMER (BRIEF INTRO TO SPSS)
9 -DEFAULT SPACE ALLOCATION.      ALLOWS FOR..     62 TRANSFORMATIONS
10  WORKSPACE      10948 DBLWORDS                   250 RECODE VALUES + LAG VARIABLES
11  TRANSPACE       1563 DBLWORDS                  1001 IF/COMPUTE OPERATIONS
12
13                    1 NUMBERD         YES
14                    2 RUN NAME           MAIN CUTTING  FORCE REGR
15                    3 FILE NAME       REGR
16                    4 VARIABLE LIST   F,S,SS,SQ
17                    5 INPUT MEDIUM    CARD
18                    6 INPUT FORMAT    FREEFIELD
19                    7 N OF CASES      4
20                    8 VAR LABELS           F MAIN CUTTIN  FORCE/
21                    9                 S SPEED/
22                   10                 SS SPEED SQUARE/
23                   11                 SQ SPEED QUPE/
24                   12 REGRESSION       VARIABLES=F,S,SS,SQ /
25                   13                  REGRESSION=F WITH S,SS,SQ(2)/
26                   14 OPTIONS        1
27                   15 STATISTICS     2
28
29
30   ***** REGRESSION PROBLEM REQUIRES     84 DBLEWORDS WORKSPACE, NOT INCLUDING RESIDUALS *****
31
32
33 1MAIN CUTTING  FORCE REGR                                          17 MAY 83 11:59:58        PAGE     2
34    --- U N I V E R S I T Y   O F   V E R M O N T   S P S S ---
35
36  SPSS NOW CONTAINS A NEW REGRESSION PROCEDURE.
37  SEE CHAPTER 3, PAGES 94-121 OF THE SPSS RELEASE 7-9 UPDATE MANUAL.
38  NEW REGRESSION WILL REPLACE THIS (OLD) REGRESSION PROCEDURE IN THE NEXT RELEASE.
39
40  TO AVOID PRINTING THIS TEXT, SPECIFY OPTION 20.
41
42  NEW REGRESSION CONTAINS MANY NEW FEATURES, INCLUDING
43
44   - TRUE STEPWISE SELECTION
45   - BACKWARD EXCLUSION
46   - REGRESSION THROUGH THE ORIGIN
47   - MEAN SUBSTITUTION OFMISSING DATA
48   - INTERNAL SELECTION FOR CROSS-VALIDATION
49   - MANY TYPES OF RESIDUALS, PREDICTED VALUES, AND DISTANCE MEASURES
50   - HISTOGRAMS, NORMAL PROBABILITY PLOTS AND OUTLIER TABLES OF RESIDUALS
51
```

```
52
53  THE SYNTAX OF NEW REGRESSION DIFFERS FROM (OLD) REGRESSION.  MOST NOTABLY, ALL
54  OPTIONS AND STATISTICS ARE REQUESTED VIA KEYWORDS ON THE NEW REGRESSION CONTROL CARD.
55  KEYWORDS IN NEW REGRESSION MAY BE ABBREVIATED TO THE FIRST THREE CHARACTERS (OR USE
56  MORE FOR READABILITY).  EQUALS SIGNS (=) ARE OPTIONAL.
57  HERE ARE EXAMPLES SHOWING COMPARABLE REQUESTS FROM (OLD) REGRESSION AND NEW REGRESSION:
58
59                      OLD                                          I                          NEW
60                                                                   I
61  REGRESSION      VARIABLES = A TO E/                              I    NEW REGRESSION  VARIABLES = A TO E/
62                  REGRESSION = A WITH B,C(2) D,E(1)/               I                    DEPENDENT = A/ENTER B,C/FORWARD D,E/
63                                                                   I
64                                                                   I  SAME REQUEST, ABBREVIATED FORM:
65                                                                   I    NEW REGRESSION  VAR A TO E/
66                                                                   I                    DEP A/ENT B,C/FOR D,E/
67                                                                   I
68  -------------------------------------------------------------------I-------------------------------------------------------------------
69                                                                   I
70  REGRESSION      VARIABLES = A, C, E TO P, R, T TO Z/             I    NEW REGRESSION  VAR = A, C, E TO P, R, T TO Z/
71                  REGRESSION = A (999,3.84,.2)                     I                    CRITERIA =  FIN(3.84) TOLERANCE(.2)/
72                             WITH C TO Z/                          I                    DEP = A/STEPWISE/
73                                                                   I
74                                                                   I  (THE USER HAS SPECIFIED TRUE STEPWISE IN NEW REGRESSION.)
75                                                                   I
76  -------------------------------------------------------------------I-------------------------------------------------------------------
77                                                                   I
78  REGRESSION      VARIABLES = A TO E/                              I    NEW REGRESSION  VARIABLES = A TO E/MISSING = PAIRWISE/
79                  REGRESSION = A WITH B TO E RESIDS=0/             I                    DESCRIPTIVE = MEAN STDDEV COR/
80  OPTIONS         2,11,12                                          I                    DEP = A/STEPWISE/
81  STATISTICS      1,2,4,5,6                                        I                    RESIDUALS/CASEWISE = ALL/
82                                                                   I                    SCATTER = (*RESID,*PRED)/SAVE = RESID PRED/
83                                                                   I
84                                                                   I  DEFAULT CASEWISE PLOT IS OF OUTLIERS ONLY:  CASEWISE/
85                                                                   I  SCATTERPLOTS OF ANY VAR IN EQUATION:  SCATTER = (A,*RESID)/
86                    16 READ INPUT DATA
87 1MAIN CUTTING  FORCE REGR                                                          17 MAY 83 11:59:58        PAGE     3
88   --- U N I V E R S I T Y   O F   V E R M O N T   S P S S ---
89  FILE     REGR   (CREATED  17 MAY 83 11:59:58)
90
91
92  VARIABLE          MEAN      STANDARD DEV     CASES
93
94    F           2343.7500          887.9694         4
95    S            153.7500           47.1478         4
96    SS         25306.2500        13516.9704         4
97    SQ       4365843.7500      3076935.6939         4
98 1MAIN CUTTING  FORCE REGR                                                          17 MAY 83 11:59:58        PAGE     4
99   --- U N I V E R S I T Y   O F   V E R M O N T   S P S S ---
100  FILE     REGR   (CREATED  17 MAY 83 11:59:58)
101 O* * * * * * * * * * * * * * * * * * * * * * * * *  M U L T I P L E   R E G R E S S I O N  * * * * * * * * * * * * *    VARIABLE LIS
102                                                                                                                        REGRESSION LIS
103  DEPENDENT VARIABLE..      F        MAIN CUTTIN  FORCE
104 OVARIABLE(S) ENTERED ON STEP NUMBER  1..      SQ       SPEED QUPE
105                                               S        SPEED
106                                               SS       SPEED SQUARE
107  ****** WARNING *****   SS     HAS TOLERANCE  0.00002.  IT HAS BEEN DROPPED.  THE SOLUTION IS NOT UNIQUE.
108
109 OMULTIPLE R           0.88577                ANALYSIS OF VARIANCE    DF      SUM OF SQUARES        MEAN SQUARE              F
110  R SQUARE             0.78459                REGRESSION               2.      1855921.38640        927960.69321          1.
111  ADJUSTED R SQUARE    0.35377                RESIDUAL                 1.       509547.36358        509547.36358
```

```
 112  STANDARD ERROR     713.62586
 113
 114
 115  ---------- VARIABLES IN THE EQUATION ----------                    ---------- VARIABLES NOT IN THE EQUATION ----------
 116
 117  VARIABLE            B          BETA      STD ERROR B        F      VARIABLE      BETA IN     PARTIAL    TOLERANCE
 118
 119    SQ        -0.3829818E-03   -1.32708      0.00061       0.388     SS         -117.54604   -1.00000     0.00002     9999
 120    S           8.624983        0.45795     40.11933       0.046
 121  (CONSTANT)    2689.698
 122
 123
 124  F--LEVEL OR TOLERANCE-LEVEL INSUFFICIENT FOR FURTHER COMPUTATION
 125 OSTATISTICS WHICH CANNOT BE COMPUTED ARE PRINTED AS ALL NINES.
 126 1MAIN CUTTING  FORCE REGR                                  17 MAY 83 11:59:58        PAGE     5
 127   --- U N I V E R S I T Y   O F   V E R M O N T   S P S S ---
 128  FILE     REGR    (CREATED  17 MAY 83 11:59:58)
 129 0* * * * * * * * * * * * * * * * * * * * M U L T I P L E   R E G R E S S I O N * * * * * * * * * * * * *    VARIABLE LIS
 130                                                                                                            REGRESSION LIS
 131  DEPENDENT VARIABLE..      F        MAIN CUTTIN  FORCE
 132 0                                                SUMMARY TABLE
 133
 134  VARIABLE                                    MULTIPLE R  R SQUARE  RSQ CHANGE   SIMPLE R          B                  BE
 135
 136    SQ        SPEED QUPE                       0.88013    0.77463    0.77463     0.88013    -0.3829818E-03          -1.3
 137    S         SPEED                            0.88577    0.78459    0.00996     0.83725      8.624983              0.4
 138  (CONSTANT)                                                                                  2689.698
 139 1MAIN CUTTING  FORCE REGR                                  17 MAY 83 11:59:58        PAGE     6
 140   --- U N I V E R S I T Y   O F   V E R M O N T   S P S S ---
 141 OCPU TIME REQUIRED..     0.63 SECONDS
 142  ELAPSED WALL TIME..       4 SECONDS
 143
 144
 145
 146                 17 FINISH          (SPSS GENERATED)
 147 1           NORMAL END OF SPSS RUN.
 148              17 COMMAND RECORDS READ
 149               0 ERRORS DETECTED
 150
```

```
** Pdn     8    3199-AIT                TERMINAL:  65              16 MAY 83 12:50:40                                  ****************
**                                                                                                                    ****** V003 ***
**                                                                                                                    ****************
```

```
1 1STATISTICAL PACKAGE FOR THE SOCIAL SCIENCES  ---  BATCH SYSTEM              16 MAY 83 12:49:47         PAGE     1
2    --- U N I V E R S I T Y    O F    V E R M O N T    S P S S ---
3  SPSS FOR HARRIS/(VULCAN 10A OR VOS 1.1), RELEASE 9.1, MAY 1, 1982
4 0                          CURRENT DOCUMENTATION FOR THE SPSS BATCH SYSTEM
5  ORDER FROM MCGRAW-HILL:  SPSS, 2ND ED. (PRINCIPAL TEXT)       ORDER FROM SPSS INC.:  SPSS STATISTICAL ALGORITHMS
6                           SPSS UPDATE 7-9 (USE W/SPSS,2ND FOR REL. 7, 8, 9)          KEYWORDS:  THE SPSS INC. NEWSLETTER
7                           SPSS POCKET GUIDE, RELEASE 9
8                           SPSS PRIMER (BRIEF INTRO TO SPSS)
9 -DEFAULT SPACE ALLOCATION.      ALLOWS FOR..     62 TRANSFORMATIONS
10   WORKSPACE      10948 DBLWORDS                  250 RECODE VALUES + LAG VARIABLES
11   TRANSPACE       1563 DBLWORDS                 1001 IF/COMPUTE OPERATIONS
12
13                     1 NUMBERD          YES
14                     2 RUN NAME            RADIAL FORCE REGR
15                     3 FILE NAME        REGR
16                     4 VARIABLE LIST    F,S,SS,SQ
17                     5 INPUT MEDIUM     CARD
18                     6 INPUT FORMAT     FREEFIELD
19                     7 N OF CASES       4
20                     8 VAR LABELS          F RADIAL FORCE/
21                     9                  S SPEED/
22                    10                  SS SPEED SQUARE/
23                    11                  SQ SPEED QUPE/
24                    12 REGRESSION        VARIABLES=F,S,SS,SQ /
25                    13                   REGRESSION=F WITH S,SS,SQ(1)/
26                    14 OPTIONS         1
27                    15 STATISTICS      2
28
29
30    ***** REGRESSION PROBLEM REQUIRES      84 DBLEWORDS WORKSPACE,  NOT INCLUDING RESIDUALS *****
31
32
33 1RADIAL FORCE REGR                                                          16 MAY 83 12:49:47         PAGE     2
34    --- U N I V E R S I T Y    O F    V E R M O N T    S P S S ---
35
36  SPSS NOW CONTAINS A NEW REGRESSION PROCEDURE.
37  SEE CHAPTER 3, PAGES 94-121 OF THE SPSS RELEASE 7-9 UPDATE MANUAL.
38  NEW REGRESSION WILL REPLACE THIS (OLD) REGRESSION PROCEDURE IN THE NEXT RELEASE.
39
40  TO AVOID PRINTING THIS TEXT, SPECIFY OPTION 20.
41
42  NEW REGRESSION CONTAINS MANY NEW FEATURES,  INCLUDING
43
44  - TRUE STEPWISE SELECTION
45  - BACKWARD EXCLUSION
46  - REGRESSION THROUGH THE ORIGIN
47  - MEAN SUBSTITUTION OFMISSING DATA
48  - INTERNAL SELECTION FOR CROSS-VALIDATION
49  - MANY TYPES OF RESIDUALS, PREDICTED VALUES, AND DISTANCE MEASURES
50  - HISTOGRAMS, NORMAL PROBABILITY PLOTS AND OUTLIER TABLES OF RESIDUALS
51
```

```
 52
 53  THE SYNTAX OF NEW REGRESSION DIFFERS FROM (OLD) REGRESSION.  MOST NOTABLY, ALL
 54  OPTIONS AND STATISTICS ARE REQUESTED VIA KEYWORDS ON THE NEW REGRESSION CONTROL CARD.
 55  KEYWORDS IN NEW REGRESSION MAY BE ABBREVIATED TO THE FIRST THREE CHARACTERS (OR USE
 56  MORE FOR READABILITY).  EQUALS SIGNS (=) ARE OPTIONAL.
 57  HERE ARE EXAMPLES SHOWING COMPARABLE REQUESTS FROM (OLD) REGRESSION AND NEW REGRESSION:
 58
 59                      OLD                                          I                        NEW
 60                                                                   I
 61  REGRESSION      VARIABLES = A TO E/                              I    NEW REGRESSION  VARIABLES = A TO E/
 62                  REGRESSION = A WITH B,C(2) D,E(1)/               I                    DEPENDENT = A/ENTER B,C/FORWARD D,E/
 63                                                                   I
 64                                                                   I  SAME REQUEST, ABBREVIATED FORM:
 65                                                                   I    NEW REGRESSION  VAR A TO E/
 66                                                                   I                    DEP A/ENT B,C/FOR D,E/
 67                                                                   I
 68  ---------------------------------------------------------------- I-------------------------------------------------------------------
 69                                                                   I
 70  REGRESSION      VARIABLES = A, C, E TO P, R, T TO Z/             I    NEW REGRESSION  VAR = A, C, E TO P, R, T TO Z/
 71                  REGRESSION = A (999,3.84,.2)                     I                    CRITERIA =  FIN(3.84) TOLERANCE(.2)/
 72                               WITH C TO Z/                        I                    DEP = A/STEPWISE/
 73                                                                   I
 74                                                                   I  (THE USER HAS SPECIFIED TRUE STEPWISE IN NEW REGRESSION.)
 75                                                                   I
 76  ---------------------------------------------------------------- I-------------------------------------------------------------------
 77                                                                   I
 78  REGRESSION      VARIABLES = A TO E/                              I    NEW REGRESSION  VARIABLES = A TO E/MISSING = PAIRWISE/
 79                  REGRESSION = A WITH B TO E RESIDS=O/             I                    DESCRIPTIVE = MEAN STDDEV COR/
 80  OPTIONS         2,11,12                                          I                    DEP = A/STEPWISE/
 81  STATISTICS      1,2,4,5,6                                        I                    RESIDUALS/CASEWISE = ALL/
 82                                                                   I                    SCATTER = (*RESID,*PRED)/SAVE = RESID PRED/
 83                                                                   I
 84                                                                   I  DEFAULT CASEWISE PLOT IS OF OUTLIERS ONLY:  CASEWISE/
 85                                                                   I  SCATTERPLOTS OF ANY VAR IN EQUATION:  SCATTER = (A,*RESID)/
 86                    16 READ INPUT DATA
 87 1RADIAL FORCE REGR                                                                16 MAY 83 12:49:47        PAGE     3
 88   --- U N I V E R S I T Y   O F   V E R M O N T   S P S S ---
 89  FILE     REGR    (CREATED  16 MAY 83 12:49:47)
 90
 91
 92  VARIABLE            MEAN      STANDARD DEV      CASES
 93
 94     F             3125.0000        1069.6573          4
 95     S              153.7500          47.1478          4
 96     SS           25306.2500       13516.9704          4
 97     SQ         4365843.7500     3076935.6939          4
 98 1RADIAL FORCE REGR                                                                16 MAY 83 12:49:47        PAGE     4
 99   --- U N I V E R S I T Y   O F   V E R M O N T   S P S S ---
100  FILE     REGR    (CREATED  16 MAY 83 12:49:47)
101 0* * * * * * * * * * * * * * * * * * * * * * * * * * * * M U L T I P L E   R E G R E S S I O N  * * * * * * * * * * * * * *    VARIABLE LIS
102                                                                                                                          REGRESSION LIS
103  DEPENDENT VARIABLE..        F        RADIAL FORCE
104 OVARIABLE(S) ENTERED ON STEP NUMBER  1..       SQ        SPEED QUPE
105
106 OMULTIPLE R           0.69384                  ANALYSIS OF VARIANCE    DF       SUM OF SQUARES         MEAN SQUARE              F
107  R SQUARE             0.79894                  REGRESSION               1.       2742368.25250       2742368.25250           7.
108  ADJUSTED R SQUARE    0.69841                  RESIDUAL                 2.        690131.74744        345065.87372
109  STANDARD ERROR     587.42308
110
111
```

```
112  ---------- VARIABLES IN THE EQUATION ----------                    ---------- VARIABLES NOT IN THE EQUATION ----------
113
114  VARIABLE            B          BETA      STD ERROR B        F      VARIABLE     BETA IN     PARTIAL    TOLERANCE
115
116    SQ          0.3107305E-03    0.87384       0.00011     7.947      S          -0.39818    -0.19348     0.04747
117  (CONSTANT)     1768.399                                             SS          -0.65315    -0.15753     0.01170
118
119
120
121  * * * * * * * * * * * * * * * * * * * * * * * * * * * * * * * * * * * * * * * * * * * * * * * * * * * * * * * * * * * * * * * * *
122 0VARIABLE(S) ENTERED ON STEP NUMBER  2..       S        SPEED
123
124 0MULTIPLE R            0.89804                    ANALYSIS OF VARIANCE    DF       SUM OF SQUARES          MEAN SQUARE              F
125  R SQUARE              0.80647                    REGRESSION               2.      2768203.36870      1384101.68430              2.
126  ADJUSTED R SQUARE     0.41941                    RESIDUAL                 1.       664296.63127       664296.63127
127  STANDARD ERROR      815.04394
128
129
130  ---------- VARIABLES IN THE EQUATION ----------                    ---------- VARIABLES NOT IN THE EQUATION ----------
131
132  VARIABLE            B          BETA      STD ERROR B        F      VARIABLE     BETA IN     PARTIAL    TOLERANCE
133
134    SQ          0.4458284E-03    1.28245       0.00070     0.403      SS         111.41665    1.00000     0.00002     9999
135    S           -9.033719       -0.39818      45.80811     0.039
136  (CONSTANT)     2567.517
137
138
139  F-LEVEL OR TOLERANCE-LEVEL INSUFFICIENT FOR FURTHER COMPUTATION
140 0STATISTICS WHICH CANNOT BE COMPUTED ARE PRINTED AS ALL NINES.
141 1RADIAL FORCE REGR                                    16 MAY 83 12:49:47        PAGE     5
142    --- U N I V E R S I T Y   O F   V E R M O N T   S P S S ---
143  FILE      REGR    (CREATED  16 MAY 83 12:49:47)
144 0* * * * * * * * * * * * * * * * * * * * * * * * * M U L T I P L E   R E G R E S S I O N * * * * * * * * * * * * *    VARIABLE LIS
145                                                                                                                    REGRESSION LIS
146  DEPENDENT VARIABLE..       F        RADIAL FORCE
147 0                                                  SUMMARY TABLE
148
149  VARIABLE                                        MULTIPLE R   R SQUARE   RSQ CHANGE   SIMPLE R          B                BE
150
151    SQ        SPEED QUPE                          0.89384     0.79894     0.79894     0.89384     0.4458284E-03          1.2
152    S         SPEED                               0.89804     0.80647     0.00753     0.85346     -9.033719             -0.3
153  (CONSTANT)                                                                                       2567.517
154 1RADIAL FORCE REGR                                    16 MAY 83 12:49:47        PAGE     6
155    --- U N I V E R S I T Y   O F   V E R M O N T   S P S S ---
156 0CPU TIME REQUIRED..     0.68 SECONDS
157  ELAPSED WALL TIME..       3 SECONDS
158
159
160
161                  17 FINISH          (SPSS GENERATED)
162 1           NORMAL END OF SPSS RUN.
163              17 COMMAND RECORDS READ
164               0 ERRORS DETECTED
165
```

```
** Pdn     8    3199-AFL                TERMINAL:  75              17 MAY 83 12:29:32                                  ****** V003 ***

1 1STATISTICAL PACKAGE FOR THE SOCIAL SCIENCES  ---  BATCH SYSTEM              17 MAY 83 12:28:44        PAGE     1
2   --- U N I V E R S I T Y   O F   V E R M O N T   S P S S ---
3  SPSS FOR HARRIS/(VULCAN 10A OR VOS 1.1), RELEASE 9.1, MAY 1, 1982
4 0                              CURRENT DOCUMENTATION FOR THE SPSS BATCH SYSTEM
5  ORDER FROM MCGRAW-HILL:   SPSS, 2ND ED. (PRINCIPAL TEXT)       ORDER FROM SPSS INC.:  SPSS STATISTICAL ALGORITHMS
6                            SPSS UPDATE 7-9 (USE W/SPSS,2ND FOR REL. 7, 8, 9)          KEYWORDS:  THE SPSS INC. NEWSLETTER
7                            SPSS POCKET GUIDE, RELEASE 9
8                            SPSS PRIMER (BRIEF INTRO TO SPSS)
9 -DEFAULT SPACE ALLOCATION..      ALLOWS FOR..     62 TRANSFORMATIONS
10  WORKSPACE      10948 DBLWORDS                    250 RECODE VALUES + LAG VARIABLES
11  TRANSPACE       1563 DBLWORDS                   1001 IF/COMPUTE OPERATIONS
12
13                     1 NUMBERD         YES
14                     2 RUN NAME        FEED FORCE REGR
15                     3 FILE NAME       REGR
16                     4 VARIABLE LIST   F,S,SS,SQ
17                     5 INPUT MEDIUM    CARD
18                     6 INPUT FORMAT    FREEFIELD
19                     7 N OF CASES      4
20                     8 VAR LABELS      F FEED FORCE/
21                     9                 S SPEED/
22                    10                 SS SPEED SQUARE/
23                    11                 SQ SPEED QUPE/
24                    12 REGRESSION       VARIABLES=F,S,SS,SQ /
25                    13                  REGRESSION=F WITH S,SS,SQ (1)/
26                    14 OPTIONS        1
27                    15 STATISTICS     2
28
29
30   ***** REGRESSION PROBLEM REQUIRES     84 DBLEWORDS WORKSPACE, NOT INCLUDING RESIDUALS *****
31
32
33 1FEED FORCE REGR                                                    17 MAY 83 12:28:44        PAGE     2
34   --- U N I V E R S I T Y   O F   V E R M O N T   S P S S ---
35
36  SPSS NOW CONTAINS A NEW REGRESSION PROCEDURE.
37  SEE CHAPTER 3, PAGES 94-121 OF THE SPSS RELEASE 7-9 UPDATE MANUAL.
38  NEW REGRESSION WILL REPLACE THIS (OLD) REGRESSION PROCEDURE IN THE NEXT RELEASE.
39
40  TO AVOID PRINTING THIS TEXT, SPECIFY OPTION 20.
41
42  NEW REGRESSION CONTAINS MANY NEW FEATURES, INCLUDING
43
44  - TRUE STEPWISE SELECTION
45  - BACKWARD EXCLUSION
46  - REGRESSION THROUGH THE ORIGIN
47  - MEAN SUBSTITUTION OFMISSING DATA
48  - INTERNAL SELECTION FOR CROSS-VALIDATION
49  - MANY TYPES OF RESIDUALS, PREDICTED VALUES, AND DISTANCE MEASURES
50  - HISTOGRAMS, NORMAL PROBABILITY PLOTS AND OUTLIER TABLES OF RESIDUALS
51
```

```
 THE SYNTAX OF NEW REGRESSION DIFFERS FROM (OLD) REGRESSION.  MOST NOTABLY, ALL
 OPTIONS AND STATISTICS ARE REQUESTED VIA KEYWORDS ON THE NEW REGRESSION CONTROL CARD.
 KEYWORDS IN NEW REGRESSION MAY BE ABBREVIATED TO THE FIRST THREE CHARACTERS (OR USE
 MORE FOR READABILITY)   EQUALS SIGNS (=) ARE OPTIONAL.
 HERE ARE EXAMPLES SHOWING COMPARABLE REQUESTS FROM (OLD) REGRESSION AND NEW REGRESSION:

                      OLD                                          I                        NEW
                                                                   I
 REGRESSION      VARIABLES = A TO E/                               I    NEW REGRESSION  VARIABLES = A TO E/
                 REGRESSION = A WITH B,C(2) D,E(1)/                I                    DEPENDENT = A/ENTER B,C/FORWARD D,E/
                                                                   I
                                                                   I  SAME REQUEST, ABBREVIATED FORM:
                                                                   I    NEW REGRESSION  VAR A TO E/
                                                                   I                    DEP A/ENT B,C/FOR D,E/
                                                                   I
-------------------------------------------------------------------I-------------------------------------------------------------------
                                                                   I
 REGRESSION      VARIABLES = A, C, E TO P, R, T TO Z/              I    NEW REGRESSION  VAR = A, C, E TO P, R, T TO Z/
                 REGRESSION = A (999,3.84,.2)                      I                    CRITERIA =  FIN(3.84) TOLERANCE(.2)/
                              WITH C TO Z/                         I                    DEP = A/STEPWISE/
                                                                   I
                                                                   I  (THE USER HAS SPECIFIED TRUE STEPWISE IN NEW REGRESSION.)
                                                                   I
-------------------------------------------------------------------I-------------------------------------------------------------------
                                                                   I
 REGRESSION      VARIABLES = A TO E/                               I    NEW REGRESSION  VARIABLES = A TO E/MISSING = PAIRWISE/
                 REGRESSION = A WITH B TO E RESIDS=O/              I                    DESCRIPTIVE = MEAN STDDEV COR/
 OPTIONS         2,11,12                                           I                    DEP = A/STEPWISE/
 STATISTICS      1,2,4,5,6                                         I                    RESIDUALS/CASEWISE = ALL/
                                                                   I                    SCATTER = (*RESID,*PRED)/SAVE = RESID PRED/
                                                                   I
                                                                   I  DEFAULT CASEWISE PLOT IS OF OUTLIERS ONLY:  CASEWISE/
                                                                   I  SCATTERPLOTS OF ANY VAR IN EQUATION:  SCATTER = (A,*RESID)/
                    16 READ INPUT DATA
1FEED FORCE REGR                                                                    17 MAY 83 12:28:44          PAGE     3
   --- U N I V E R S I T Y   O F   V E R M O N T   S P S S ---
 FILE     REGR   (CREATED  17 MAY 83 12:28:44)


 VARIABLE            MEAN       STANDARD DEV      CASES

    F             2556.2500          96.5553          4
    S              153.7500          47.1478          4
    SS           25306.2500       13516.9704          4
    SQ         4365843.7500     3076935.6939          4
1FEED FORCE REGR                                                                    17 MAY 83 12:28:44          PAGE     4
   --- U N I V E R S I T Y   O F   V E R M O N T   S P S S ---
 FILE     REGR   (CREATED  17 MAY 83 12:28:44)
0* * * * * * * * * * * * * * * * * * * * * * * * *  M U L T I P L E   R E G R E S S I O N  * * * * * * * * * * * * * *    VARIABLE LIS
                                                                                                                        REGRESSION LIS

 DEPENDENT VARIABLE..       F         FEED FORCE
OVARIABLE(S) ENTERED ON STEP NUMBER  1..       SQ        SPEED QUPE

OMULTIPLE R           0.56512                    ANALYSIS OF VARIANCE    DF       SUM OF SQUARES         MEAN SQUARE              F
 R SQUARE             0.31935                    REGRESSION               1.         8931.95934          8931.95934             0.
 ADJUSTED R SQUARE   -0.02097                    RESIDUAL                 2.        19036.79066          9518.39533
 STANDARD ERROR      97.56226
```

```
 ------------------- VARIABLES IN THE EQUATION -------------------                    ------------- VARIABLES NOT IN THE EQUATION ---------

 VARIABLE              B              BETA      STD ERROR B          F                VARIABLE       BETA IN      PARTIAL    TOLERANCE

   SQ        -0.1773349E-04     -0.56512        0.00002           0.938                 S            3.76150      0.99339     0.04747         7
 (CONSTANT)    2633.672                                                                 SS           7.60499      0.99692     0.01170        16



* * * * * * * * * * * * * * * * * * * * * * * * * * * * * * * * * * * * * * * * * * * * * * * * * * * * * * * * * * * * * * * * * * * * *
OVARIABLE(S) ENTERED ON STEP NUMBER  2..       SS        SPEED SQUARE

OMULTIPLE R            0.99790                          ANALYSIS OF VARIANCE    DF      SUM OF SQUARES         MEAN SQUARE             F
 R SQUARE              0.99581                          REGRESSION              2.        27851.48430          13925.74215           118.
 ADJUSTED R SQUARE     0.98742                          RESIDUAL                1.          117.26570            117.26570
 STANDARD ERROR       10.82893


 ------------------- VARIABLES IN THE EQUATION -------------------                    ------------- VARIABLES NOT IN THE EQUATION ---------

 VARIABLE              B              BETA      STD ERROR B          F                VARIABLE       BETA IN      PARTIAL    TOLERANCE

   SQ        -0.2549808E-03     -8.12550        0.00002         184.180                 S           -8.14004     -1.00000     0.00006      9999
   SS         0.5432442E-01      7.60499        0.00428         161.339
 (CONSTANT)    2294.709


 F-LEVEL OR TOLERANCE-LEVEL INSUFFICIENT FOR FURTHER COMPUTATION
OSTATISTICS WHICH CANNOT BE COMPUTED ARE PRINTED AS ALL NINES.
1FEED FORCE REGR                                                                      17 MAY 83 12:28:44        PAGE    5
 --- U N I V E R S I T Y   O F   V E R M O N T   S P S S ---
 FILE      REGR    (CREATED  17 MAY 83 12:28:44)
0* * * * * * * * * * * * * * * * * * * * *  M U L T I P L E   R E G R E S S I O N  * * * * * * * * * * * * * *   VARIABLE LIS
                                                                                                                            REGRESSION LIS
 DEPENDENT VARIABLE..        F            FEED FORCE
                                                                    SUMMARY TABLE
0
                                                           MULTIPLE R  R SQUARE  RSQ CHANGE   SIMPLE R          B                   BE
 VARIABLE
 .
   SQ         SPEED QUPE                                    0.56512    0.31935    0.31935    0.56512    -0.2549808E-03          -8.1
   SS         SPEED SQUARE                                  0.99790    0.99581    0.67645    0.47285     0.5432442E-01           7.6
 (CONSTANT)                                                                                               2294.709
1FEED FORCE REGR                                                      17 MAY 83 12:28:44        PAGE    6
 --- U N I V E R S I T Y   O F   V E R M O N T   S P S S ---
OCPU TIME REQUIRED..       0.68 SECONDS
 ELAPSED WALL TIME..          3 SECONDS



                   17 FINISH           (SPSS GENERATED)
1              NORMAL END OF SPSS RUN.
                17 COMMAND RECORDS READ
                 0 ERRORS DETECTED

```

Pdn 8 3199-AFL TERMINAL: /5 17 MAY 83 12:38:31 No of Pages 4 V003

APPENDIX II

REFERENCES

1. Special report — "Lucas announce SYALON ceramics", a new family of Eng. materials, March 1983.

2. Finnie, I. — "Review of metal cutting analyses of the past hundred years", Mech. Eng., V.78, No.8, p.715, Aug. 1956.

3. Cocquilhat, M. — "Experiences sur la resistance utile produite dans le forage", Ann. Trav. publ. en Belgique, V.10, p.199, 1851

4. Time, I. — "Soprotivienie Maetaalov i Dereva Rezaniju", St. Petersburg, 1870.

5. Tresca, H. — "Memoire sur le rabotage des metaux", Bull. Soc. d'Encouragement pour l'Industries National, pp. 585 and 685, 1873.

6. Mallock, A. — "The action of cutting tools", proc. Roy. Soc., V.33, p.127, 1881-1882.

7. Taylor, F.W. — "On the art of cutting metals", Trans. ASME, V.28, p.31, 1906

8. Ernst, H. and Merchant M. — "Chip formation, friction and high quality machined surfaces : surface treatment of metals", Am. Soc. of metals, N.Y., V.29, p.299, 1941.

9. Merchant M.E. — "Mechanics of the metal cutting process", J. Appl. Physics, V.16, No.5, p.267, May 1945.

10. Lee, E.H. and Shaffer, B.W. — "Theory of plasticity applied to the problem of machining", J. Appl. Mech., V.18, p.405, 1951.

11. Shaw, et al — "Shear angle relationship in metal cutting", Trans. ASME, V.75, p.273, 1953.

12. Oxley, P.L.B. — "A strain Hardening Solution for the Shear Angle in orthogonal Metal Cutting", Int. J. Mech. Sci., V.3, p.68, 1961.

13. Oxley, P.L.B. & Hatton, A.P. — "Shear Angle Solutions Based on Experimental shear zone and Tool-chip Interface Distributions", Int. J. Mech. Sci., V.5, p.41, 1963.

14. Colding, B.N. — "A yield Criterion Applied to the Shear Angle Relationship", Microtecnic, V.14, p.47, 1960.

15. Armarego, E.J.A. & Brown, R.H. "The Machining of Metals", Prentice-Hall Inc., 1969

16. Piispanen, V. "Lastunmoudostimisen Teoriaa", Teknillinen Aika Kauslehti, V.27, p.315, 1937.

17. Palmer, W.B. & Oxley, P.L.B. "Mechanics of orthogonal Machining", Proc. I. Mech. E.,V.173, p.623, 1959.

18. Okushima, K & Hitomi, K. "An Analysis of the Mechanics of orthogonal cutting and its Application to Discontinuous chip formation", Trans. ASME series B J. of Eng. for Ind., V.83, p.545, 1961.

19. Bitans, K. & Brown, R.H. "An Investigation of the Deformation in orthogonal cutting", Int. J. Mach. Tool-Des-Res., V.5, p.155, 1965

20. Zorev, N.N. "Interrelation between shear processes occurring along tool face and on shear plane in metal cutting", Int. Res. in Prod. Eng., Pittsburgh, p.42, 1963.

21. Usui, E. and Takeyama, H. "A photoelastic analysis of machining stresses", Trans. ASME, J. Eng. Ind., V.82, pp.303-308, 1960.

22. Wilcox, A.B. "Negative rake metal cutting", Ph.D. Thesis 1971, Birmingham Univ.

23. Kudo, H. "Some new slip-line solutions for two dimensional steady-state machining", Int. J. Mech. Sci. V.7, p.43, 1965.

24. Kato, S. "Stress distribution at the interface between tool and chip in machining", Trans. ASME J. of Eng. for Ind.,V.94, p.683, May 1972.

25. Barrow, et al "Determination of rake stress distribution in orthogonal machining." Int. J. Mech Tools, Des & Res. V.22, No.1, p.77, 1981

26. Zorev, N. "Metal Cutting Mechanics", 1966, (Pergammon).

27. Trent, E.M. "The relationship between machinability and tool wear", Proc. conf. Machinability, 1965.

28. Boothroyd, G. et al — "Effect of Tool Flank wear on the temperature generated during metal cutting", Advances in MTDR., p.667, 1967.

29. Shaw, M.C. — "metal cutting principles" M.I.T. Press, 1952.

30. Lenz, E., Katz, Z & Ber, A. — "Investigation of the flank wear of cemented carbide tools", Trans. ASME, p.246, Feb.1976.

31. Barrow — "A review of experimental & theoretical Techniques of Assessing cutting temperature", CIRP V.2212, 1973.

32. Boothroyd, G. — "Fundamentals of Metal Machining and Machine Tools", McGraw-Hill, 1975.

33. Reeht, R.F — "Catastrophic thermoplastic shear", Trans. ASME, J. Appl. Mech., pp.189, June 1964.

Pekelharing, A.J. — "Why and how does the chip curl and break?", Annals of the CIPR 12, pp.144-147, 1964.

34. Chao, B.T. and Bisacre, G.H. — "The effect of speed & feed on the mechanics of metal cutting", Proceedings, I. Mech. E., V.165, p.1, 1951.

35. Chao, B.T. et al — "Therophysical Aspects of Metal Cutting", Trans. ASME, V.74, p.1039, 1952.

36. Tobias, S.A. — "Machine-tool vibration", John Wiley and Sons, Inc., N.Y., 1965

37. Skelton, R.C. & Tobias, S.A. — "A Survey of Research on cutting with oscillating tools", Int. J. of Machine Tool DR p.5.

38. Loladze, T.N. — "Requirements of a tool material", 8th Int. M.T.D.R. Conf., Manchester. 1967.

39. Trent, E.M. — "Metallurgical Reviews", 127.

40. Boulger, F.W. — "Superior machinability of Mx explained.IRON Age", pp.90-95, May 1951.

41. Paliwoda, E.J. "The influence of chemical composition on the machinability of rephosphorised open hearth screw steel." Trans. ASM, V.47, p.680, 1955.

42. Schrader, C.F. "Statistical study on the effect of chemical composition on the machinability of 12L14 steel.", Proc. AIME Met. Soc. Conv. Mechanical working of steel 2, V.26, p.83, 1964.

43. Armarego, E.J. and Brown, R.H. "The machining of metals", Pergman Press, Oxford, 1969.

44. Kronenberg, M. "Machining Science and Application", Pergman Press, 1966.

45. Trent, E.M. The wear rate of carbide cutting tools . Powder Met., 12, 24, 568, 1969.

46. Trent, E.M. Wear processes which control the life of cemented carbide cutting tool. Conf. Mat. for Met. Cut., ISI 126, 1970.

47. Trent, E.M. SME Tech paper, MR71-913, 1971.

48. Trent, E.M. "Metal Cutting", Butterworths, 1977.

49. Bhattacharyya, A. and Ghosh, A. "Diffusion wear of Cutting Tools", Proc. of 5th Int. MTDR Conf., 1964.

50. Bhattacharyya, A. and Ghosh, A. "Diffusion wear of cutting tools", Ann CIRP, Oct. 1967.

51. Opitz, H. and Konig, W. "On the wear of cutting tools", 8th Int. M.T.D.R. Conf., Manchester, 1967.

52. Cook, N.H. "Tool wear and tool life", Trans. of ASME J. of Eng. for Ind., pp.931-938, 1973.

53. Trent, E.M. "Conditions of seizure at the tool work interface", I.S.I. special report 94, 11, 1967.

54. Opitz, H. "Unsolved problems Associated with Metal Removal Operations", Proc. 2nd. Buhl. International Conf. on Materials, Pittsburgh, 1966.

55. Blankenstein, B. SME Tech. paper, MR71-914, 1971.

56. Zorev, N.N. "Machining steel with a carbide Tipped Tool in Interrupted heavy cutting conditions", Russian Eng. J. V.43, No.2, p.43, 1963.

57. Trent, E.M. "Hot Compressive strength of Cemented Carbide", presented at the 8th Int. M.T.D.R. Conf. University of Manchester, 12th-15th Sept., 1967.

58. Ekemar, S. "Plastic deformation of cemented carbide cutting tools", MTDR, 1966.

59. Trent, E.M. "Tool wear and machinability", J. Inst. Prod. Eng., March 1959.

60. Venkatesh & Colding "A Discussion on Tool Life Criteria and Total Failure Causes. Publ. Ass. CIRP, V.29 - 1 - 1980.

61. Mecheletti "In Process Tool Wear sensor for cutting operation", Ann. CIRP, V.25/2/76.

62. "Syalon for high speed cutting" The production Engineer, p.37, Nov.1984.

63. Katz, R.N. and Lenoe, E.M. "Properties of sialon ceramic", AMMRC sp 75-4, Army Materials and Mechanics Research Centre, May, 1970.

64. Lumby, R.J., North, B. and Taylor, A.J. "Properties of sintered sialons and some applications in metal handling and cutting", proc. of 5th U.S. Army Materials Technology Conf., 1978

65. Arrol, W.J. "The sialons-properties and fabrication." Ceramics for high performance Applications, Brook Hill, 1974.

66. Rama, G. et al "Electrical and Thermal conductivity of sialon ceramics", ceramic bullent V.57, No.6, 1978.

67. 'Special report' Metal working production, Jan. 1981.

68. Cother, N.E. and Hodgson, P. "The development of syalon ceramics and their Engineering Applications", Tran. J. Br. Ceram. Soc. V.81, pp.141-144, 1982.

69. Bhattacharya, S.K., Wallbank, J. and Jawaid, A. "Sialon proves its point in cutting ability and life research", Metal-working Production, Feb.1982.

70. Kato, S. et al "Measurement of temperature distribution within tool using powders of constant melting point", J. of Eng. for Ind., Trans. ASME series B, V.98, No.2, pp.607-613, 1976.

71. Leong Yee-Foong "An Investigation into the basic actions of cutting fluids". M.Sc. thesis. The Victoria Univ. of Manchester, May 1976.

72. Opitz, H. et al "The heat treatment of steel for good machinability", Metals prog., April 1956.

73. Kurimoto, T. & Barrow, G. "The wear of high speed steel cutting tools under the action of several different cutting fluids". Annals of the CIRP V.31/1/1982.

74. Ansell, C.T. & Taylor, T. "The surface finishing properties of a carbide and ceramic cutting tool." 3rd Int. MTDR conf. Birmingham, pp.225-243, 1962.

75. Solaja, V. "Wear of carbide tools and surface finish generated in finishing turning of steel." Wear 2, pp.40-58, 1958.

76. Shaw, M.C. et al "Groove formation in the machining of high temperature alloys", Trans. ASME, J. Eng. for Ind., 88, No.2, 1966.

77. Pekelharing, A.J. & Schuermann, R.A. "Wear of carbide tools. Its Effect on surface finish and Dimensional Accuracy", Tooling Engineer V.31, No.4, pp.51-57, 1953.

78. Chambers, A.R. "The wear of cemented carbide cutting tools", Ph.D. thesis, Birmingham University, 1975.

79. Phillips "Effect of Machining on high strength low alloy steels", ISI special Report No.94, Machinability.

80. Bhattacharys, S.K. et al — "The application of polycrystalline compacts for ferrous machining" Matador Conf., 1978.

81. Draper, W.A. — "An Investigation into the optimum Machining Conditions of high strength steels", Ph.D. Thesis, UMIST, 1974.

82. Meyer — "Data Analysis for scientists and Engineers", Wiley, 1976.

83. Norman et al — "Statistical package for the social science".

84. Deleeuw, A.L. — "Metal cutting tools", McGraw-Hill Book Co., N.Y., p.18, 1922.

85. Klopstock, H. — Recent Investigations in Turning and Planning and a New Form of Cutting Tool, Trans ASME, J. Eng. Ind., 47, 345, 1925.

86. Herbert, E.G. — Cutting Tools Research Committee Report on Machinability, Inst. Mech. Eng., 5, 19, 1928.

87. Armitage, J.B. & Schmidt, A.O. — An Investigation of Radial Angles in Face Milling, Trans. ASME, J. Eng. Ind., 66, 633, 1944.

88. Jensen, M.G. — Carbide Tools of Special Form for Interrupted Cutting, Machinery, 92, 17, 1958.

89. Chao, B.T. and Trigger, K.J. — Controlled Contact Cutting Tools, Trans. ASME, J. Eng. Ind., 66, 633, 1944.

90. Kibby, D.R. and Moore, H.D. — Ceramic or Carbide Tools - Which? Am. Mach./Metalwork Prod., 104, 63, 1960.

91. Hitomi, K. — Fundamental Machinability Research in Japan, Trans. ASME, J. Eng. Ind., 83, 531, 1961.

92. Bagley, F.L. — Turning Hardened Tool Steels with Ceramic Tool, The Tool and Manufacturing Engineer, 46, 99, 1961.

93. Albrecht, P. — High Strength Tool Geometry - A Result of Research in Tool Geometry, Trans. ASME, J. Eng. Ind., 86, 70, 1964.

94. Clark, W.T. and Ludig, B.W. "Influence of tool geometry on machining performance in some turning and face milling operations", B.I.S.R.A. / I.S.I. Conf., Materials for metal cutting, Scarborough, 1970.

95. Braiden, P.M. "Resolving the problems of machining unconventional materials", Tooling, Dec., 1972.

96. Agnew, J.D. Choosing a Fighting Edge for Carbide Tools, Tool Prod., 39, 59, 1974.

97. Agnew, J.D. Edge Preparation, Its Importance and How, Tool Prod., 38, 42, 1973.

98. Lenz, E., Moskowitz, D., Mayer, J.E. Jr. & Stauffer, D.J. Optimal Edge Geometry for Maximum Tool Life, 77-WA/Prod. 43, 1977.

99. Draper, W.A. and Barrow, G. Double Rake Tooling - The Development of High Strength Tool Geometry, 1st Joint Polytechnic Symposium on Manuf. Eng., Leicester Polytechnic, England, E1-1, June 14th & 15th, 1977.

100. Yellowley, I. & Barrow, G. The Stress-Temperature Method of Assessing Tool Life, Proc. 14th MTDR Conf., Macmillan, 733, 1974.

101. Yellowley, I. An Investigation into the Variables Affecting the Life of Cutting Tools, M.Sc. Thesis, UMIST, England, 1970.

102. Kendrick, G.D "Parameters for Tool Life Optimisation with respect to face milling", M.Sc. Thesis, University of Aston in Birmingham, 1981.

103. Fowler, J.O., Draper, W.A. and Derricott, R.T. "Influence of hard surface coatings on performance of double rake cutting tools", proc. of Int. Conf. organised jointly by National Physical Laboratory and the Metal Society, 28-29 April 1981.

104. Fowler, J. The Cutting Performance of Coated Carbide Tools, Ph.D. Thesis, C.N.A.A. - The Polytechnic, Wolverhampton, England, 1980.

105. Ahmmed M. "Analysis of Cutting Performance of double rake tool", Ph.D. Thesis, Wolverhampton Polytechnic, Aug.1982.

106. Friedman, M.Y. et al — "Investigation of the tool-chip contact length in metal cutting", Int. J. MTDR, V.10, pp.401-416, 1970.

107. Hoshi, K. and Usui, E. — Wear Characteristics of Carbide Tools with Artificially Controlled Tool Chip Contact Length, MTDR Conf., 121, 1962.

108. Usui, E. — Free Machining Steel-Tools with Reduced Contact Length, Trans. ASME, J. Eng. Ind., 84, 89, 1962.

109. Enahoro, H.E. — "Optimisation of factors influencing the efficiency of finish machining operations", College of Aeronautics, Cranfield, Memo. No.181.

110. Wu, S.M. — "Tool Life Testing by response surface methodology", Trans. of ASME J. of Eng. for Ind., Pt.1, pp.105-110, 1964.

111. Wu, S.M. — "Tool-life testing by response surface methodology" Trans. of ASME J. of Eng. for Ind., pt.2, pp.111-115, 1964.

112. Vickerstaff, T.J. Lafta, A.F. — The influence of edge geometry on the cutting performance of sialon tool. 2nd Joint Int. Conf. on Production Engineering, Leicester Polytechnic, April 1982.

113. Chiffre, L.de — "Cutting Tools with restricted contact", Int. J. Mach. Tool Des. Res., V.22, No.4, pp.321- 1982.

114. Barrow, G. — Private communications.

115. Draper, A. — Private communications.